Trinity College Dublin
Coláiste na Tríonóide, Baile Átha Cliath
The University of Dublin

Influence of Mechanical Environment on Limbal and Corneal Epithelial Cells

A thesis submitted to the University of Dublin in partial fulfilment of the requirements for the degree of

Doctor in Philosophy

Sophia Masterton, B.Sc., M.Sc.

January 2021

Supervisor: Prof Mark Ahearne

Declaration

I declare that this thesis has not been submitted as an exercise for a degree at this or any other university and is entirely my own work. I agree to deposit this thesis in the University's open access institutional repository or allow the library to do so on my behalf, subject to Irish Copyright Legislation and Trinity College Library conditions of use and acknowledgement.

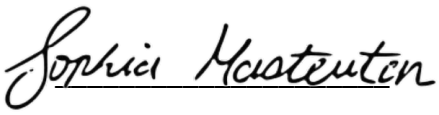

Summary

A transparent cornea is vital for vision. Corneal blindness is the 4th leading cause of blindness worldwide. It is the most transplanted tissue in the world but there is estimated to be only 1 donor cornea available for every 70 required. This coupled with donor rejection has led to research into alternative therapies for treating corneal blindness. The outermost layer of the cornea is the corneal epithelium. Maintenance of the corneal epithelium occurs at the corneal periphery where the limbus is located. This contains a pool of stem cells that replenishes the epithelial layer by migrating centripetally to the centre, differentiating and replacing any lost or dead cells. Limbal stem cell deficiency results in the loss of this function. Treatments for this condition use either limbal tissue transplanted directly onto the affected eye or expanded limbal stem cells from donor tissue that form sheets of cells. While these treatments are successful, there is still donor rejection and suboptimal visual acuity. There has been much research into how different biochemical environments can improve the expansion and transplantation of limbal stem cells, but the effect that the cells physical environment has on their behaviour is less well understood. This thesis aims to explore how mechanical cues affect limbal stem cells during expansion to aid in our understanding of corneal mechanobiology.

The aim of the first study of this thesis was to examine how glucose and calcium concentration in a corneal epithelial cell line media affected cell growth, differentiation and focal adhesion expression. The supplier's recommended media was compared to a typical corneal epithelial media used in the lab with varying glucose and calcium concentrations. Results showed that the supplier's media was best at retaining stem cell characteristics and promoting proliferation while a high glucose high calcium media should be avoided when culturing these cells.

After determining the optimal chemical environment for these cells, substrate stiffness was examined to determine how the physical environment affects the cells behaviour. Polydimethylsiloxane was used to create a wide range of stiffnesses (10 – 1500

kPa) to determine how stiffness affects cell morphology, proliferation, differentiation and mechanobiological responses over 3 and 7 days on these uncoated substrates. Results showed that culturing cells on a material with a Young's modulus in the range of 10 kPa – 105 kPa would be the most suited for retaining stem cell characteristics while also promoting a transient amplifying cellular phenotype. Focal adhesion expression decreased at day 3 but was significantly increased at day 7 suggesting these cells may migrate at a later stage repopulating terminally differentiated cells. Proliferation was increased across all stiffnesses with 820 kPa displaying the highest level of proliferation as a measure of pERK and Ki67 protein expression. This study showed that over a wide range of stiffness, the corneal epithelial phenotype is significantly affected and this data could be used in optimising biomaterial design and culturing environments for these cells.

Laminar shear stress was next examined using a fluid flow bioreactor. Human limbal stem cells were subjected to either 1 or 3 days of low or high shear stress. After culturing cells under both 1 day and 3 days of shear stress, stem cell and mature gene expression was significantly increased across three donors with variation in donor response evident. Donor age affected the shear stress response. The 1 day low shear group showed the most significant upregulation of stem cell markers among donors which was decreased over 3 days. After 3 days of high shear, the transient amplifying marker CK14 was significantly upregulated in all donors with the oldest donor showing the most significant upregulation of this marker after 3 days of high shear stress. Both shear stress rates significantly increased integrin β 1 expression after 3 days in donor 2 and 3. Cellular alignment was also observed in the high shear stress groups after 1 and 3 days, which suggests an enhanced migratory capability. This showed that after exposure to laminar unidirectional shear these cells while expressing stem cell markers also retain the ability to express CK14 and integrin β 1, which aids in wound healing and migration capability. Mature markers CK3/12 were significantly upregulated under either shear stress rates in some donors. There was no obvious trend observed for these mature markers but cells stratified after 3 days of high shear. This suggested that a more in vivo like phenotype is

observed with a heterogeneous population of stem cell and mature markers. Barrier function was also measured which is an essential function of the corneal epithelium to protect the eye from pathogens and environmental insults. Due to variations in ZO-1 expression it was difficult to determine exactly how these shear stress rates affect barrier function. However, it can be concluded that donor age will influence the cells response to shear stress and formation of an intact barrier function. Expression of TRPV4 gene expression was also examined as this channel has been implicated in the fluid shear response of MSCs. TRPV4 was significantly upregulated across all shear groups and donors compared to static culture, providing a therapeutic target to mimic this shear stress response in vitro during the ex vivo expansion of these limbal stem cells for transplantation. This work has shown that rather than using typical static culture, a new way of culturing these cells under shear stress produces a more conducive cellular phenotype. This may aid in higher success rates of transplantation while also aiding in our knowledge of corneal epithelial mechanobiology.

The next study explored a possible regulatory mechanism of the shear stress response. The aim of this study was to determine if TRPV4 activation using an agonist or inhibition using an antagonist effects the behaviour of human limbal stem cells after 2 days of cell culture supplemented with these treatments. Donor response was compared to media or vehicle treatment. A significant increase in stem cell markers was observed after TRPV4 treatment. However, only one donor had a significant increase in stem cell marker NP63α gene expression after 50nM antagonist treatment compared to the 50nM agonist group in the vehicle-controlled groups. Stem cell markers ABCG2, CK15 and Nestin expression showed a similar result among donors with only one donor displaying a significant increase in gene expression after 50nM antagonist treatment compared to the control and 50nM agonist group in both the vehicle and media-controlled groups. Based on these results, TRPV4 antagonist treatment affected stem cell marker expression with donor variation observed. Further experimentation investigating the effect of DMSO is required to determine how much it effects cellular response to TRPV4 treatment as only

one donor displayed significant increases in stem cell expression in vehicle-controlled groups while other donors displayed significant increases in stem cell marker expression compared to the agonist treatment rather than the vehicle control.

The final study of this thesis combined both stiffness and shear stress for 1 day of human limbal stem cell culture to determine if a synergistic relationship exists between these two stimuli. This study showed that the stiffer flow group which has an elastic modulus of approximately 1.5 MPa combined with low shear stress for 1 day significantly enhanced both stem cell and transient amplifying gene expression with no detection of mature marker gene expression. Therefore, when culturing limbal stem cells it would better to combine shear stress with a substrate that has a stiffness of 1-2 MPa. This work may serve as a model to mimic a more in vivo environment of the limbal stem cells for drug toxicity testing and culturing these cells before transplantation.

In conclusion, this thesis demonstrated that the mechanical environment of limbal derived corneal epithelial cells has a major role on the cellular phenotype. These findings should be taken into consideration when optimising culture environments or developing new therapies for limbal stem cell transplantation.

.

Acknowledgements

Firstly, I would like to thank my supervisor Prof. Mark Ahearne for giving me the opportunity to do a PhD in his lab and allowing me to explore many different research avenues throughout, helping me to develop significantly as a scientist. During my PhD, I was able to attend and present at many conferences both in Ireland and abroad and feel very lucky and grateful to have been given these experiences.

To everyone in the Trinity Centre for Biomedical Engineering thank you all for your guidance and collaboration, which proved invaluable to my research. The kindness and generosity displayed by everyone across the multiple labs allowed for a positive and fun workplace, I will never forget my time spent among everyone will be forever grateful for such a rewarding and fun experience.

In particular, I would like to thank Dr. Julia Fernández-Pérez who taught me many things in the lab and never faltered in her willingness to give up her time to help others. I'd also like to thank Dr. Olwyn Mahon, a true supportive friend and an inspiring scientist, the memories that we have made over the past 4 years I will always cherish.

Finally, I would like to thank all members of my family for their unwavering support and tolerance of me during the highs and lows of completing this PhD. This work is dedicated to my baby who as I write this is due to join us in exactly 1 week and was there with me writing and defending this thesis, I cannot wait to meet you.

Table of Contents

List of Figures

List of Tables

Nomenclature

ABCG2	ATP binding cassette subfamily G member 2
AMT	Amniotic membrane transplantation
ANOVA	Analysis of variance
AP-1	Activator protein 1
BCA	Bicinchoninic acid
BM	Basement membrane
BSA	Bovine serum albumin
CECs	Corneal epithelial cells
CK12	Cytokeratin 12
CK14	Cytokeratin 14
CK15	Cytokeratin 15
CK3	Cytokeratin 3
CLAU	Conjunctival limbal autograft
CLET	Cultivated limbal epithelial transplantation
DAPI	4’,6-diamidino-2-phenylindole
DMEM	Dulbecco's modified eagle medium
DMSO	Dimethyl sulfoxide
ERK	Extracellular related kinase
GAG's	Glycosaminoglycan’s
HAM	Human amniotic membrane
HC	High calcium
HCEC	Human corneal epithelial cells
HG	High glucose
HRP	Horseradish peroxidase
HS	High shear
hTCEpi	human telomerase-immortalised corneal epithelial cell line
ICAM-1	Intercellular adhesion molecule-1
IF	Intermediate filament
IgG	Immunoglobulin G

IL	Interleukin
IOP	Intraocular pressure
ITS	Insulin-transferrin-selenium
kDa	Kilodaltons
KGM-2	Keratinocyte Growth Medium 2
KLAL	Keratolimbal graft
kPa	Kilopascal
LASIK	Laser-assisted in situ keratomileusis
LC	Low calcium
LESC	Limbal epithelial stem cells
LG	Low glucose
LS	Low shear
LSCD	Limbal stem cell deficiency
mAb	Monoclonal antibody
MAPK	Mitogen-activated protein kinase
MMP	Matrix metalloproteinase
MPa	Megapascal
MSC	Mesenchymal stem cell
NP63	Nuclear Protein p63
OGB	Oregon Green 488 BAPTA-1AM
Paam	Polyacrylamide
PBS	Phosphate buffered saline
PDMS	Polydimethylsiloxane
pERK	Phosphorylated extracellular related kinase
PFA	Paraformaldehyde
Plk3	Polo like kinase 3
PVDF	Polyvinylidene difluoride
pYAP	phosphorylated yes-associated protein
RIPA	Radioimmunoprecipitation
ROS	Reactive oxygen species
RT-PCR	Reverse transcription polymerase chain reaction

SD	Standard deviation
SDS-PAGE	Sodium dodecyl sulfate–polyacrylamide gel electrophoresis
SLET	Simple Limbal epithelial transplantation
TAZ	Tafazzin
TBS	Tris-buffered saline
TCP	Tissue culture plastic
TERK	Total extracellular related kinase
TNF	Tumour necrosis factor
TRITC	Tetramethylrhodamine
TRPV4	Transient receptor potential cation channel subfamily V member 4
vCJD	Variant creutzfeldt–jakob disease
WHO	World Health Organisation
YAP	Yes-associated protein
ZO-1	Zonula-occludens-1

Publications

1. Masterton, S. and M. Ahearne (2018). "Mechanobiology of the corneal epithelium." Experimental Eye Research.
2. Masterton, S. and M. Ahearne (2019). "The Effect of Calcium and Glucose Concentration on Corneal Epithelial Cell Lines Differentiation, Proliferation, and Focal Adhesion Expression." BioResearch open access 8(1): 74-83.
3. Masterton, S. and M. Ahearne "Influence of polydimethylsiloxane substrate stiffness on corneal epithelial cells." Royal Society Open Science 6(12): 191796.
4. Ahearne, M., J. Fernández-Pérez, S. Masterton, P. W. Madden and P. Bhattacharjee (2020). "Designing Scaffolds for Corneal Regeneration." Advanced Functional Materials 30(44): 1908996.

Conference Abstracts

1. Bioengineering in Ireland, 23rd Annual Conference, Belfast, Ireland, January 2017. **Masterton S.**, Ahearne M. Examining the Effect of Mechanical Conditions on Corneal Epithelial Cells.
2. European Chapter Meeting of the Tissue Engineering and Regenerative Medicine International Society, Davos, Switzerland, June 2017. **Masterton S.**, Ahearne M. Examining the Effect of Mechanical Conditions on Corneal Epithelial Cells. Abstract published in eCM Journal.
3. Bioengineering in Ireland, 24th Annual Conference, Meath, Ireland, January 2018. **Masterton S.**, Ahearne M. Influence of Material Stiffness on a Human Corneal Epithelial Cell Line.
4. 8th World Congress of Biomechanics, Dublin, Ireland, July 2018. **Masterton S.**, Ahearne M. Influence of Material Stiffness on a Human Corneal Epithelial Cell Line.
5. XXIII Biennial Meeting of the International Society for Eye Research, Belfast, Ireland, September 2018. **Masterton S.**, Ahearne M. Influence of Material Stiffness on a Human Corneal Epithelial Cell Line.
6. Bioengineering in Ireland, 25th Annual Conference, Limerick, Ireland, January 2019. **Masterton S.**, Ahearne M. Influence of Material Stiffness on a Human Corneal Epithelial Cell Line.
7. Bioengineering in Ireland Conference, 26th Annual Conference, Carlow, Ireland, 2020. **Masterton S.**, Ahearne M. Shear Stress Enhances Stem Cell Characteristics, Stratification and Barrier Function in Human Corneal Epithelial Cells.
8. International Cell Culture Under Flow Meeting, Munich, Germany, February 2020. **Masterton S.**, Ahearne M. Shear Stress Enhances Stem Cell Characteristics, Stratification and Barrier Function in Human Corneal Epithelial Cells.

Chapter 1

Introduction

In 2016 the WHO stated that corneal opacities were the fourth leading cause of blindness globally (5.1%) proceeding cataract, glaucoma and age-related macular degeneration. Depending on the severity of corneal blindness, corneal transplantation or 'keratoplasty' may be required. Corneal tissue is the most transplanted tissue worldwide but the supply does not meet demand which poses a problem in both developed and developing countries (WHO 2016). In Ireland it is not possible to donate corneas due to a risk of Variant Creutzfeldt–Jakob disease (vCJD) transmission further adding to donor shortage (IBTS 2021). Graft failure occurs in up to 10% of corneal transplants and normally requires a regraft which can then fail in 50% of cases (Dunn, Gal et al. 2014). When combined with an ageing population and an increase in popularity of laser eye surgery (LASIK) which alters the cornea, making it unsuitable for donation, the need for alternative therapies to treat corneal blindness is increasing.

There are multiple types of corneal blindness that are mainly caused by physical or genetic conditions. Damage to the corneal epithelium due to trachoma, limbal stem cell deficiencies or physical abrasion can result in pain, inflammation, vascularisation and blindness due to the conjunctiva proliferating over the cornea leading to opacification and vascularisation.

The corneal epithelium, the outermost layer of the cornea, acts as a first line of defence for the eye in combination with the tear film providing a barrier to pathogens. It contains a pool of stem cells in the limbus located at the corneal periphery between the cornea and opaque sclera which replenishes this layer replacing any lost or dead cells (Van Buskirk 1989). During wound healing or homeostatic conditions, these stem cells migrate from the limbus to the corneal epithelium replacing any lost or dead cells and

differentiating into epithelial cells. When this function is lost, limbal stem cell deficiency (LSCD) occurs and results in blindness in severe cases. Patients with LSCD can develop physical and psychological distress, fractures, falls, depression and premature mortality (Di Girolamo 2015). LSCD can occur due to severe ocular surface disease leading to decreased vision, pain and photophobia. When this occurs allogeneic or autologous limbal stem cell transplantation is performed, which can be from a donor or from the contralateral unaffected eye . However, as mentioned previously, there is a worldwide donor tissue shortage coupled with graft failures. This results in high healthcare costs and an increased economic burden from loss of income, especially as the most common cause being chemical injury occurs in patients of working age. (Geerling, Liu et al. 2002, Di Girolamo 2015).

Biomaterial, tissue engineering and cell-based therapies to generate or repair corneal tissue have the potential to treat corneal blindness. Several reviews on the progress made in cultivating corneal tissue within the lab have previously been published with some studies using these cultivation techniques to grow a full epithelium for transplantation (Zhang, Zhang et al. 2016, Yin and Jurkunas 2018, Ngan, Chau et al. 2019, Shanbhag, Patel et al. 2019, Jackson, Myklebust Ernø et al. 2020). Corneal epithelial cells can be isolated from animals such as rabbits using an enzyme digestion with dispase and growth on a feeder layer (3T3 fibroblasts). Explant culture of rabbit corneal epithelial cells was also performed in the same study to compare isolation techniques. Explants were placed epithelium side up onto culture dishes after treatment with dispase for 1 hour, following attachment media is added (Zhang, Sun et al. 2005). Limbal epithelial cells from human donor corneas have been cultivated for 4 weeks using an amniotic membrane carrier and co cultured with 3T3 fibroblasts. These cells were subsequently transplanted

onto patients after air lifting cultures to create a new epithelium (Nakamura, Koizumi et al. 2003).

Transplantation of the limbal stem cells can be achieved by transplanting a piece of limbal tissue directly onto the eye or via ex vivo expansion on a carrier material (usually amniotic membrane) which can then be transplanted onto the eye. This process is known as cultivated limbal epithelial transplantation (CLET). While this increases the use of stem cells acquired from donor tissue for transplantation the overall success rate stands at 70% with visual acuity remaining suboptimal after successful transplantation (Haagdorens, Van Acker et al. 2016).

While there has been much research that has examined how different biochemical environments can improve the expansion and transplantation of limbal stem cells, the effect that the cells physical environment has on their behaviour is less well understood. Studying this may help to improve current transplantation techniques while also contributing to the knowledge of corneal mechanobiology.

1.1 Aims and objectives

When culturing cells on a substrate or fabricating biomaterials for cell transplantation it is important to consider the mechanical characteristics of the materials since these will influence how the cells behave (Discher, Janmey et al. 2005). The overall goal of this thesis is to elucidate how different mechanical stimuli affect the corneal epithelium, specifically focusing on stiffness and shear stress. Furthermore, can these mechanical stimuli be used to enhance stem cell expression in the ex vivo expansion of these limbal stem cells for transplantation.

This thesis aims to answer the following questions:

- How does glucose and calcium in combination affect the epithelial layers stem cell phenotype to optimise culturing conditions for a corneal epithelial cell line?
- What is the optimum stiffness for growing a corneal epithelial cell line to retain the stem cell phenotype?
- How does shear stress affect the stem cell characteristics and barrier function of the corneal epithelium?
- Can the effect of shear stress be mimicked in vitro removing the need for shear?
- Is the combination of stiffness and shear synergistic or opposing?

Chapter 2

Literature Review

2.1 Corneal anatomy, structure and function

The cornea is the multi-layered transparent outer layer of the eye consisting of the epithelium, bowman's layer, stroma, Descemet's membrane and the endothelium as depicted in Figure 2.1. It provides two thirds of the refractive power of the eye. In order to carry out its functions effectively it must be tough as well as transparent with high tensile strength. Its collagenous structures enables the cornea to do this (Maurice 1957). In corneal pathologies changes in the corneal layers can result in increased light scattering and a loss of transparency (Meek and Knupp 2015). The corneal epithelium, which is the focus of this review, is covered by the tear film. This aids in lubrication, nutrition and protection from the external environment. The composition of the tears can be an indication of disease and health state (Azkargorta, Soria et al. 2017).

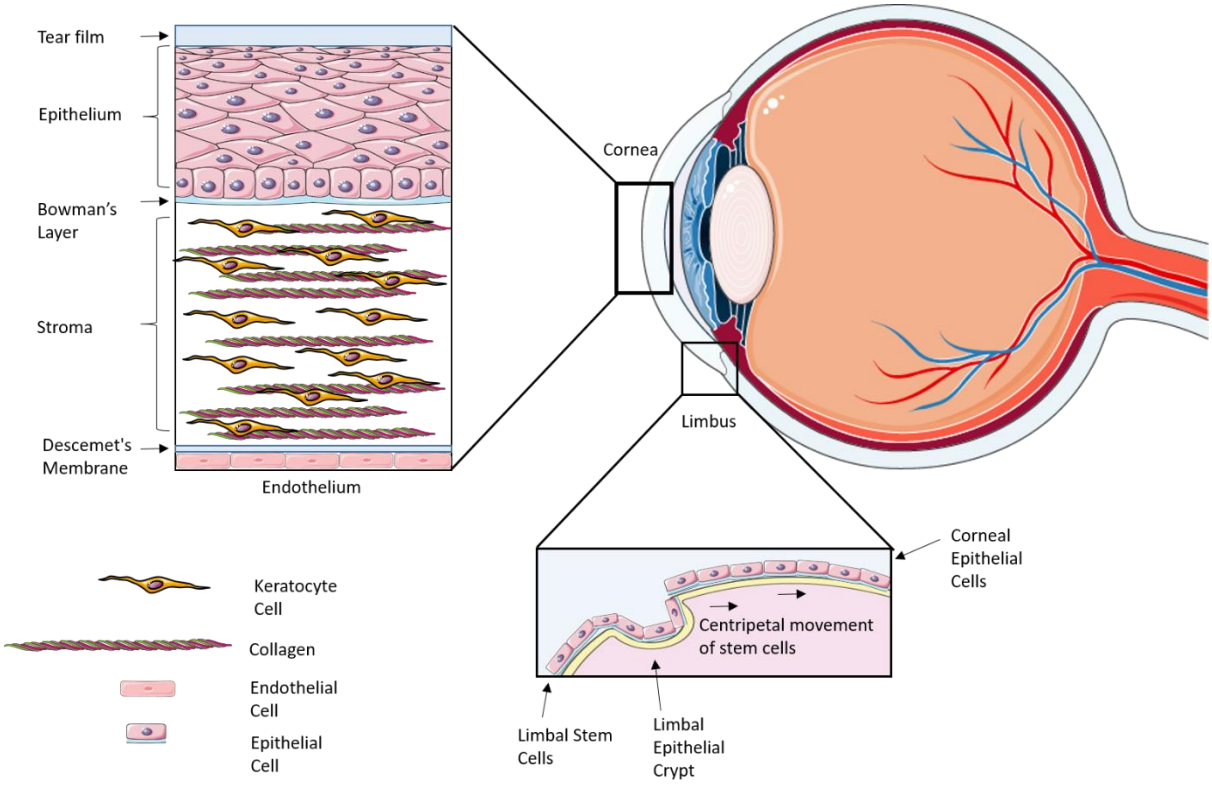

Figure 2.1 Anatomy of the cornea Schematic representation of the structure and composition of the cornea and limbus.

2.1.1 *Endothelium*

The endothelium is a single layer of cells that forms a border between the stroma and anterior chamber. It regulates stromal hydration and maintains corneal transparency. A decrease in endothelial cell density occurs with age and suggests that either it proliferates very slowly which cannot compensate for cell loss or it does not proliferate at all. Loss of function of the endothelium results in corneal edema due to fluid flow into the stroma from the aqueous humor (Joyce 2003).

2.1.2 *Descemet's membrane*

The Descemet's membrane is located between the stroma and endothelium and increases in thickness with age from 3µm to 10µm (Johnson, Bourne et al. 1982). Nanoscale topographical studies revealed that the surface of the membrane consists of a meshwork of fibres and pores all interwoven in a more dense appearance than the Bowman's Layer (Abrams, Schaus et al. 2000). Detachment of the Descemet's membrane is uncommon but does occur after cataract surgery, this can cause no effect on corneal clarity but larger detachments can result in severe corneal edema and could lead to potential corneal transplant (Kim, Shin et al. 2005).

2.1.3 *Stroma*

The stroma makes up the bulk of the cornea and consists of collagen fibrils which are precisely aligned to allow for transparency (Daxer, Misof et al. 1998). In order to allow light to focus onto the retina while achieving minimum scatter, the arrangement of the collagen fibrils is paramount. These fibrils change direction near the limbus and fuse with limbal collagen present in the circumference (Meek and Boote 2004). Keratocytes are quiescent mesenchymal derived cells of the stroma. These cells contain crystallins, which

contribute to transparency. Upon injury, the cells will either undergo cell death or adopt a repair phenotype and lose their quiescence. This results in either fibrotic scarring leading to a decrease in transparency and possible blindness depending on severity or promote regeneration (West-Mays and Dwivedi 2006).

2.1.4 *Bowman's layer*

The Bowman's layer lies between the epithelium and the stroma of the cornea. It serves as the basement membrane of the epithelium. Formation of the layer is through cytokine-mediated interactions between keratocytes in the stroma and corneal epithelial cells in early development. The functionality of the Bowman's Layer is debated and it is commonly destroyed in conditions such as bullous keratopathy (Wilson and Hong 2000). It has been hypothesized that the Bowman's layer could act as a biological barrier against pathogens as well as modulating the epithelial-stromal wound healing process (Tong, van Dijk et al. 2019). A study performed in 2009 examined the role of the Bowman's layer in corneal regeneration after phototherapeutic keratectomy (Lagali, Germundsson et al. 2009). The authors concluded that removal of the layer delayed sub basal nerve regeneration and sub epithelial keratocyte density and reflectivity. This study provided the first evidence of a role of the Bowman's Layer in rapid stromal wound healing and recovery of transparency in addition to epithelial innervation after trauma.

2.1.5 *Epithelium*

The corneal epithelium is the outermost section of the cornea underneath which lies the Bowman's layer, this lies on the collagen rich stroma, which makes up the bulk of the cornea. The epithelium contains 5-7 layers of stratified squamous epithelial cells. A

more detailed description of the structure and physiology of the epithelium is described in section 2.3.

2.1.6 *Limbus*

The limbus is located at the corneal periphery. A pool of stem cells or 'epithelial progenitors' are located in the limbus which during wound healing or homeostatic conditions migrate centripetally replenishing any lost or dead cells. Limbal stem cells play an important role in homeostasis of the corneal epithelium maintaining the dynamic stability by progressive division into transient amplifying cells and terminally differentiated cells. These cells are located in a specialised microenvironment within the limbus termed palisades of Vogt (Tseng, Chen et al. 2020). This microenvironment contains the cells, extracellular matrix, exosomes and secreted cytokines required for LSCs to maintain their stemness (Guo, Jia et al. 2021). This stem cell niche is required for the behaviour of these cells and their ability to respond to the needs of the corneal tissue (Seyed-Safi and Daniels 2020).

2.1.7 *Development*

The cornea's embryonic geneses includes the neural crest derived periocular mesenchyme and surface ectoderm. Cells in the surface ectoderm are from where the corneal epithelium originates which is adjacent to both sides of the lens placode, which is the precursor to the lens. Once the lens thickens, invaginates and separates from the surface ectoderm the corneal epithelium is formed. A protein called Pax6 in cells is required in this process to prevent corneal defects occurring including epithelial thinning, vascularisation and improper separation of the lens and cornea. The corneal epithelial cells are multipotent at this stage which may develop as lens or epidermal cells. The

presence of neural crest and epiblast cells expressing BMP inhibitors restricts lens fate. Epidermal fate is restricted by suppressing WNT signalling and cytokeratin protein expression. The cornea begins as 1-2 cell layers thick, growing to 6-8 cell layers with morphology of the cell layer dependent on it's final location. The endothelium is formed through a wave of neural crest cells from the periocular mesenchyme, which migrate from the dorsal neural tube to populate the space between the lens and corneal epithelium. This is a similar process for the stroma with a periocular mesenchyme origin.(Miesfeld and Brown 2019).

2.1.7.1 *Circadian rhythm*

Melatonin modulates a wide range of circadian rhythms, which is influenced by light stimulation of the retina. Melatonin is synthesised in the eye and pineal gland which acts on ocular structures mediating physiological processes within the eye. Melatonin receptors have been identified in corneal epithelial cells facilitating desquamation of the epithelium by modulating tight junction formation; it also affects corneal hydration in vitro, wound healing and mitotic activity. Melatonin has been shown to be required for corneal growth in chicks in vivo. Research into the mechanism of action of melatonin in ocular systems may aid in development of targeted therapeutic and environmental interventions, which may be used to treat a variety of ocular conditions (Ostrin 2019).

2.1.8 *Corneal Nutrition and REM*

The study of rapid eye movement (REM) in the cornea has not yet been fully understood with little research performed to date. Implications of REM and corneal nutrition has been linked however. An early study hypothesised recurrent corneal erosion occurring in the morning may be due to mechanical irritation from REM during early

morning REM sleep phases. Corneal nutrition is nocturnally deficient due to closed eyelids leading to corneal hypoxia as well as temperature rise impairing thermal circulation and obstructs the aqueous supply of amino acids and glucose to the cornea. This results in glycolytic corneal metabolism under anaerobic conditions as well as decreased tear film pH resulting in failure of the pH-dependent epithelium pumps which promote drainage when the eyelids are open during the day. Therefore, the cornea becomes thicker at night and rapid eye movements during REM sleep phases ameliorate this nocturnal deficiency of the healthy cornea by shaking the aqueous humour of the eye located in the anterior chamber which stagnates during sleep (Hoffmann and Curio 2003). This hypothesis remained controversial and unproven over the years (Fitt and Gonzalez 2006). However, a study published in 2014 used computational modelling to replicate aqueous humour motion in the eye subjected to REM motions. This study proved that anterior chamber flow generated by REM could transfer nutrients to the posterior corneal surface during sleep (Modarreszadeh, Abouali et al. 2014).

2.1.9 *Blindness and treatment*

Corneal blindness represents the second leading cause of blindness in most developing countries. It is estimated that almost 5 million corneal blind people worldwide could potentially have their eyesight restored via corneal transplantation (Oliva, Schottman et al. 2012). There are multiple types of corneal blindness, which are mainly caused by physical or genetic conditions. As the cornea is the outermost layer of the eye, it is the most susceptible to physical injuries.

The type of corneal blindness that a patient is afflicted with will determine what treatment will be used. Table 1 below outlines the main causes of corneal blindness and treatments performed.

Table 1 Corneal blindness, causes and treatments

Name	Cause	Definition	Treatment	Reference
Trachoma	Bacterial infection *Chlamydia trachomatis*	Irreversible condition spread through personal contact. Repeated infection can cause eyelashes to be drawn in and rub on the surface of the eye. This can permanently damage the cornea.	Antibiotic treatment and surgical treatment.	(Taylor, Burton et al. 2014)
Xerophthalmia	Vitamin A deficiency	Leading cause of childhood blindness. Leads to corneal melting and perforation. Close association with Measles	Widespread immunizations and high dose vitamin A capsules.	(Khatry, West et al. 1995)
Opthalmia neonatorum	Bacterial infection – *Neisseria gonorrhoeae/C. trachomatis*	Conjunctivitis of new-born. Risk of blindness differs depending on which infective pathogen caused the disease.	Tetracycline ointment. Prevention of sexually transmitted diseases and antenatal screening.	(Brocklehurst 2000)

Name	Cause	Definition	Treatment	Reference
Onchocerciasis (river blindness)	Parasitic infection – *Onchocerca volvulus*	Major cause of blindness in the world. Causes severe blindness and keratitis as an inflammatory response to dead and degenerating microfilaria in the stroma. Results in corneal scarring and vascularisation.	Development of ivermectin to sterilise adult worms in infected individuals. Administration of two tablets per year in endemic areas estimates that the disease will be eradicated by 2020-2025.	(Boussinesq, Fobi et al. 2018)
Mucopolysaccharidosis 1 (MPS1)	Genetic – autosomal recessive lysosomal storage disorder.	Caused by null/nonsense mutations of gene encoding alpha-L-iduronidase (IDUA) which breaks down glycosaminoglycan's (GAGs). This results in a build-up of GAGs in lysosomes. Over 95% of patients manifest cornea clouding with 50% progressing to blindness.	Corneal transplants result in high rejection rate in MPS1 patients. IDUA enzyme replacement therapy and hematopoietic stem cell transplantation is also used to treat the disease.	(Parini, Deodato et al. 2017)

Name	Cause	Definition	Treatment	Reference
Keratoconus	Complex – Genetic and Environmental	Degenerative disease causing progressive thinning of the stroma which causes a cone shaped stroma that bulges out the eye. Results in myopia and visual impairment	Keratoplasty or gas permeable contact lenses.	(Fournié, Touboul et al. 2013)
Fuchs' Dystrophy	Genetic	A combination of epithelial and stromal edema. The epithelium can detach from the basement membrane and form a painful bullae. Results in a thickened cornea and blurred vision	Keratoplasty	(Matthaei, Hribek et al. 2019)
Stevens-Johnson Syndrome	Viral infection or adverse allergic reaction	Characterised by blistery lesions on skin and mucous membranes. Corneal blisters can occur causing blindness.	Anti-histamine and anti-viral drugs or in severe cases corneal transplantation may be required if scarring has occurred.	(Jain, Sharma et al. 2016)

2.2 Corneal epithelium

The corneal epithelium is a multi-layered non-keratinised squamous epithelium containing proliferating basal cells that rest on a basement membrane (BM) structure named the Bowman's layer. Overlying this cell layer is suprabasal 'wing' epithelial cells and above these cells contain flat post mitotic superficial epithelial cells. The cornea is one of the most innervated tissues in the body in which these sympathetic nerves and axons

pierce the BM terminating between the epithelial layer. The limbus located at the corneal periphery contains pools of limbal stem cells that replenish the epithelium. In this region, the Bowman's Layer disappears and is replaced by papillae-like invaginations known as the 'palisades of Vogt'. The location of these structures allow access to a rich vascular network where soluble signals and nutrients may diffuse to support LESCs and there is added protection in the deep stromal location to allow for protection against environmental insults (Sridhar 2018).

2.2.1 *Barrier function*

The corneal epithelium serves and the major barrier to pathogens and environmental insults. This is achieved from production of tight junctions, differentiation and maturation of cells which allows for constant repopulation of cells in its basal layer (Eghrari, Riazuddin et al. 2015). The barrier function also allows the cornea to stay dehydrated which preserves transparency for transmission of light. Disruption of the barrier function can lead to a number of ocular surface conditions including dry eye, persistent epithelial defects, infectious keratitis and allergic keratoconjunctivitis (Leong and Tong 2015)

2.2.2 *Homeostasis*

There are two main theories of how the corneal epithelium is maintained. The limbal epithelial stem cell hypothesis is more widely accepted and states that the epithelium is maintained by stem cells located in the limbus in the corneal periphery. The corneal epithelial stem cell hypothesis proposes that during normal homeostasis the epithelium is maintained by stem cells in the basal corneal epithelium and that the stem cells in the limbus contribute only during wound healing (Mort, Douvaras et al. 2012).

Cells in the corneal epithelium are shed after terminal differentiation reducing the risk of pathogenic entry into the stroma which is not particularly immunogenic (Ruberti, Roy et al. 2011). However, viable cells can also be shed by apoptosis as shown in early studies using shear stress to determine how cells are shed from the cornea (Ren and Wilson 1996).

2.2.2.1 *Nutrition*

Due to the avascular nature of the cornea, which is required for transparency, delivery of nutrients and gases are supplied directly from the tear film (Tiffany 2008). The tear film provides nutrition to the cornea in addition to its role in lubrication and protection from the external environment. Tears contain electrolytes, proteins, mucins, metabolites and lipids (Azkargorta, Soria et al. 2017). The secretion of electrolytes, protective proteins and the watery component of tears is achieved through the lacrimal glands. The conjunctival and corneal epithelia release mucins allowing for aqueous tears to transform into a muco-aqueous gel, increasing lubrication. The Meibomian glands secrete lipids which forms the outermost layer of the tear film and prevents evaporation (Pellegrini, Senni et al. 2020).

The tear film is spread evenly across the ocular surface in short periods and maintained with each blink, suggesting an even nutritional supply to the limbus and central cornea (Yokoi, Bron et al. 2014). In order to measure tear film stability, a fluorescein break up time test is performed which in a faster break up time observed in dry eye patients compared to a normal ocular surface (Paugh, Tse et al. 2020).

2.2.2.2 *Metabolism*

Glucose diffusion into the cornea is achieved by the aqueous humour of the eye to the epithelium (McCarey and Schmidt 1990). The corneal epithelium utilises this glucose as an energy source to produce ATP via aerobic glycolysis with some of this glucose being added to glycogen stores. Under hypoxic conditions, anaerobic glycolysis is used for ATP production with stored glycogen phosphorylated for use as an additional energy source (Kosaku, Harada et al. 2018).

Due to the avascular nature of the stroma, corneal epithelial cells are very glycogen rich functioning as the major endogenous supply of glucose. Proliferation and migration of corneal epithelial cells which is key in their homeostasis is dependent on a balance between the synthesis and catabolism of glycogen. The limbal epithelial cells have less glycogen than the corneal epithelial cells. This may be due to the fact that limbal epithelium is supported by a highly vascularised stroma acting as another source of energy as well as the inherent reduced need of glycogen because a portion of the basal cells in the limbus are putative stem cells with differing metabolic needs (Peng, Katsnelson et al. 2013).

The corneal epithelium is also subjected to differing oxygen levels due to eyelash closure during sleep. This hypoxic stress that the corneal epithelium experiences results in a decrease in glycogen stores in corneal epithelial cells but the epithelium is still well maintained. This suggests that the cornea has a high tolerance for hypoxic stress which was shown in mice corneas subjected to 10% oxygen environment for 140 days (Kosaku, Harada et al. 2018).

2.2.3 *Wound healing and cell migration*

During both homeostatic and wound healing conditions, the corneal epithelium is in a constant state of migration and renewal to maintain or replace any dead or lost cells. This enables maintenance of a smooth optical surface and barrier function (Liu and Kao 2015). The migratory capacity of the corneal epithelial cells is central to its role in regenerating this layer and allowing for adequate barrier control and clear vision.

The role of mechanical stimuli in this process is key to its function. Primarily, shear stress from the tear film and eyelid combined aid in cellular migration and sloughing off terminally differentiated cells to allow the cell layer to be renewed (Eberwein and Reinhard 2015).

Studies examining how the corneal epithelial cells migrate have shown that the cells adopt a type of swirl pattern as shown in Figure 2.2 associated with their migration and that this is done in cellular sheets (Iannaccone, Zhou et al. 2012). Other studies have shown the cells migratory capacity to migrate back toward the limbus when this has been surgically removed and the cells undergo a de differentiation process (Nasser, Amitai-Lange et al. 2018).

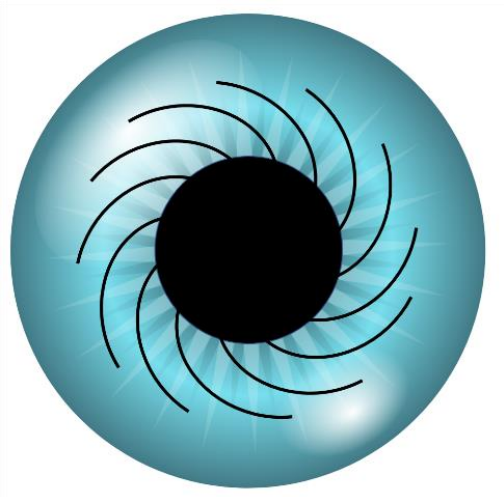

Figure 2.2 Swirl pattern of corneal epithelium. Cells migrating to the centre of the cornea do so in a swirl formation as shown in this image.

2.2.4 *Phenotype*

There are different phenotypical characteristics associated with cells in different areas of the corneal epithelium as shown in Figure 2.3. Cells located in the limbus contain a pool of stem cells which express markers associated with their stem cell phenotype (Nowell and Radtke 2017). As these cells migrate toward the centre, they become transient amplifying cells and finally fully differentiated cells in the central cornea where they stratify (West, Dorà et al. 2015).

In the limbus, cells express a number of different markers associated with a stem cell phenotype. These include ABCG2, Nestin – a multipotent stem cell marker, NP63 which has a number of different isoforms associated with different corneal epithelial cell types (Chen, de Paiva et al. 2004) and cytokeratin 15 (Gouveia, Lepert et al. 2019). The marker associated with a transient amplifying phenotype in the corneal epithelium is cytokeratin 14 while mature marker expression of cytokeratin 3 and cytokeratin 12 is expressed in the central cornea where mature differentiated cells reside (Guo, Zhang et al. 2018).

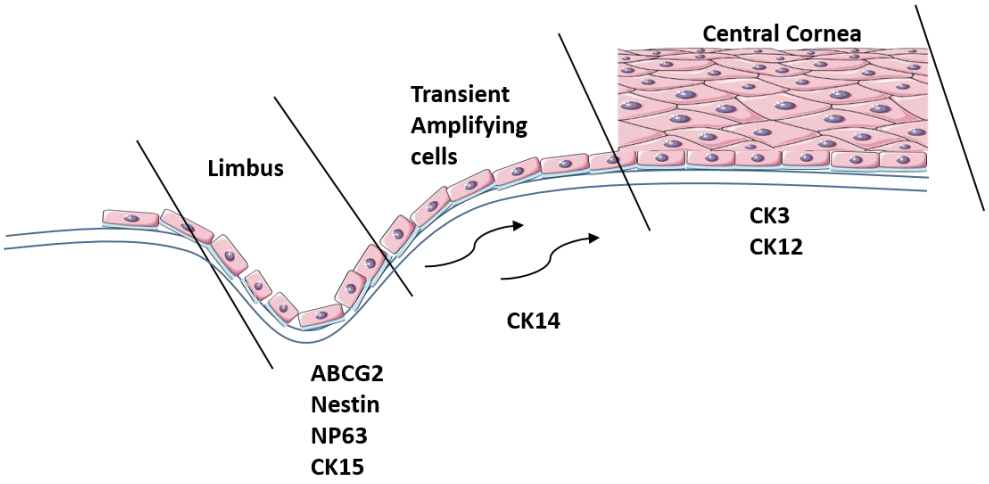

Figure 2.3 Corneal epithelial markers. Cells located in the limbus express a number of markers including ABCG2, Nestin, NP63 and CK15. Migratory cells, which are transiently amplifying cells making their way to the centre of the cornea, express CK14. The central mature corneal epithelial cells express CK3 and CK12.

This pathway can also occur in the absence of the limbal stem cell niche. One study showed that surgical removal of this limbal stem cell niche in the limbus resulted in corneal committed cells dedifferentiating into limbal stem cells, which retained marker expression described in the limbus. However, this effect required an intact stroma (Nasser, Amitai-Lange et al. 2018).

2.2.5 *Diseases*

In the corneal epithelium, blindness can occur due to genetic conditions or physical insults as discussed previously. This will result in the inability to replenish the corneal epithelium with stem cells from the limbus resulting in corneal blindness as shown in Figure 2.4

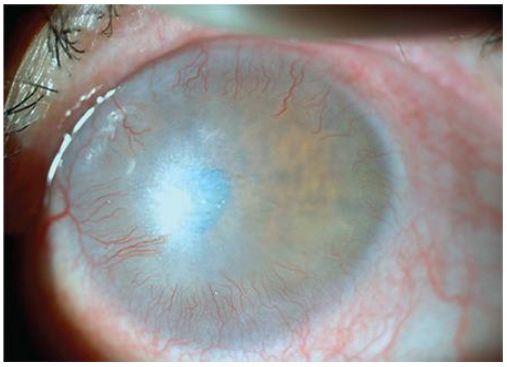

Figure 2.4 Limbal Stem cell deficiency causing blindness. Photograph of the eye of a patient with limbal stem cell deficiency caused by chemical injury. Advanced vascularization toward the central cornea as well as conjunctivalisation can be seen causing blindness (Barut Selver, Yagci et al. 2017).

Previous research has shown that epithelial-mesenchymal transition (EMT) may be a way in which ophthalmic diseases progress, effecting damage repair and corneal epithelial healing (Liu and Dong 2008). One study showed that EGF inhibits TGF-β1-induced EMT enhancing the corneal epithelial cell's proliferation and migration increasing the wound healing process (Chen, Xie et al. 2020). This transition of cells from epithelial to mesenchymal phenotypes has been proposed as a possible therapeutic target in fibrotic disorders including the cornea(Di Gregorio, Robuffo et al. 2020).

2.2.6 *Treatments*

An early form of treatment for corneal epithelial defects was introduced in the 1980s called 'Keratoepithelioplasty'. The procedure included using lenticules of donor cornea covered by epithelium placed at the corneoscleral limbus to eventually spread and cover the centre of the cornea (Thoft 1984). However, penetrating keratoplasty, which is a procedure to replace the full thickness of the cornea, is the dominant procedure at present. Table 2 below details limbal stem cell deficiency treatments. The

procedures used to treat limbal stem cell deficiencies and the mechanism of action is detailed in the table below (Haagdorens, Van Acker et al. 2016).

Table 2 Limbal stem cell deficiency procedures.

Procedure:	Mechanism of action	References
Autologous serum drops	Promote proliferation and migration of healthy epithelium.	(Yeh, Chu et al. 2020)
Therapeutic contact lenses	Prevents further epithelial defects while promoting healing of persistent epithelial defects.	(Harthan and Shorter 2018)
Corneal scraping and amniotic membrane transplantation (AMT)	Overgrown conjunctiva removed to allow re epithelialization by residual CESCs AMT proceeds this to promote proliferation and migration of residual LESCs.	(Sabater and Perez 2017)
Conjunctival limbal autograft/allograft (CLAU)	A graft from the patient's healthy unaffected eye or a donor using the conjunctiva as a carrier tissue, which may induce LSCD in the healthy donor eye. Increased risk of infection and neoplasia due to immunosuppressant use.	(Yin and Jurkunas 2018)
Keratolimbal graft (KLAL)	Cornea used as a carrier tissue from deceased donor, increased risk of disease transmission and neoplasia.	(Yin and Jurkunas 2018)

Procedure:	Mechanism of action	References
Ex vivo cultivated limbal epithelial stem cells (CLET)	Transplantation of allogeneic or autologous cultivated limbal stem cells using most commonly human amniotic membrane (HAM) or fibrin as a carrier for the graft. Decreased risk of immunological rejection and inducing LSCD in the healthy donor eye. However, using HAM may cause disease transmission. Some culturing methods also use animal derived products, which may cause zoonotic disease transmission or cause immune rejection.	(Yin and Jurkunas 2018)
Simple limbal epithelial transplantation (SLET)	Autologous transplantation of small limbal grafts secured onto HAM. Epithelialization achieved in vivo with reduced risk of immunological rejection.	(Yin and Jurkunas 2018)

2.3 Cultivating corneal epithelial cells

Ex vivo limbal expansion and grafting (CLET) or transplanting limbal tissue directly onto the affected eye (SLET) is a common way to treat corneal blindness caused by limbal stem cell deficiency. In 1997, Pellegrini et al showed that CLET was effective in restoring the corneal surface using a small piece of autologous limbal tissue; this could also be used for long-term regeneration of the corneal epithelium in patients with chemical or thermal burns (Pellegrini, Traverso et al. 1997, Rama, Bonini et al. 2001).

The advantages of ex vivo limbal grafting include decreased risks to the donor eye, ability to regraft after failure, storing cells to allow for additional transplantation if required and combination with gene therapy (Sacchetti, Rama et al. 2018). The success rates of CLET can vary with rates from 45% to 100% which is influenced by age with

younger patients achieving a lower success rates (less than 15 years old) compared to adults and can be costly (Ramachandran, Basu et al. 2014).

Although CLET is becoming the standard of care for repairing corneal damage the cost and success rates are not ideal. In addition to this, immune rejection has been reported following allogeneic CLET resulting in patients receiving immunosuppressive therapy (Qi, Xie et al. 2013). Alternative methods to culture these cells should be investigated to increase the chances of the cells transplanting successfully into the patient's eye.

2.3.1 *Media supplementation*

Cultivation of limbal stem cells requires a nutrient media containing a number of growth factors and supplements. Limbal biopsies can be cultured initially using a drop of FBS for 24 hrs followed by addition of the nutrient media. Briefly the media includes DMEM/F12 media (1:1 mixture) FBS, hydrocortisone, cholera toxin, insulin-transferrin-selenium (ITS), dimethyl sulfoxide, human epidermal growth factor and gentamicin (Qi, Xie et al. 2013). There are variations of media in the literature with all containing similar components and in a low calcium environment. Ideally, xenogenic substances are not introduced and the cells express >70% positivity for limbal progenitor cell phenotype markers NP63.

2.3.2 *Biological substrates*

There have been a number of biological substrates used as a substrate for corneal epithelium growth including silk films (Jia, Ghezzi et al. 2016), feeder layers such as irradiated human fibroblasts as well as fibrin and collagen type IV substrates (Rama, Bonini et al. 2001, Chakraborty, Dutta et al. 2013, Le-Bel, Guérin et al. 2019).

Amniotic membrane is widely used as a carrier substrate for the corneal epithelium which can be transplanted directly with cells as well as using amniotic membrane transplantation alone as a therapy for ocular chemical injury (Zeng, Wang et al. 2014, Zhang, Zou et al. 2016, Eslani, Baradaran-Rafii et al. 2019). However, issues with variability among batches of amniotic membrane, low transparency and risk for disease transmission reduce the effectiveness of amniotic membrane as a biological substrate for corneal epithelial transplantation (Yazdanpanah, Haq et al. 2019).

The previously described substrates that have been investigated for corneal epithelial transplantation are still in animal study phase but offer novel alternative substrates for corneal epithelial transplantation.

2.3.3 *Transplantation*

The two main transplantation techniques used in corneal epithelial transplants are shown in Figure 2.5 below. A piece of donor tissue can be used from either allogeneic or autologous sources and expanded ex vivo followed by transplantation (CLET) or a piece of limbal tissue may be transplanted directly onto the affected eye (SLET).

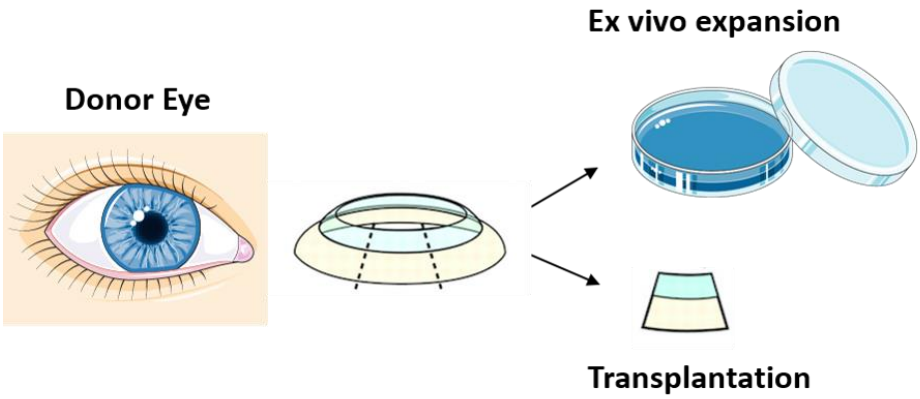

Figure 2.5 Transplantation techniques for the corneal epithelium. A limbal biopsy is taken from the donor eye which can be either cultured ex vivo and cells transplanted (often on a carrier substrate such as amniotic membrane) or the tissue can be transplanted directly onto the eye**.**

2.4 Mechanobiology

When cells are subjected to physical forces this normally results in a series of intracellular biochemical processes that regulate both the cells physiological and pathological responses (Chen 2008). Examples of how mechanical forces can influence the behavior of cells in tissue and organs can be seen throughout the body such as the effect of fluid pressure and shear stress from pumping blood on the regulation of endothelial vasculature (Resnick, Yahav et al. 2003) or in the ability of bone to remodel to adapt to differing loading regimes (Orr, Helmke et al. 2006).

A wide variety of signaling molecules and structures have been shown to contribute to mechanotransductive events in the cell including integrins, extracellular matrix components and cadherin molecules. Structures such as nuclei and stretch activated ion channels also contribute to mechanotransductive events (Ingber 2006). There are a wide variety of these mechanosensitive processes, for example, activation of membrane pores by osmotic swelling to reduce intracellular pressure and tension in the membrane leading to an increase in cell survival. The fusion of intracellular membrane

vesicles occurs through tension sensitive fusion with the cell membrane. This leads to transmitter release implicated in a wide range of important physiological processes (Hamill and Martinac 2001). Physical forces have been shown to provide a way of altering the conformation of proteins to generate signals for both widely expressed and specialized mechanosensitive systems (Orr, Helmke et al. 2006). Mechanosensitive mechanisms in the nucleus may also regulate both its structure and function where the nuclear envelope appears to have a role in functioning during adhesion and migration (Aureille, Belaadi et al. 2017). In addition to this, cytoskeletal organization is also affected by the nuclear envelope mechanosensitivity. In relation to the corneal epithelium specifically, a variety of mechanical stimuli are applied to the limbal and epithelial regions on the cornea in vivo and these can affect both intracellular and extracellular functions. These forces influence how the epithelium is maintained and its ability to undergo repair. The sources of stimulation include shear stress from the tear film motion, fluctuations in the strain and stiffness of the basement membrane and stroma and external compressive

and shear forces from rubbing of the eyelid or contact lens wear as shown in Figure 2.6 below.

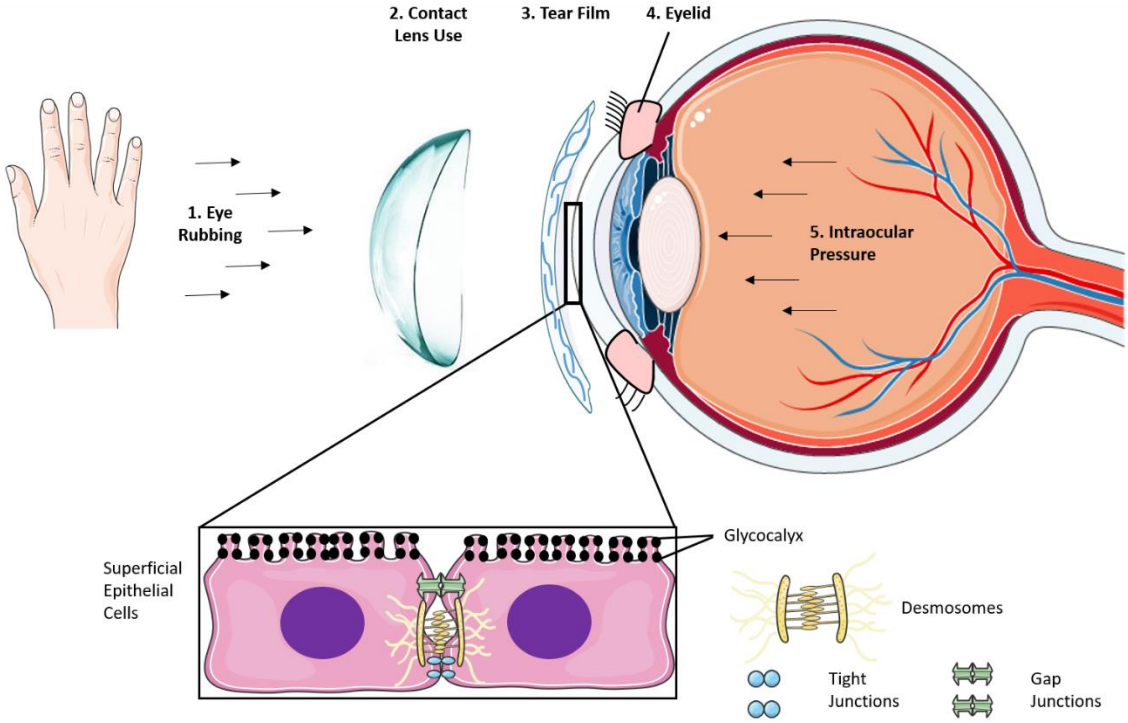

Figure 2.6 Mechanical Stimuli experienced by the corneal epithelium. Image depicting different sources of mechanical stimuli that can be applied to the cornea and the subcellular structures in superficial epithelial cells that respond to these mechanical signals.

2.4.1 *External stimuli*

Several studies have examined the mechanical and viscoelastic characteristics of the cornea using techniques such as extensometry, inflation or micro-indentation (Hjortdal 1994, Ahearne, Yang et al. 2007, Elsheikh, Wang et al. 2007, Hatami-Marbini and Rahimi 2014), to measure the mechanical properties of the epithelium or epithelial cells. A wide range of values for the elastic modulus of the cornea have been reported from 0.1-57 MPa (Garcia-Porta, Fernandes et al. 2014). Therefore, a more sophisticated approach is required. Since the corneal epithelium is subjected to a wide range of mechanical stimuli it needs to have sufficient strength and stiffness to withstand these forces. Two common

examples of methods by which external forces are applied to the cornea are by rubbing and wearing contact lenses. The following section describes studies which have examined the effect of eyelid rubbing and contact lens use on the corneal epithelium. These are important factors to consider when designing alternative therapies to ensure that materials to be transplanted into the eye as an alternative therapy can withstand these forces.

2.4.2 *Eyelid rubbing*

The eyelids are composed of skin, fibrous tissue, muscle and a mucous membrane to protect the eye from injury and excess light. In addition, it also spreads the tear film evenly over the ocular surface while blinking. Electrohydrodynamic studies have shown that the tear film lubricates and protects the cornea from the eyelid during blinking and eye lid closure (Jones, Fulford et al. 2008). However, when the eyelid is being rubbed, it is pushed back against the corneal epithelium, reducing the tear film thickness under the compressed area. In addition to compression, the motion during rubbing can result in shear forces being applied to the epithelium. The combination of these forces can have a negative effect on the health of the cornea.

A number of cases have reported an association between eye rubbing and the progression of keratoconus (Lindsay, Bruce et al. 2000, Jafri, Lichter et al. 2004, Ioannidis, Speedwell et al. 2005). For example, Lindsay et al., (2000) reported a patient who experienced frequent eye rubbing due to epiphora from punctal agenesis developed unilateral keratoconus in the affected eye (Lindsay, Bruce et al. 2000). Eye rubbing has been shown to reduce 'corneal hysteresis' which is a reflection of the capacity of the cornea to absorb and dissipate energy and affects intraocular pressure (Liu, Lee et al.

2011). This study found that after eye rubbing the biomechanical properties of the cornea were significantly decreased and this was a cumulative effect with increasing episodes of eye rubbing. The mechanical stimulation applied to the cells during rubbing results in an increase in proteases and inflammatory markers such as MMP-13, IL-6 and TNF released into the tear film after 60 seconds of rubbing (Balasubramanian, Pye et al. 2013).

Rubbing may also lead to changes in the thickness of the epithelium. One study found that there was an 18.4% reduction in the thickness of the epithelium immediately after rubbing (McMonnies, Alharbi et al. 2010). It was hypothesized that the applied force resulted in cell displacement and flattening. However, a more recent study found no significant change in the epithelium thickness after rubbing (Prakasam, Schwiede et al. 2012). One of the difficulties in investigating the effect of rubbing on the epithelium is the wide variations in how people rub their eyes, the frequency of rubbing and the amount of force they apply. There is no set of standard rubbing forces or techniques resulting in wide variations in data collected by researchers. For this reason, while the force applied by rubbing does appear to affect corneal epithelial cells, the precise effect of rubbing on the health of the cornea remains unclear.

2.4.3 *Contact lens use*

Contact lenses are commonly used to improve vision, however there are some risks associated with their use, infections usually caused by poor lens care and improper use results in blindness in 1 out of every 500 users annually (Dart, Radford et al. 2008). One risk with wearing contact lenses is adhesion occurring between the lens and the cornea. Proteins and other molecules from the tear film may bind to the contact lens and these allow cells from the epithelium to adhere. Depending on the adhesion force, this

can result in damage to the epithelium when the lens is being removed from the eye. One study found that this adhesion to the contact lens can tear the epithelium upon detachment (Elkins, Qi et al. 2014). However, a limitation to the study was the use of cell monolayers rather than a stratified multilayer model hence further study will be required to fully elucidate the mechanical effects of contact lens adhesion on the corneal epithelium.

Contact lenses may also impart a mechanical effect on the epithelium by restricting the tear film flow over the corneal surface (Mann and Tighe 2013, Muntz, Subbaraman et al. 2015). As previously mentioned, the motion of the tear film results in shear forces being applied to the epithelium. By restricting the tear flow under the lens, the mechanical stimulation that these cells are normally subjected to is inhibited. Proteins and lipids also may become entrapped under the contact lens leading to an immune reaction (Mann and Tighe 2013). Furthermore, the thickness of the tear film has been shown to change pre- and post- contact lens wear (Lin, Graham et al. 1999, Nichols and King-Smith 2003, Wang, Fonn et al. 2003). This would likely result in changes to the magnitude of shear force being applied to the cells.

While contact lenses are designed to be oxygen permeable they still result in a decrease of oxygen uptake by the epithelium (Takatori, Lazon de la Jara et al. 2013). Contact lenses have also been shown to inhibit cell proliferation in the central cornea after prolonged wear (Ladage, Ren et al. 2003) and delay the migratory capacity of cells (Robertson 2013). Poor oxygen permeability may lead to hypoxic conditions that can cause various conditions including epithelial keratitis and loss of corneal transparency. Under closed eyelid conditions this is made worse with the minimum oxygen requirement

for the cornea not being met (Lee, Kim et al. 2015). This is leading to alternative contact lens designs such as new lens materials containing organosilicon moieties in their polymers (Long, Schweizer et al. 2009).

Hypoxic conditions activate Polo-like kinase 3(Plk3) signalling and c-Jun/AP-1 transcription complexes that in turn lead to apoptosis of corneal epithelial cells (Lu, Sheyla et al. 2016). Hypoxic stress has a different effect on human limbal stem cells by inducing a differentiation response through down regulation of the Plk3 activity. Corneal hypoxia also leads to corneal edema which is well documented in low oxygen transmissible contact lenses. One study reports a biochemical description of the cornea to quantify hypoxic swelling (Leung, Bonanno et al. 2011). Inflammation has also been associated with hypoxia of the cornea and this can lead to vascularization and have detrimental effects on vision (Safvati, Cole et al. 2009). For these reasons contact lens manufacturers have been interested in developing lenses with higher oxygen permeability.

Understanding the effects that a contact lens has on the mechanobiological behavior of the corneal epithelium provides valuable information on how to improve the design of biomaterials for culturing and transplanting these cells.

2.4.4 *Corneal stiffness*

Fluctuations in intraocular pressure (IOP) can also lead to changes in the corneal epithelium. As IOP increases, the shape of the cornea may change leading to strain being applied to the corneal epithelial cells although the overall stiffness of the cornea is not believed to change significantly (Johnson, Mian et al. 2007, Pierscionek, Asejczyk-Widlicka et al. 2007). Early studies examining the link between corneal edema and intraocular pressure observed that epithelial edema appeared sooner and progressed faster as

intraocular pressure was increased and/or after endothelial damage leading to stromal swelling increase (Ytteborg and Dohlman 1965). This study was performed on human subjects with low, normal or raised IOP. Specifically, stromal hydration and the presence or absence of corneal edema was studied focusing on the etiology of bullous keratopathy. The authors postulated that raised IOP or endothelial malfunction with stromal edema may cause epithelial edema by pressure of the stromal interstitial fluid. Due to the corneal epithelium's high resistance to fluid flow the positive pressure of the stromal interstitial fluid may then force fluid into the epithelium causing the observed edema.

2.4.5 *Basement membrane*

Several studies have shown that the mechanical characteristics of the substrate on which cells adhere can influence their phenotype (Discher, Janmey et al. 2005, Engler, Sen et al. 2006). In the cornea, changes to the stroma or Bowman's layer resulting from damage or disease can affect how the epithelial cells behave. Extracellular matrix proteins secreted by the stroma in response to chronic inflammation or in homeostatic conditions can alter the mechanical integrity of the extracellular matrix and lead to the activation of a YAP/TAZ and β-catenin signaling pathways that in turn promotes the epidermal differentiation of the epithelium. This can lead to corneal squamous cell metaplasia which causes blindness. (Nowell, Odermatt et al. 2016). The expression of YAP is believed to be increased with increase in substrate stiffness (Foster, Jones et al. 2014) while the regulation of YAP/TAZ has also been shown to be dependent on topographical cues (Raghunathan, Dreier et al. 2014). This pathway has been shown in multiple studies to be involved in the relaying of mechanical signals given by cell shape and extracellular matrix rigidity. The pathway is also required to control the differentiation of mesenchymal stem cells induced by varying matrix stiffness (Dupont, Morsut et al. 2011). Hence it is not

surprising that it has a role to play in the corneal epithelium's response to underlying matrix stiffness.

2.4.6 *In vitro environments before transplantation*

Ex vivo expansion of limbal epithelial cells will usually involve culture of these cells on a substrate in the laboratory (Utheim, Aass Utheim et al. 2018). Limbal stem cells are generally grown in a static environment using biological cues to enhance limbal stem cell proliferation. Cultivation of limbal stem cells on amniotic membrane is the most common in vitro environment that these cells encounter. However, issues with immune rejection and storage means that a tissue-engineering alternative is required (Hancox, Heidari Keshel et al. 2020). These include amniotic membranes which are widely used as a tissue carrier in reconstruction surgery (Zhang, Zou et al. 2016). Amniotic membrane has also been used as a temporary patch in emergency cases of LSCD as well as in ex-vivo cell expansion (Sabater and Perez 2017). Transplantation of limbal epithelium grown on amniotic membrane in vitro has restored a non inflamed ocular surface and corneal phenotype (Pauklin, Steuhl et al. 2009).

2.4.7 *Studying substrate stiffness in vitro*

Several different biomaterials including Polyacrylamide (Paam) gels and collagen have been used to examine the effect of matrix stiffness on cell behaviour (Engler, Sen et al. 2006, Wen, Vincent et al. 2014). Human corneal epithelial cells cultured on Paam gels with differing elastic moduli displayed no significant variation in cell proliferation, integrin expression and intercellular adhesion molecule-1 (ICAM-1) expression although apoptosis and necrosis were increased on softer substrates (Molladavoodi, Kwon et al. 2015). The migration of cells was also analyzed and showed that cells on medium and stiff substrates

migrated significantly more than the softer. When the cytoskeletal structure of the cells was assessed, cells on compliant or softer substrates were lacking actin filaments while the formation of actin filaments increased on a high substrate stiffness. Actin is known to be vital for cells to exert pulling forces onto their environment (Ahearne, Liu et al. 2010), disrupted actin fibers as well as a higher number of apoptotic cells on soft substrates would explain the cells inability to migrate. One limitation with using Paam gels is that their surface topography and the availability of adhesion sites can vary with varying stiffness introducing additional parameters that could affect cell behaviour (Trappmann, Gautrot et al. 2012).

Collagen hydrogels have also been used as a substrate for examining the influence of stiffness on epithelial and limbal cells. Plastic compression of collagen hydrogels can be used to vary their stiffness by removing water and increasing the overall collagen density and stiffness (Abou Neel, Cheema et al. 2006, Cheema, Chuo et al. 2007, Levis, Brown et al. 2010). Jones et al. (2012) used collagen substrates to demonstrate that stiffness can control the phenotype of limbal stem cells to aid in the ex vivo expansion of limbal stem cells for transplantation and keep the cells in an undifferentiated state (Jones, Hamley et al. 2012). The authors showed that limbal derived stem cells cultured on stiffer collagen substrates (2.9 kPa) had greater expression of cytokeratin 3 a commonly used limbal epithelial cell differentiation marker as well as a higher cell number than on softer collagen substrates (0.003 kPa) using immunohistochemistry and western blotting. The modulus of the anterior basement membrane is believed to be between 2 kPa and 15 kPa (Last, Liliensiek et al. 2009, Last, Thomasy et al. 2012). The phenotype of the limbal epithelial cells was affected by the stiffness of the hydrogels and this could be useful for

the design of ocular surface constructs or models to aid in ex vivo expansion of limbal epithelial cells.

Foster et al. (2014) showed the expression of the transcriptional co activator Yes-associated protein (YAP) in the Hippo signalling pathway by epithelial cells varied on collagen hydrogels of differing stiffness (Foster, Jones et al. 2014). Localization of YAP was selected to assess the effect of substrate stiffness on differentiation and centripetal migration of limbal epithelial cells during normal homeostasis. The expression of YAP was compared between the limbus and central cornea in situ and in vitro using limbal epithelial stem cells on collagen hydrogels which were biomimetic (use of synthetic materials to mimic biological processes). The nuclear expression of YAP was increased with increasing stiffness; this was also used as a molecular probe to look at the mechanical microenvironment in situ in a normal ocular surface. Localization of YAP in situ was cytoplasmic in the basal limbal epithelial cells and nuclear in the basal central corneal epithelial cells. This study concluded that YAP and the distinct cell populations studied indicated that cells experience a different mechanical environment between the central cornea and limbus. This has led to a new hypothesis in which differences in substrate stiffness drives migration and differentiation of limbal epithelial cells controlling homeostasis.

2.5 Shear stress

The corneal epithelium is covered by a thin tear film to protect the eye against bacteria and other pathogens. It plays an important role in light refraction and has the largest change in refractive index of the eye (Montés-Micó, Alió et al. 2005). The dynamic nature of the tear film means its motion results in shearing forces being applied to the

underlying cells (Braun, King-Smith et al. 2015). The amount of force applied is regulated by a number of factors including the tear film thickness, composition, viscosity and flow pattern resulting from blinking.

2.5.1 *Tear film composition*

The tear film must be stable with uniform thickness over the entire corneal surface to allow for acute vision and health of the ocular surface (Svitova and Lin 2016). While early studies on tear film thickness and protein composition were inconclusive, making it difficult to accurately characterize tear film dynamics, more recent studies have established that tear lipids exist as multi layered films that range between 30-100nm in thickness and that the total tear film thickness varies between individuals and is dependent on the measurement techniques applied with values ranging from 3-10μm (Hodson and Earlam 1994). However, the structure of tears is still poorly understood due to their complexity and variability in composition with over 1500 proteins believed to be present (Moon, Kim et al. 2016).

2.5.2 *Flow dynamics*

The flow pattern of the tear film can be altered by several medical conditions such as Sjögrens syndrome or rheumatoid arthritis both of which can result in dry eye syndrome (Fujita, Igarashi et al. 2005). Variations in the tear film dynamics associated with dry eye can effect wavefront aberrations after blinking (Montes-Mico, Alio et al. 2005, Wang, Xu et al. 2009). Wavefront aberrations are optical flaws that occur in the eye preventing light focusing effectively on the retina. These aberrations can be low order (e.g. astigmatism) and can be corrected using glasses or surgery. However higher order

aberrations are untreatable and the tear film flow can effect these aberrations (Resan, Vukosavljevic et al. 2012).

Dry eye is very common worldwide and is treated primarily using artificial tear drops. Tear additives increase the viscosity of tears and significantly increased shear stress on the ocular surface during a blink. This in turn increases the cell shedding rate of corneal epithelial cells (McElwain, Jones et al. 2007). Moisture chamber spectacles can be used in severe cases but these have limitations and require a great amount of optimisation for the patient to be able to use them effectively. However, these methods have been optimised using 3D printing to aid in design of personalised moisture chamber spectacles (Moon, Kim et al. 2016).

Evaporation is another factor that can influence the dynamics of the tear film and is affected by environmental factors including temperature and humidity. The intact lipid layer decreases this evaporation rate and has an impact on tear film dynamics, stability and osmolality (Stahl, Willcox et al. 2012). The stability of the tear film has also been shown to be affected by age with the break up time significantly shorter for older age groups. Age also affects the lipid layer, becoming thinner in older subjects and showed a synergic effect of gender and age (Maïssa and Guillon 2010).

It is clear that the tear film has a complex flow configuration that is influenced by several different factors and is vital in maintaining the health of the corneal epithelium. Physical forces imparted on the tear film such as blinking have downstream effects on the corneal epithelium as discussed and is something that should be considered when studying the mechanobiology of the corneal epithelium. These include imparting a shear force on the corneal epithelium as well as ensuring adequate lubrication for the corneal

epithelium to prevent evaporation. Replication of the flow conditions in-vitro may improve our understanding of the precise mechanisms by which fluid shear forces affects epithelial cells and assist in optimizing the culture conditions for generating epithelial sheets with a view to mimic the in vivo environment of the corneal epithelium

2.5.3 *Eyelid*

The tear film is partially displaced by the eyelid during blinking. The blink cycle can be broken into different parts (downstroke, turning point, upstroke and interblink) each of which affect the tear film dynamics in differing ways. This includes lipid compression in a thick layer under the upper eyelid during downstroke with the release of a thick and narrow band at the start of the upstroke. A 'rippling' effect is also observed during lid motion. (Braun, King-Smith et al. 2015). Lipids are an important aspect of the tear film which are located in the tear film lipid layer, this provides a smooth surface over the cornea and prevents evaporation from the eye. (Wizert, Iskander et al. 2014). Several mathematical and computational models have been developed to predict the fluid behaviour during blinking (Heryudono, Braun et al. 2007, Winter, Anderson et al. 2010, Braun, King-Smith et al. 2015).

2.5.4 *Simulation of fluid flow in vitro*

The most common approach to applying fluid flow in vitro is to use a bioreactor system (Weyand, Israelowitz et al. 2009). Studies performed using bioreactors have the potential to reduce costs and may facilitate the growth of specific engineered tissues. Bioreactors can also enable the automation and standardization of tissue manufacturing processes in closed controlled systems (Martin, Wendt et al. 2004). There have only been a limited number of studies involving their application with corneal epithelial cells.

One type of bioreactor system that has been used to study corneal epithelial cells involves the use of a flow chamber that allows fluid to pass over a substrate onto which the cells are adhered (Molladavoodi, Robichaud et al. 2017). Shear stress was found to up-regulate integrin β1 expression which is normally associated with cell adhesion. In contrast to this, integrin α3 and ICAM-1 showed minimal changes with shear stress. Changes to the cytoskeleton resulting from shear forces were found to enhance the rate of wound healing although fluid shear needed to be applied prior to the damage occurring.

Kang et al. (2014) used a purpose-built bioreactor to examine the effect of flow induced shear stress on the stemness of limbal epithelial stem cells (Kang, Shin et al. 2014). Their aim was to mimic the flow induced shear stress from the blinking of an eye. It was found that steady flow had a positive effect on maintenance of stemness of the cells while intermittent flow caused the cells to differentiate into transient amplifying cells as evident from the appearance of holoclones.

Shear forces may also affect the cell-shedding rate of the corneal epithelium. In this case the fluid shearing effect was studied using an in vitro whole eye perfusion experiment (Ren and Wilson 1997). A magnetic stir plate and test tube placed on top filled with tear solution was constructed to allow the entire corneal surface to be exposed to the solution for 6 hours. The authors concluded that over time the rate of cell shedding increased in shear conditions with 3,500 cells shed from static conditions and 20,000 cells shed from stirred corneas. A follow up study examined the shed cells for DNA fragmentation as a marker for apoptosis. The study concluded that nonviable epithelial cells are shed after terminal differentiation but viable cells can be shed via apoptotic mechanisms. This

demonstrated that there is more than one mechanism for the removal of cells from the surface of the cornea (Ren and Wilson 1996).

2.6 Impact of mechanobiology on biomaterial design

Biomaterials are materials that are engineered for use in biological applications. They may be synthetic, natural or biological in origin and they play a pivotal role in the field of tissue engineering and regenerative medicine (Hubbell 1995). For corneal epithelial regeneration, amniotic membranes isolated from the placenta have been used to treat ocular surface conditions due to their high biocompatibility, anti-inflammatory properties and promotion of epithelial wound healing in the eye from the presence of growth factors (Rahman, Said et al. 2009, Meller, Pauklin et al. 2011). However, drawbacks including transmission of bacterial infections due to a lack of donor screening or improper storage and processing of membranes can lead to complications for the patients. The inherent donor variation is also an issue (Malhotra and Jain 2014). This has increased the demand for alternative biomaterials to be designed to treat corneal epithelial defects.

One important factor that needs to be considered when choosing a biomaterial is its physical and mechanical characteristics since these will affect how the cells respond (Mitragotri and Lahann 2009). For the corneal epithelium, the biomaterial must have sufficient strength and stiffness to withstand the external and internal forces experienced by the corneal epithelium as discussed earlier. The Young's modulus describes the tensile elasticity of a material and is a useful parameter when selecting suitable biomaterials as the cells will behave differently on materials with differing moduli. For the corneal epithelium, this value must be sufficiently high to withstand different mechanical forces acting on the epithelium and may need to be strong enough to withstand suturing if

needed. It may also be beneficial to try to replicate the mechanical characteristics of the basement membrane or Bowman's layer to create a more in-vivo like environment. This can create a problem since there may be some discrepancies between what the optimal Young's modulus would be for resisting forces and the modulus of the basement membrane. Taking the amniotic membrane as an example, the Young's modulus in full term membranes ranges from approximately 1.5-3MPa (Benson-Martin, Zammaretti et al. 2006) which is considerable higher than the Young's modulus of the anterior basement membrane on which the corneal epithelium rests with a value between 2-15kPa (Last, Liliensiek et al. 2009). However, there has been a very wide range of reported values for the mechanical properties of the cornea, primarily due to different methods of measurement, differing methods of sample preparation and the viscoelastic nature of the tissue. Despite these issues, studies that have examined the effect that mechanical environments have on the corneal epithelium should assist researchers trying to optimise parameters to drive cells to form a healthy epithelium.

In addition to mimicking the mechanical characteristics of tissues, many biomaterials aim to mimic in vivo biochemical and biophysical conditions in order to create microenvironments that allow for effective in vitro studies and assist in tissue regeneration. Many biomaterials incorporate specific biological components such as growth factor and cytokines to replicate conditions cells experience in vivo (Chen and Liu 2016) or to promote matrix deposition (Ahearne, Liu et al. 2014). These biological components can influence how cells behave and the matrix proteins they deposit which in turn affect the mechanical properties of the environment (Glatt, Evans et al. 2016). As cells change the mechanical properties of their environment, the new environment can affect how the cells behave thus creating a dynamic reciprocity between cells and their

environment (Ahearne 2014). Recently, one study found that ascorbic acid promotes stemness of the corneal epithelial stem cells though regulation of extracellular matrix components and accelerates wound healing (Chen, Lan et al. 2017). Other studies have also shown that the extracellular matrix which provides structural and mechanical support also plays a role in limbal epithelial stem cell homeostasis (Mei, Gonzalez et al. 2012). This highlights the importance of studying what the effect the mechanical environment has on the corneal epithelium to aid in biomaterial or 3D microenvironment design and optimise the chemical environment to which the cells are subjected.

2.7 Conclusion

From the literature presented, it can be seen that while there has been much research conducted on the corneal epithelium and limbal stem cells, several questions remain to be answered. This thesis will aim to answer the following questions:

- How does glucose and calcium in combination affect the epithelial layers stem cell phenotype to optimise culturing conditions for a corneal epithelial cell line?
- What is the optimum stiffness for growing a corneal epithelial cell line to retain the stem cell phenotype?
- How does shear stress affect the stem cell characteristics and barrier function of the corneal epithelium?
- Can the effect of shear stress be mimicked in vitro removing the need for shear?
- Is the combination of stiffness and shear synergistic or opposing?

Chapter 3

The Effect of Calcium and Glucose Concentration on a Corneal Epithelial Cell Line's Differentiation, Proliferation and Focal Adhesion Expression

3.1 Introduction

The corneal epithelium is the stratified squamous outer layer of the cornea that is maintained by limbal epithelial stem cells located in crypts along the cornea-scleral border(Ludwig, Lopez et al. 2020). Severe damage to the epithelium can cause blindness and require either keratoplasty from donor tissue or the transplantation of limbal stem cells in cases of limbal stem cell deficiency. These cells may also be expanded in vitro and undergo epithelial differentiation to generate cell sheets suitable for transplantation (Pellegrini, Traverso et al. 1997). While there has been much research undertaken using different culture media, further work is still required to find an optimal media formulation expanding the cell population and promoting epithelial differentiation.

Two factors that can influence the behaviour of corneal epithelial and limbal cells are the glucose and calcium concentrations within the culture media. Glucose concentration has been associated with changes in matrix metalloproteinase (MMP) activity (Takahashi, Akiba et al. 2000), immune response (Ni, Yan et al. 2011) and growth factor signalling (Xu, Li et al. 2009) in corneal epithelial cells as well as being the primary energy source for the corneal epithelium in vivo via diffusion of glucose from the aqueous humour (McCarey and Schmidt 1990).

Calcium concentration has been shown to effect both the proliferation and differentiation of mice corneal epithelial cells in-vitro (Ma and Liu 2011). While the role of each of these two important reagents has been examined, their reciprocal role on cell behaviour has not previously been explored. The present study uses a human corneal epithelial cell line isolated from the limbus that is used widely in corneal epithelial research (Robertson, Li et al. 2005, Dreier, Raghunathan et al. 2012, McMahon, Gallagher

et al. 2014) to determine how different glucose and calcium concentrations in combination effect the cell's ability to proliferate and differentiate. Proliferation was determined by examining the proliferative marker extracellular related kinase (ERK) at both the gene and protein level in addition to measuring metabolic activity and cell growth over 7 days. Differentiation was characterized by examining epithelial stem cell marker NP63 and mature corneal epithelial marker cytokeratin 3 (CK3) which are both well-established markers of a stem cell by NP63 being present exclusively in the limbus and CK3 present in the central corneal superficial cells and absent from the limbus (Di Iorio, Barbaro et al. 2005, Jones, Hamley et al. 2012). In addition, the effects that the media had on cellular focal adhesions, which are critical to cellular communication and migration, was also examined. This study will assist researchers in understanding the effect of different media formulations on corneal epithelial cells and may be applied to primary culture cells for ex vivo expansion or for researchers using this cell line.

The recommended media from the cell line provider was used as a control group in this study. However, in the media which contain varied calcium and glucose concentrations a DMEM/F12 media was used which is typical in the media of primary culture isolations (Yang 1991). Other studies have also used DMEM/F12 to establish cell lines in the early stages of developing them (Fan, Xu et al. 2011). This was to give a more representative medium in corneal epithelial isolation rather than varying calcium and glucose in the manufacturer's media alone, which does not describe in detail the exact components of the media.

A recent study showed that access to an adequate amount of eye tissue is difficult for some researchers and that research findings are questioned due to the poor quality of

tissue received. The study concluded that an online portal would be beneficial in tackling these issues (Stamer, Williams et al. 2018). The use of cell lines in corneal epithelial research may therefore be more beneficial not only for reduced donor variation and for increased compatibility among research labs but also to allow researchers to have enough cells to conduct their research on.

Therefore, how different media and components effect these cell lines is required to allow researchers to better understand cellular responses and design novel experiments in which these components may be varied. This research will give better insights into how the use of typical corneal epithelial media used in primary culture isolation effects these cell lines, which are also used for research.

3.2 Materials and Methods

3.2.1 *Cell culture*

A vial of an immortalized human corneal epithelial cell line (hTCEpi, Evercyte) was used on all the experiments in this study. The cells ectopically express the catalytic subunit of human telomerase. The cell line was thawed by pre-warming in hand and transferring the contents to a tube filled with 9ml pre-warmed Keratinocyte Growth Medium 2 (KGM-2, PromoCell). The cells were centrifuged at 170 G for 5 minutes and the pellet resuspended in 1ml media. This was transferred to a T25 culture flask containing 6ml media and incubated at 37^{o}C. The culture medium was changed after 24 hrs and passaged if already confluent.

Cells were seeded at 5,000 cells/cm^2 into cell culture plates. Cells were used between passage 4 and 6 for testing media formulations. The cells were fed three days a week with corneal epithelial media containing Dulbecco's Modified Eagle's Medium

(DMEM) and Ham's F12 medium in a 3:1 ratio. Three DMEM solutions containing different glucose and calcium concentrations (low glucose, high calcium (LG-HC); high glucose, high calcium (HG-HC); high glucose, low calcium (HG-LC)) were compared in this study. A media supplementation recipe adapted from Bray et al, 2011 (Bray, George et al. 2011) was used and consisted of 10% Foetal Bovine Serum (FBS), 0.1% penicillin/streptomycin solution, 1% non-essential amino acids, 400mM L-Glutamine, 6.8mg 3,3,5-triiodo-L-thyronine sodium salt (T3), 1µg/ml Insulin, 180µM Adenine, 10ng/ml Epidermal Growth Factor (EGF), 1µg/ml isoproterenol, 0.4µg/ml hydrocortisone and 5µg/ml Transferrin. Cells were also grown in the suppliers recommended media, KGM-2, as a control group. The table below (Table 1) outlines the different calcium and glucose concentrations for each group.

Table 3.1 Glucose and calcium concentrations of the different media.

Media	Low Glucose High Calcium (LG-HC)	High Glucose High Calcium (HG-HC)	High Glucose Low Calcium (HG-LC)	KGM-2 Media (Control)
Calcium Concentration (mM)	1.896	1.896	0.096	0.06
Glucose Concentration (mM)	5.5	25	25	6

3.2.2 *Cell growth curve*

After seeding cells in all media formulations cell growth was measured every day for 7 days in each group. Cells were trypsinised from three separate wells for each group and counted using a hemocytometer and trypan blue exclusion assay to determine the cell suspension per ml using the formula: cell count x 10,000 x 2.

3.2.3 *Metabolic activity*

A PrestoBlue assay (Thermo Fisher Scientific) was used to assess metabolic activity of cells after 7 days in all groups. This commercially available kit was used following the manufacturer's instructions. Media was aspirated from each well and a 1:10 mixture of PrestoBlue reagent to media was prepared and added to wells. This was incubated at 37°C for 1 hour, the reagent and media was placed in triplicate into a 96-well plate as well as a blank and absorbance read at a wavelength of 570 nm.

3.2.4 *RT-PCR*

RT-PCR was performed using a similar protocol to those previously described (Ahearne and Lynch 2015, Lynch, O'Sullivan et al. 2016, Lynch and Ahearne 2017). RNA was isolated from monolayer cultures using Trizol (Invitrogen). 1ml of Trizol was added per well (on a 6 well plate) followed by cell scraping. The Trizol-cell solution was collected in RNAse-free eppendorf tubes, snap frozen in liquid nitrogen and transferred to -80°C for storage until further use. When ready to be used the solution was placed on ice to allow it to thaw slowly. 200µl of chloroform was added to each tube and centrifuged at 12,000 G at 4°C. RNA located in the upper phase was transferred to a new RNAse free tube, isopropanol was added at the same volume as well as 4µl glycoblue to allow visualisation of the RNA in the following steps. The tubes were stored at -20° C for 12 hours, again placed on ice to allow the solution to thaw, and centrifuged at 12000 G at 4°C for 15 minutes. A visible blue RNA pellet was formed, supernatant was discarded and the tubes dried. 1ml of 70% ethanol (in RNAse free water) was added to wash the pellet. Another centrifugation step was performed at 12,000g at 4°C for 15 minutes, ethanol was removed and the pellet air-dried. RNAse free water (11µl) was used to dissolve the pellet. A NanoDrop-1000 (Thermo Fisher Scientific) was used to quantify RNA yield and purity.

Transcription of mRNA to cDNA was performed using a high capacity cDNA reverse transcription kit (Invitrogen). A mastermix was added to 500ng of RNA and placed in a thermocycler. The following temperature sequence was applied: 10 minutes at 25°C, 2 hours at 37°C, 5 minutes at 85°C, 1 minute at 4°C. Quantitative PCR was performed with TaqMan reagents, 4.5µl cDNA, 5µl TaqMan universal mastermix II and 0.5µl primer. The following primers were used: ERK (Hs00385075_m1), CK3 (Hs00365080_m1), NP63 (custom-made primer sequence adapted from Robertson et al. (Robertson, Ho et al. 2008) and GAPDH (Hs02758991_g1). All samples were run in triplicate with a GAPDH housekeeping gene control. Fold change expression was calculated using the ΔΔCt method.

3.2.5 *Western blot*

To evaluate the expression of ERK protein in the cells grown with different media formulations western blot analysis was performed on all groups at day 7. The proteins examined included phosphorylated ERK and Total ERK as a loading control. Cell lysates were isolated from monolayer culture using RIPA Lysis buffer with a phosphatase inhibitor cocktail followed by cell scraping. Samples were centrifuged at 13,000 RPM for 5 minutes and the supernatant used for western blotting. Protein concentration was determined using a BCA protein assay kit (Thermo Fisher Scientific) to ensure equal loading of protein across all conditions which was 7µg. The cell lysates were subjected to sodium dodecyl sulfate–polyacrylamide gel electrophoresis (SDS-PAGE) using a 12% precast polyacrylamide gel at 200V for 40 minutes in an electrophoresis rig (Bio-Rad). A molecular weight ladder was added to each gel, proteins were transferred to Polyvinylidene difluoride (PVDF) membrane via semi dry transfer (Thermo Fisher). Membranes were blocked in 3% Bovine serum albumin (BSA) in Tris-Buffered

Saline and 1% Tween 20 (pH 7.6) for 1 hour RT. The membranes were incubated with anti-rabbit phospho-p44/42 MAPK (Erk1/2) (Thr202/Tyr204) antibody #9101 and p44/42 MAPK (Erk1/2) antibody #9102 (Cell Signalling) at 1:1000 in 3% Bovine serum albumin (BSA) in Tris-Buffered Saline and 1% Tween 20 (pH 7.6) O/N at 4^{o}C with agitation to analyse expression of phosphorylated and total ERK protein respectively. Membranes were washed three times for 5 minutes with Tris-Buffered Saline and 1% Tween 20 followed by secondary antibody incubation for 1 hour RT. Anti-rabbit IgG, horseradish peroxidase (HRP) linked antibody (Cell Signalling) was prepared at 1:2000 in Tris-Buffered Saline and 1% Tween 20. Membranes were washed three times for 5 minutes with Tris-Buffered Saline and 1% Tween 20 and membranes developed using an immunodetection kit (enhanced chemiluminescence western blotting substrate – Thermo Fisher) and developed using GelDoc system (Bio-Rad). Densitometry was performed on all blots using ImageJ software and graphed using GraphPad Prism 7.

3.2.6 *Immunocytochemistry*

To perform Immunocytochemical staining cells were seeded onto coverslips, which were activated using HCl treatment followed by PBS washing. After 7 days, cells were fixed using 4% paraformaldehyde (PFA) for 15 minutes at room temperature (RT) followed by rinsing in phosphate buffered saline (PBS) 3 times and stored in PBS until ready to stain. Cells were blocked and permeabilised using 2% FBS and 0.5% Triton-X in PBS (blocking buffer) for 30 minutes RT, followed by primary antibody incubation at 4^{o}C O/N in 1:10 blocking buffer in PBS (antibody buffer). Antibodies for mouse anti-vinculin antibody ab18058 (Abcam) and anti-p63 (ΔN), poly6190, rabbit polyclonal 619002 (Biolegend) was used at a 1:500 dilution and CK3 K3/K76 antibody (Sigma Aldrich) at 1:200 dilution. Cells were washed three times with antibody buffer to remove excess primary

antibody and incubated with secondary antibody donkey anti-Mouse IgG H&L (Alexa Fluor® 488) (ab150105) (Abcam) for vinculin and CK3 and goat anti Rabbit IgG (H+L) 647 (ab150079) (Abcam) for NP63 for 2 hours @ RT at twice the primary antibody dilution. Cells stained with NP63 and CK3 were stained for cellular actin to visualise the cytoskeleton using Phalloidin-TRITC P1951 (Sigma Aldrich) at 1:1000 for 2 hours @ RT with the secondary antibody incubation. All groups were also stained for cellular nuclei using fluoroshield with DAPI (Sigma Aldrich). Cells were imaged using a confocal microscope. Mean fluorescence intensity was determined using ImageJ software and corrected for background.

3.2.7 *Statistical analysis*

All data was analysed using GraphPad Prism 6. Data are presented as the mean $\pm$ standard deviation (SD), significance calculated via one-way ANOVA with Post-Tukey test. All data are presented as N=3.

3.3 Results

3.3.1 *Cell growth curve*

A cell growth curve was prepared over 7 days on all groups as shown in Figure 3.1. The control group had a significantly higher rate of growth over 7 days compared to all other groups. The cells grown in varying calcium and glucose concentrations showed a similar rate of cell growth. However, the LG-HC group did show an increase in cell growth at day 6 and 7 compared to cells grown in HG-HC and HG-LC. The LG-HC group had a significantly higher rate of growth compared to the HG-HC and HG-LC group.

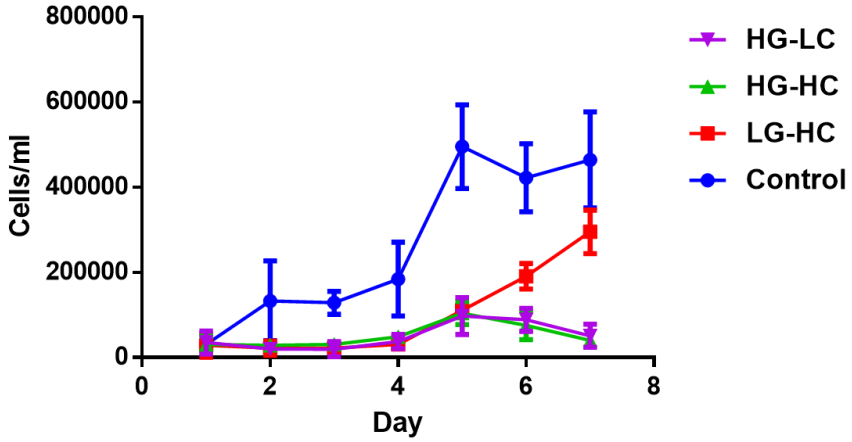

Figure 3.1 Cell growth curve of hTCEpi cells grown in different media formulations over 7 days. Cells grown in the commercial media displayed a significantly higher cell number over 7 days compared to all other groups. The LG-HC group had a significantly higher rate of growth compared to the HG-HC and HG-LC group. Data are presented as the mean ± SD. HG-HC, high glucose, high calcium; HG-LC, high glucose, low calcium; LG-HC, low glucose, high calcium.

3.3.2 *Metabolic activity*

A PrestoBlue assay was performed on all groups after 7 days in culture as shown in Figure 3.2 to examine the effect that the media formulation had on the cell populations' metabolic activity. Cells cultured using the different glucose and calcium concentrations had significantly less metabolic activity compared to the control group. There was no significant difference in metabolic activity between the three test groups. However, the HG-LC group displayed the least metabolic activity of all the groups tested.

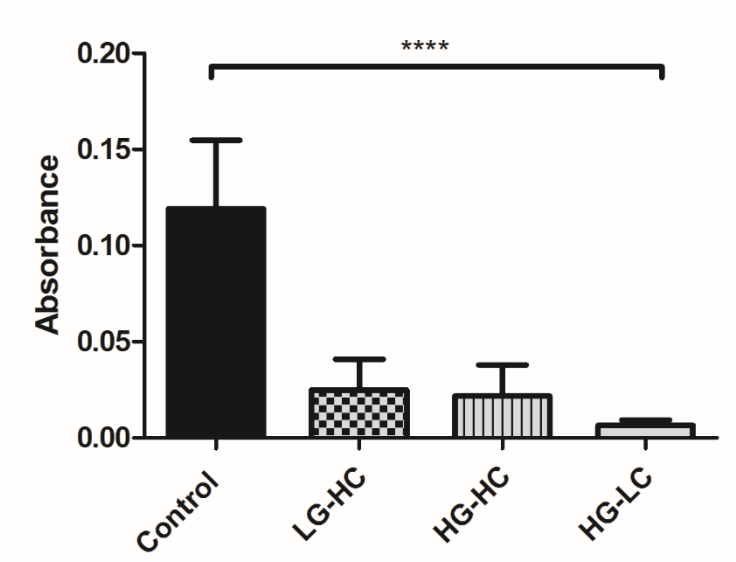

Figure 3.2 Metabolic activity of hTCEpi cells after 7 Days in culture. Cell metabolic activity was significantly decreased in all groups compared with commercial media-cultured cells (control). Data are presented as the mean ± SD, N=3, **** = P ≤ 0.0001.

3.3.3 *RT-PCR*

Gene expression analysis of the cellular proliferation marker ERK was also performed on all groups after 7 days in culture the specified culture media (Figure 3.3). The HG-HC and LG-HC groups expressed significantly less ERK than the control group. HG-HC fed cells expressed ERK significantly lower than the LG-HC fed cells but not the control. The HG-LC group did not show any significant difference in gene expression of ERK when compared to all other groups including the control.

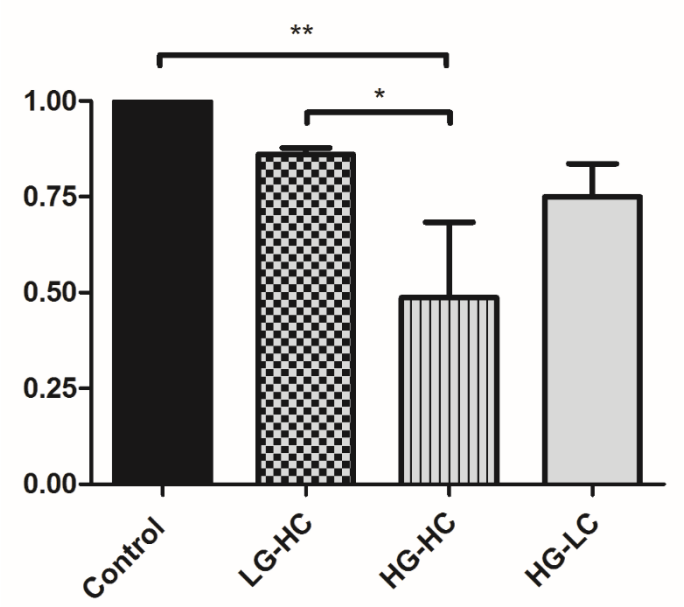

Figure 3.3 Real time PCR to determine relative expression of ERK after 7 Days in culture. HG-HC fed cells expressed ERK significantly lower than the control group and the LG-HC group. Data are presented as the mean ± SD, N=3, *= P ≤ 0.005, **= P≤ 0.01

The corneal epithelial stem cell marker NP63 was analysed for gene expression after 7 days (Figure 3.4). The HG-LC and HG-HC groups showed the most significant decrease in NP63 expression compared to the control, followed by the LG-HC group. In addition to this, a significant reduction in NP63 expression was observed between groups in the HG-HC group and the HG-LC as well as the LG-HC group.

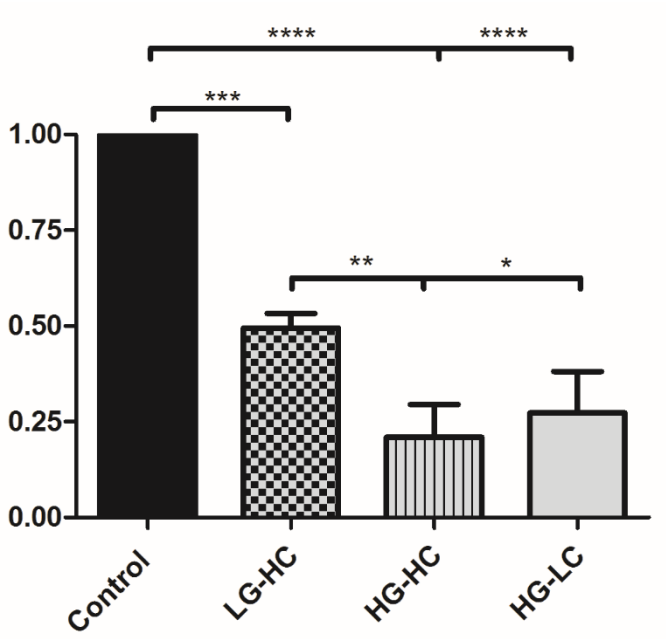

Figure 3.4 Real time PCR to determine relative expression of NP63 after 7 Days in culture. HG-LC and HG-HC groups had the most significant decrease in NP63 expression compared to the control followed by LG-HC. Between groups the HG-HC group and the HG-LC expressed NP63 significantly lower than the LG-HC group. Data are presented as the mean ± SD, N=3, * = P ≤ 0.05, ** = P ≤ 0.01, *** = P ≤ 0.001, **** = P ≤ 0.0001.

Gene expression of a mature corneal epithelial marker was also examined (Figure 3.5). CK3 was expressed in both the LG-HC and HG-LC groups. However, CK3 was not detected in the HG-HC group. The expression of CK3 was lowest in the control group but no significant differences were observed either between the test groups or compared to the control.

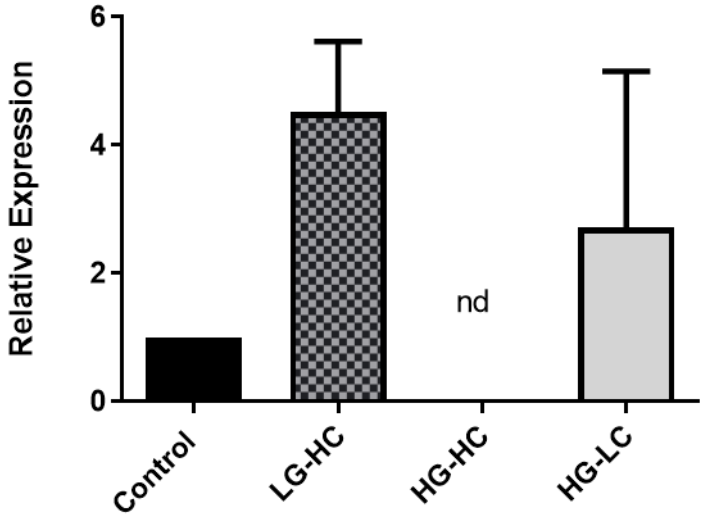

Figure 3.5 Real time PCR to determine relative expression of CK3 after 7 Days in culture. Cells fed in LG-HC and HG-LC media expressed CK3 higher than the control group, CK3 was not detected (nd) in the HG-HC group. No significance was observed between groups or compared to control. Data are presented as the mean ± standard deviation (SD), N=3.

3.3.4 *Western blot*

After 7 days in all media formulations cells were analysed for phosphorylated ERK protein expression as a marker for proliferation (Figure 3.6). The HG-HC group appeared to express less pERK protein compared with all other groups. The LG-HC and commercial media group produced the highest level of pERK protein, although statistically there was no significant difference in pERK found between any of the groups. When a similar western blot was performed for CK3, there were insufficient proteins detectable to generate a band.

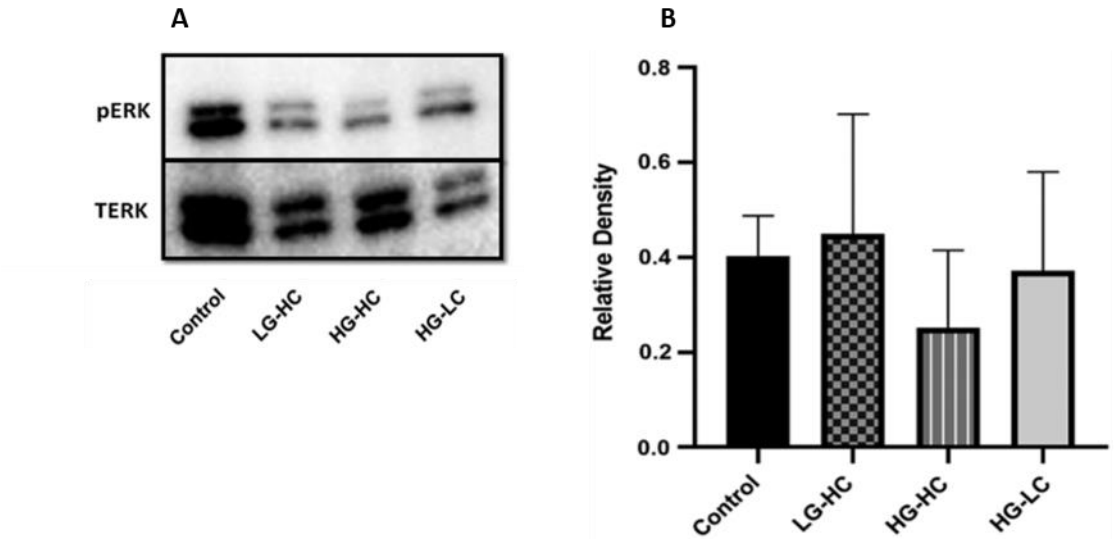

Figure 3.6 Western blot and densitometry analysis of a corneal epithelial cell line cultured in different media formulations after 7 days. No significant differences between groups observed of pERK expression (b). Data are presented as the mean ± SD, N=3.

3.3.5 *Immunocytochemistry*

Cells were analysed by immunocytochemistry as shown in Figure 3.7 and imaged using confocal microscopy at day 7 for stem cell marker NP63 in order to visualise nuclear localisation of the protein as well as mature corneal epithelial marker CK3. In addition, to corneal epithelial markers focal adhesions were examined using a vinculin stain.

The morphological characteristics of the cells were different between the different groups. In the control group, cells exhibited the typical cobblestone morphology that corneal epithelial cells display with consistent morphology between the cells (Figure 3.7 A,E,I). Control group cells also were smaller and more densely packed together. In comparison, cells grown using the different test media formulations were more globular

and less cobblestone in shape with some irregular cell shapes present. In particular, LG-HC fed cells had very irregular cell shapes and adopted a more globular appearance (Figure 3.7 B,F,J). HG-HC fed cells were also globular and bigger in size compared to controls (Figure 3.7 C,G,K). The HG-LC fed cells appeared smaller and more regular in cell shape compared to the other test groups (Figure 3.7 D,H,L).

Nuclear localisation of the stem cell marker NP63 was the highest in the control group with little expression in the cytoplasm (Figure 3.7 A). Among the test groups, LG-HC fed cells expressed NP63 the most in the nucleus with some expression in the cytoplasm (Figure 3.7B). The lowest nuclear expression of NP63 appeared in the HG-HC fed group (Figure 3.7 C). The HG-LC group expressed NP63 in both the nucleus and cytoplasm in similar levels (Figure 3.7 D). The mature corneal epithelial cell marker CK3 was least detectable in the control and HG-HC groups (Figure 3.7 E + G). The LG-HC and HG-LC fed groups displayed more CK3 with similar expression levels (Figure 3.7 F + H).

Focal adhesions were visualised using vinculin staining. All groups stained positive for the protein, however the amount of staining did vary between groups. The control group exhibited an even distribution of staining of the protein over most of the cells although some cells appeared to show no staining (Figure 3.7 I). In the LG-HC group the intensity of the vinculin stain varied between cells (Figure 3.7 J). The HG-LC group (Figure 3.7 L) also displayed differing amounts of vinculin between different cells but not to the same extent as the LG-HC (Figure 3.7 J) fed cells. The HG-HC group had the least vinculin present of all the groups (Figure 3.7 K).

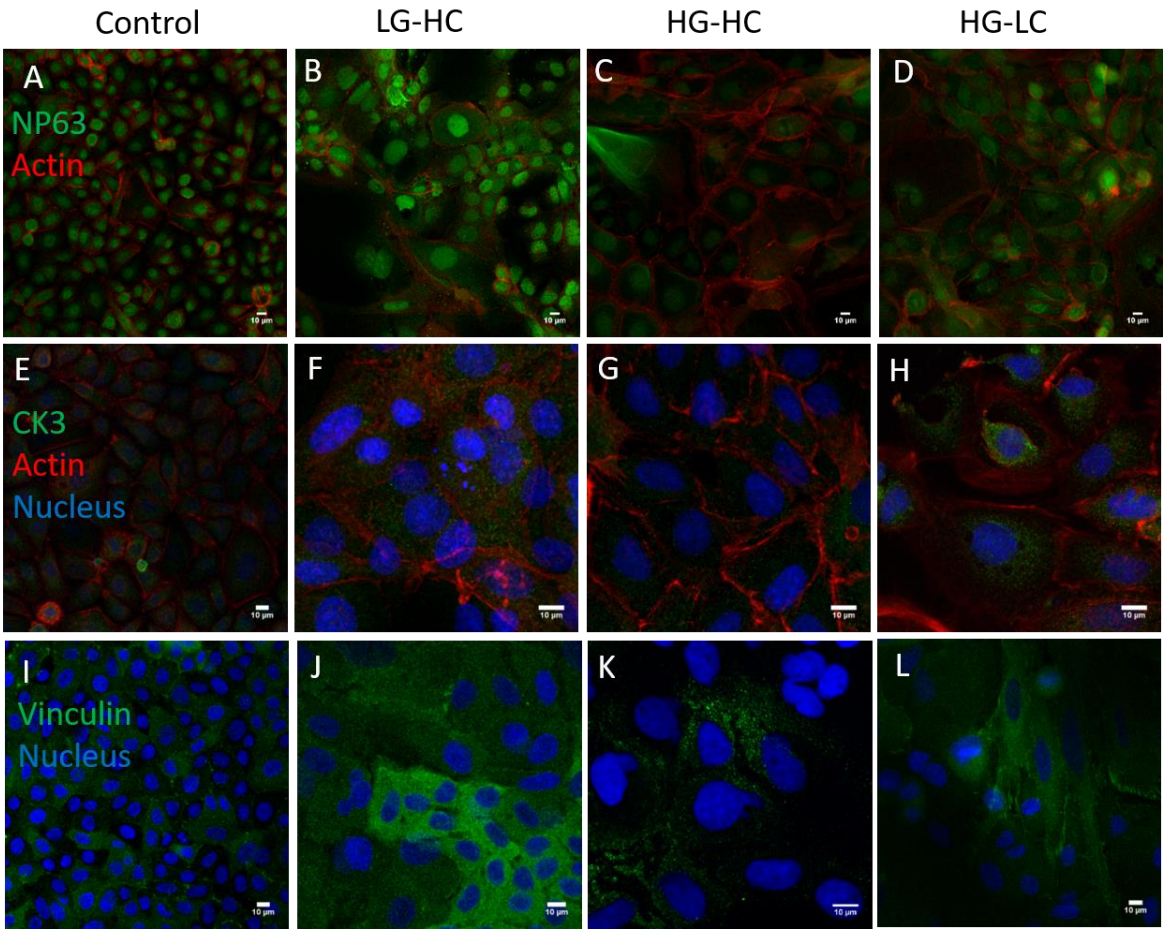

Figure 3.7 Immunocytochemistry analysis of a corneal epithelial cell line cultured in different media formulations after 7 Days. Top row (A-D) cells stained in green for NP63 (green); second row (E-H) cells stained in green for CK3 and bottom row (I-L) cell stained in green for vinculin. All cells were counterstained for f-actin (red) and DAPI (blue). First column (A,E,I) shows cells cultured in control media; second column (B,F,J) shows cells cultured in LG-HC; third column (C,G,K) shows cells cultured in HG-HC and forth column (D,H,L) shows cells cultured in HG-LC. (Scale bar = 10µm).

3.4 Discussion

In order to assess the effect of glucose and calcium concentrations on the growth of this cell line it was decided to use the recommended manufacturer's media to expand the cells and then switch to a LG-HC, HG-HC or HG-LC media. A DMEM/F12 basal media formulation was used as this is most commonly applied in primary culture media and has

not been used with this cell line in the literature. The control group was kept in the manufacturer's media. The control group served as the LG-LC media in this study, however, using the typical primary culture media with LG-LC concentrations would be useful in future work to determine how this compares to the manufacturer's media.

Glucose was selected to vary concentration in cell culture media in this study. However, other sugars in cell culture media such as galactose has not been studied on this cell line in detail. It is important to consider this for future work as there a number of other carbohydrates in nature, which these cells may use as an energy resource. Other studies have shown that galactose in cell culture media can affect protein glycosylation and increase cellular susceptibility to mitochondrial toxicants (Marroquin, Hynes et al. 2007, Hossler, Racicot et al. 2017).

Cellular growth was assessed over 7 days in each media formulation using a trypan blue exclusion assay. It was observed that the control group had a significantly higher level of cell growth compared to all groups. Between groups with varying calcium and glucose concentrations cellular growth was similar, however, the LG-HC group had a significant increase in cellular growth compared to the other test groups at day 6 and 7 suggesting that calcium increases cellular growth after 5 days.

The metabolic activity of the cells in the different media conditions was examined to provide an indicator of cell proliferation. This was achieved using a presto blue assay which is a resazurin-based metabolic assay which uses the mitochondrial activity to reduce the blue non-florescent resazurin to the florescent pink resorufin (Sonnaert, Papantoniou et al. 2015). While metabolic activity has been previously used to quantify cell proliferation opinion differs as to how well it truly represents the number of cells

present (Quent, Loessner et al. 2010, Sonnaert, Papantoniou et al. 2015). While there was no difference between the LG-HC and HG-HC groups, the HG-LC group appeared to demonstrate less metabolic activity, albeit not significantly different. These results suggest that calcium concentration plays a role in the proliferation of these cells. Calcium signalling is known to be a key regulator of proliferation for many cell types (Martinez and Santibanez 1993, Munaron, Antoniotti et al. 2004, Pinto, Kihara et al. 2015). A study by Ma and Liu (2011) found that calcium inhibits proliferation and triggers differentiation in mouse corneal epithelial cells (Ma and Liu 2011) while a study by Kruse and Tseng (1992) showed that the effect of calcium on rabbit corneal epithelial proliferation was dependent on the initial cell seeding density and culture time (Kruse and Tseng 1992). Interestingly, the highest metabolic activity was recorded for the control media that had the least calcium. While this might suggest that low calcium is better for proliferation, it should be noted that other components present in the control media differed in concentration or were absent when compared to the test media and this may also have contributed toward the cells proliferation. The cell number was also higher in the control group which may have contributed to this result.

To analyse further the effect of glucose and calcium on the proliferative capacity of the cells, ERK gene expression was examined. This protein is involved in many cellular processes including proliferation (Mebratu and Tesfaigzi 2009). The HG-HC group had a significantly lower expression of ERK compared to LG-HC and control media. In one previous study, high glucose (25mM) media impaired the EGFR signalling pathway in porcine eyes which is the same pathway that ERK acts on and this delayed epithelial wound healing most likely though ROS (Xu, Li et al. 2009). Interestingly, HG-HC also had a lower expression of ERK compared to HG-LC, which appears to indicate that the

combination of high glucose and high calcium have a particularly detrimental effect on proliferation. This finding, to our knowledge, has not been previously reported in the literature and should be considered for researchers using this cell line in corneal epithelial research.

It is worth noting also that activation of ERK occurs post transcriptionally via phosphorylation and subsequent translocation to the nucleus where it activates proliferation. Quantification of western blots found no significant differences between groups; however, HG-HC clearly displayed the least pERK. The LG-HC had a higher expression of pERK compared with the commercial media control group. This trend was similar to ERK gene expression and the cell growth curve, showing a significant increase in proliferation after 5 days in the LG-HC group. This may have been due to the observed contact inhibition of the cells grown in the commercial media in which the EGFR pathway has been implicated. Contact inhibition occurs when cells cease proliferation once confluency has been achieved, which is important for tissue homeostasis (Swat, Dolado et al. 2009). Therefore, it is not surprising that due to the confluency observed in the commercial media-fed cells that pERK is downregulated.

Extracellular calcium has been show to activate the ERK 1/2 signalling pathway via a calcium sensing receptor enhancing proliferation in porcine bone marrow MSCs (Ye, Ai et al. 2016). The cross talk between the calcium sensing receptor and the ERK signalling pathway has also been implicated in human cancer cells. Modulation of the calcium signalling receptor may serve as a therapeutic target in cancer (Fang, Liu et al. 2020). Given the implications of calcium and ERK mediated proliferation in this study, further research into the calcium sensing receptor in corneal epithelial cells may provide further insight

into the cellular signalling pathway taking place in these cells in response to calcium alterations. High glucose conditions have been shown to activate the ERK pathway, promoting proliferation which has had implications in cancer progression, by upregulating insulin receptor expression in cancer epithelial cells (Wei, Duan et al. 2017). Epithelial-mesenchymal transition can also be induced by high glucose concentration in human kidney cells. Glucose concentration in cell culture media for corneal epithelial cells have not been studied in detail in the literature. Cross talk between calcium and glucose receptors on cells may be occurring with further experimentation required to elucidate cell-signalling mechanisms on the effect of this on ERK activation and subsequent proliferative consequences.

Stem cell marker NP63 was examined by both RT-PCR and immunocytochemistry. This is a well-established marker of a corneal epithelial stem cell phenotype and is present in the limbus of the cornea where stem cells reside (O'Sullivan and Clynes 2007) The highest gene expression was in the control group, indicating that this media retains its stem cell phenotype. This was confirmed by immunocytochemistry analysis where the control group has almost exclusively nuclear localisation of the protein. In the test groups NP63 gene expression was significantly lower than the control group. The most significant decrease in NP63 gene expression and nuclear staining was the HG-HC group. This result shows that high glucose and high calcium both inhibit proliferation and cause the cells to lose their stem cell phenotype.

CK3 was used to determine if the cells were differentiating towards a mature epithelial cell phenotype. It has been shown that CK3 is present only in the suprabasal and superficial cells indicating that these cells have undergone terminal differentiation

(Merjava, Neuwirth et al. 2011). HG-HC cells did not produce any gene expression for CK3 and it was not visible after staining. This result may indicate that the cells grown in this media formulation begin to differentiate towards an alternative cell phenotype. Gene expression of CK3 was higher in LG-HC and HG-LC cultured cells compared to control cells. Immunocytochemistry analysis of these groups showed a similar result with the control group displaying little staining for CK3 while the LG-HC and HG-LC groups both displayed higher levels of the protein. When combined with the data for NP63, these results show that while the control media is more beneficial for maintaining a stem cell phenotype, the LG-HC and HG-LC media were better at promoting mature epithelial differentiation.

Vinculin is a focal adhesion protein that is associated with cell signalling, spreading and migration (Jannie, Ellerbroek et al. 2015) hence it was decided to examine its localization using immunocytochemical staining. For the corneal epithelium focal adhesion sites are important to allow the cells to migrate and repopulate regions for both homeostatic and wound healing responses (Ljubimov and Saghizadeh 2015). Previous studies have shown that vinculin becomes polarized within corneal epithelial cells to allow migration in a specific direction. (Soong 1987, Zieske, Bukusoglu et al. 1989) However, in our study the staining was more homogeneous within individual cells although the total amount of vinculin present varies from cell to cell depending on the media used. The confluency of the cells may be a factor in the distribution of vinculin in our study since this would have limited movement of the cells. The HG-HC group had the least vinculin staining of all the groups. High glucose levels have previously been associated with inhibition of focal adhesions for some cell types (Tamura, Osajima et al. 2003) while calcium can also effect vinculin localization and density (O'Keefe, Briggaman et al. 1987).

The morphology of the cells was also very different compared to the cells grown in the control media. In the control group cells exhibit the typical cobblestone morphology with consistent cell shape and number while the test groups had a far more globular appearance with a lower cell number and high nucleus to cytoplasm ratio. Cell shape was not consistent and some cells were a lot larger than others which has been observed in other papers that have investigated calcium concentrations on murine corneal epithelial cells (Ma and Liu 2011).

3.5 Conclusion

This study showed that the combination of different glucose and calcium concentrations can affect the metabolic activity, proliferative capacity, differentiation and focal adhesion of a corneal epithelial cell line. The cell line suppliers recommended media appeared to be the best at maintaining stem like characteristics while also promoting proliferation. LG-HC and HG-LC media both had reduced expression of NP63 and enhanced expression of CK3 suggesting that these media formulations may be useful for promoting differentiation towards a mature epithelial phenotype. HG-HC media should be avoided when culturing these cells. Having determined the optimal chemical environment for these cells, next we wanted to explore how the physical environment affects the cells behaviour in Chapter 4.

Chapter 4

Influence of polydimethylsiloxane substrate stiffness on corneal epithelial cells

4.1 Introduction

Damage to the corneal epithelium can occur due to a variety of conditions including limbal stem cell deficiencies or physical abrasion. Limbal derived stem cells allow the epithelium to undergo renewal following injury by migrating into the damaged region and differentiating into epithelial cells. However if the injury is too severe or if there is a lack of healthy stem cells in the limbus then additional therapeutic approaches may be required to repair the ocular surface such as cell transplantation (Atallah, Palioura et al. 2016). Allogeneic limbal tissue may be taken from a donor and applied directly to a patient to provide a new stem cell source (Ahmad, Osei-Bempong et al. 2010), however a lack of suitable donor tissue can limit this option. The alternative is to isolate and culture limbal epithelial stem cells in-vitro and then to transplant these cells on a biomaterial carrier. This approach has the advantages of allowing a higher number of cells to be transplanted and allowing autologous cells from a patient biopsy to be used. However, optimization of the culture environment, including the physical substrate onto which the cells are adhered, is required to control the cell phenotype.

When culturing cells on a substrate or fabricating biomaterials for cell transplantation it is important to consider the mechanical characteristics of the materials since these will influence how the cells behave (Discher, Janmey et al. 2005). Examples of how material stiffness effects cells include by directing the differentiation of mesenchymal and adipose stem cells (Engler, Sen et al. 2006, Xie, Zhang et al. 2018), influencing the proliferation, migration and resistance to chemotherapy of cancer cells (Tilghman, Cowan et al. 2010, Schrader, Gordon-Walker et al. 2011) and modulating inflammatory cells such as macrophages (Sridharan, Cavanagh et al. 2019). In the cornea, only a small number of

studies have examined the role that material stiffness has on the behaviour of corneal epithelial and limbal cells (Zhao, Shen et al. 2019) . Factors affecting epithelial cells that have been examined in response to changes in stiffness include cell migration and viability (Molladavoodi, Kwon et al. 2015) as well as stratification and differentiation (Gouveia, Vajda et al. 2019), generation of tractional force by cells (Onochie, Zollinger et al. 2019), nuclear Yes-associated protein (YAP) expression (Foster, Jones et al. 2014) and cytokeratin expression (Jones, Hamley et al. 2012). One limiting factor with these studies is that since they use either polyacrylamide or collagen gels as substrates, only a narrow range of stiffness values could be examined. The mechanical environment of epithelial cells can vary with the cells in contact with soft substrates such as the basement membrane (modulus ≈ 7.5 kPa) (Last, Liliensiek et al. 2009, Last, Thomasy et al. 2012), stiffer substrates such as the corneal stroma (0.17 to 1.5 MPa) (Singh, Han et al. 2018, Xie, Zhang et al. 2018, Zappone, Patil et al. 2018, Karimi, Razaghi et al. 2019) following the loss of the bowman's layer after laser photorefractive keratectomy (Lagali, Germundsson et al. 2009) or even stiffer substrates such as an amniotic membrane (≈ 2.6 MPa) (Benson-Martin, Zammaretti et al. 2006).

The aim of this study was to examine the influence of material stiffness on a limbal derived epithelial cell line using a wide range stiffness values at day 3 and 7 and cell line suppliers recommended media. The corneal epithelium is replaced after approximately 7 days, therefore, an early and late stage response to stiffness was studied to determine how cells responded at different stages in their typical lifecycle in vivo (Mort, Douvaras et al. 2012). PDMS was used to fabricate substrates with a Young's modulus ranging from 10 kPa to 1500 kPa. No protein coating was used for this study, which eliminates the influence of the coating on the cellular phenotype. Cell morphology, differentiation,

proliferation and mechanobiological responses were assessed to determine the relationship between cell behaviour and material stiffness. Cells cultured on tissue culture plastic (TCP) were used as the control group for this study.

4.2 Materials and Methods

4.2.1 *PDMS fabrication*

PDMS blends of varying stiffnesses were made using a commercially available product of Sylgard 184 and Sylgard 527 (Dow Corning). The softest blend of Sylgard 527 was prepared as per the manufacturer's instructions mixing equal quantities of parts A and B. Sylgard 184, the stiffest substrate, was also prepared as per manufacturer's instructions blending 10 parts base to 1 part curing agent. Equal amounts of Sylgard 527 and Sylgard 184 were blended to create a 1:1 ratio of the stiffest and softest PDMS blends to make the medium group. A blend of five parts 527 to one part 184 was prepared and used as the medium-soft group. All samples were centrifuged at 650 G for 5 min to reduce air bubbles before casting into 6 or 24 well plates. Samples were cured at 60 °C overnight. Dog-bone moulds were used to cast samples for tensile testing**.** The groups used in this study were a tissue culture plastic (TCP) control, stiff, medium, medium-soft and soft.

For the purposes of immunocytochemistry, PDMS groups were spin coated onto 12 mm glass coverslips to allow for confocal microscopy imaging. Each group was spin coated onto coverslips at 863 G for 15 seconds using a spin coater. The thickness of PDMS spin coated samples was determined using white light interferometry. After spin coating, a scratch was made in each sample as an indirect measure of thickness to ensure that cells were sensing the substrate and not the glass.

4.2.2 *Mechanical characterisation*

The Young's modulus of each sample was determined using a Zwick tensile tester with each blend tested at least 4 times. A 10% strain was applied using a 5 N load cell at a loading rate of 4 mm/min. Young's modulus was calculated from the slope of the linear elastic region of the stress-strain curves.

4.2.3 *Cell culture*

Cell culture was performed using the protocol previously described in Chapter 3. Cells were cultured for 3 to 7 days and analysed using RT-PCR, immunocytochemistry and western blot. Cells were fed using the cell line suppliers recommended media

4.2.4 *Cell adhesion*

Cells were imaged on a brightfield microscope, four hours after seeding onto PDMS and TCP and counted using the cell counter on ImageJ. The number of adhered cells/ cm^2 was calculated and used to determine percentage of adhered cells using the initial seeding density value of 5,000 cells/cm^2 .

4.2.5 *Contact angle*

The contact angle of each PDMS substrate and TCP was determined using a FTA125 contact angle analyser (First Ten Angstroms, Inc.). The contact angle of each material was calculated via a static sessile drop technique using water. Each material was tested for contact angle three times with the contact angle determined after approximately 10 sec of dropping water onto the surface to ensure the droplet was static. An average of the three measurements was used to determine contact angle of each PDMS substrate and TCP.

4.2.6 *Metabolic activity*

Metabolic activity was measured using the same protocol described in Chapter 3.

4.2.7 *RT-PCR*

RT-PCR was performed using the same protocol described in Chapter 3. The following primers were used: CK3 (Hs00365080_m1), CK14 (Hs00265033_m1) ΔNP63 (custom-made primer adapted from (Robertson, Ho et al. 2008), ABCG2 (Hs01053790_m1) and GAPDH (Hs02758991_g1). All samples were run in triplicate with a GAPDH housekeeping gene control. Fold change expression was calculated using the ΔΔCt method with TCP as control.

4.2.8 *Western blot*

Western blot was performed using the same protocol described in Chapter 3. To evaluate the expression of pERK, TERK, cytokeratin 3 (CK3), cytokeratin 14 (CK14) and NP63 protein in the cells western blot analysis was performed at day 7. The following antibodies were used: phospho-p44/42 MAPK (137F5) rabbit monoclonal antibody (mAb) (ERK 1/2)(Th202/204) antibody #9101 and p44/42 MAPK (L34F12) mouse mAb (ERK 1/2) antibody #9102 at 1:1000 to analyse expression of phosphorylated and total ERK protein respectively. Other antibodies included anti-cytokeratin 3 mouse mAb (ab77869 – Abcam) at 1:500 dilution, anti-cytokeratin 14 (MAC3232 – Sigma-Aldrich) at 1:1000 dilution and anti-NP63 (619002 – Biolegend) at 1:500 dilution. The loading control for all proteins was GAPDH (ab9484 - Abcam) at 1:1000 dilution. All secondary antibody dilutions were double that of the primary. Anti-rabbit IgG, horseradish peroxidase (HRP) linked antibody (Cell Signalling) was prepared at 1:1000 for NP63 and 1:2000 for ERK and GAPDH membranes respectively in TBS and 1% Tween 20. Rabbit anti-mouse IgG HRP (ab6728 – Abcam) was prepared at 1:1000 in TBS and 1% Tween 20 for CK3 detection. Membranes were washed three times for 5 minutes with TBS and 1% Tween 20 and the membranes developed using an immunodetection kit (enhanced chemiluminescence western blotting substrate –

Thermo-Fisher) and developed using GelDoc system (Bio-Rad). Densitometry was performed using ImageJ software and graphed using GraphPad Prism 7.

4.2.9 *Immunocytochemistry*

Immunocytochemistry was performed using the same protocol described in Chapter 3. The following antibodies and dilutions were used; Anti-Ki67 (ab15580 –Abcam) was made up in 1:1000 dilution, anti-ABCG2 (sc-58222 – Santa Cruz) at 1:500 dilution, anti-NP63 (619002 – Biolegend) in 1:500 dilution, mouse anti-vinculin (ab18058 – Abcam) at 1:1000 dilution, rabbit anti-vimentin (ab92547 – Abcam) at 1:1000 dilution and anti-pYAP (Ser127) antibody #4911 – Brennan and Co at 1:100 dilution.

Cells were washed three times with antibody buffer to remove excess primary antibody and then incubated with a secondary antibody at double the primary antibody dilution for 2 hours at room temperature. For ABCG2 and vinculin goat anti-mouse IgG H&L (Alexa Fluor® 488) (ab150113 - Abcam) was used. For all other proteins donkey anti-rabbit IgG H&L (Alexa Fluor® 488) (ab150073 - Abcam) was used. Cells were also stained for actin to visualize the cytoskeleton using Phalloidin-TRITC (Sigma-Aldrich) at 1:1000 in parallel to the secondary antibody incubation. All groups were also stained for cellular nuclei using fluoroshield with DAPI (Sigma-Aldrich). Cells were imaged using a confocal microscope. Day 3 cells were imaged at a higher magnification to appreciate cellular morphology and distribution of proteins tested. At day 7 a lower magnification was used to appreciate the confluent monolayer formed. Mean fluorescence intensity was determined using ImageJ software and corrected for background.

4.2.10 *Statistical analysis*

All experiments were carried out in triplicate, statistical analysis and outlier calculation was performed using GraphPad Prism software. Data are presented as the mean $\pm$

standard deviation (SD), significance was calculated either via one-way or two-way ANOVA with Post-Tukey test, significance deemed as $p \leq 0.05$ for all data sets.

4.3 Results

4.3.1 *Mechanical characterisation*

The thickness of all samples that were spin coated onto glass coverslips were between 10 and 25 μm with no significant differences between groups (Figure 4.1 A). Each PDMS group was tensile tested and the elastic modulus obtained using the slope of the linear regression on the stress strain curve. The stiff group had an average elastic modulus of 1500 kPa, the medium group 820 kPa, the medium-soft group 105 kPa and the soft group 10 kPa. The stiff group had a significantly higher elastic modulus that all other groups. The medium group had a significantly higher elastic modulus than the medium-soft and soft group (Figure 4.1 B).

Contact angle was measured for all groups before cell seeding. The control group had a significantly lower contact angle than all the PDMS groups. The stiff group had a significantly lower contact angle than the medium soft and soft group. The soft group had a significantly higher contact angle than the medium group (Figure 4.1 C). The percentage of adhered cells was calculated 4 hours after seeding. Between each PDMS group no significant differences in adhesion was observed. The control group displayed significantly less adhesion compared to the medium, medium soft and soft groups (Figure 4.1 D).

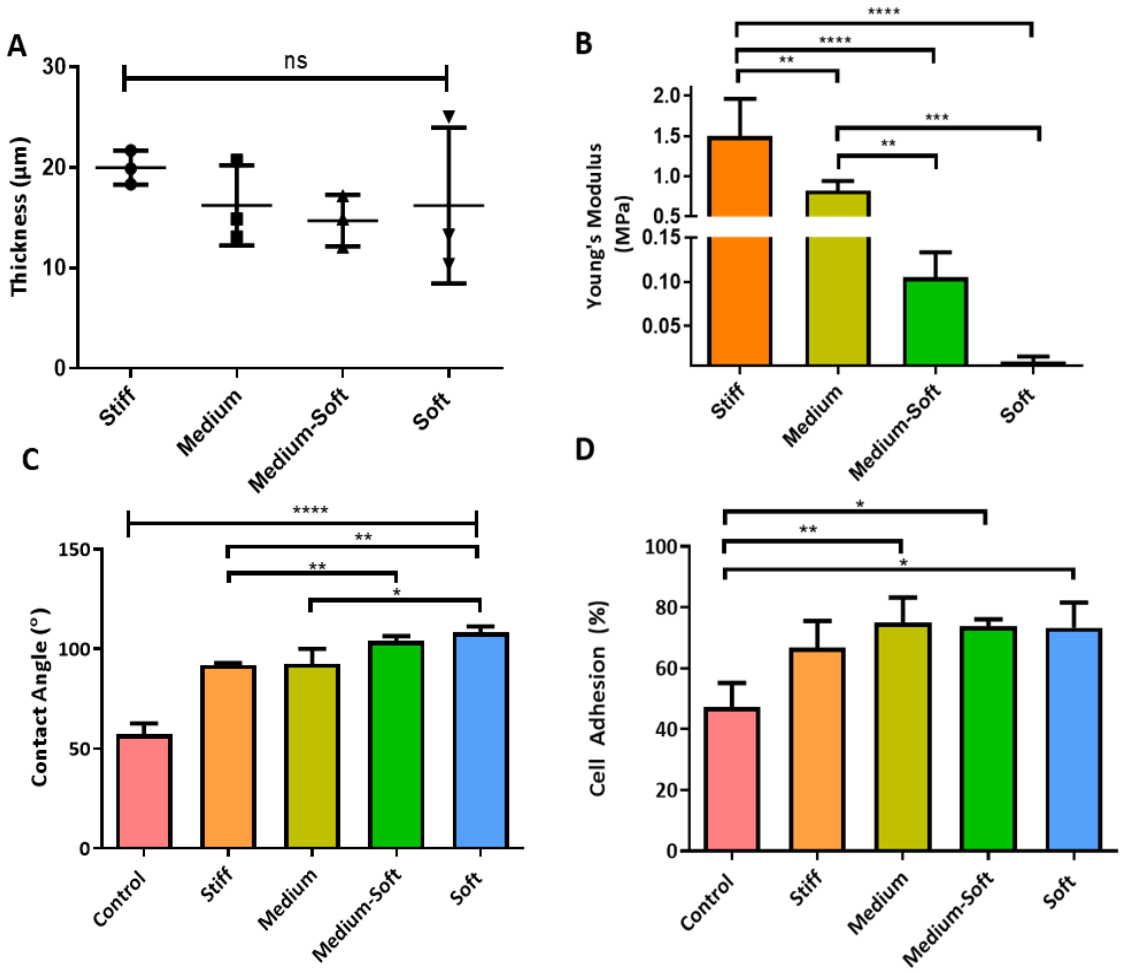

Figure 4.1 Characterization of PDMS substrates. (A) Thickness of spin coated PDMS; (B) Young's modulus of PDMS; (C) Contact angle of PDMS and TCP; (D) Percentage of cell adhered to substrates after 4 h seeding. Data are presented as the mean + standard deviation, significance calculated via one-way ANOVA with Post-Tukey test, N=4-6, * = P ≤ 0.05** = P ≤ 0.01, *** = P ≤ 0.001, **** = P ≤ 0.0001.

4.3.2 *Cell proliferation and metabolic activity*

After 7 days in culture all cells on PDMS had a significantly higher rate of cell metabolic activity compared to cells on the control cell culture plastic (Figure 4.2A). Between PDMS test groups, the stiff group had a significantly higher cell metabolic activity when compared to the soft group.

The proliferative marker ERK was analysed using western blot at day 7, the active form of this protein occurs post transcriptionally therefore a western blot was performed to examine phosphorylation of the protein and subsequent activation. Phosphorylated ERK (pERK) was normalized to total ERK (TERK) and a housekeeping protein GAPDH rather than β-actin as the expression of this protein was seen to be affected by the substrates (Figure 4.2 B). Densitometry analysis was performed to quantify differences in protein expression between the groups (Figure 4.2 C). The medium group showed the highest-level activation of pERK at day 7 and was significantly higher than the other groups. The least pERK expression was observed in the medium soft and soft groups.

Ki67, a marker of actively proliferating cells was examined by immunocytochemical staining (Figure 4.2 E). At day 3 the control and stiff groups showed similar levels of Ki67 staining indicating a similar proliferative rate (Figure 4.2 E (i) (ii)). The medium group at day 3 showed the highest quantity of Ki67 (Figure 4.2 E(iii)), significantly so compared to the soft group indicating a more proliferative phenotype at this stiffness (Figure 4.2D (i)). The medium soft displayed a significantly higher level of Ki67 compared to the soft group indicating decreased proliferation on soft substrates (Figure 4.2D (i)). At day 7 (Figure 4.2E (vi)-(x)) the control, stiff and medium groups showed similar levels of Ki67 staining. The medium soft and soft group again had less Ki67 staining indicating less proliferative activity (Figure 4.2D (ii)).

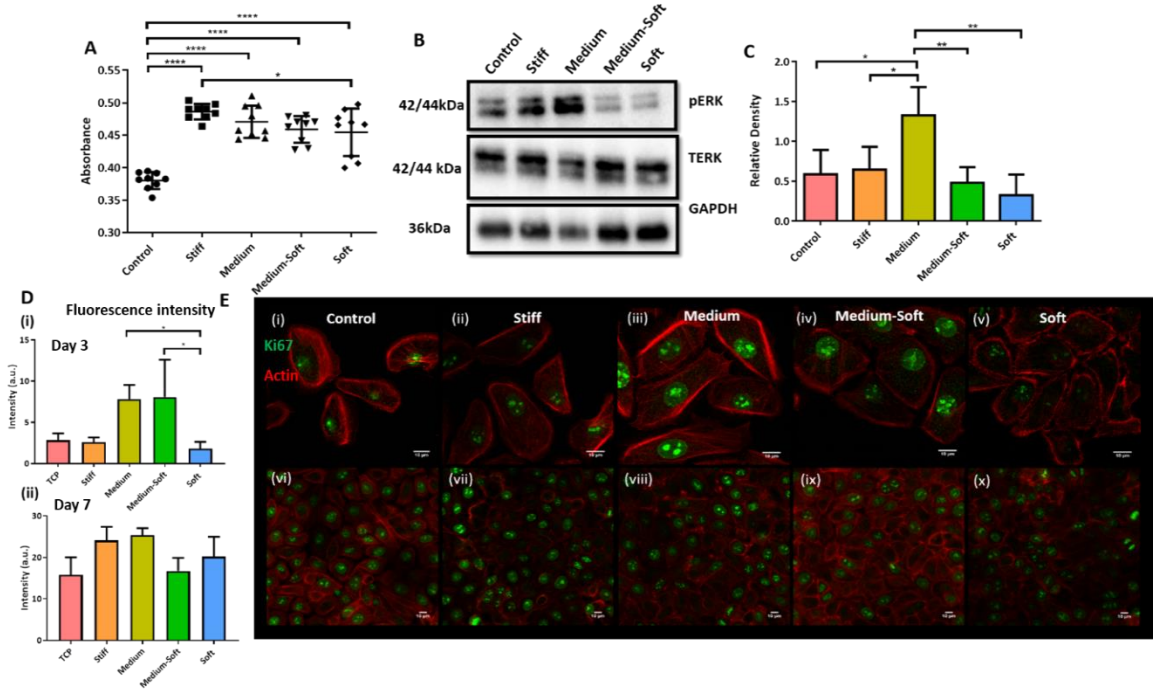

Figure 4.2 Metabolic activity and proliferation of cell in response to different substrate stiffness. (A) Metabolic activity of cells after 7 days in culture; (B) Western blot of cells grown on different substrates for pERK, TERK and GAPDH proteins at day 7; (C) Densitometry analysis of western blot data at day 7, all data normalized to TERK and GAPDH; (D) Fluorescence intensity of Ki67 staining at day 3 (i) and day 7 (ii); (E) Ki67 staining of cells grown on different substrates at day 3 (i)-(v) and day 7 (vi)-(x), (Scale bar = 10µm). Data are presented as the mean (±SD), significance calculated via one-way ANOVA with Post-Tukey test, N=3-6, * = $P \leq 0.05$, ** = $P \leq 0.01$, **** = $P \leq 0.0001$.

4.3.3 *Cell differentiation*

The mature corneal epithelial marker CK3 was examined using RT-PCR, western blot and immunocytochemistry. There was significantly higher gene expression of CK3 in the stiff group compared to the control, medium soft and soft groups (Figure 4.3) indicating that stiffer substrates promote differentiation towards a more mature corneal epithelial

phenotype. However, this was not detected on a protein level with both immunocytochemical staining and western blotting being negative for CK3.

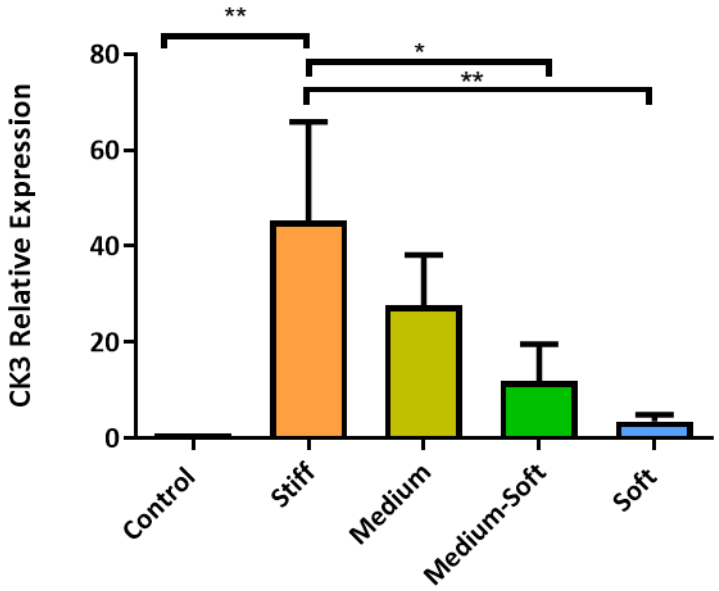

Figure 4.3 Real time PCR of CK3 to determine relative expression 7 days. CK3 gene expression at day 7, there was no detection of CK3 at day 3 in any groups. Data are presented as the mean (±SD), significance calculated via one-way ANOVA for CK3 with Post-Tukey test, N=3, * = $P \leq 0.05$, ** = $P \leq 0.01$.

Gene expression of CK14, a marker of hemidesmosome formation by basal epithelial cells, in the stiff medium soft and soft groups was significantly higher than the control group (Figure 4.4A) at day 7. The medium soft and soft groups also had significantly higher expression compared to the medium group. In western blot analysis (Figure 4.4B (i)) the medium soft group expressed this protein significantly higher compared to all other groups I. The soft group also expressed this protein higher than other groups but this was not significant. These results suggest the medium soft group produced a basal epithelial phenotype.

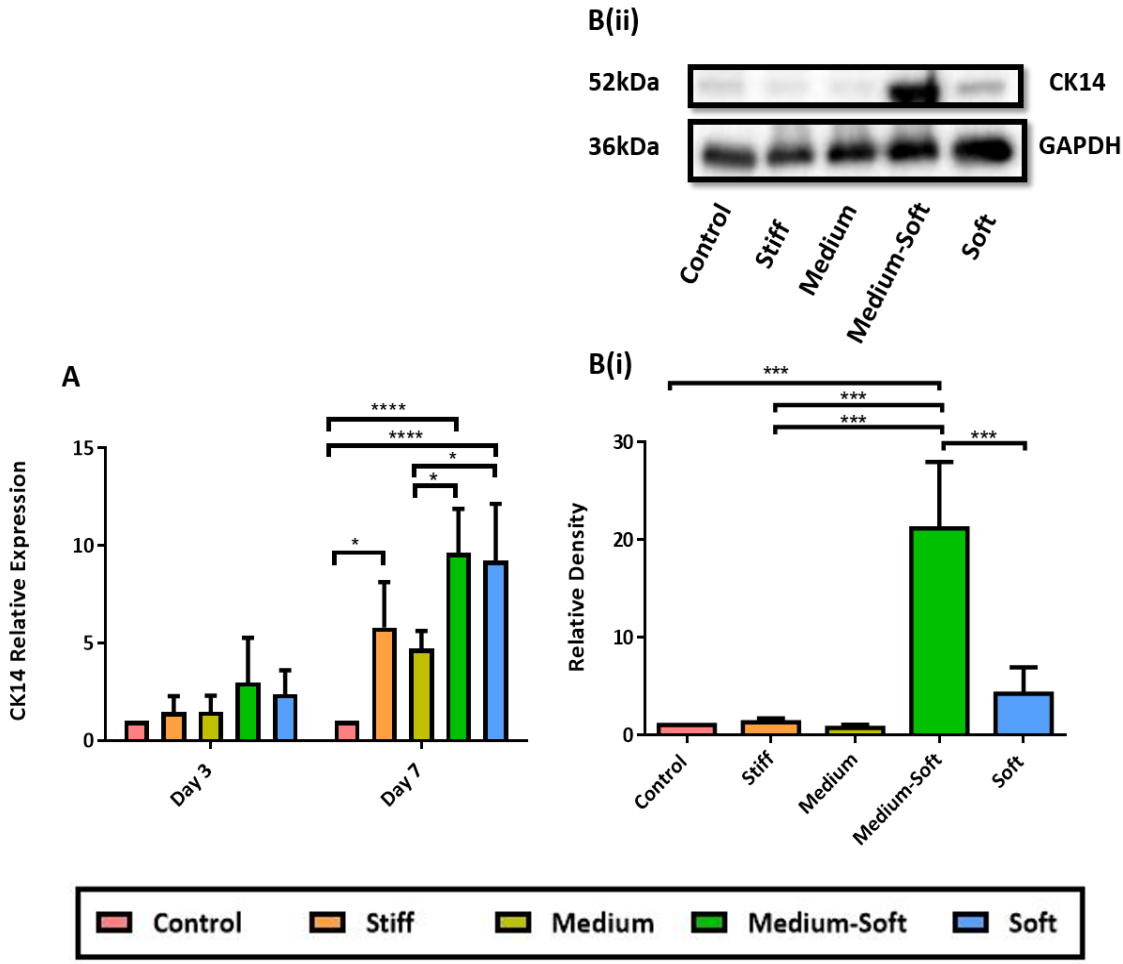

Figure 4.4 Real time PCR and western blot of CK14 at 3 and 7 days. (A) CK14 gene expression at day 3 and day 7; (B)(i) Densitometry analysis for CK14 and GAPDH; (B)(ii) Sample western blot for CK14 and GAPDH loading control. Data are presented as the mean (±SD), significance calculated via two-way ANOVA for CK14 gene expression and one-way ANOVA for densitometry analysis with Post-Tukey test, N=3, * = $P \leq 0.05$, *** = $P \leq 0.001$, **** = $P \leq 0.0001$.

The stem cell marker ATP Binding Cassette Subfamily G Member 2 (ABCG2) was examined at day 3 and 7 using RT-PCR (Figure 4.5 A). No significant changes were seen in gene expression in any of the groups. However, at day 3 over all the medium-soft and soft group produced the highest level of ABCG2 gene expression but by day 7 the stiff and soft group had the highest level of ABCG2 gene expression albeit not significant.

Immunocytochemical analysis was also carried out for this protein at day 7 (Figure 4.5 C (i) – (v)). Nuclear localization was seen in all groups with the highest expression observed in the medium group (Figure 4.5 B). However, in general all groups expressed this marker at a similar level.

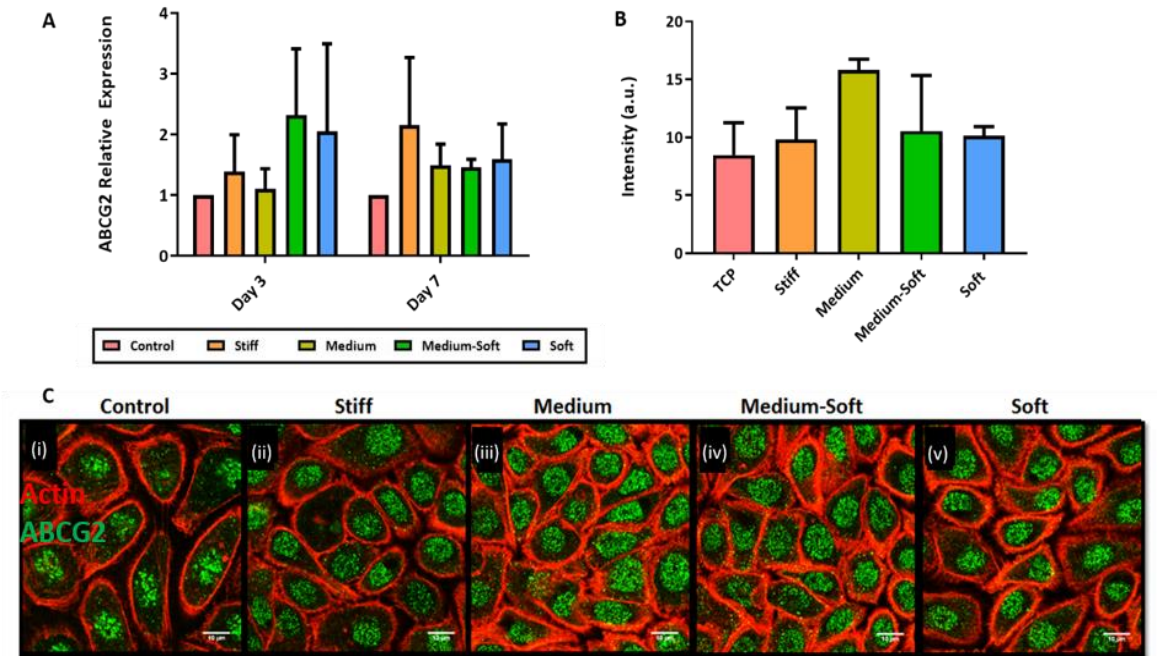

Figure 4.5 Gene expression and Immunocytochemical staining for ABCG2. (A) ABCG2 gene expression at day 3 and 7; (B) Fluorescence intensity of ABCG2 at day 7; (C) Immunocytochemical staining of ABCG2 at day 7 (green). All cells were counterstained with f-actin (red) and DAPI (blue). (Scale bar = 10µm) Data are presented as the mean (±SD), N=3.

A second marker for a stem cell phenotype NP63 was examined. At day 7 gene expression analysis for ΔNP63 showed no significant difference between groups (Figure 4.6 A). However, a similar expression pattern to ABCG2 was observed with the medium-soft and soft group producing the highest level of ΔNP63 gene expression but by day 7 the stiff and soft group had the highest level of ΔNP63 gene expression albeit not significant.

Nuclear localization of this protein is an indication of its activation in cells. Therefore, immunocytochemical analysis was performed (Figure 4.6 C (i)-(v)). The control and stiff group showed cytosolic and nuclear expression of NP63. The softer groups had little to no cytosolic expression with all cells showing a nuclear localization of the protein indicating a stem cell phenotype in softer substrates. The fluorescent intensity was highest in the TCP group indicating more staining on the cytoplasm (Figure 4.6 B) however, no significant changes were observed between groups.

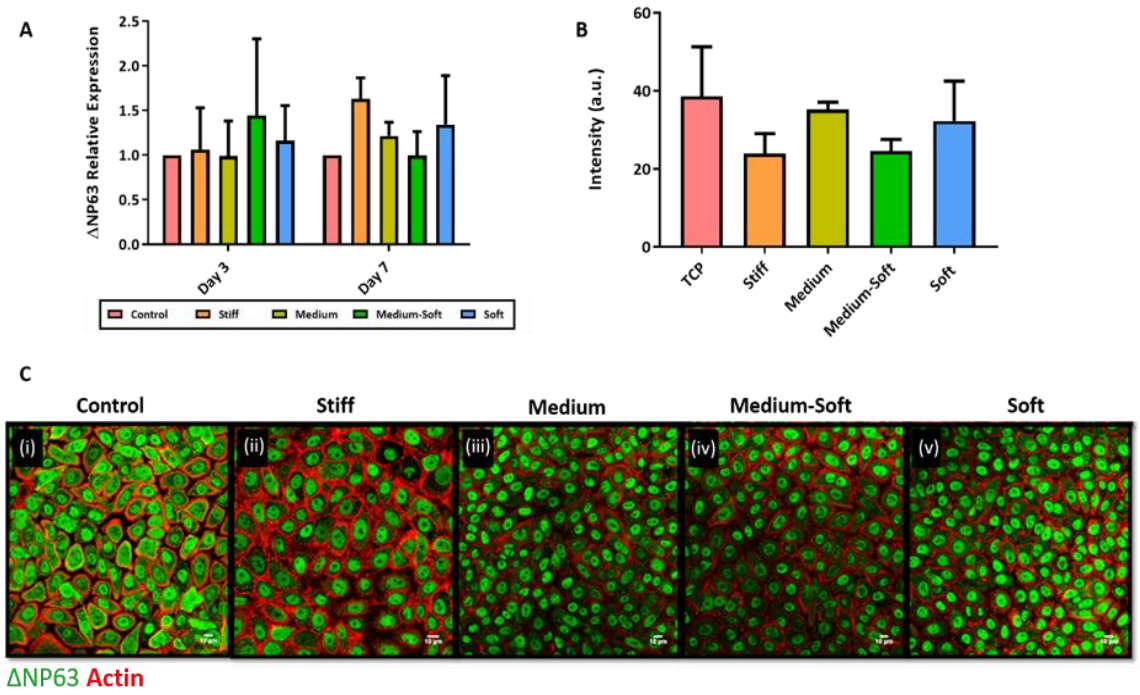

Figure 4.6 Gene expression and Immunocytochemical staining for ΔNP63. (A) ΔNP63 gene expression at day 3 and 7; (B) Fluorescence intensity of ΔNP63 at day 7; (C) Immunocytochemical staining of ΔNP63 at day 7 (green). All cells were counterstained with f-actin (red) and DAPI (blue). (Scale bar = 10μm) Data are presented as the mean (±SD), N=3.

Due to the presence of isoforms associated with different phenotypes in the corneal epithelium a western blot was performed. Figure 4.7 A shows the three isoforms of NP63α,β,γ with the housekeeping protein GAPDH used as a loading control. Densitometry analysis showed that no significant differences were observed between

groups. However, alpha and beta isoforms were expressed at a higher level in the stiff and medium groups (Figure 4.7 B).

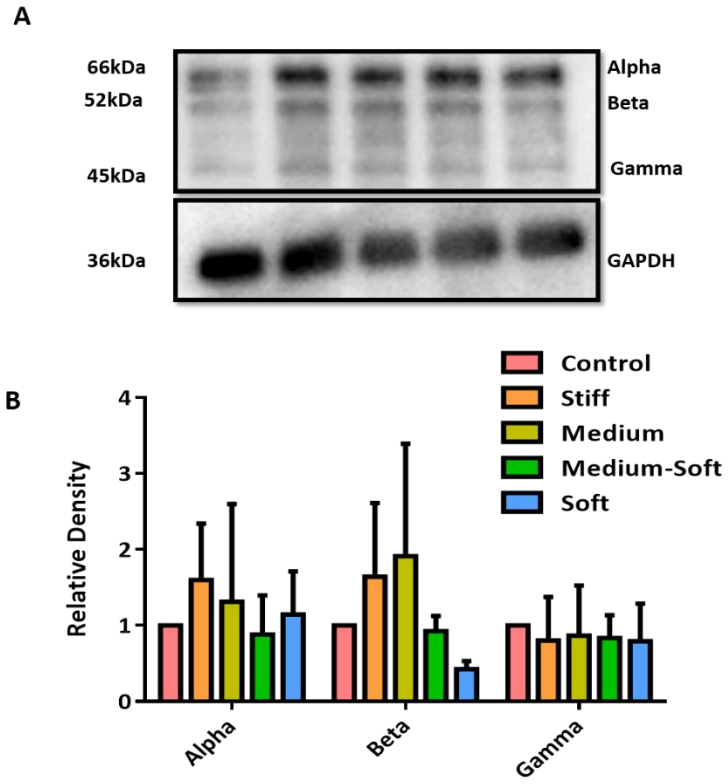

Figure 4.7 Western blot analysis of NP63 isoforms. (A) Sample western blot for NP63 isoforms alpha, beta, gamma and GAPDH; (B) Densitometry analysis of each NP63 isoforms. Data are presented as the mean (±SD), N=3.

4.3.4 *Mechanobiology*

Mechanobiological responses of cells to stiffness were assessed at day 3 and 7 (Figure 4.8). At day 3, cells grown on tissue culture plastic (control group) displayed a smaller, more circular cell shape with little actin and fewer cellular projections compared to the cells grown on the different PDMS formulations. By day 7, these cells displayed projections and a polygonal shape but had more extracellular space compared to the other groups.

The stiff group displayed more of a spread cellular shape at day 3 (Figure 4.8 B) with visible filopodia extending from the cells edge and increased actin production compared to control. By day 7 (Figure 4.8 G) cells had little extracellular space with compacted cell morphology.

The medium group at day 3 (Figure 4.8 C) displayed stress fibers extending throughout the cell as well as longer cellular projections between each cell. A more spread cellular phenotype was also evident in this group with circular actin formations. Lamellipodia were evident in this group extending from the cells edge toward neighbouring cells. At day 7 (Figure 4.8 H) there were larger nuclei compared to the stiff and control group but less stress fiber formation across the cell compared to the cells at day 3.

The medium soft group had a similar cell shape as the medium group with more pronounced stress fibers at day 3 (Figure 4.8 D). The cells also appear to be longer and more spread in comparison to all other groups. Cellular projections were not as evident in this group but rather cellular sheets extending from the cells were visible. By day 7 the medium soft group (Figure 4.8 I) had more stress fiber formation compared to all other groups and increased nuclear size, similar to cells grown on medium stiffness. Decreased formation of circular structures in the actin cytoskeleton also occurred at day 7 in this group.

The soft group had less striking actin filaments with more of a triangular cell shape evident at day 3 (Figure 4.8 E). These cells displayed a sheet like projection from the cells along with these projections which were seen in other groups, in particular the medium group, however this was a lot more apparent in the soft group. The soft group at day 7 (Figure 4.8 J) had very little stress fiber formation and little to no circular actin formations.

The cells appeared to have a much more defined cell membrane connection between each other and larger nuclei similar to that seen on the medium group at day 7.

All test groups showed a similar morphology at day 7 with more compacted cell phenotypes and less extracellular space compared to control group cells. Stiff, medium and medium-soft groups contained more actin between cells compared to the soft group and displayed circular structures in their actin cytoskeleton. The medium-soft group had the most stress fiber formation at day 7 compared to all other groups. The soft group had the least actin compared to all other groups as well as the least extracellular space.

Focal adhesions were examined by staining for vinculin (Figure 4.8). At day 3, vinculin was high in the control group (Figure 4.8 (i)) and more visible at the cell's edge (Figure 4.8 A). In the cells grown on PDMS vinculin was more diffuse in the cytoplasm with the medium stiffness group showing the least focal adhesions (Figure 4.8 A-E) however this was not significant (Figure 4.8 (i)). At day 7, the number of focal adhesions per cell decreased in the control group and was significantly higher in the medium, medium soft and soft group compared to the control (Figure 4.8 (ii)) with some cells displaying more focal adhesions at the cells edge. The stiff group had significantly less vinculin compared to the other PDMS groups at day 7.

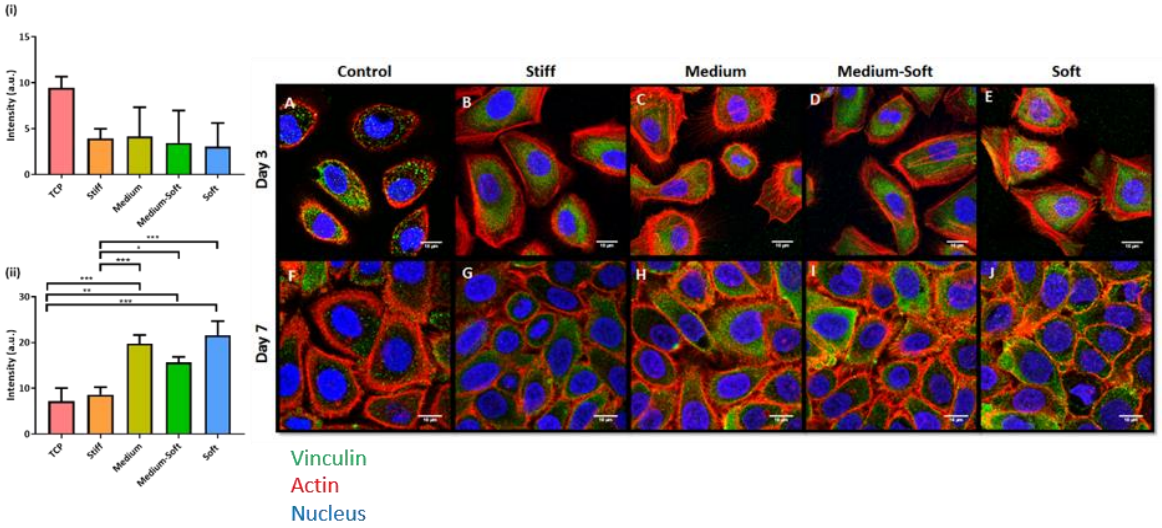

Figure 4.8 Immunocytochemical staining for vinculin. (i) Fluorescence intensity of vinculin at day 3 and (ii) day 7. Top row (A-E) shows cells stained in green for vinculin at day 3. Bottom row (F-J) shows cells at day 7. All cells were counterstained with f-actin (red) and DAPI (blue). (Scale bar = 10µm). Data are presented as the mean (±SD), significance calculated via one-way ANOVA with Post-Tukey test, N=3, * = $P \leq 0.05$, ** = $P \leq 0.01$, *** = $P \leq 0.001$.

Vimentin, an intermediate filament (IF) protein was examined at day 3 and 7 (Figure 4.9). The control and stiff group had the most vimentin with IF's extending over the cellular nuclei in the medium group at day 3. No significant changes in vimentin expression was observed at either time points (Figure 4.9 (i), (ii)). The soft group had the lowest number vimentin positive cells and the lowest production of the protein within the cell. At day 7, the control group cells displayed the highest level of IF expression as well as the highest number of vimentin positive cells.

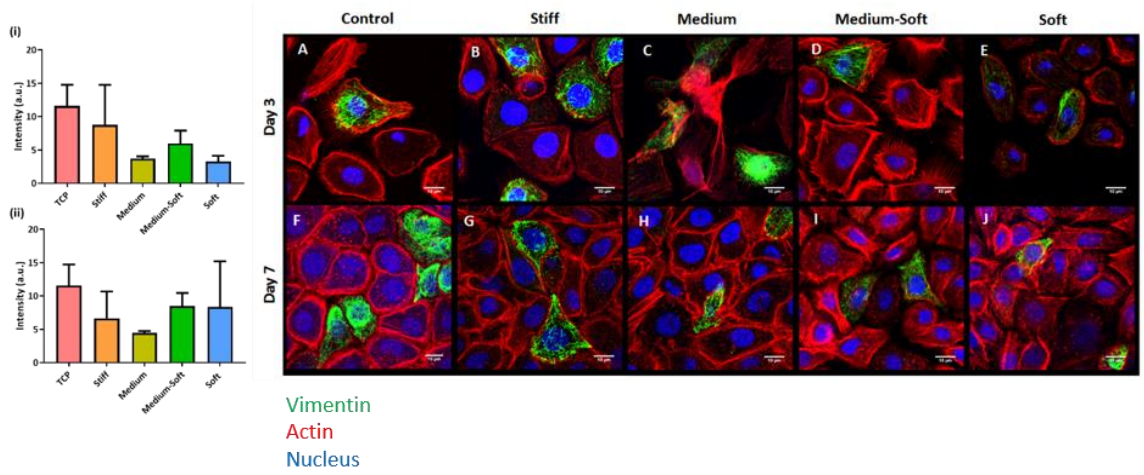

Figure 4.9 Immunocytochemical staining for vimentin. (i) Fluorescence intensity of vimentin at day 3 and (ii) day 7. Top row (A-E) shows cells stained in green for vimentin at day 3. Bottom row (F-J) shows cells at day 7. All cells were counterstained with f-actin (red) and DAPI (blue). (Scale bar = 10μm).

At day 3 and 7 the activated phosphorylated form of yes-associated protein (pYAP) was studied (Figure 4.10). At day 7 the stiff group showed the lowest amount of total pYAP expression with a significant decrease in expression compared to the medium soft group. By day 7, the soft group had a significantly higher amount of total pYAP production compared to control stiff and medium groups (Figure 4.10 (ii)) Control and stiff groups had the lowest pYAP production at day 7. Nuclear localisation of the protein was also quantified (Figure 4. 11).

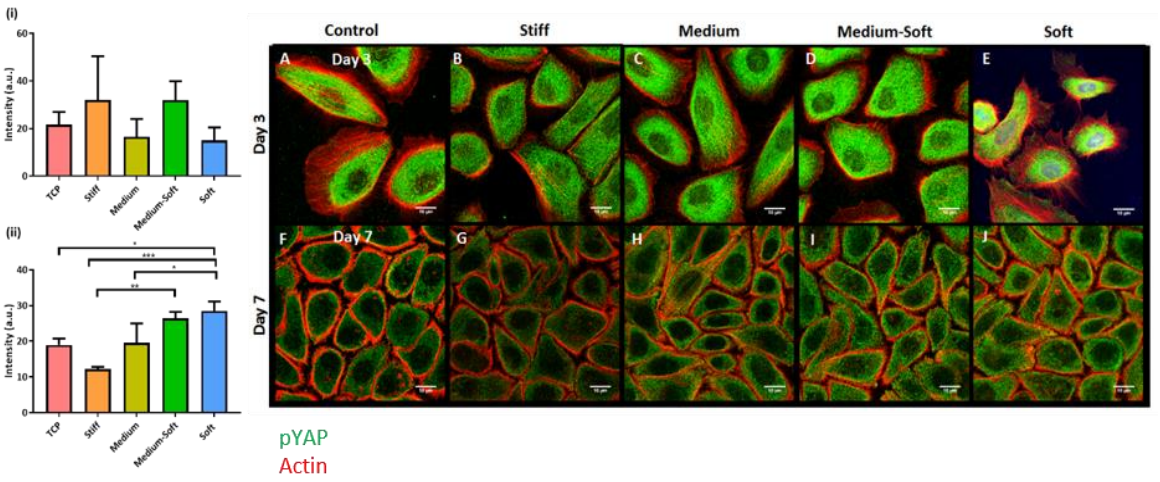

Figure 4.10 Immunocytochemical staining for phosphorylated yap (pYAP) protein. (i) Fluorescence intensity of total pYAP at day 3 and (ii) day 7. Top row (A-E) shows cells stained in green for pYAP at day 3. Bottom row (F-J) shows cells at day 7. All cells were counterstained with f-actin (red). (Scale bar = 10µm). Data are presented as the mean (±SD), significance calculated via one-way ANOVA with Post-Tukey test, N=3, * = $P \leq 0.05$, ** = $P \leq 0.01$, *** = $P \leq 0.001$.

At day 3 and 7 the nuclear localisation of activated phosphorylated form of yes-associated protein (pYAP) was studied (Figure 4. 11). There were no significant differences in nuclear pYAP expression at day 3, however, the soft group had the highest nuclear pYAP expression overall compared to all groups (Figure 4. 11 A). At day 7, the medium soft and soft groups displayed a significant increase in nuclear pYAP expression compared to all groups.

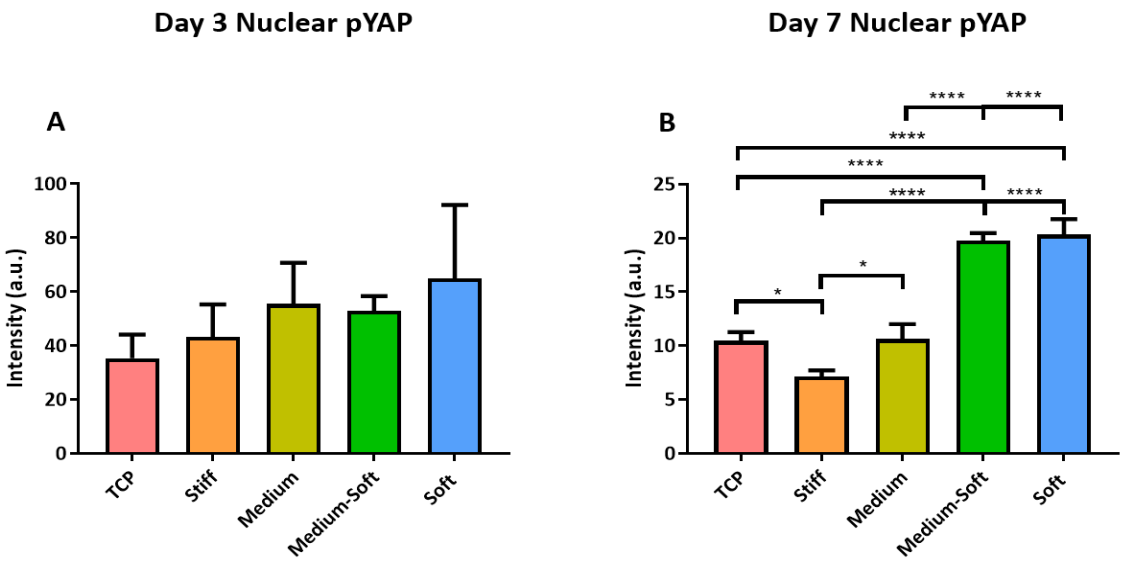

Figure 4. 11 Fluorescence quantification of nuclear pYAP localisation. (A) Fluorescence intensity of nuclear pYAP at day 3 and (B) day 7. Data are presented as the mean (±SD), significance calculated via one-way ANOVA with Post-Tukey test, N=3, * = P ≤ 0.05, **** = P ≤ 0.0001.

4.4 Discussion

In this study, PDMS was used to evaluate the effect of substrate stiffness on the behaviour of corneal epithelial cells. In most previous PDMS stiffness studies, Sylgard 184 with differing ratios of base to curing agents was used to generate substrates with a narrow variation in stiffness. To achieve a wider range of stiffness values for this study, two PDMS solutions (Sylgard 184 and 527) were mixed at different ratios. This technique was originally developed by Palchesko et al., (2012) and has previously been used to examine the effect of substrate stiffness several different cell types (Palchesko, Zhang et al. 2012, Palchesko, Lathrop et al. 2015) but not corneal epithelial cells. In this study, white light interferometry was used to determine thickness of spin coated substrates, which was consistent across all substrates and did not exceed 10 µm. Previous studies have shown that single cells can only sense underlying materials through soft hydrogel materials at thicknesses below 10 µm, which is measured by the degree of cell spreading (Tusan, Man

et al. 2018). Other studies have shown that cells can be influenced by underlying structures hundreds of microns away (up to 130µm). However, this is influenced by the structure of the substrate in question with fibrous substrates that are similar to the fibrous nature of biological substrates allowing cells to propagate forces through the individual fibers over longer distances (Mullen, Vaughan et al. 2015). In this presented study, cells were spread at all stiffnesses and more rounded on the TCP group at day 3, indicating that cells were sensing the PDMS substrate rather than the glass. This coupled with the significant differences in gene and protein expression as well as the homogenous non-fibrous nature of PDMS indicated that the cells were reacting to the stiffness of the PDMS and not the underlying coverslip. Therefore, this study ensured that all spin-coated substrates exceeded this value.

To further characterise the PDMS substrates, water contact angle was used to measure hydrophobicity and how this influences adhesion of the cells. There was a significant difference between the hydrophobicity of TCP and PDMS. This result correlates with fewer cells adhering on the TCP compared to PDMS after 4 hours despite TCP being less hydrophobic. While this suggests that hydrophobic surfaces may be better at supporting corneal epithelial cell adhesion, some studies have postulated that water contact angle may not be an accurate predictor of biological responses to materials (Alexander and Williams 2017). Values for the optimal contact angles for cell adhesion vary considerably between publications most likely due to the use of different cell types and materials (Wei, Yoshinari et al. 2007, Dowling, Miller et al. 2011, Tang, Akiyama et al. 2012, Meng, Yang et al. 2017).

Most studies which examine cellular response to stiffness coat surfaces with biological substances such collagen or laminin (Engler, Sen et al. 2006, Gouveia, Lepert et al. 2019),

however, this study has shown that a more hydrophobic surface can still support corneal epithelial cell adhesion and that a coating may not be required to study cellular responses. Previous studies have shown that collagen coating can penetrate deeper on softer substrates compared to stiffer ones (Lo, Wang et al. 2000) which may affect cellular responses. This cell line is used for culturing on TCP which is why this was chosen as the control group.

Stiffness was shown to influence the proliferation and cell metabolic activity of the cells. Only small variations in metabolic activity were detectable probably due to the lack of sensitivity of the assay due to the colour changing quickly with time as well as its use as a measure of cell viability rather than cellular metabolism (Xu, McCanna et al. 2015). A clearer trend was detectable when proliferative markers such as Ki67 and pERK were examined. Expression of pERK was measured using western blot analysis at day 7 only as higher protein yields were obtained at this point which made it possible for the protein bands to be visualised compared to day 3. The stiff and medium groups had the highest level of Ki67 while the medium group had significantly higher pERK production compared to the other groups. The increase in proliferative markers in the stiffer groups suggests that cells on the softer substrates are slower cycling. In the eye it is necessary for epithelial cells to undergo proliferation to maintain homeostasis, however a subpopulation of cells have been found to undergo a slower cycle that can accelerate if necessary to support homeostasis or response to damage (Sartaj, Zhang et al. 2017). Ki67 protein accumulation occurs in the S, G2 and M phase of the cell cycle and degraded in G1 and G0 (quiescence) of the cell cycle (Miller, Min et al. 2018). It is evident from Ki67 staining that although not actively proliferating or dividing the number of cells present is similar among groups,

which indicates cells in a quiescent state retaining their slow cycling yet proliferative abilities in repairing the ocular surface.

Material stiffness was shown to affect cell phenotype. In vivo, cells from the limbus proliferate and migrate along the basal region of the corneal epithelium cells where they undergo transient amplifying behaviour (Yoon, Ismail et al. 2014). These cells then divide, producing mature, differentiated epithelial cells in the superficial region of the epithelium. To distinguish between different phenotypes, CK3 was used as a marker of a mature, differentiated phenotype and CK14 was used to identify transient amplifying cells like those found in the basal epithelium but are absent from the central cornea (Jones, Hamley et al. 2012). During wound healing CK14 positive cells have been identified in the basal epithelium of mice (Park, Richardson et al. 2019). Gene expression analysis at day 7 showed there was significantly more CK3 in cells on stiffer substrates than softer while expression of CK14 was higher on the softer substrates compared to the stiff. This indicates that stiffer substrates produce a more mature corneal epithelial phenotype while the softer substrates support a more stem like phenotype. The medium-soft group in particular had a significant increase in CK14 protein expression as shown in the western blot, this suggests that this stiffness is suitable for upregulating this transient amplifying phenotype in these cells. Previous research looking at substrate stiffness using collagen hydrogels yielded similar results with stiffer substrates displaying increased CK3 expression in bovine limbal stem cells while softer substrates increased the expression of CK14. It is worth noting that the stiff group in that study was only 2.9 kPa compared to 1500 kPa in this presented study (Jones, Hamley et al. 2012). However, a recent study showed that using compressed collagen gels in vitro a more mature phenotype expressing CK3 was observed in the stiffer group of 4.8 ± 3.5 MPa and a stem cell phenotype

expressing CK15 in the softer group of 0.7 ± 0.4 MPa. This study used a laminin coating that may have influenced cellular response to stiffness (Gouveia, Lepert et al. 2019).

Expression of markers associated with a limbal stem cell phenotype, ABCG2 and NP63, were also examined with no significant changes observed. Western blot analysis of NP63 isoforms associated with different phenotypes in the corneal epithelium also had no significant difference. However, using immunocytochemistry it was clear that in softer substrates nuclear localisation of NP63 was higher than in stiff substrates. It has been shown that nuclear localisation of NP63 is lost in differentiated superficial cells of the cornea (Robertson, Ho et al. 2008), further supporting the hypothesis that softer substrates induce more of a limbal stem cell phenotype. It may be possible that differentiated corneal epithelial cells can still express genes for stem cell markers and allow the ocular surface to repopulate the stem cell niche if required. A recent study showed in a mouse model that differentiated committed cells in the central cornea have the ability to migrate back toward the limbus when this stem cell niche is removed and repopulate this niche (Nasser, Amitai-Lange et al. 2018). Additionally, other papers have proposed a corneal epithelial stem cell hypothesis where stem cells are distributed in the basal layer which have stem cell functionality in regenerating the ocular surface and these cells don't necessarily originate from the limbus (West, Dorà et al. 2015). Furthermore, a recent study showed using an in vivo model of wounded corneas that by softening these damaged corneas using collagenase that a limbal epithelial stem cell like phenotype can be promoted improving wound healing (Gouveia, Lepert et al. 2019).

Immunocytochemistry was used to visualise localisation of pYAP in the cells. YAP is involved in the Hippo signalling pathway and in the cytoskeletal responses to substrate rigidity and topography along with its co activator PDZ binding motif (TAZ) and has

previously been investigated in the corneal epithelium (Raghunathan, Dreier et al. 2014). YAP mediated gene expression can lead to stem cell proliferation, apoptosis evasion and cell proliferation, however, YAP regulation by mechanical stress is not completely understood (Zhu, Li et al. 2015). Regulation of YAP occurs through phosphorylation whereby unphosphorylated YAP is sequestered in the nucleus and acts as a transcriptional co activator, phosphorylated YAP by a Lats kinase inhibits its functionality and sequesters YAP in the cytoplasm where it is targeted for subsequent degradation (Hong and Guan 2012). All groups displayed cytoplasmic distribution of pYAP with little nuclear staining. This was more pronounced at day 7 whereby all groups displayed a lower level of pYAP expression compared to day 3. This indicates that degradation of pYAP occurs over seven days and perhaps earlier time points would be more beneficial to see when it is sequestered into the nucleus to act as a transcriptional co activator. Immunocytochemical staining at day 7 also showed a significant increase in pYAP in the softer groups compared to the control and stiff group. This may indicate that softer substrates retain stem cell characteristics over a longer time compared to stiffer substrates. Ectopic expression of YAP has been shown to maintain stem cell phenotypes even under differentiation conditions (Lian, Kim et al. 2010). Nuclear quantification of pYAP showed that softer substrates at day 7 had a significant increase in pYAP protein expression. This combined with lower levels of total pYAP and day 7 indicates that softer substrates sequesters YAP in the nucleus over 7 days, promoting stem cell proliferation as previously reported in the literature. This result further supports the theory that culturing corneal epithelial cells on softer substrates leads to increased stem cell expression.

Focal adhesions between cells and their surrounding matrix play an important role in dictating cell migration, cytoskeletal structure and cell signalling. In this study, vinculin

was used to study localisation of focal adhesions. At day 3, the control group showed the highest vinculin intensity while all other groups had similar levels. Staining was localized to the cytoplasm rather than along the cells edge as would be expected for this protein. By day 7 this trend seemed to differ with the medium, medium soft and soft groups producing significantly higher levels of vinculin compared to the control and stiff group. This finding suggests that at earlier time points, cells on softer substrates, which have also shown a stem cell phenotype, have a lower migratory capacity. However, by day 7 the production of focal adhesions are higher in these groups, suggesting that these cells migrate at a later stage, presumably to repopulate cells that have been terminally differentiated and shed from the ocular surface. As this study was performed in a monolayer, a stratified model would be required to confirm this finding.

Vimentin was examined as it has been described as a highly motile early differentiating corneal epithelial cell marker associated with other early differentiating markers including ΔNP63α and α6 integrin in one study (Castro-Munozledo, Meza-Aguilar et al. 2017) and previous studies have shown it to be involved in wound healing of the corneal epithelium (Walker, Bleaken et al. 2018). At day 3, more cells in the stiffer groups appeared to display this protein compared to the softer group, possibly indicating that cells on stiffer substrates have initiated differentiation towards a more mature epithelial phenotype. This would then correlate with gene expression analysis of CK3 at day 7.

Study results have implications for the design and application of biomaterials for culturing or transplanting limbal derived epithelial stem cells. For example, amniotic membrane have been widely used for transplantation and ex vivo expansion of limbal stem cells however, variations in the membranes stiffness can result from donor variations and whether the pregnancy reached term (Benson-Martin, Zammaretti et al.

2006) could affect how the cells in contact with this material behave. One study that has investigated the effect of amniotic membrane stiffness on limbal cell behaviour concluded that stiffer substrates drive a more mature differentiated corneal epithelial phenotype which would appear to agree with our findings (Chen, Jones et al. 2012). Validation of these results using a primary cell source would be beneficial, however, the use of a coating for these studies also limits their findings and the cell line used in this study has been validated as a model for corneal epithelial studies when compared to primary cells (Robertson, Ho et al. 2008).

The stiffness ranges used in this study is also useful for recapitulating reported stiffnesses in vivo. The values of these stiffnesses can vary in vivo from the basement membrane (modulus ≈ 7.5 kPa) (Last, Liliensiek et al. 2009, Last, Thomasy et al. 2012) to the stiffer corneal stroma (0.17 to 1.5 MPa) (Singh, Han et al. 2018, Xie, Zhang et al. 2018, Zappone, Patil et al. 2018, Karimi, Razaghi et al. 2019). Epithelial cells can become exposed to the stroma following the loss of the bowman's layer after laser photorefractive keratectomy (Lagali, Germundsson et al. 2009). Limbal stem cells have even been cultured on the stiffer amniotic membrane (≈ 2.6 MPa) as a method to generate transplantable sheets for corneal surface repair (Benson-Martin, Zammaretti et al. 2006). Due to the wide range of reported stiffnesses of the cornea in vivo it is difficult to conclude whether the optimal stiffness for culturing these cells in this study is similar to what is reported in vivo. However, it can be concluded that the limbus does experience a softer environment compared to the stiffer central cornea (Gouveia, Lepert et al. 2019).

Overall, this study shows that over a wide range of stiffnesses reported in the literature, differentiation, proliferation, focal adhesion and intermediate filament expression is significantly affected. Future studies looking at cell surface receptors on how

these mechanical signals are relayed as well as earlier time points to determine p-YAP response would further aid in our understanding of the corneal epithelial response to stiffness.

4.5 Conclusion

This study demonstrates that stiffness plays a major role on the differentiation, proliferation and morphology of limbal derived epithelial cells using a corneal epithelial cell line as a model. Culturing cells on a material with a Young's modulus in the range of 10 kPa-105 kPa would appear to be the most suitable for retaining the cell's stem like characteristics. Limitations with this study include that is used a cell-line rather than primary cells, there was no air-liquid interface when culturing the cells and the topography of the PDMS substrates will differ from the corneas basement membrane. Despite this, these findings could be applied when optimizing the design of biomaterials for limbal epithelial cell culture and transplantation.

Chapter 5

Donor Dependent Response of Limbal Derived Stem Cells to Fluid Shear Stress

5.1 Introduction

The corneal epithelium is subjected to oscillatory shear stress from tear fluid and the eyelid combined. This process aids in homeostasis, wound healing, lubrication and nutrition. In the corneal periphery, a pool of stem cells which replenish this epithelial layer are located in the limbus. When this function is lost due to injury or chemical insults, blindness may result. Cellular programming into corneal epithelial differentiation is highly complex with a recent study showing 4897 genes differentially expressed among these stages (Ortiz-Melo, Garcia-Murillo et al. 2021). In order to restore this limbal stem cell niche, donor cells or autologous cells from the other unaffected eye may be transplanted. To do this, limbal epithelial stem cells (LESCs) can be grown ex vivo as sheets or use a carrier material for transplantation. However, rejection of these transplants, use of animal products such as FBS which may pose immunological risks, low basal stem cell population and poor culturing systems or non-approved biomaterials pose a problem for restoring the limbal stem cell niche (Chew 2011, Mason, Stewart et al. 2016, Hernáez-Moya, González et al. 2020).

Little is known about the magnitude of shear stress in vivo in the eye or how these mechanical cues affect the cornea. Previous studies have mimicked the in vivo environment to recapitulate eye blinking using custom-designed bioreactors for the purposes of studying drug toxicity as well as determining how the corneal epithelium responds to fluid shear mechanistically (Abdalkader and Kamei 2020). Research has also examined how this affects differentiation and barrier function of the corneal epithelium (Hampel, Garreis et al. 2018). The shear stress rates of studies performed vary widely from 0.07 dyn/cm^2 to 50 dyn/cm^2 (Kang, Shin et al. 2014, Hampel, Garreis et al. 2018) as well

as the length of time that the cells are exposed to shear with some studies exposing cells to shear for a couple of hours or seconds at particular days in culture. Studies thus far have shown that oscillatory shear stress increases differentiation and apoptosis of corneal epithelial cells and effect their migratory capacity and wound healing (Utsunomiya, Ishibazawa et al. 2016, Molladavoodi, Robichaud et al. 2017).

The aim of this study was to examine how laminar fluid shear on human limbal epithelial stem cells (LESCs) effects differentiation, orientation, tight junction formation and stratification using a commercial pump system. Cells undergoing flow were subjected to high shear (2.43 dyn/cm^2) or low shear stress (1.1 dyn/cm^2) for either 1 or 3 days. Static cultures were used as controls. The time points of 1 and 3 days were chosen to reflect what has been explored in the literature to add to this knowledge as well as allowing the cells to experience a longer cell culture under shear stress which has not been widely explored in the literature. This allows for differences in stem cell expression to be examined to determine what is the optimum time point for cell culture under shear stress and to see how cells respond to shear stress after this length of time cultured under shear.

Overall, the goal of this study was to determine how laminar flow effects human limbal epithelial stem cells and whether this effect is exacerbated over time. This study will try to identify the optimal flow conditions for culturing human LESCs that increase stem cell characteristics by examining gene expression of both mature and stem cell markers. Barrier function of the cells was studied using immunocytochemistry analysis of tight junction protein ZO-1 to determine how shear stress effects this vital function of the corneal epithelium. Vimentin and integrin beta 1 expression was also examined which are key proteins involved in the migration of the cells during wound healing and how they

relay these mechanical cues (Carter 2009, Castro-Munozledo, Meza-Aguilar et al. 2017). Finally, gene expression of TRPV4 – a mechanosensitive ion channel was also studied to determine if this was implicated in the shear stress response.

5.2 Materials and Methods

5.2.1 *Cell culture*

Human corneal rims were obtained from the Royal Victoria Eye and Ear bank in Dublin after use in transplantation. The source of the rims were from the Lions Eye bank and donated for research. Explant culture was performed to isolate human limbal epithelial stem cells (LESCs). Three donors of varying ages (25, 45 and 66 years old referred to as donor 1, 2 and 3 respectively) were used for fluid flow experiments as shown in Table 3.

Table 3 Donor age and number

Donor	1	2	3
Age (Years)	25	45	66

Corneal epithelial media was used to culture explants containing low glucose Dulbecco's Modified Eagle's Medium (DMEM) and Ham's F12 medium in a 3:1 ratio. A media supplementation receipt adapted from Bray et al, 2011 (Bray, George et al. 2011) was used and consisted of 10% Foetal Bovine Serum (FBS), 0.1% penicillin/streptomycin solution, 1% non-essential amino acids, 400 mM L-Glutamine, 6.8 mg 3,3,5-triiodo-L-thyronine sodium salt (T3), 1 µg/ml Insulin, 180 µM Adenine, 10 ng/ml Epidermal Growth Factor (EGF), 1 µg/ml isoproterenol, 0.4 µg/ml hydrocortisone and 5 µg/ml Transferrin.

A 6 well plate was coated with gelatin (1 mg/ml) at 37 °C for 1 hour, gelatin was aspirated and the plate left to dry under a laminar flow hood for 1 hr while preparing explant cultures. Each rim was rinsed with PBS, quartered and placed epithelial side down onto a gelatin coated 6 well plate. In order for each explant to attach, 1 ml of media was placed on top of each explant and left overnight at 37 °C, the next day 2 ml media was

then added to each explant culture. The cells were fed three days a week with corneal epithelial media until the cells grown out of the explant occupied 80% of the well. Accutase treatment was used to isolate the cells and expanded into a T25 flask. Remaining explants from the initial expansion were fed again with corneal epithelial media and the process repeated to increase cell number which can be done up to three times from one explant while retaining stem cell properties (López-Paniagua, Nieto-Miguel et al. 2013) . Upon confluence in the T25 flask, cells were further expanded in a T75 flask and used for fluid flow experiments. All cells used in the experiment were at passage 4 or below.

5.2.2 *Fluid flow bioreactor*

A commercially available fluidic unit quad and pump (IBIDI) (Figure 5.2) was used for shear stress experiments which allows 8 samples to be run in parallel as seen in Figure 5.3. Slides designed for the fluidic unit were used to apply defined shear onto the cells, the µslide I Leur 0.8 (IBIDI) was used for all experiments. The system works using a pump to generate constant pressure which pumps media from one reservoir to the other. This applied pressure results in a specific flow rate (ml/min) which depends on the channel height, pressure input, medium viscosity and flow resistance of the perfusion system (slide and tubing). The flow rate (ml/min) results in a wall shear stress (dyn/cm^2) to which the cells are exposed. The calculation shown in Figure 5.1 is used to determine the flow rates for the corresponding shear stress.

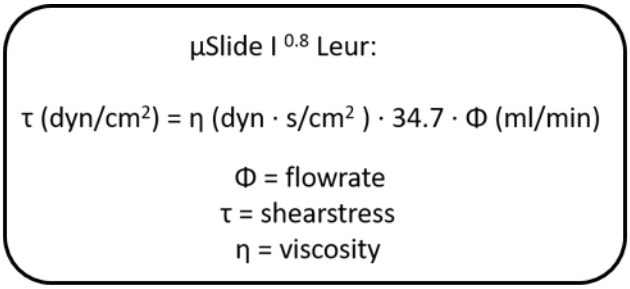

Figure 5.1 Shear Stress calculation. Wall shear stress depends on the flow rate and viscosity of perfusion medium.

The constant air pressure from the pump to the reservoirs of the fluidic unit generates a constant flow of medium within the slides; before these reservoirs run dry the medium is pumped back and forth between the two reservoirs. To create a laminar flow two valves are integrated in the fluidic unit that are simultaneously switched between two states.

The slides were coated with gelatin for 1 hour at 37 °C, LESC's were then seeded at 500,000 cells/slide (200,000 cells/cm^2) in 200µl of media to allow a fully confluent layer to be achieved. Cells were left to attach for 5 hours and washed with media to remove any unattached cells. For the static cultures, cells were left in the slides with daily media changes for either 1 or 3 days. Cells undergoing flow were attached to the fluidic unit and subjected to high shear (2.43 dyn/cm^2) or low shear (1.1 dyn/cm^2) for either 1 or 3 days. After shear had been applied to cells for the appropriate amount of time cells were prepared for RT-PCR or fixed for immunocytochemical analysis.

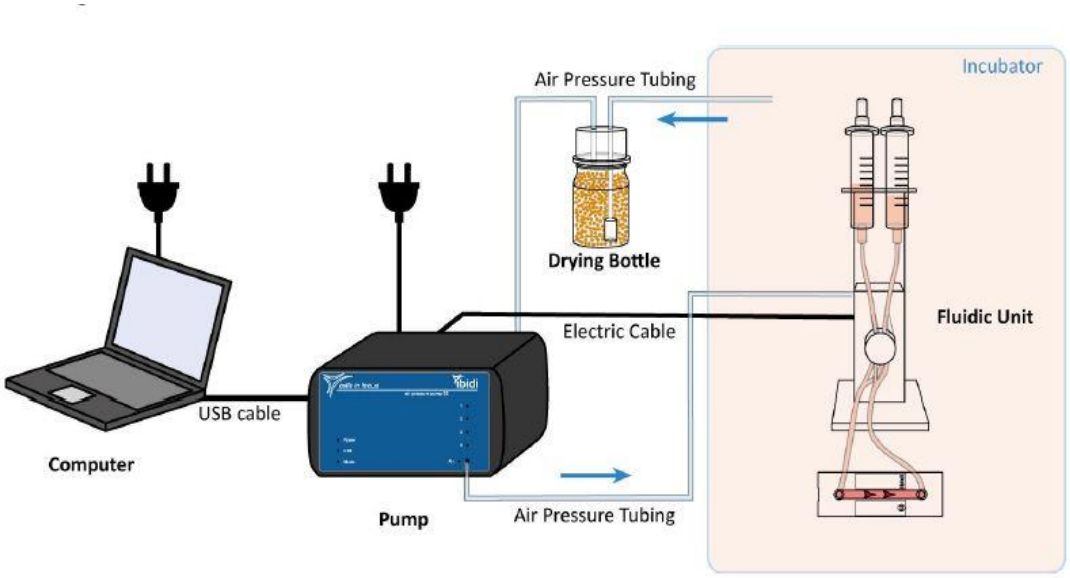

Figure 5.2 Fluid Flow Bioreactor. The fluidic unit is placed inside an incubator connected to the pump by air pressure tubing and a drying bottle to prevent condensation from the incubator entering the pump. The computer connected to the pump allows the desired shear stress to be applied to the cells.

Figure 5.3 Quad Fluidic Unit in Flow Hood. The Quad unit allows for 8 samples to undergo shear stress at one time. This picture depicts the cells seeded onto slides connected to the quad unit.

5.2.3 *RT-PCR*

RT-PCR was performed using the same protocol described in Chapter 3. The following primers were used: NP63α (custom made primer sequence adapted from Robertson et al.) (Robertson, Ho et al. 2008) ABCG2 (Hs01053790_m1), CK15 (Hs00267035_m1), Nestin (Hs00707120_s1), CK14 (Hs00265033_m1), CK3 (Hs00365080_m1), CK12 (Hs00165015_m1), TRPV4 (Hs01099348_m1) and GAPDH (Hs02758991_g1).

5.2.4 *Immunocytochemistry*

Immunocytochemistry was performed using the same protocol described in Chapter 3. The following antibodies and dilutions were used: Integrin β1 at 1:1000 dilution (ab24693 - Abcam), Vimentin at 1:1000 (ab92547 - Abcam), ZO-1 at 1:200 dilution (40-

2200 - Biosciences). For integrin β1 goat anti-mouse IgG H&L (Alexa Fluor® 488) (ab150113 - Abcam) was used. For all other proteins donkey anti-rabbit IgG H&L (Alexa Fluor® 488) (ab150073 - Abcam) was used.

Mean fluorescence intensity was determined using ImageJ software and corrected for background. 3D projection and orthogonal views were viewed to measure stratification of the cell layer. An image of the middle of each stack was acquired to observe morphology and distribution of the proteins in the cell.

5.2.5 *Orientation*

Using the ImageJ plugin OrientationJ, a colour map of the orientation of the cells was created. A max projection of the actin channel was used for this purpose. The coherency was also measured to measure the level of isotropy in each sample.

5.2.6 *Statistical analysis*

All experiments were carried out in triplicate, statistical analysis and outlier calculation was performed using GraphPad Prism software. Data are presented as the mean $\pm$ standard deviation (SD), significance was calculated either via one-way or two-way ANOVA with Post-Tukey test, significance deemed as $p \leq 0.05$ for all data sets.

5.3 Results

5.3.1 *Differentiation*

Gene expression of a panel of limbal stem cell markers (NP63α, ABCG2, CK15 and Nestin), transient amplifying marker CK14 and mature markers CK3 and CK12 were examined for each donor and time point.

5.3.1.1 *Stem cell marker expression*

1 day

Stem cell marker expression was significantly increased across all donors exposed to shear stress after 1 day (Figure 5.4). Variation among donors was evident with the youngest donor (donor 1) showing a significant increase in stem cell expression under both low and high shear compared to static (Figure 5.4 A-D). In particular, the high shear stress group induced the highest level of stem cell marker expression (NP63α, ABCG2 and CK15) with the exception of Nestin, which was expressed at a similar level in both the low and high shear group significantly increasing Nestin gene expression compared to the static group. In contrast, donor 2 (45 year old donor) showed a significant increase in stem cell marker expression (NP63α, ABCG2 and CK15) in the 1 day low shear group only, with Nestin gene expression significantly increased in the high shear group only compared to static treatment (Figure 5.4 E-H). The oldest donor (Donor 3) had a more varied response with NP63α significantly decreased after 1 day high shear while ABCG2, and Nestin were significantly increased after 1 day low shear compared to static culture (Figure 5.4 I-L). After 1 day high shear stress ABCG2 and CK15 were significantly increased compared to static culture for ABCG2 and both static and 1 day low shear culture for CK15 (Figure 5.4 J + K).

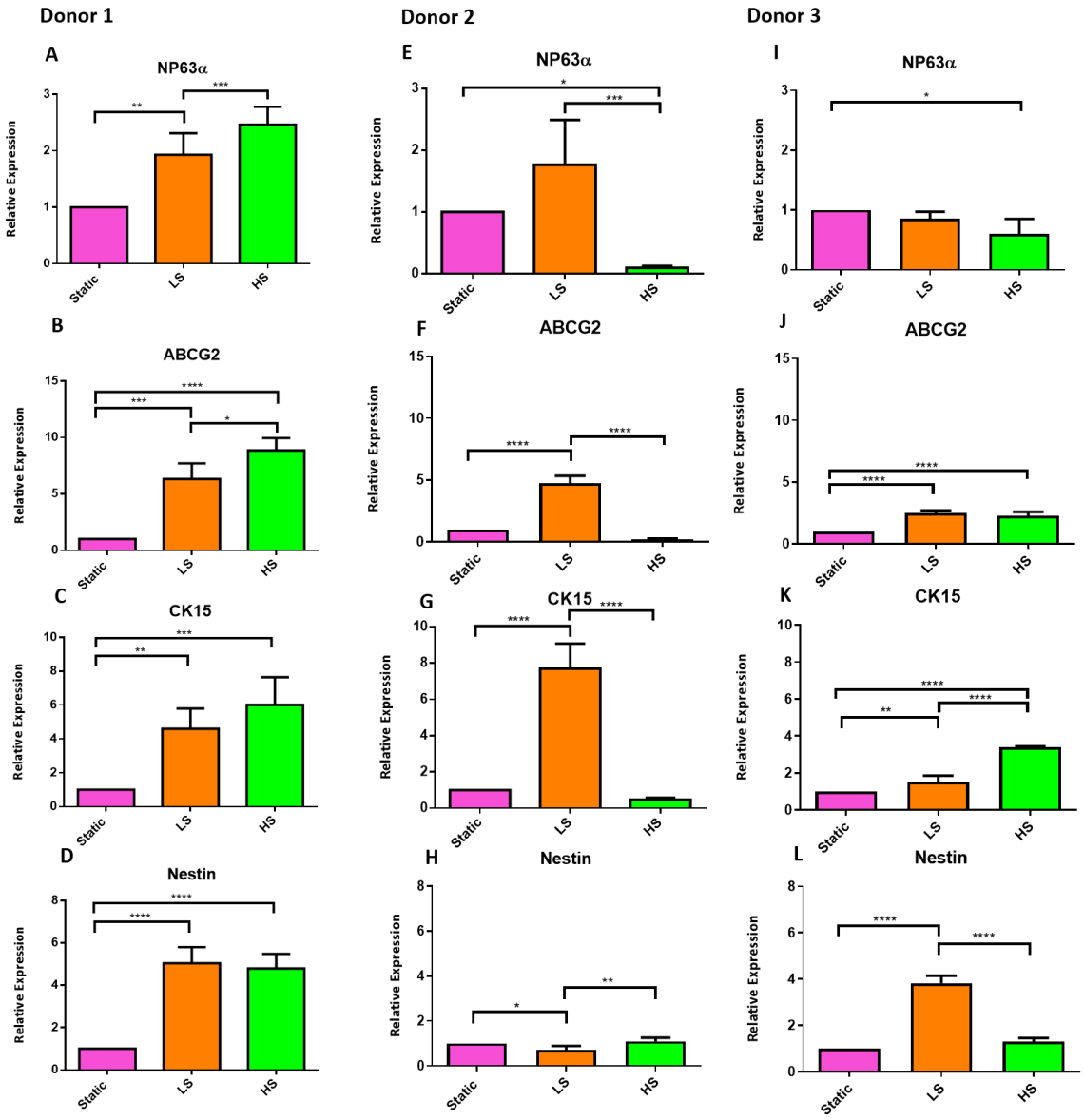

Figure 5.4 Real time PCR of NP63α, ABCG2, CK15 and Nestin after 1 day static, low shear (LS) and high shear (HS) culture. (A) – (D) Donor 1 gene expression, (E) – (H) Donor 2 gene expression, (I) – (L) Donor 3 gene expression of NP63α, ABCG2, CK15 and Nestin after 1 day static, low shear and high shear culture. Data are presented as the mean (±SD), significance calculated via one-way ANOVA with a Post-Tukey test, N=4, * = $P \leq 0.05$, ** = $P \leq 0.01$, *** = $P \leq 0.001$, **** = $P \leq 0.0001$.

3 day

Cells exposed to shear for 3 days affected stem cell marker expression in all donors (Figure 5.5). Similar to the 1 day group, donor variations were observed. All donors expressed a significant increase in NP63α gene expression with the most significant upregulation observed after 3 days of high shear stress (Figure 5.5 A,E,I). The youngest donor significantly increased ABCG2 gene expression under 3 days low shear (Figure 5.5 B). In contrast, ABCG2 was significantly increased in the high shear stress group in the older donors (donors 2 and 3) (Figure 5.5 F + J) with the low shear group significantly reducing ABCG2 expression compared to both static and high shear cultures. High shear promoted CK15 expression in donor 1 and 2 (Figure 5.5 C + G). Donor 3 had a similar expression of CK15 compared to the static group with no significant increase in any of the shear groups (Figure 5.5 K). The low shear group in donor 1 (Figure 5.5 D) significantly increased Nestin expression while in donor 2 (Figure 5.5 H) expressed Nestin significantly higher under high shear, with the low shear group significantly decreasing Nestin expression over 3 days compared to both the static and high shear groups. Donor 3 had a similar expression of Nestin compared to the static group with no significant increase in any of the shear groups (Figure 5.5 L).

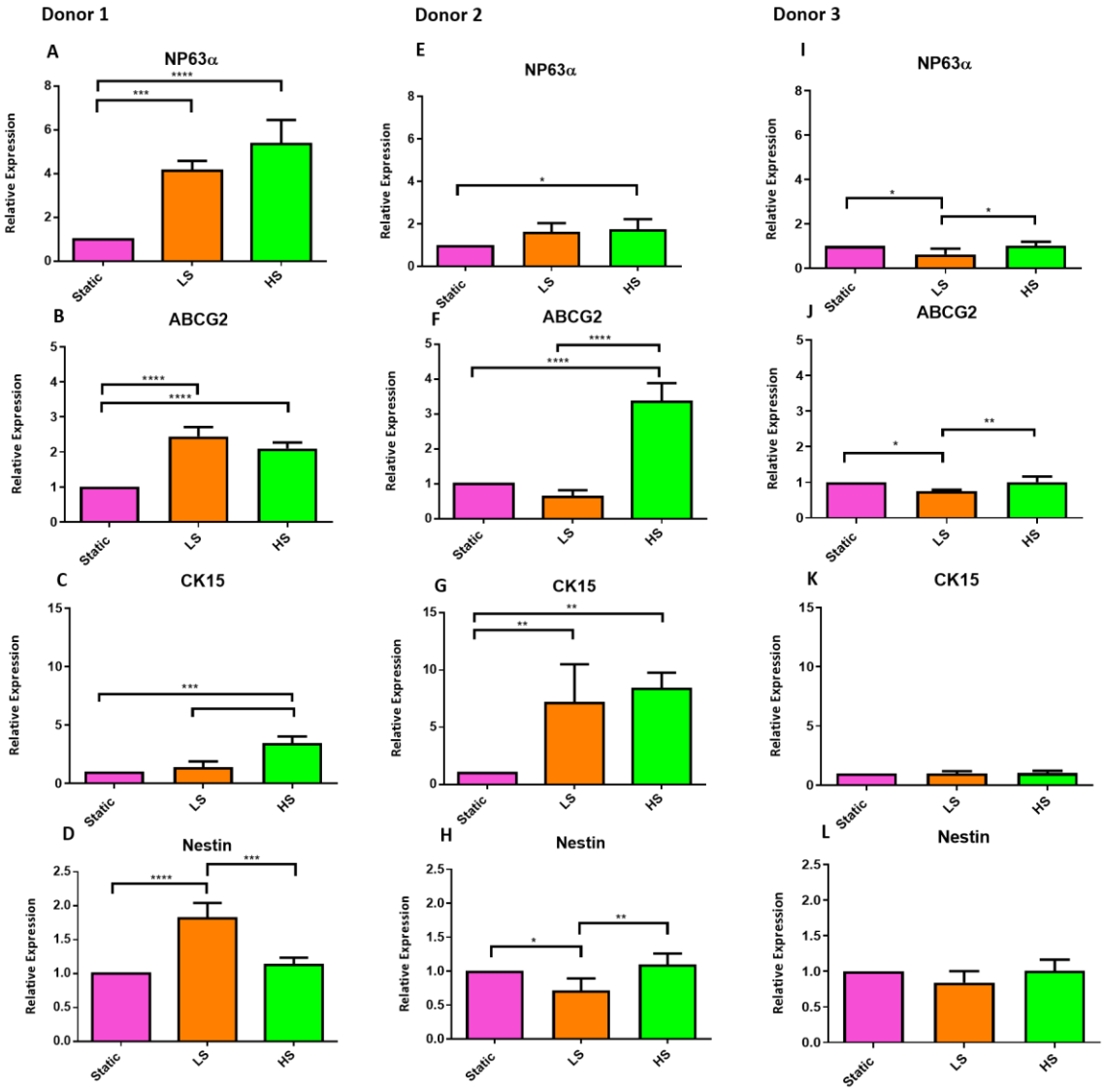

Figure 5.5 Real time PCR of NP63α, ABCG2, CK15 and Nestin after 3 days static, low shear (LS) and high shear (HS) culture. (A) – (D) Donor 1 gene expression, (E) – (H) Donor 2 gene expression, (I) – (L) Donor 3 gene expression of NP63α, ABCG2, CK15 and Nestin after 1 day static, low shear and high shear culture. Data are presented as the mean (±SD), significance calculated via one-way ANOVA with a Post-Tukey test, N=4, * = $P \leq 0.05$, ** = $P \leq 0.01$, *** = $P \leq 0.001$, **** = $P \leq 0.0001$.

5.3.1.2 *Transient amplifying marker expression*

Cells exposed to low shear stress for 1 day significantly increased CK14 expression in both the donor 1 and 2 compared to static and high shear stress culture (Figure 5.6 A,C). The high shear stress group significantly decreased CK14 expression in both donors. Donor 3 did not induce any significant change in CK14 expression, but overall this was decreased in expression compared to the static group (Figure 5.6 E).

After 3 days of high shear cell culture, donor 1 and 2 significantly increased CK14 expression compared to the low shear group (Figure 5.6 B,D). There was also a significant difference between the high shear and static group for donor 2 (Figure 5.6 D). Low shear significantly decreased CK14 expression compared to static in donor 1 (Figure 5.6 B). When donor 3 was exposed to both low and high shear over 3 days there was a significant decreased CK14 expression, the most significant being the low shear group compared to the static group as well as the high shear group (Figure 5.6 F).

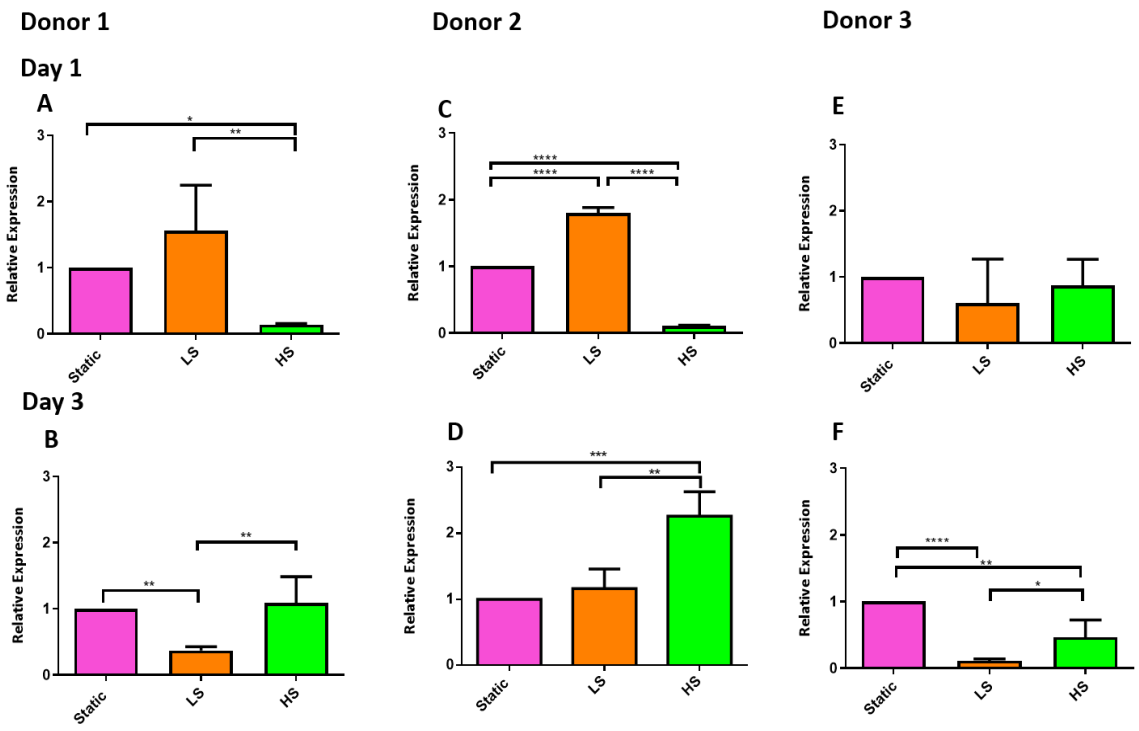

Figure 5.6 Real time PCR of CK14 after 1 day and 3 days static, low shear and high shear culture. (A) + (B) Donor 1 gene expression, (C) + (D) Donor 2 gene expression, (D) + (E) Donor 3 gene expression of CK14 after 1 day (A, C, E) and 3 day (B, D, F) static, low shear and high shear culture. Data are presented as the mean (±SD), significance calculated via one-way ANOVA with a Post-Tukey test, N=4, * = P ≤ 0.05, ** = P ≤ 0.01, *** = P ≤ 0.001, **** = P ≤ 0.0001.

5.3.1.3 *Mature marker expression*

Mature marker CK3 and CK12 expression was significantly increased under 1 day of high shear compared to static for donor 1 as shown in Figure 5.7 A + B. There was no CK3 expression detected after 3 days of shear stress exposure (Figure 5.7 C) and CK12 expression was not significant in the same donor after 3 days (Figure 5.7 D), although 3 day low shear showed the highest CK12 expression over all.

Donor 2 showed a significant increase in CK3 and CK12 after 1 day of low shear stress culture compared to the high shear group for CK3 expression and compared to both

static and high shear for CK12 expression (Figure 5.7 E + F). This donor also showed higher CK3 expression after 3 days (Figure 5.7 G) in both shear stress groups but this was not significant. The CK12 expression in this donor was not detected under low shear but was significantly increased under high shear stress compared to static after 3 days (Figure 5.7 H).

Donor 3 showed no significant expression of any of the mature marker expression under any shear stress culture (Figure 5.7 I - L). In the one day groups, CK3 expression was highest under low shear (Figure 5.7 I) and CK12 was expressed at a higher level in both low and high shear groups, albeit not significant (Figure 5.7 J). The 3 day groups showed a higher CK3 expression under high shear stress (Figure 5.7 K) with no detection of CK12 under low shear and lower CK12 expression in high shear compared to static cell culture, albeit not significant (Figure 5.7 L).

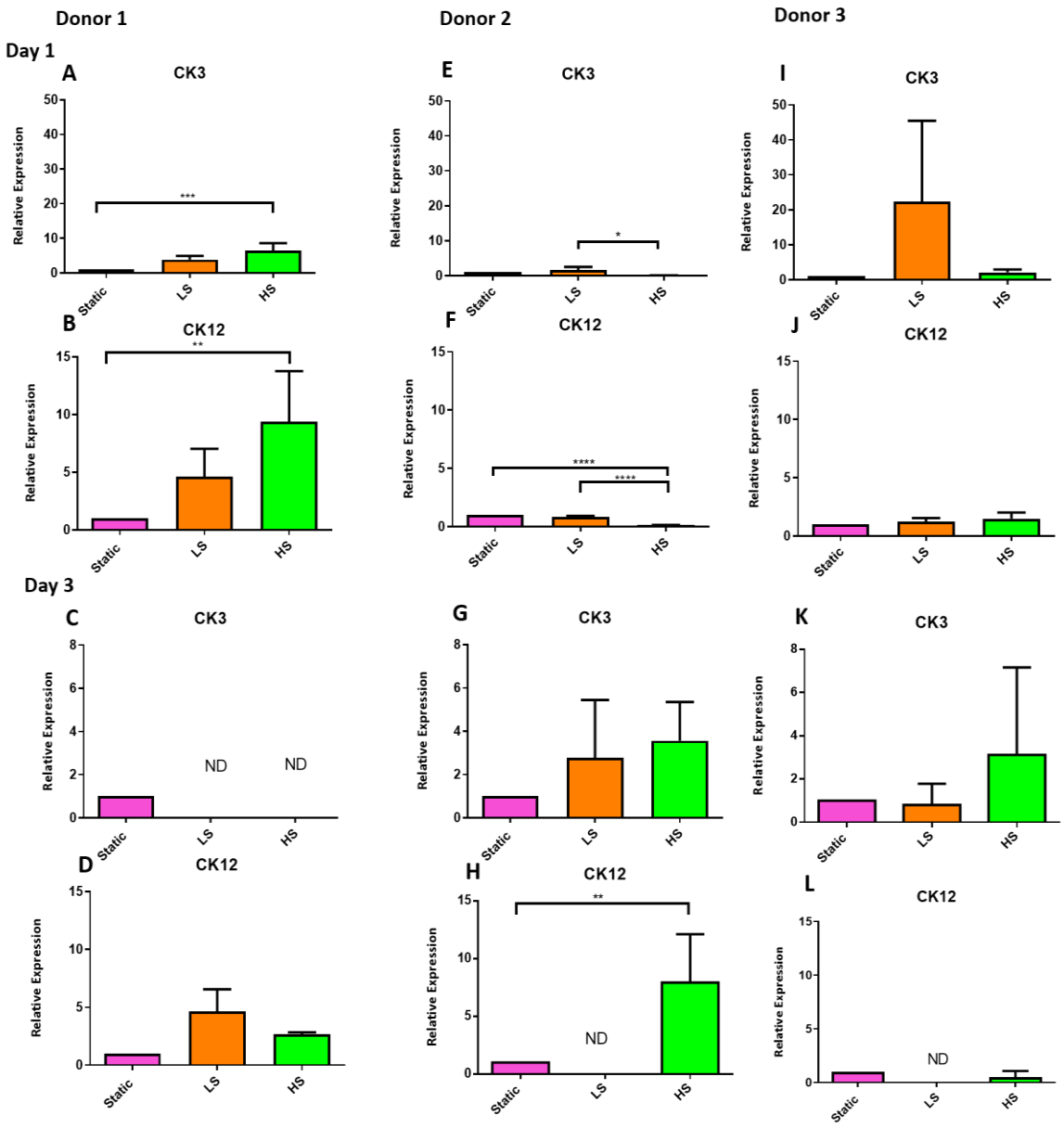

Figure 5.7 Real time PCR of CK3 and CK12 after 1 day and 3 days static, low shear and high shear culture. (A + B) Donor 1 CK3 and CK12 gene expression after 1 day of shear stress culture, (C + D) Donor 1 CK3 and CK12 gene expression after 3 days of shear stress culture. (E + F) Donor 2 CK3 and CK12 gene expression after 1 day of shear stress culture, (G + H) Donor 2 CK3 and CK12 gene expression after 3 days of shear stress culture. (I + J) Donor 3 CK3 and CK12 gene expression after 1 day of shear stress culture, (K + L) Donor 3 CK3 and CK12 gene expression after 3 days of shear stress culture. Data are presented as the mean (±SD), significance calculated via one-way ANOVA with a Post-Tukey test, N=4, * = $P \leq 0.05$, ** = $P \leq 0.01$, *** = $P \leq 0.001$, **** = $P \leq 0.0001$. ND = not detected.

5.3.2 *TRPV4 expression*

Expression of TRPV4 was significantly upregulated in all donors under low shear culture after 1 and 3 days compared to static culture (Figure 5.8). Donor 1 had a significant upregulation of TRPV4 after 1 day in both low and high shear conditions compared to the static control group (Figure 5.8 A). After 3 days the high shear group was more significantly upregulated compared to the static control group (Figure 5.8 B). Donor 2 had a significant upregulation of TRPV4 in the low shear stress cell culture after both 1 and 3 (Figure 5.8 C, D), the high shear group also significantly increased TRPV4 expression compared to the static control group after 1 day (Figure 5.8 C). Donor 3 had the most significant upregulation of TRPV4 gene expression after 1 day in the low shear group compared to static control group; this was also significantly upregulated in the high shear (Figure 5.8 E). After 3 days of shear stress, TRPV4 was significantly upregulated in the high shear group in this donor compared to both the low shear and static groups in this donor. The low shear group also significantly enhanced TRPV4 gene expression after 3 days compared to the static control group (Figure 5.8 F).

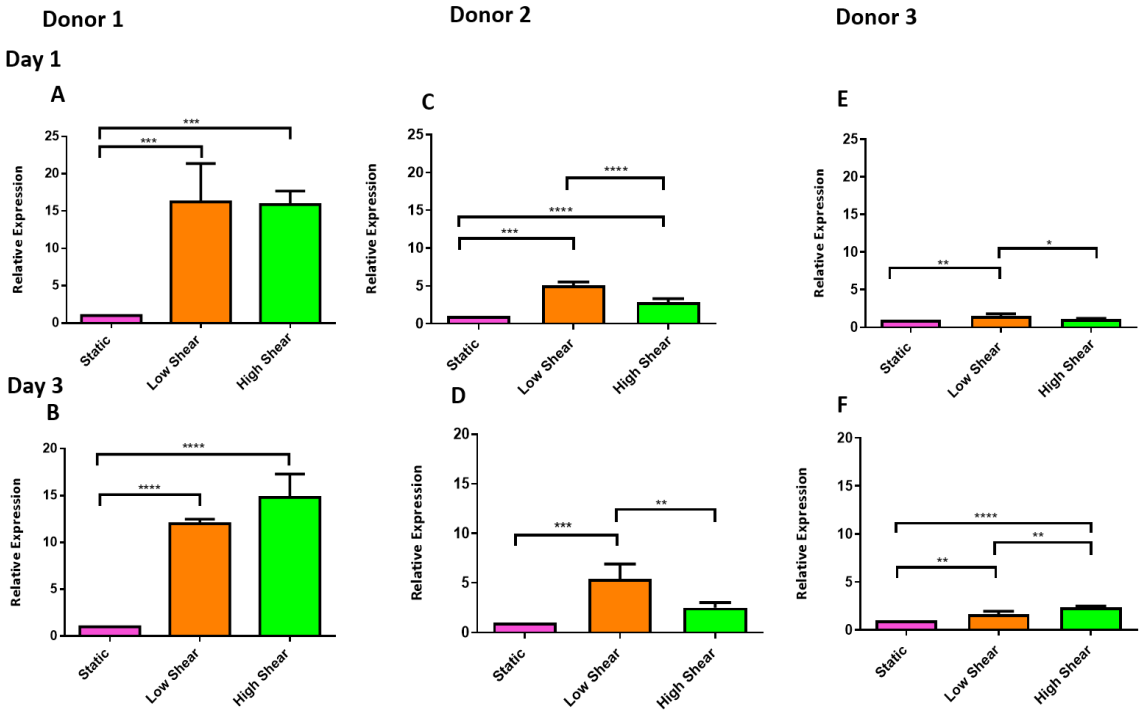

Figure 5.8 Real time PCR of TRPV4 after 1 day and 3 days static, low shear and high shear culture.

(A) + (B) Donor 1 gene expression, (C) + (D) Donor 2 gene expression, (D) + (E) Donor 3 gene expression of CK14 after 1 day and 3 day static, low shear and high shear culture. Data are presented as the mean (±SD), significance calculated via one-way ANOVA with a Post-Tukey test, N=4, * = P ≤ 0.05, ** = P ≤ 0.01, *** = P ≤ 0.001, **** = P ≤ 0.0001.

5.3.3 *Orientation*

Confocal microscopy was used to determine whether cells aligned to the direction of flow. Using the actin channel, each cell stack was max projected and the Image J plugin OrientationJ was used on each image. A colour map corresponding to different angles of directionality in each cell was created as shown in Figure 5.9 below.

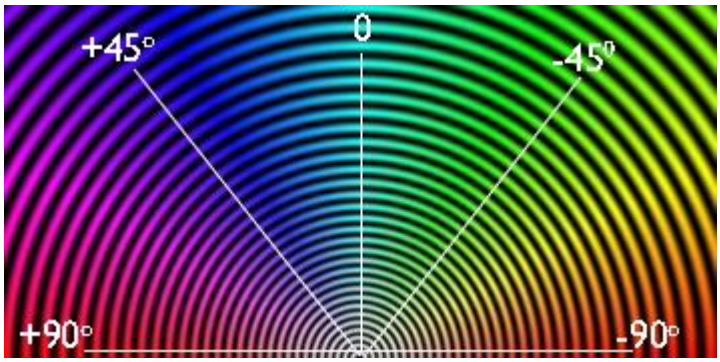

Figure 5.9 Orientation colour map. A colour map was made using OrientationJ in which the angles of the cells correspond to the colour map (Püspöki, Storath et al. 2016).

In the 1 day shear groups, all 1 day static groups did not show any directionality in their actin cytoskeletal arrangement as shown in Figure 5.10 A, D, G. This was also observed for cells exposed to 1 day low shear stress rates (Figure 5.10 B, E, H), however, the oldest donor (donor 3) did show cellular alignment after 1 day low shear (Figure 5.10 I). All donors aligned perpendicular to the flow direction after 1 day of high shear stress (Figure 5.10 C, F, I).

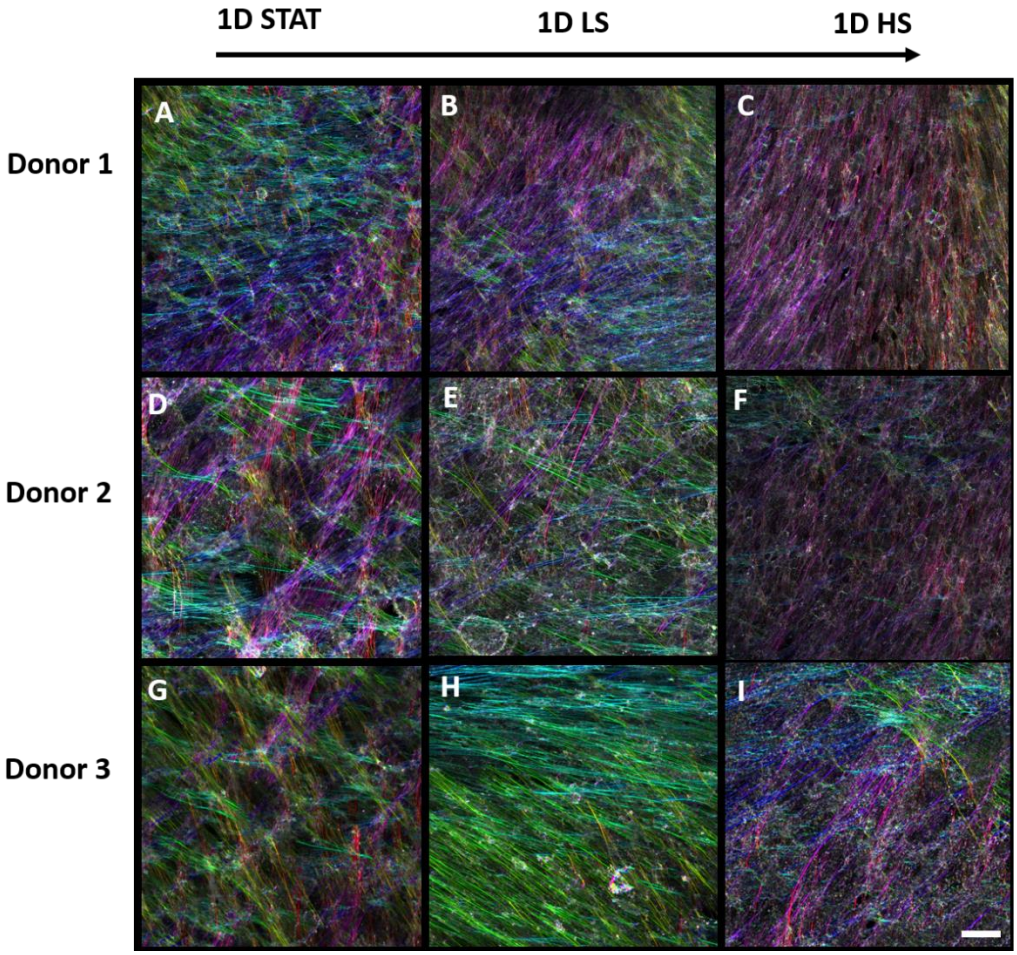

Figure 5.10 Immunocytochemical staining of cellular orientation after 1 day shear stress culture. (A) – (C) Orientation of Donor 1, (D) – (F) Orientation of Donor 2, (G) – (I) Orientation of Donor **3.** Cells were stained with f-actin and the OrientationJ plugin was used to create a colour map of orientation of cells. Arrow indicates direction of flow, Scale bar = 20µm.

Cells exposed to static or shear stress for three days were also examined for orientation (Figure 5.11). The 3 day static group had random alignment and showed no directionality (Figure 5.11 A, D, G) apart from donor 3 showing some more directionality compared to the other donors (Figure 5.11 G). Donors 1 and 3 aligned to the flow direction after 3 day low shear (Figure 5.11 B, H) whereas donor 2 remained random in its alignment (Figure 5.11 E). All donors aligned perpendicular to flow direction in the 3 day high shear stress group (Figure 5.11 C, F, I).

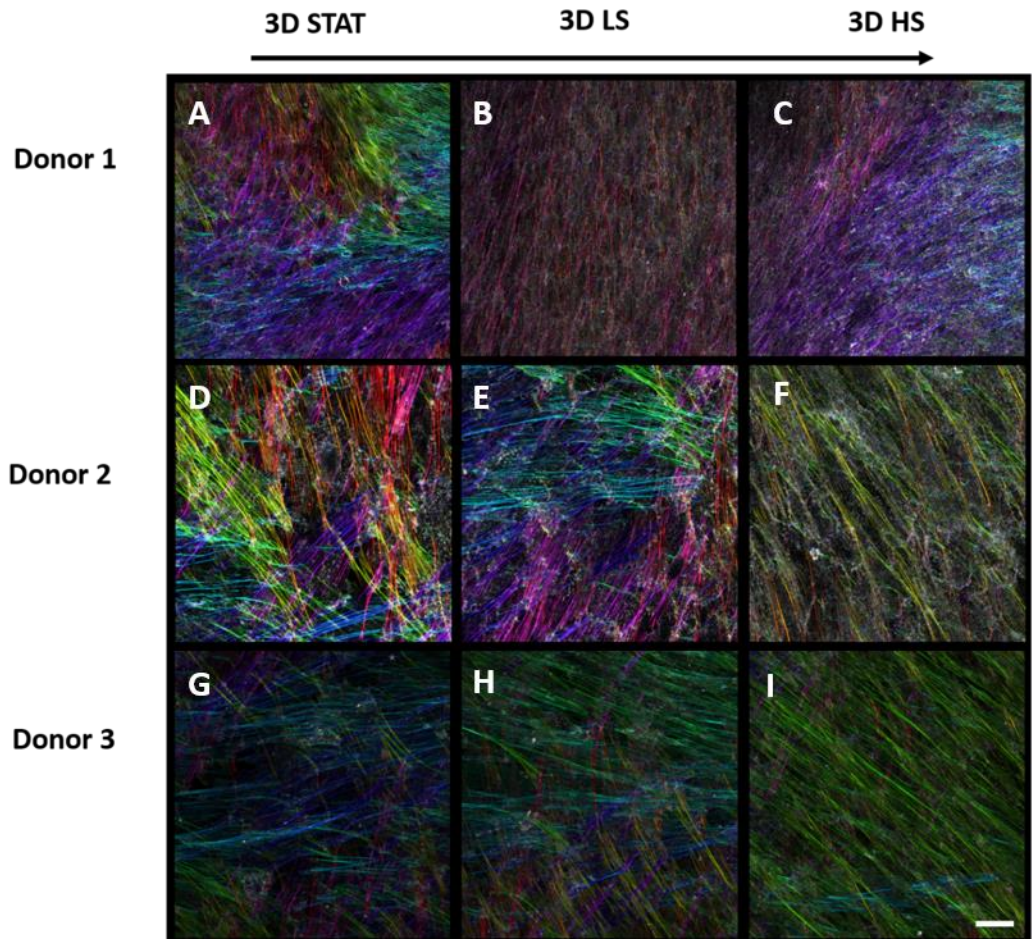

Figure 5.11 Immunocytochemical staining of cellular orientation after 3 days shear stress culture. (A) – (C) Orientation of Donor 1, (D) – (F) Orientation of Donor 2, (G) – (I) Orientation of Donor 3. Cells were stained with f-actin and the OrientationJ plugin was used to create a colour map of orientation of cells. Arrow indicates direction of flow, Scale bar = 20μm.

5.3.4 *Stratification*

All donors in the 1 day (Figure 5.12 A, D, G) and 3 day (Figure 5.12 J, M, P) static group remained as a monolayer with no stratification observed. Donor 3 stratified to form a 2-3 cell layer after 3 days of low shear stress (Figure 5.12 Q) with all other donors not showing any stratification. The high shear group after 1 day showed some stratification to a 2 cell layer in the older donor (donor 3) (Figure 5.12 I) but cells did not stratify in the other donors exposed to 1 day high shear (Figure 5.12 C, F). Cells exposed to 3 days of high shear

stratified to form a 4-5 cell layer in both the younger and middle age donor (donor 1 and 2) as shown in Figure 5.12 L, O with a 2-3 cell layer observed after 3 day high shear in donor 3 (the older donor) as shown in Figure 5.12 R.

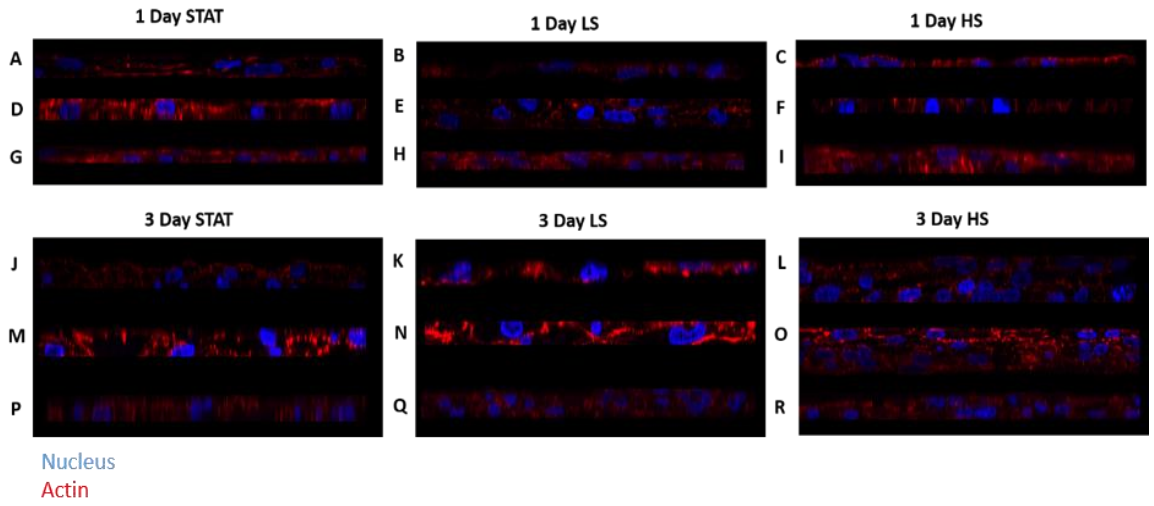

Figure 5.12 Immunocytochemical staining for cellular stratification. (A – C) Donor 1 cellular stratification, (D – F) Donor 2 cellular stratification, (G – I) Donor 3 cellular stratification after 1 day static, low shear and high shear cell culture. (J – L) Donor 1 cellular stratification, (M – O) Donor 2 cellular stratification, (P – R) Donor 3 cellular stratification after 3 days static, low shear and high shear cell culture.

Stratification was quantified by manually counting cell number using the Image J cell counter plugin on three separate orthogonal sections per donor in each condition. Cell number from each donor and shear stress group was quantified and these values used to calculate percentage increase of cell number using the static group as the control as shown in Figure 5.13. An increase in cell number or percentage increase indicates stratification due to more cells being present in the cell layer.

All donors displayed a significant increase in cell number after 3 days high shear stress compared to static culture as shown in Figure 5.13 C, J, K. Donor 2 displayed a

significant increase in cell number after 1 day low shear and high shear stress culture (Figure 5.13 E), the percentage increase of cells was significantly increased in donor 2 after 1 day low shear stress culture compared to 1 day high shear stress culture (Figure 5.13 F).

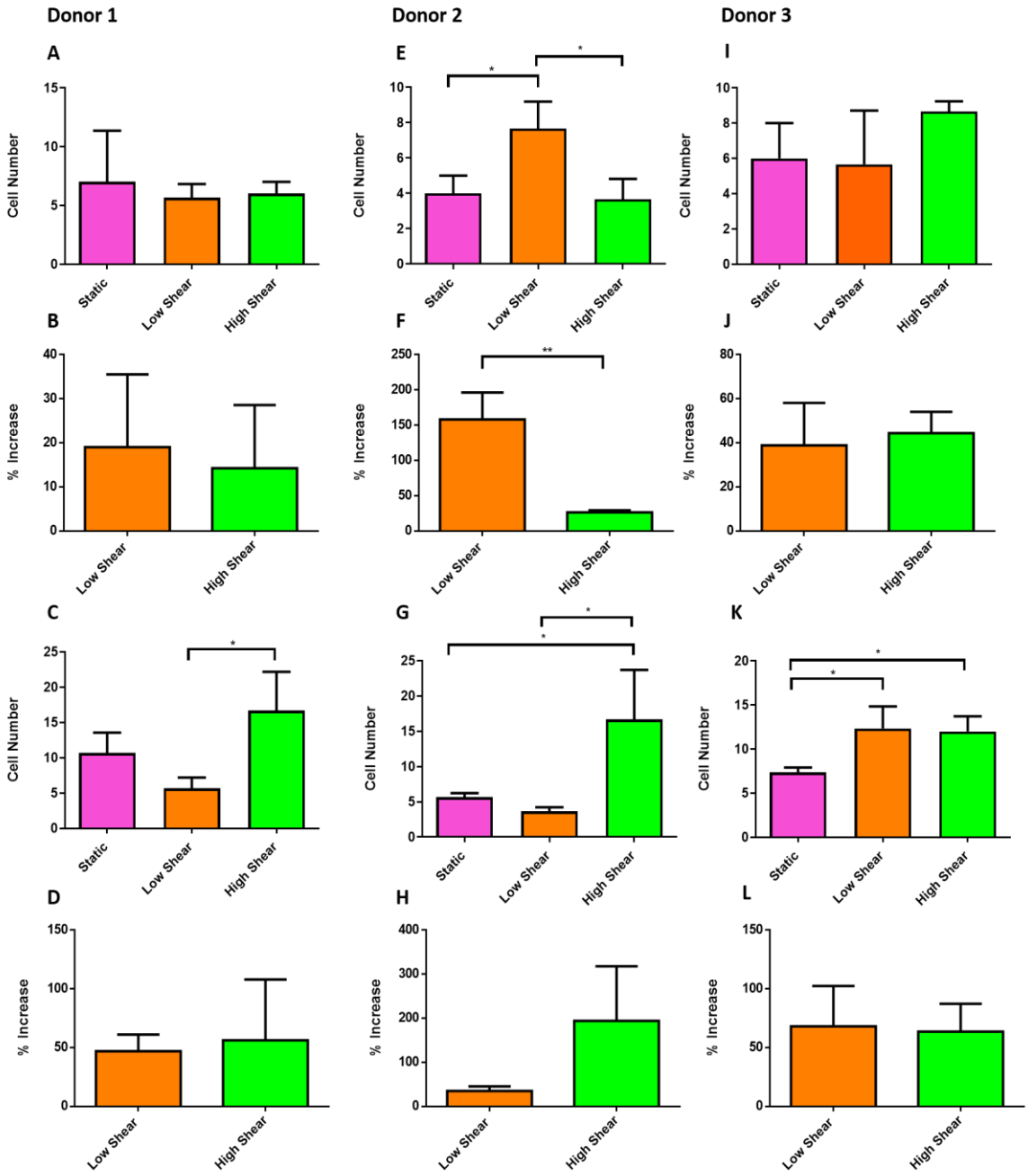

Figure 5.13 Stratification of cells as a measure of cell number and percentage increase. (A + B) Donor 1, (E + F) Donor 2, (I + J) Donor 3 cell stratification of cells after 1 day static, low shear or high shear stress culture. (C + D) Donor 1, (G + H) Donor 2, (K + L) Donor 3 cell stratification of cells after 3 days static, low shear or high shear stress culture. Data are presented as the mean (±SD), significance calculated via one-way ANOVA with a Post-Tukey test, N=3, * = $P \leq 0.05$, ** = $P \leq 0.01$.

5.3.5 *Wound healing*

Two markers for wound healing in the corneal epithelium were examined. Confocal microscopy was used to look at expression and distribution of integrin β 1 and vimentin.

5.3.5.1 *Integrin β1*

Confocal microscopy was used to determine levels of expression of integrin β1 as well as protein distribution and morphology. For donor 1, 1 day groups showed even distribution of integrin β 1 in the static group (Figure 5.14 A) while the 1 day low shear and 1 day high shear groups had more of a scattered distribution ((Figure 5.14 B, C). Donor 2 had a more even distribution of integrin β 1 in all 1 day groups (Figure 5.14 D-F). Donor 3 had random integrin β 1 distribution in the 1 day low shear group (Figure 5.14 H) but this was even across the 1 day static and 1 day high shear groups (Figure 5.14 G, I). This distribution did not seem to be affected by alignment of the cells.

All donors had an elongated cellular morphology in both of the shear groups while the static groups were more rounded and displayed the typical cobblestone shape associated with the corneal epithelial cells.

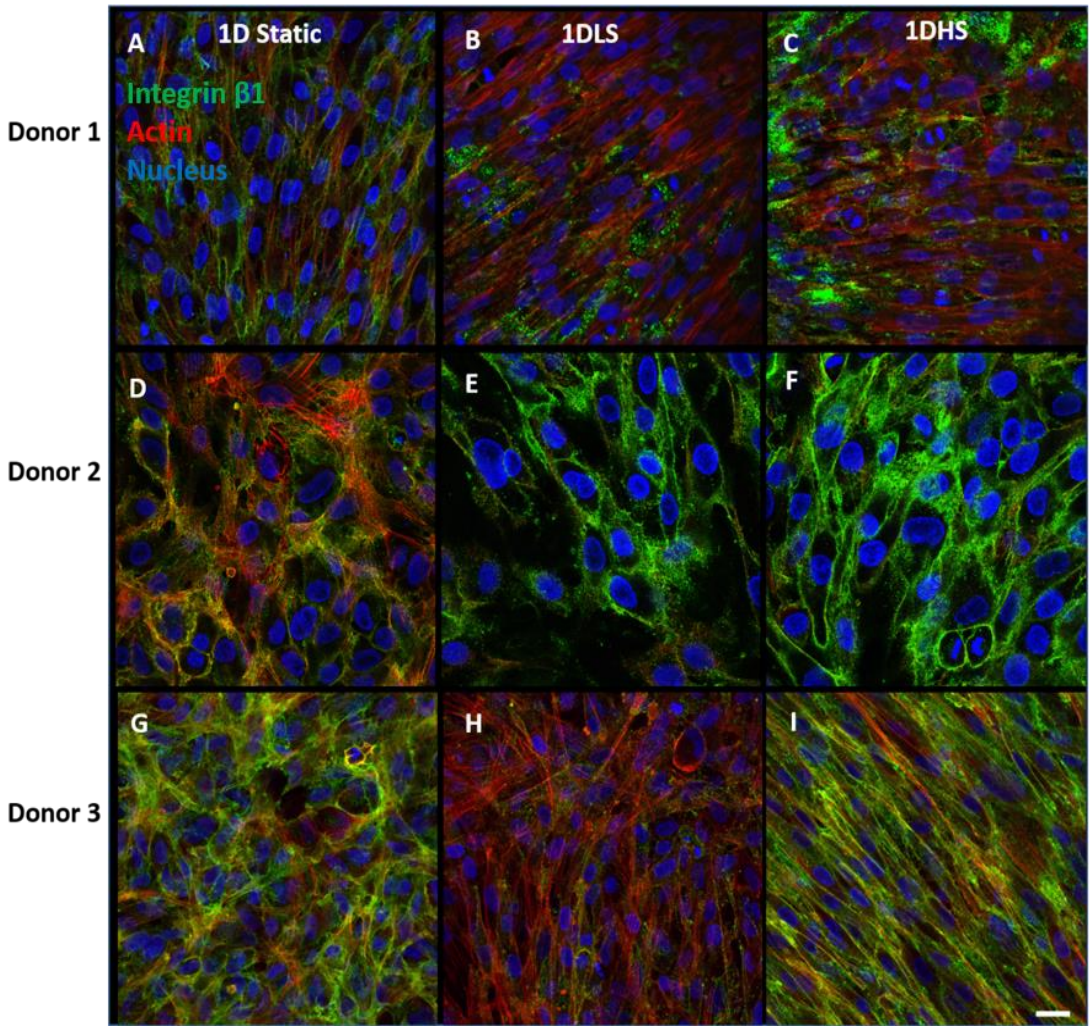

Figure 5.14 Immunocytochemical staining for Integrin β 1 (green) after 1 day shear stress culture. A – C Donor 1 integrin β1 staining. D – F Donor 2 integrin β1 staining. G – I Donor 3 integrin β1 staining. Integrin β1 is stained in green. All cells were counterstained with f-actin (red) and DAPI (blue), Scale bar = 20µm.

The 3 day groups had a random distribution of integrin β 1 for donor 1 (Figure 5.15 A-C). This was similar to results seen in the 1 day group for the donor 1 shear stress groups (Figure 5.14 A-C). Donor 2 had an even distribution of integrin β 1 in the 3 day shear groups but this was more scattered in the 3 day static group (Figure 5.15 D-F), again similar to the 1 day experimental group (Figure 5.14 A-C). Donor 3 had a scattered integrin β 1 protein

distribution in the static and low shear group. This was more evenly distributed in the 3 day high shear group (Figure 5.15 G-I).

All donors displayed an elongated cell shape with the 3 day low shear group showing some more cobblestone morphology compared to the other groups (Figure 5.15 B, E, H).

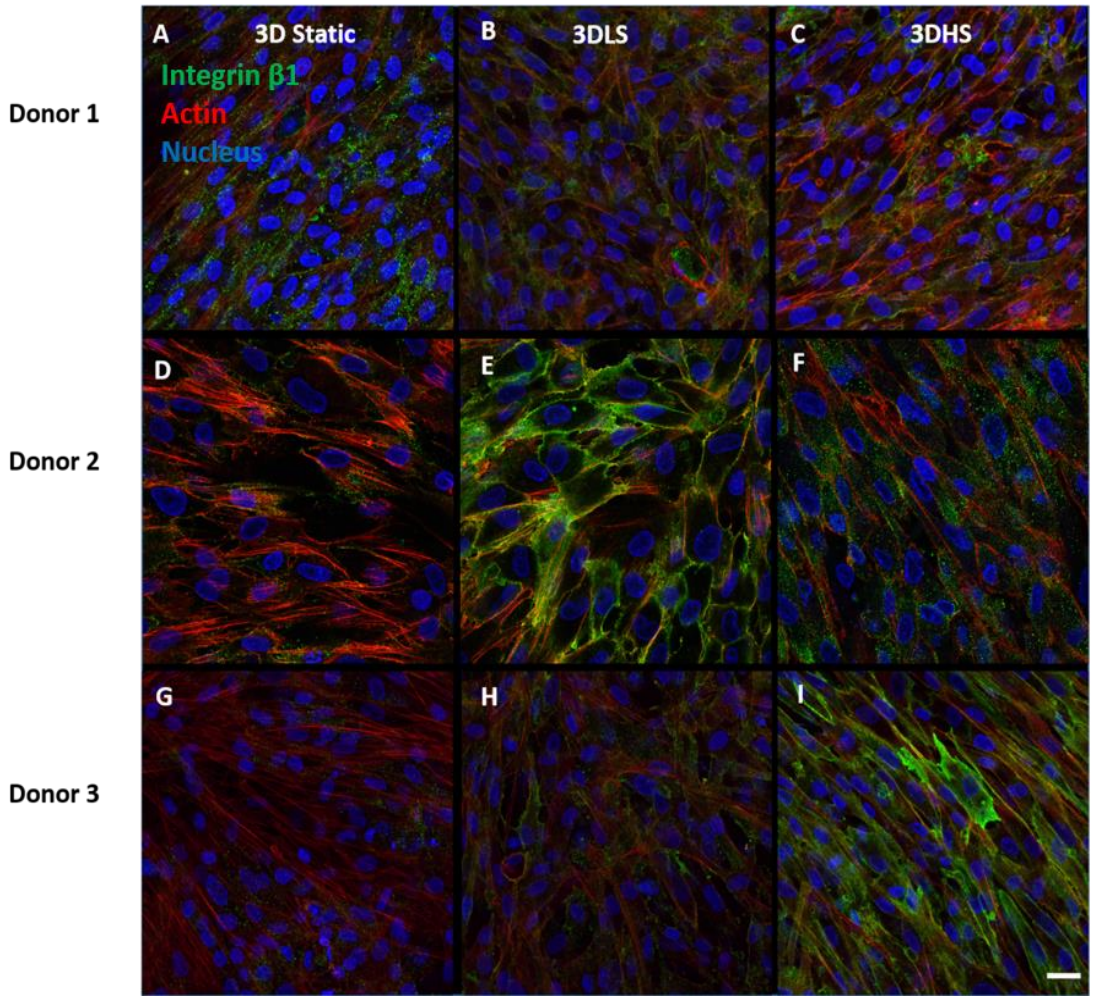

Figure 5.15 Immunocytochemical staining for Integrin β 1 (green) after 3 days shear stress culture. A – C Donor 1 integrin β1 staining. D – F Donor 2 integrin β1 staining. G – I Donor 3 integrin β1 staining. Integrin β1 is stained in green. All cells were counterstained with f-actin (red) and DAPI (blue), Scale bar = 20µm.

Fluorescence intensity was calculated for integrin β 1 protein expression. Among all donors, there were significant differences in expression of integrin β1 (Figure 5.16). Donor 1 and 3 had a significant decrease in expression of integrin β1 after 1 day of low shear with a significant increase of integrin β1 expression after 1 day of high shear (Figure 5.16 A (i), C (i)). Donor 2 in contrast significantly increased integrin β1 expression after 1 day of low shear (Figure 5.16 B (i)). There was a significant increase in integrin β1 expression after 3 days of both low and high shear stress in both donor 2 and 3 compared to the static group (Figure 5.16 B (ii), C (ii)). Donor 3 significantly enhanced integrin β1 expression after 3 days high shear stress compared to the 3 day low shear group while the 3 day low shear group significantly enhanced integrin β1 expression compared to the static group (Figure 5.16 C (ii)).

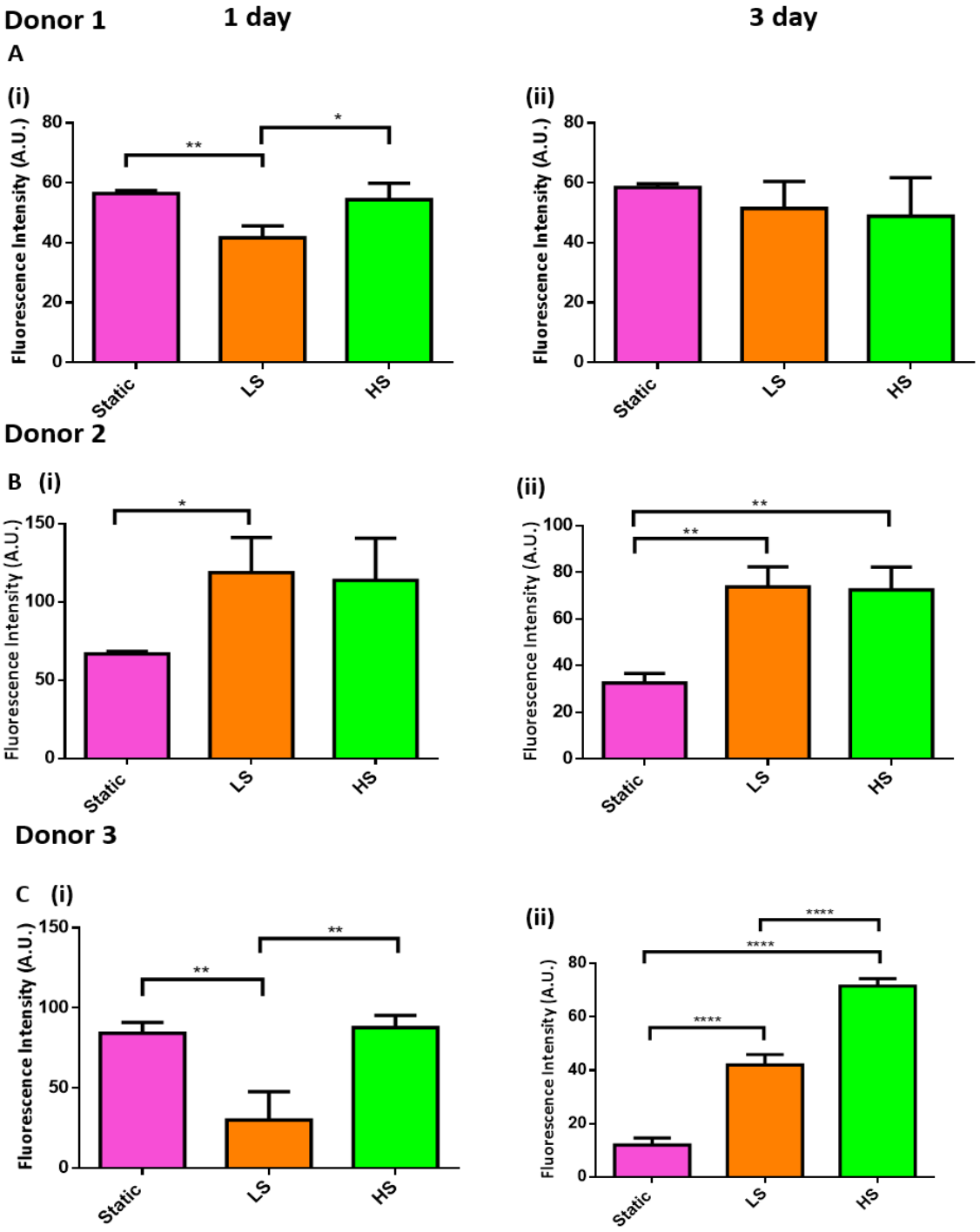

Figure 5.16 Fluorescence intensity of Integrin β 1 after 1 and 3 day static, low shear and high shear stress. (A) Donor 1 (i) 1 day and (ii) 3 day, (B) Donor 2 (i) 1 day and (ii) 3 day, (C) Donor 3 (i) 1 day and (ii) 3 day Integrin β 1 fluorescence intensity. Data are presented as the mean (±SD), significance calculated via one-way ANOVA with a Post-Tukey test, N=3, * = P ≤ 0.05, ** = P ≤ 0.01, *** = P ≤ 0.001, **** = P ≤ 0.0001.

5.3.5.2 *Vimentin*

Vimentin was distributed mostly at the top of the monolayer of cells. The images in the results below are from the middle of each stack (Figure 5.17). Donor 1 showed vimentin distribution concentrated to one side of the cell monolayer (Figure 5.17 A-C). Donor 2 showed an even distribution of vimentin in the static and low shear group, with distribution centrally in the high shear group (Figure 5.17 D-F). Donor 3 produced little vimentin protein at this stack with it visible in just a few cells (Figure 5.17 G - I).

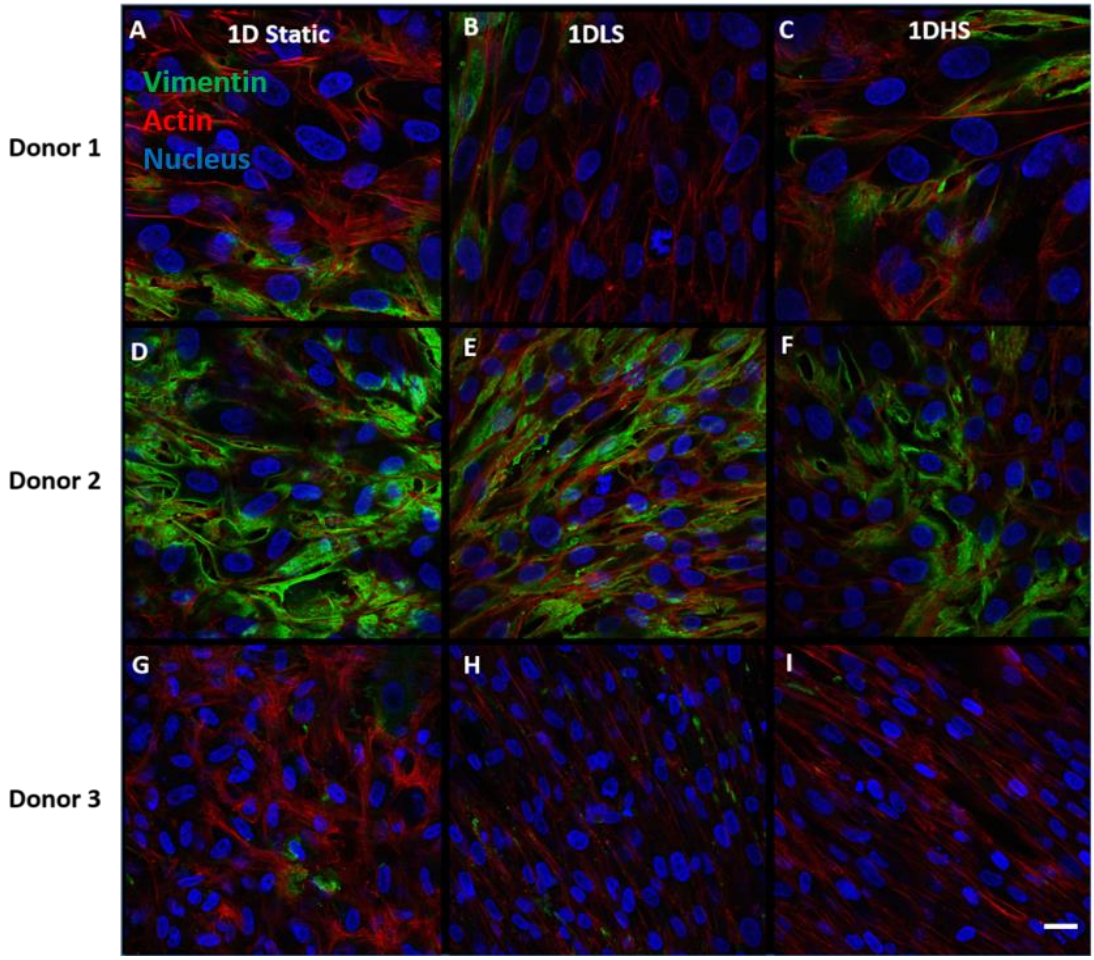

Figure 5.17 Immunocytochemical staining for Vimentin (green) after 1 day shear stress culture. A – C Donor 1 integrin β1 staining. D – F Donor 2 integrin β1 staining. G – I Donor 3 integrin β1 staining. Vimentin is stained in green. All cells were counterstained with f-actin (red) and DAPI (blue), Scale bar = 20μm.

Donor 1 of the 3 day groups showed an appearance of even distribution of vimentin in the static and low shear group (Figure 5.18 A, B). The high shear group showed random distribution of vimentin in some cells (Figure 5.18 C). Donor 2 had even distribution of vimentin across all groups in the 3 day time point (Figure 5.18 D - F). Donor 3 did not show much vimentin protein in this area of the stack, any protein that was visible was quite scattered (Figure 5.18 G – I).

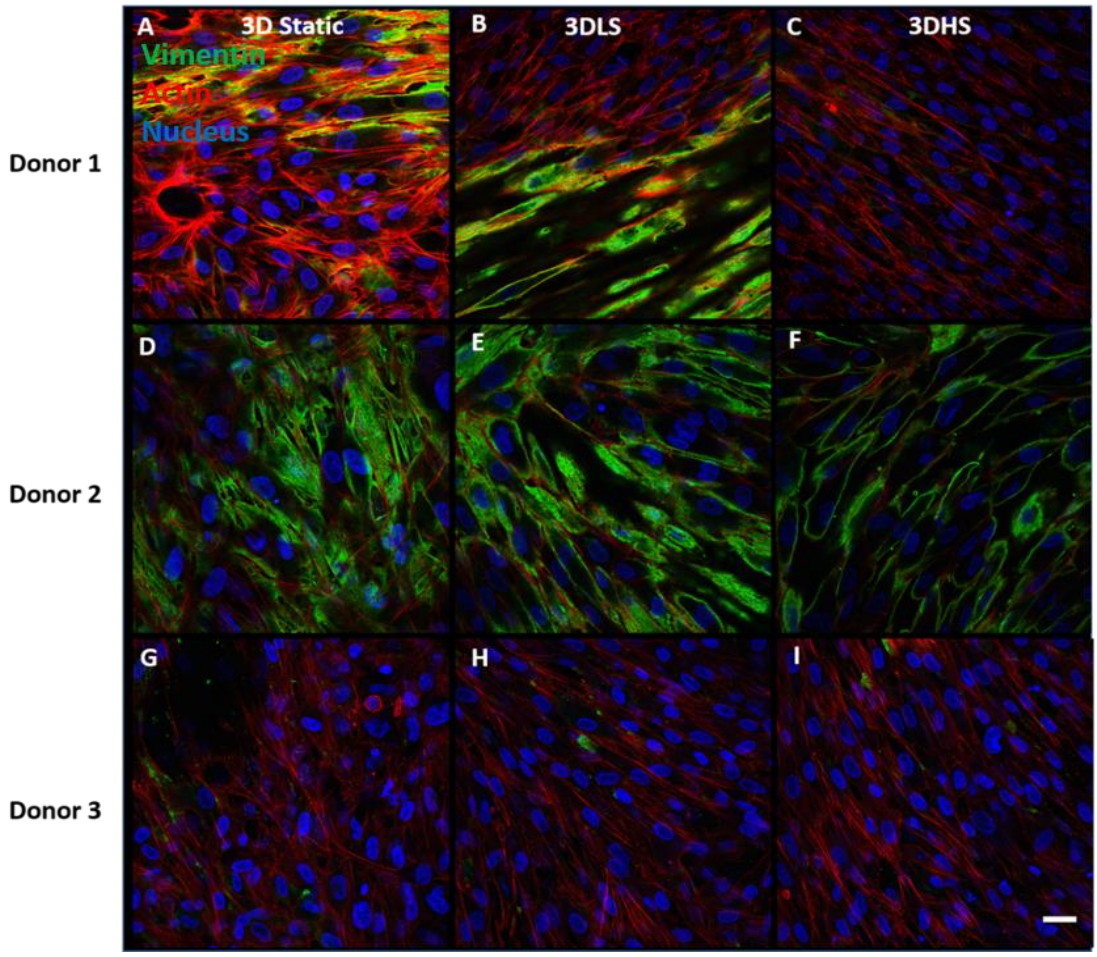

Figure 5.18 Immunocytochemical staining for Vimentin (green) after 3 days shear stress culture. A – C Donor 1 integrin β1 staining. D – F Donor 2 integrin β1 staining. G – I Donor 3 integrin β1 staining. Vimentin is stained in green. All cells were counterstained with f-actin (red) and DAPI (blue), Scale bar = 20µm.

Fluorescence intensity was quantified for vimentin. Donor 1 had a significant decrease in vimentin expression after 1 day of low shear stress (Figure 5.19 A (i)). There was a significant decrease in vimentin expression after 1 day of low shear stress compared to both static and 1 day high shear stress cultures donor 2 (Figure 5.19 B (i)). The 1 day high shear stress group significantly decreased vimentin expression compared to the static group in donor 3 also (Figure 5.19 C (i)). There was no significant differences in vimentin expression in any donors after 3 days of either low shear stress or high shear stress (Figure 5.19 A (ii), B (ii), C (ii)).

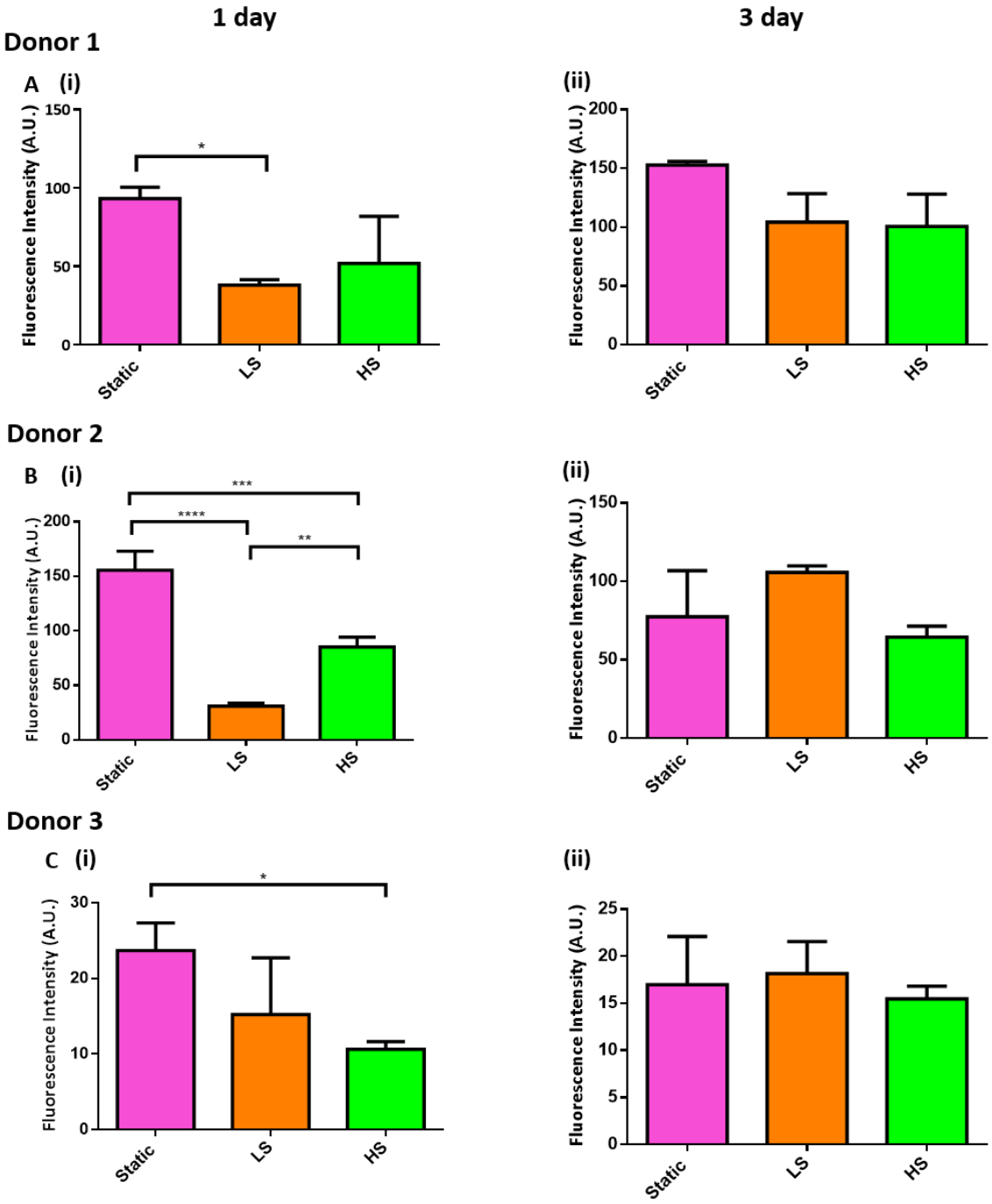

Figure 5. 19 Fluorescence intensity of Vimentin after 1 and 3 day static, low shear and high shear stress. (A) Donor 1 (i) 1 day and (ii) 3 day, (B) Donor 2 (i) 1 day and (ii) 3 day, (C) Donor 3 (i) 1 day and (ii) 3 day vimentin fluorescence intensity. Data are presented as the mean (±SD), significance calculated via one-way ANOVA with a Post-Tukey test, N=3, * = P ≤ 0.05, ** = P ≤ 0.01, *** = P ≤ 0.001, **** = P ≤ 0.0001.

5.3.6 *Barrier function*

Confocal microscopy was used to determine if shear stress affected barrier function as shown in Figure 5.20 and Figure 5.21. ZO-1 protein was studied to determine expression and distribution of this protein under shear stress. At day 1 there was an even distribution of ZO-1 among the cells in the static group. The protein was sparser and scattered in both of the shear groups (Figure 5.20 A, D, G).

Donor 2 had even ZO-1 distribution with clear tight junctions forming at cell boundaries in the static group (Figure 5.20 D). In both of the shear groups the ZO-1 distribution was very sparse with little protein observed in the cells (Figure 5.20 E, F). Donor 3 showed even ZO-1 distribution among all groups with the protein being concentrated at the apical sides of the cell where other cells are connecting (Figure 5.20 G–I).

The static groups showed a more cobblestone cellular morphology. All shear groups were more spindle shaped and elongated.

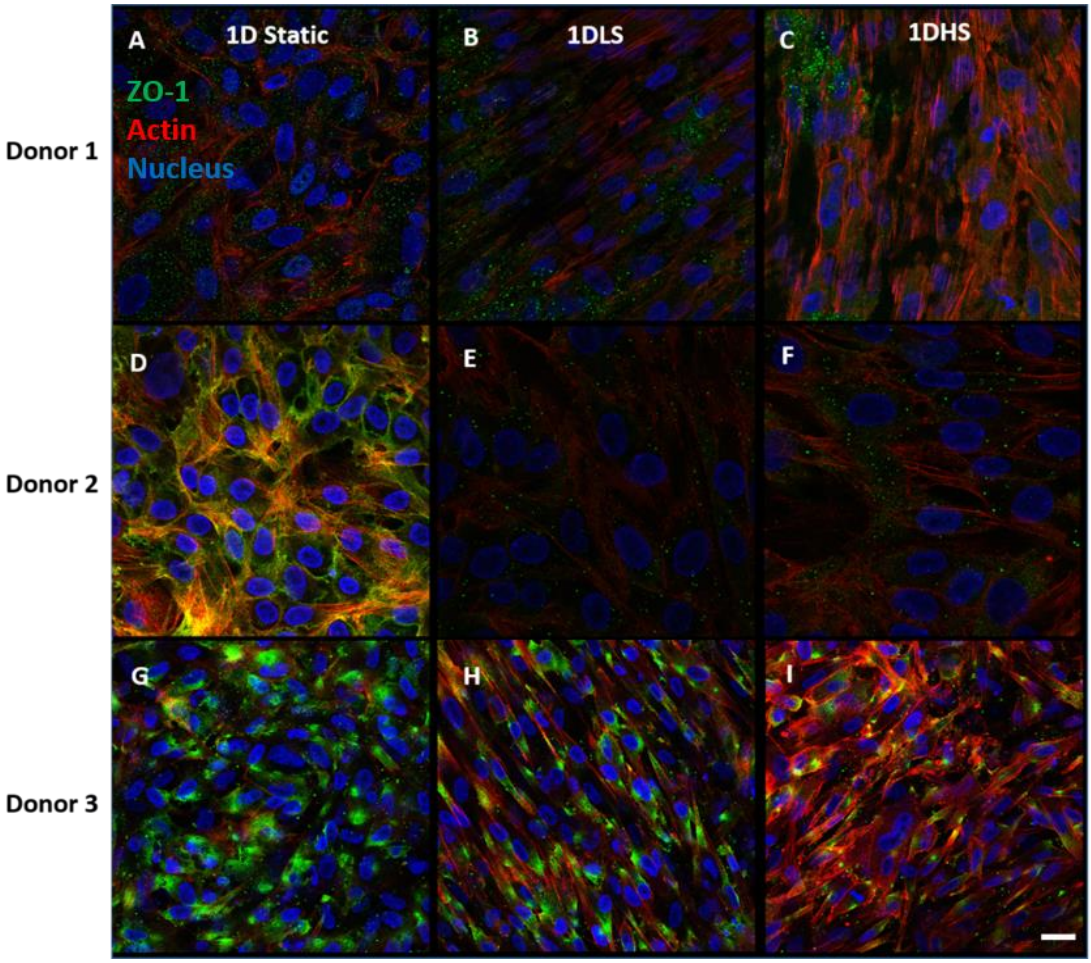

Figure 5.20 Immunocytochemical staining for ZO-1 (green) after 1 day shear stress culture. A – C Donor 1 ZO-1 staining. D – F Donor 2 ZO-1 staining. G – I Donor 3 ZO-1 staining. ZO-1 is stained in green. All cells were counterstained with f-actin (red) and DAPI (blue), Scale bar = 20µm.

Immunocytochemical staining for ZO-1 after 3 days was also performed (Figure 5.21). Donor 1 had even distribution in the 3 day static and high shear group. The 3 day low shear group showed more sparse distribution of the protein (Figure 5.21 A-C). Donor 2 had less visible ZO-1 protein in the static group with this quite scattered in distribution. The 3 day low shear group showed an even ZO-1 distribution with clear tight junction formation at cellular boundaries. This was also seen in the 3 day high shear group with less ZO-1 protein at each cell boundary (Figure 5.21 D-F). Donor 3 had even ZO-1 distribution among each group. This was most pronounced in the 3 day low shear group

with the 3 day static and high shear group having more ZO-1 distribution at the apical cellular sides (Figure 5.21 G-I).

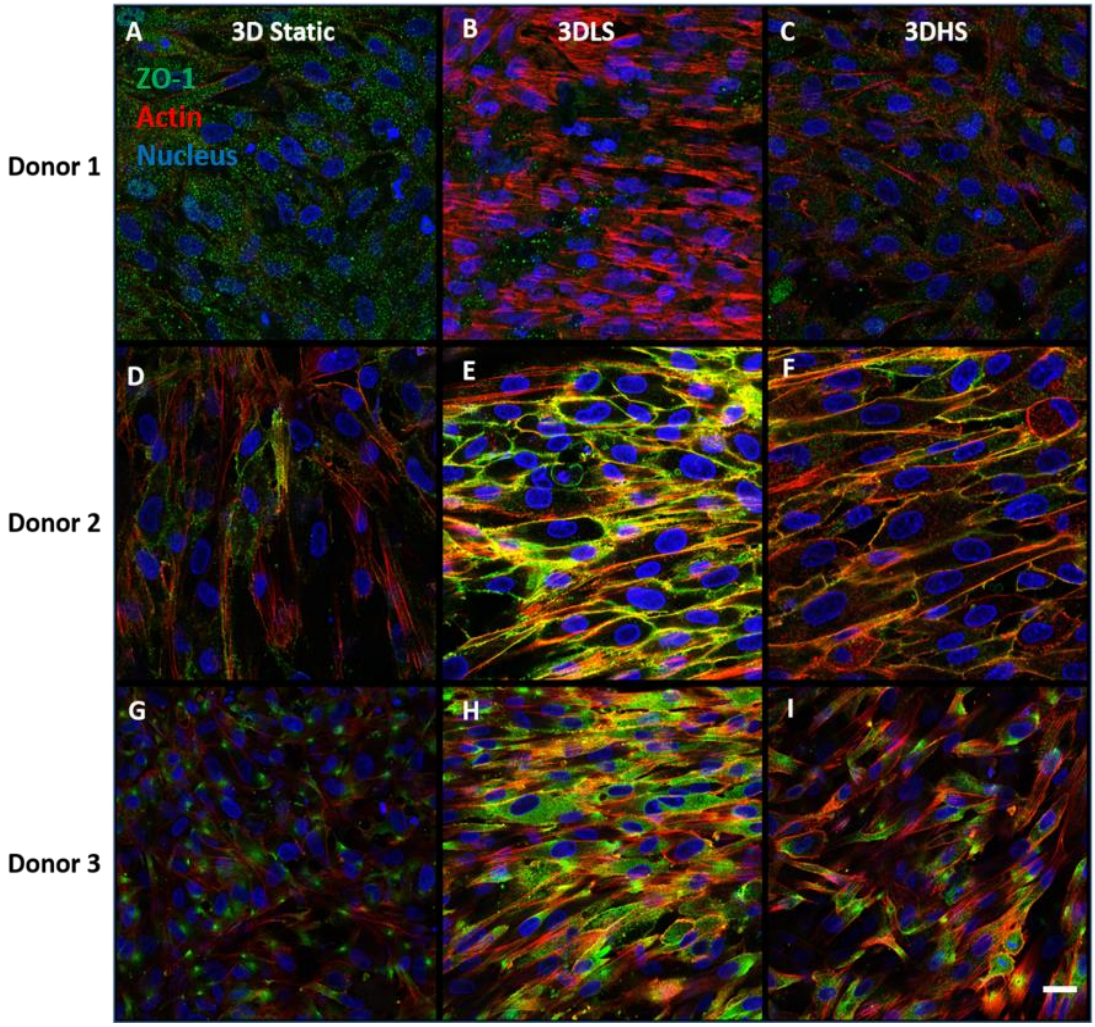

Figure 5.21 Immunocytochemical staining for ZO-1 (green) after 3 days shear stress culture. A – C Donor 1 ZO-1 staining. D – F Donor 2 ZO-1 staining. G – I Donor 3 ZO-1 staining. ZO-1 is stained in green. All cells were counterstained with f-actin (red) and DAPI (blue), Scale bar = 20µm**.**

Fluorescence intensity was quantified for ZO-1 protein expression (Figure 5.22). Expression of ZO-1 in donor 1 was significantly increased after 1 day of high shear stress compared to both the low shear stress and static groups (Figure 5.22 A (i)). Donors 2 and 3 in contrast had a significant decrease in ZO-1 expression after 1 day of high shear stress compared to 1 day static culture and low shear stress culture respectively (Figure 5.22 B

(i), C (i)). Donor 2 had a significant decrease in ZO-1 expression after 1 day of low shear stress. In contrast, donor 3 had a significant increase in ZO-1 expression after 1 day of low shear stress compared to the 1 day high shear stress group (Figure 5.22 C (i)).

After 3 days of shear stress, donor 1 had a significant decrease in ZO-1 expression in both the low shear and high shear stress group compared to the static group. The 3 day high shear stress group significantly increased ZO-1 expression compared to the 3 day low shear group (Figure 5.22 A (ii)). Donors 2 and 3 significantly increased ZO-1 expression after 3 days of low shear stress compared to the static group. The middle age donor also had a significant increase in ZO-1 expression after 3 days of high shear stress compared to the static group (Figure 5.22 B (ii) C (ii)). Donor 3 had a significant decrease in ZO-1 after 3 days of high shear stress compared to the 3 day low shear stress group (Figure 5.22 C (ii)).

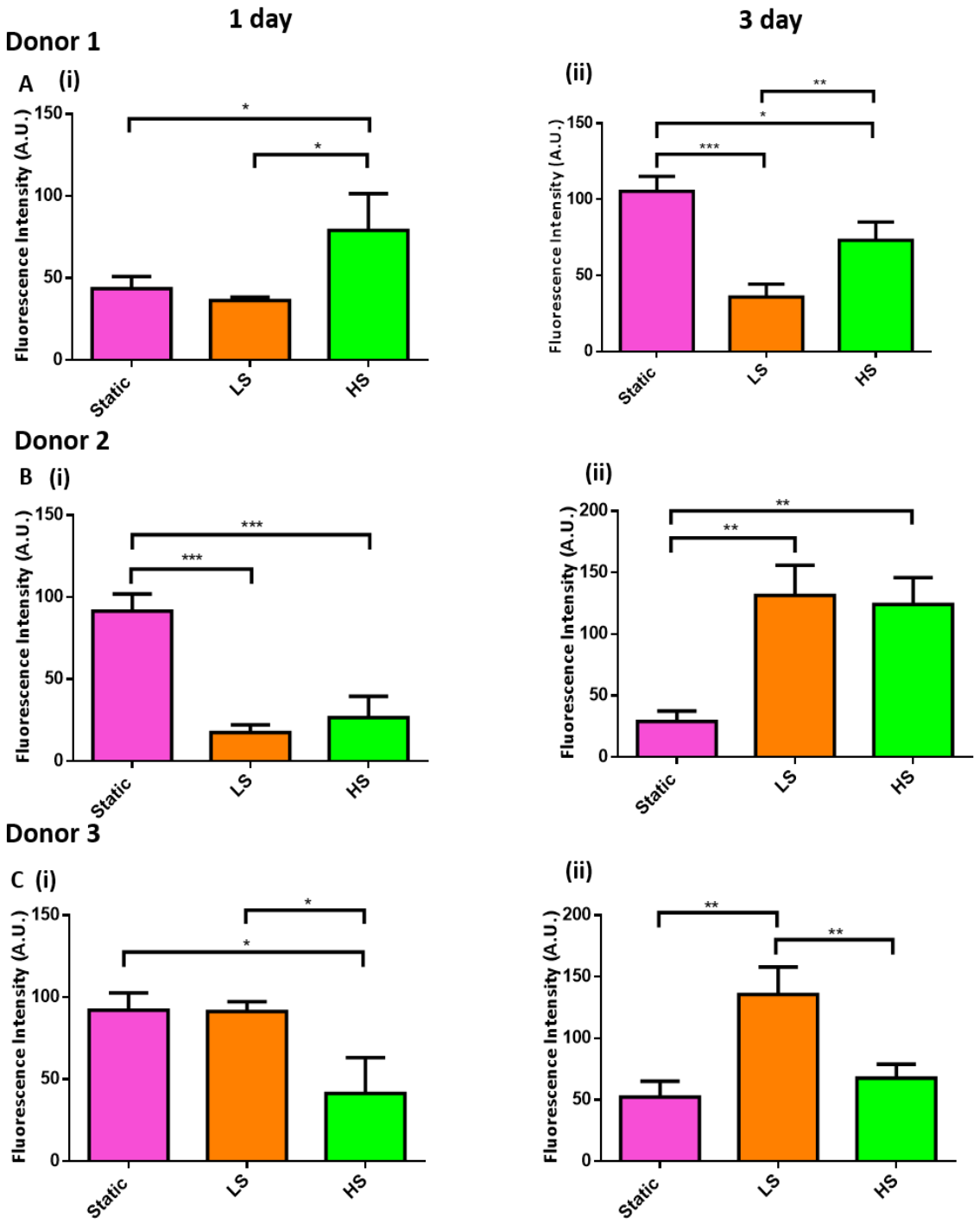

Figure 5.22 Fluorescence intensity of ZO-1 after 1 and 3 day static, low shear and high shear stress. (A) Donor 1 (i) 1 day and (ii) 3 day, (B) Donor 2 (i) 1 day and (ii) 3 day, (C) Donor 3 (i) 1 day and (ii) 3 day ZO-1 fluorescence intensity. Data are presented as the mean (±SD), significance calculated via one-way ANOVA with a Post-Tukey test, N=3, * = P ≤ 0.05, ** = P ≤ 0.01, *** = P ≤ 0.001.

All donors were compared for vimentin, integrin β 1 and ZO-1 expression as shown in Figure 5.23 Significant differences were observed between donors in each marker. Significant differences with a P<0.0001 are shown in the graph. Vimentin expression after 1 day static culture was significantly increased in donor 2 compared to donor 1 and 3 (Figure 5.23 A). Vimentin expression after 1 day high shear stress culture was significantly decreased in donor 3 compared to donor 2 (Figure 5.23 A). There was no significant changes in vimentin expression after 1 day low shear stress among donors. After 3 day static culture (Figure 5.23 B), Donor 1 had the most significant increase in vimentin expression after 3 days static culture compared to donor 2. Donor 3 had a significant decrease in vimentin expression after 3 days of low shear stress culture compared to donor 1 and 2. Donor 3 had a significant decrease in vimentin expression after 3 days of high shear stress compared to donor 1 and 2.

There were no significant differences between donors in integrin β 1 expression of static culture between donors after 1 day (Figure 5.23 C). Donor 2 had a significant increase in integrin β 1 expression after 1 day low shear stress compared to donor 1 and 3. After 3 days (Figure 5.23 D) of static culture, donor 1 displayed a significant increase in integrin β 1 expression compared to donor 3.

ZO-1 expression was significantly increased after 1 day (Figure 5.23 E) low shear compared to donor 2. After 1 day high shear stress culture donor 1 ZO-1 expression was significantly increased in donor 1 compared to donor 2 and 3. After 3 days (Figure 5.23 F) of static culture, donor 1 displayed a significant increase in ZO-1 expression compared to donor 2. After 3 days low shear stress culture donor 2 and 3 had a significant increase in ZO-1 expression compared to donor 1.

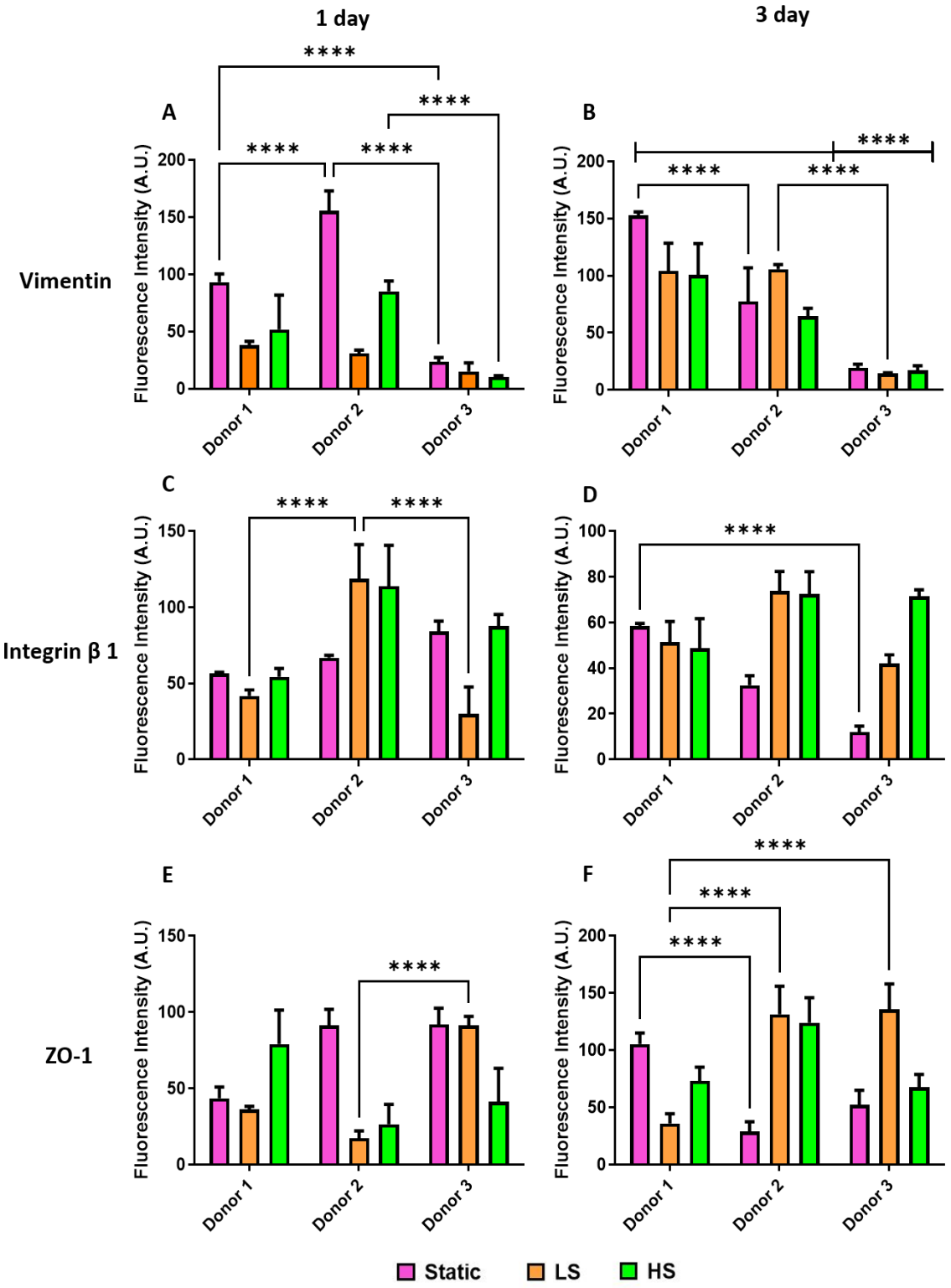

Figure 5.23 Fluorescence intensity of vimentin, Integrin β 1 and ZO-1 after 1 and 3 day static, low shear and high shear stress in all donors. (A + B) Vimentin, (C + D) Integrin β 1, (E + F) ZO-1 protein expression. Data are presented as the mean (±SD), significance calculated via two-way ANOVA with a Post-Tukey test, N=3, **** = P ≤ 0.0001.

5.4 Discussion

A panel of markers for the corneal epithelium were selected to create a phenotypic profile of the stem cell status of the cells after shear was applied. The markers selected range from stem cell markers expressed exclusively in the limbus where the stem cells are located, namely NP63α, ABCG2 and CK15 to the multipotent marker Nestin and the transient amplifying marker CK14. In addition, two mature epithelial markers CK3 and CK12 were examined. This allowed for a wide range of phenotypes to be examined including the limbal stem cell phenotype, transient amplifying phenotype and central corneal epithelial cell phenotype. Unlike previous studies in the literature, this study used unidirectional rather than bidirectional oscillatory shear which has been used in the literature to mimic the conditions of eye blinking (Hampel, Garreis et al. 2018, Abdalkader and Kamei 2020). The aim of this study was not to mimic a more in vivo phenotype of the corneal epithelium but rather elucidate what shear stress rate in a unidirectional manner would increase stem cell expression of the corneal cells and use this information to guide culturing conditions for expanding these cells ex vivo for transplantation, something that has not been previously explored.

The cornea's shear plane has been described previously (Elsheikh and Anderson 2005, Joseph Antony 2015) but the distribution of shear stress in the human cornea is not yet well understood. It is thought that shear is distributed in the cornea in a diamond like pattern that is both in horizontal and vertical planes. (Joseph Antony 2015) This presented work may aid in elucidating what shear stress environments the corneal epithelial cells are experiencing as well as if it is possible to use these mechanical stimuli to aid in cultivating these cells.

Among the shear stress environments examined, 1 day low shear showed the most significant upregulation of stem cell markers among donors which was decreased over three days. This suggests that exposing cells to 1 day of low shear can increase their expression of stem cell markers and that priming these cells to shear before culturing in static conditions may work to increase stem cell expression in the cells before using them for transplantation. There were observable differences in these results when comparing different donor ages, which may influence what shear stress should be used to increase stem cell marker expression depending on the age of the donor tissue. The youngest donor after 1 day high shear and low shear stress rather than low shear in the middle aged donor significantly increased stem cell marker expression. The older donor upregulated stem cell markers under both low and high shear stress after 1 day. Therefore, donor age should be taken into consideration when using these shear stress rates to increase stem cell marker expression.

After 3 days of shear stress both low and high shear stress upregulated stem cell markers. This was most significant in the youngest donor. The middle-aged donor varied in which shear stress upregulated each stem cell maker while the oldest donor significantly increased stem cell marker expression (NP63α and ABCG2) after 3 days of high shear stress. Longer-term shear stress culture again was influenced by donor age with each marker being less expressed with increased donor age. Perhaps, an intermediate shear stress rate between the low and high shear stress rates presented in this study may be more suitable for all donor ages to increase stem cell marker expression.

The transient amplifying marker CK14 was also significantly upregulated in response to 1 day low shear, this was the most significant in the middle age donor while

the oldest donor showed no significant differences. After 3 days of high shear stress this marker was significantly upregulated in all donors with the middle aged donor showing the most significant upregulation of this marker after 3 days of high shear stress. This would suggest that an initial low shear stress followed by a higher shear stress may increase the potential for cells to become more of a transient amplifying phenotype. As the corneal epithelial cells must have this transient amplifying capability at all times to allow continuous renewal of the epithelium it is not surprising that this marker was upregulated in both shear conditions. This is encouraging to observe that after exposure to unidirectional shear these cells while expressing stem cell markers also retain the ability to express CK14, which aids in wound healing and migration capability.

Mature markers CK3/12 were significantly upregulated under high shear stress in some donors or low shear stress in others. After 3 days in some cases these markers were not detected. As no obvious trend was observed for these mature markers it cannot be concluded how shear affects mature markers of the corneal epithelium. However, coupled with increased stratification after 3 days of high shear this may suggest that a more in vivo like phenotype is observed with a heterogeneous population of stem cell and mature markers.

TRPV4 is a mechanosensitive ion channel implicated in MSC shear stress response (Corrigan, Johnson et al. 2018) but has not been studied in relation to the fluid shear response and the corneal epithelium. In this study, it was shown that the TRPV4 gene was significantly upregulated in all donors in response to shear stress suggesting that TRPV4 may be involved in relaying mechanical signals in the fluid shear stress response. TRPV4

may serve as a therapeutic target in mimicking this shear stress response in vitro during cultivation of these cells for limbal stem cell transplantation.

Cellular alignment of cells was observed in the high shear stress groups after both 1 day and 3 days. The perpendicular cellular alignment observed in the high shear stress groups after both 1 day and 3 days has been shown to occur in other cell types where cells oriented perpendicular to flow in the region of maximum wall shear stress (Michalaki, Surya et al. 2020). This perpendicular alignment has been shown to effect endothelial cell migration patterns (Lin and Helmke 2009). Previous studies have shown that corneal epithelial cells exposed to a shear stress of 4 dyn/cm^2 align and migrate to aid in wound healing, whereas those that were exposed to higher shear stress (8 dyn/cm^2) had impaired wound healing capability (Molladavoodi, Robichaud et al. 2017). This would suggest from this presented study that those cells, which aligned under shear conditions, may also have enhanced migratory capability. Coupled with increased CK14 expression, these culturing conditions could aid in cultivating pro-migratory cellular phenotypes for the corneal epithelium while also retaining stem cell marker expression capabilities. Further research looking at wound healing after cells have been exposed to shear would be required to confirm this would be required to confirm this. Interestingly, those cells that did not show any obvious alignment in both static and low shear cell culture adopted a swirl pattern similar to what is seen in vivo in the migration patterns of these cells (Findlay, Panzica et al.).

Stratification of the cells after 3 days high shear coupled with a more mature phenotype suggests that this shear stress rate may be used to create a more in vivo like model of the corneal epithelium in vitro. It could also be used to cultivate cellular sheets

for transplantation. Corneal epithelial cells which have differentiated to a mature phenotype have shown their capability to de differentiate into stem cells to repopulate the stem cell niche when the limbus has been removed (Nasser, Amitai-Lange et al. 2018). Therefore, exposing these cells to shear stresses may enable this functionality when transplanted into the eye.

The role of integrin proteins in the corneal epithelium are vital for function in the stratified corneal epithelium, this is dependent upon the localisation, cell adhesion function and production (Stepp, Spurr-Michaud et al. 1993). Integrin β 1 has been implicated in the wound healing capabilities of the corneal epithelium that are vital for its function in the eye (Murakami, Nishida et al. 1992). A previous study that looked at integrin β 1 in HCECs exposed to shear and then examined wound healing capabilities showed that integrin β 1 was upregulated in cells exposed to shear suggesting an enhanced wound healing capability. In the presented study, 1 day high shear stress significantly increased integrin β 1 expression but this was influenced by donor age with the middle aged donor showing significantly increased integrin β 1 expression after 1 day of low shear and high shear compared to the other two donors. Both shear stress rates significantly increased integrin β 1 expression after 3 days in donor 2 and 3. This suggests that the after 3 days exposure to shear stress the migratory capacity of these cells are enhanced. This coupled with CK14 expression supports this result that 3 days of shear stress with the rate of shear stress dependent upon donor age can induce a pro migratory phenotype in the corneal epithelium while also expressing stem cell markers making it an attractive option for cultivation of these cells ex vivo.

The intermediate filament protein vimentin has been associated with an early differentiating highly motile phenotype of the corneal epithelium which is also involved in wound repair (SundarRaj, Rizzo et al. 1992, Castro-Munozledo, Meza-Aguilar et al. 2017). The effect that shear stress has on this protein has not been studied in the literature previously. Results showed that vimentin expression was significantly down regulated after 1 day of high and low shear stress, which was not surprising as this shear group did express more stem cell markers which would be slower cycling and not as migratory. No significant differences were observed after 3 days of shear exposure either, suggesting that shear stress does not affect vimentin expression after 3 days. When comparing donors together, donor 2 had the most significant increase in vimentin expression after 1 day high shear, while donor 1 had the most significant increase in vimentin expression after 3 days high shear culture. This suggests that donor age influences vimentin expression in fluid shear stress response of limbal epithelial cells.

Finally, barrier function as a measure of ZO-1 protein production measured by confocal microscopy was studied. The effects of ZO-1 and barrier function after shear stress exposure to the corneal epithelial cells have not been studied previously. Barrier function is an essential function of the corneal epithelium to protect the eye from pathogens and environmental insults. ZO-1 is concentrated at contact points of cells to create a seal between the cells (Sugrue and Zieske 1997). Results from this study showed that expression of the protein was significantly increased in the youngest donor after 1 day of high shear and 1 day low shear in the oldest donor while the middle aged donor showed a significant decrease in ZO-1 protein after 1 day high shear. However, after 1 day of low or high shear stress the cells did not show any good barrier function between cells but the protein was distributed inside the cell. The oldest donor did show distribution of

ZO-1 at contact points in all groups but this did not form a good barrier function of the cells as a whole monolayer. After 3 days, the middle-aged donor showed enhanced barrier function after 3 days low shear and high shear with the other two donors showing no obvious barrier formation between cells. Expression of ZO-1 protein varied a lot between donors with the oldest donor significantly increasing ZO-1 protein expression after 3 days of low shear while the middle aged donor significantly increasing ZO-1 protein in both shear groups. While it is difficult to determine exactly how these shear stress rates affect barrier function it can be concluded that donor age will influence the cells response to shear stress and formation of an intact barrier function. Perhaps a longer culture period with a more sophisticated experimental set up such as trans epithelial resistance measurements could help to elucidate how shear stress affects the barrier function capability of the corneal epithelium.

A total of three human donors were used for this study, analysis of each donor separately was conducted due to the variation of ages between donors which influences gene and protein expression in limbal epithelial stem cells (Dayoub, Cortese et al. 2018). Other stem cell types have also been shown to have their therapeutic efficacy affected by donor age including adipose derived stem cells (Yang, Kim et al. 2014) mesenchymal stem cells(Yamaguchi, Horie et al. 2018), hematopoietic stem cells transplantation(Lozano Cerrada, Altaf et al. 2018) and for T-cell therapy specifically (Azuma, Hirayama et al. 2002). This study also showed that donor age affected limbal stem cell response to fluid flow. However, further factors which may affect donor response to fluid flow include gender, health, time from death to enucleation, storage time and cause of death which weren't considered in this study. In order to more clearly identify if age is the factor that is influencing results, a much larger study with multiple donors from each age group would

be required but due to the limited availability of tissue this was not possible for this study (Van Meter, Katz et al. 2005, Lagali, Stenevi et al. 2009, Baylis, Rooney et al. 2013).

Results showed that LESCs exposed to 1 day low shear stress significantly enhances stem cell characteristics. After 3 days under shear conditions, in particular the high shear group displayed a more stratified epithelial layer with increased expression of the tight junction protein ZO-1 and a more in vivo orientation of cells were observed. TRPV4, a mechanosensitive ion channel implicated in shear stress in MSCs (Corrigan, Johnson et al. 2018) was significantly upregulated in both shear conditions, suggesting that this pathway is implicated in the corneal epithelium's shear stress response and may be a therapeutic target for mimicking this response in vitro, removing the need for shear.

This data suggests that culturing LESCs under low shear laminar flow rate would be optimum for upregulating stem cell markers in LESCs under culture for transplantation. Additionally, culturing LESCs under high shear conditions allow the cells to adopt a more stratified mature phenotype with enhanced barrier function, which may serve as an in vitro model of the corneal epithelium to study. The next chapter examines TRPV4 and it's role in how the corneal epithelium relays it's shear stress response.

5.5 Conclusion

This study has shown that culturing corneal epithelial cells under either a low shear stress (1.22 dyn/cm^2) or high shear stress (2.42 dyn/cm^2) significantly affects the corneal epithelial cells stem cell marker expression, wound healing capability and barrier function. This effect is enhanced over time with the cells adopting a more mature phenotype over three days in addition to expressing pro migratory proteins while also expressing (to a lower extent) stem cell markers, an attractive phenotypic profile for cells to be used in

limbal stem cell transplantation. This work has shown that rather than using typical static culture, a new way of culturing these cells under shear stress produces a more conducive cellular phenotype. This may aid in higher success rates of transplantation while also aiding in our knowledge of the corneal epithelial mechanobiology. The following chapter will explore the possible regulatory mechanism of this shear stress response and if it can be mimicked in vitro, removing the need for shear.

Chapter 6

Regulation of the Shear Stress Response in the Corneal Epithelium: TRPV4

6.1 Introduction

The results from Chapter 5 demonstrated that fluid shear stress significantly enhanced stem cell characteristics, wound healing capability and barrier function in the corneal epithelium with this effect increased over time. The shear stress rates of studies performed vary widely from 0.07 dyn/cm^2 to 50 dyn/cm^2 (Kang, Shin et al. 2014, Hampel, Garreis et al. 2018) as well as the length of time that the cells are exposed to shear with some studies exposing cells to shear for a couple of hours or seconds at particular days in culture. Studies thus far have shown that oscillatory shear stress increases differentiation and apoptosis of corneal epithelial cells and effect their migratory capacity and wound healing (Utsunomiya, Ishibazawa et al. 2016, Molladavoodi, Robichaud et al. 2017). However, little is known about how shear stress regulates corneal epithelial cells despite this being studied in many other cell types including MSCs (Corrigan, Johnson et al. 2018) and endothelial cells (Lu, Martino et al. 2021). Therefore, we wanted to investigate how shear stress regulates the corneal epithelium.

A study in 2016 showed that TGFβ signalling was involved in decreased wound healing and proliferation in the corneal epithelium following shear stress exposure (Utsunomiya, Ishibazawa et al. 2016). TRPV4, a mechanosensitive calcium signalling ion channel, has been shown to regulate TGFβ signalling in epithelial-mesenchymal transition as well as being essential in the nuclear translocation of YAP/TAZ in response to stiffness (Sharma, Goswami et al. 2019). In regards to fluid shear specifically, pharmacological activation of this channel has been shown to be required for MSC mechanotransduction, mediating osteogenic gene expression (Corrigan, Johnson et al. 2018).

Recent research into the role of TRPV4 in ocular function and pathologies has highlighted the therapeutic potential of TRPV4 in the ocular surface (Guarino, Paruchuri et al. 2020), corneal epithelial differentiation and barrier function (Martínez-Rendón, Sánchez-Guzmán et al. 2017) as well as corneal inflammation and fibrosis (Okada, Shirai et al. 2016). It was recently shown that the TRPV4 transcriptome is dominated by TRPV4 in the mouse corneal epithelium, localised at the basal and intermediate epithelial strata (Lapajne, Lakk et al. 2020). Another study looking at sensory nerve TRPV4 showed that it is critical in maintaining stemness of limbal basal cells and is an important mechanism of homeostasis and maintenance of the corneal epithelium (Okada, Sumioka et al. 2019). Gene expression analysis in Chapter 5 showed that an upregulation of the TRPV4 gene was observed under all flow conditions. Therefore, we wanted to determine whether using a TRPV4 agonist or antagonist would replace the need for culturing cells under shear.

Trafficking of TRPV4 is regulated by the activator GSK1016790A (Doñate-Macián, Enrich-Bengoa et al. 2019). The use of this activator allows TRPV4 to be trafficked to the cell membrane and allow influx of calcium, thereby increasing differentiation of the LSCs. Therefore, using an antagonist in the cell culture medium to culture LSCs may mimic the shear stress response previously observed, or at least increase stem cell marker expression in these cells. It may also decrease the number of cells adopting a more differentiated phenotype during the cell culture period. The aim of this study is to determine if TRPV4 activation or inhibition effects the behaviour of the cells.

6.2 Materials and Methods

6.2.1 *Cell culture*

Cell culture was performed using the same protocol described in Chapter 5. Three donors of varying ages (45, 54 and 66 years old) – named Donor 1, 2, and 3 as shown in Table 4. All cells used in the experiment were at passage 4 or below.

Table 4 Donor age and number

Donor	1	2	3
Age (Years)	45	54	66

6.2.2 *TRPV4 activation/inhibition*

TRPV4 agonist GSK-1016790A (Abcam) and TRPV4 antagonist HC067047 (ab145868) (Abcam) were dissolved in DMSO up to 1 M. A 1 M vehicle control with DMSO and sterile PBS was also prepared. Each solution was diluted to 50 nM in cell culture media for subsequent treatment of cells. Samples used for calcium imaging used phenol free media.

Cells were left overnight in fluid flow slides before treatment of cells with either the TRPV4 agonist, TRPV4 antagonist, vehicle DMSO control or media alone control. The vehicle DMSO control group serves to determine how the DMSO which is required to dissolve the TRPV4 agonist or antagonist effects cell behaviour. The media alone control is just corneal epithelial media with no DMSO, agonist or antagonist treatment. Cells were treated for 2 days with a media exchange each day. After treatment of cells with the appropriate media formulation cells were prepared for RT-PCR, metabolic activity, calcium imaging or fixed for immunocytochemical analysis.

6.2.3 *Calcium imaging*

The cell permeant calcium indicator Oregon Green 488 BAPTA-1AM (OGB) (Invitrogen) was used to observe changes in calcium signalling. OGB stock was prepared in DMSO at 2 mM, all further dilutions were in phenol red free DMEM, 0.5% FBS. The slides were coated with gelatin for 1 hour at 37 °C, LESC's were then seeded at 500,000 cells/slide (200,000 cells/cm^2) in 200 µl of media to allow a fully confluent layer to be achieved. Cells were left to attach for 5 hours and washed with media to remove any unattached cells. Cells were incubated in 40 µM OGB at 37 °C for 1.5 hours before rinsing twice in PBS (Sigma). Slides were placed onto the microscope stage and treated with TRPV4 agonist GSK-1016790A. The slides were imaged using an Olympus IX83 epifluorescent microscope (Olympus, Germany) at 40x. Exposure was kept constant between control and treatment groups below 600 milliseconds. Image acquisition occurred every 1.29 seconds for approximately 11 minutes. The fold change in fluorescence over baseline was used to calculate response where baseline was taken as 30 seconds prior to treatment. A fold change over baseline greater than 1.2 fold was considered as responsive to treatment.

6.2.4 *RT-PCR*

RT-PCR was performed using the same protocol described in Chapter 3. The following primers were used: NP63α (custom-made primer sequence adapted from Robertson et al. (Robertson, Ho et al. 2008) ABCG2 (Hs01053790_m1), CK15 (Hs00267035_m1), Nestin (Hs00707120_s1), CK14 (Hs00265033_m1), CK3 (Hs00365080_m1), CK12 (Hs00165015_m1), TRPV4 (Hs01099348_m1) and GAPDH (Hs02758991_g1).

6.2.5 *Immunocytochemistry*

Immunocytochemistry was performed using the same protocol described in Chapter 3. The following antibodies and dilutions were used: CK3 at 1:500 dilution (CBL218 - Sigma), anti-p63 (ΔN), poly6190, rabbit polyclonal 619002 (Biolegend) at 1:1000, ZO-1 at 1:200 dilution (40-2200 - Biosciences). For CK3 goat anti-mouse IgG H&L (Alexa Fluor® 488) (ab150113 - Abcam) was used. For all other proteins donkey anti-rabbit IgG H&L (Alexa Fluor® 488) (ab150073 - Abcam) was used.

Mean fluorescence intensity was determined using ImageJ software and corrected for background. An image of the middle of each stack was acquired to observe morphology and distribution of the proteins in the cell.

6.2.6 *Metabolic activity*

Cell Metabolic activity was measured using the same protocol described in Chapter 3.

6.2.7 *Calcium imaging*

After treatment with the agonist the average fold change in fluorescence from three cells in each donor over the first 100 frames (approximately 2 minutes) was calculated using the following formula:

$$\frac{F_{ROI} - F_{background}}{Average\ (F_{ROI} - F_{background}) prior\ to\ OFF}$$

Where F_{ROI} = fluorescence in region of interest (inside the cell) minus $F_{background}$ = fluorescence in region outside of the cell divided by the average of this value before treatment was applied to the cell (Prior to OFF).

6.2.8 *Statistical analysis*

All experiments were carried out in triplicate, statistical analysis and outlier calculation was performed using GraphPad Prism software. Data are presented as the mean $\pm$ standard deviation (SD), significance was calculated either via one-way ANOVA with Post-Tukey test or two-way ANOVA with Šídák's multiple comparisons test. Significance deemed as $p \leq 0.05$ for all data sets.

6.3 Results

6.3.1 *Calcium imaging*

Results from calcium imaging experiments were used to graph cellular response to TRPV4 agonist treatment as shown in Figure 6.1. Cells were considered responsive to treatment if a fold change over baseline was greater than 1.2 (Corrigan, Johnson et al. 2018). When cells were treated with the agonist, all donors displayed a fold change greater than 1.2, which decreased over time indicating that all donors were responsive to agonist treatment; in particular, donor 3 exhibited the most satisfactory response (Figure 6.1). The 1.2 fold change threshold is represented as a dashed line in the figure.

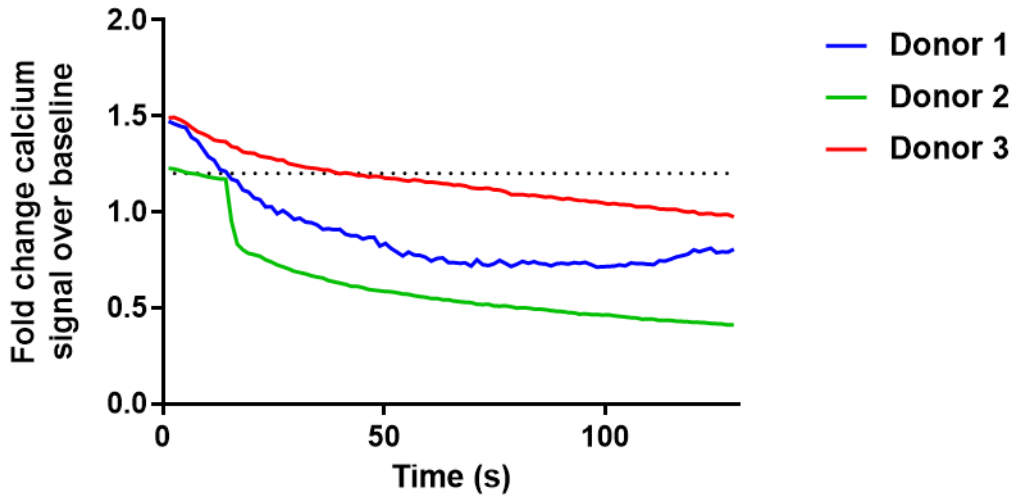

Figure 6.1 Calcium profile of 3 donors during TRPV4 agonist treatment. Treatment with agonist begins at t = 0s. Dashed black line at 1.2 represents fold change threshold that cells are considered responsive.

6.3.2 *Differentiation*

Gene expression of a panel of limbal stem cell markers (NP63α, ABCG2, CK15 and Nestin), transient amplifying marker CK14 and mature markers CK3 and CK12 were examined for each donor.

6.3.2.1 *Stem cell marker expression*

After treatment with either a TRPV4 agonist, TRPV4 antagonist, vehicle control or media alone changes in both gene and protein expression of stem cell markers as well as mature markers were examined. This data was normalised to either media treatment or vehicle control treatment. Confocal microscopy was used to determine protein CK3 and NP63 expression in the cells.

Stem cell marker expression was significantly increased across all donors after TRPV4 treatment. Donor 1 displayed a significant increase in NP63α expression after 50nM antagonist treatment compared to the control media treatment alone, no

significant differences were observed in the vehicle controlled group (Figure 6.2 A). Donor 2 displayed a significant increase in NP63α expression after 50nM antagonist treatment compared to 50nM agonist treatment in both the media and vehicle controlled groups (Figure 6.2 C). Donor 3 displayed a significant increase in NP63α expression after 50nM antagonist treatment compared to 50nM agonist treatment and the media treatment control with no significant differences observed in the vehicle controlled group (Figure 6.2 E).

ABCG2 gene expression was significantly increased in donor 1 after 50nM agonist treatment in the vehicle controlled group compared to the control (Figure 6.2 B). Donor 2 ABCG2 gene expression was significantly increased after 50nM antagonist treatment compared to 50nM agonist and control groups in both the media and vehicle-controlled groups (Figure 6.2 D). Donor 3 also had a significant increase in ABCG2 expression after 50nM antagonist treatment in the media controlled group compared to all other treatments, no significant differences were observed between groups in the vehicle controlled group (Figure 6.2 F).

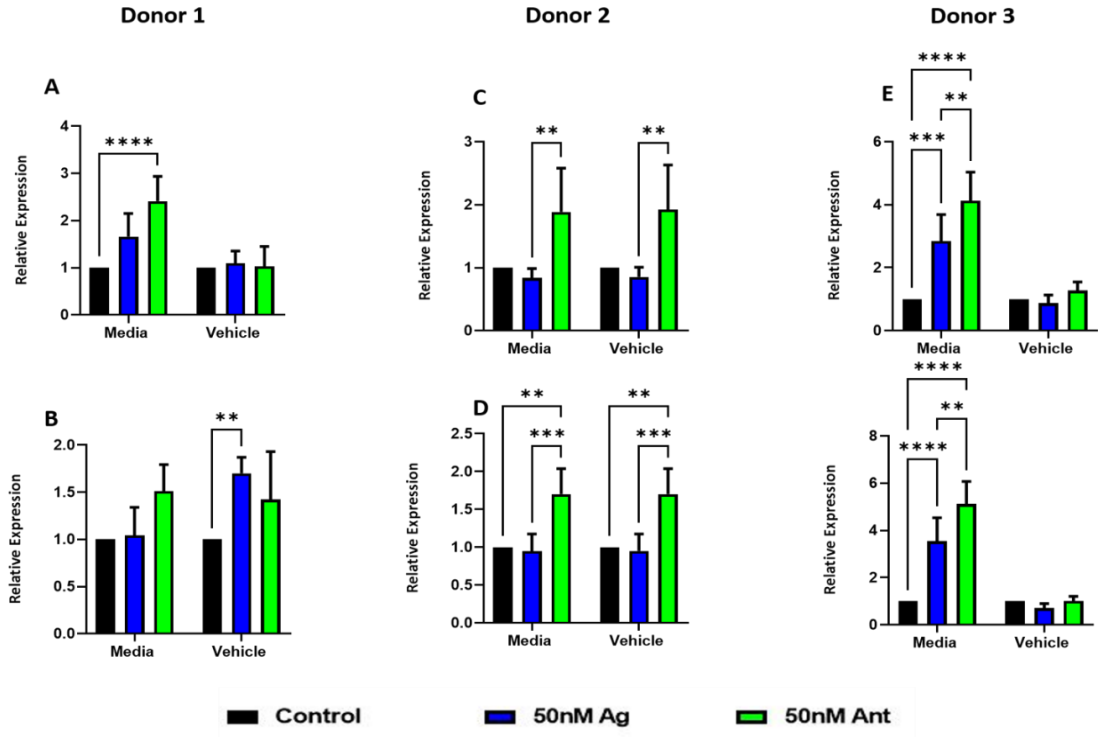

Figure 6.2 Real time PCR of stem cell markers NP63α and ABCG2 after vehicle, media, 50nM agonist and 50nM antagonist treatment. (A + B) Donor 1, (C + D) Donor 2, (E + F) Donor 3 NP63α and ABCG2 gene expression. Data are presented as the mean (±SD), normalised to either media or vehicle control, significance calculated via two-way ANOVA with a Šídák's multiple comparisons test, N=4, ** = P ≤ 0.01, *** = P ≤ 0.001, **** = P ≤ 0.0001.

Two other stem cell markers CK15 and Nestin were examined (Figure 6.3). Donor 1 had a significant increase in CK15 gene expression after 50nM antagonist treatment in the vehicle-controlled group compared to control treatment (Figure 6.3 A). Donor 2 also had a significant increase in CK15 gene expression in the media and vehicle-controlled groups after 50nM antagonist treatment compared to 50nM agonist and control treatment (Figure 6.3 C). Donor 3 had a significant increase in CK15 gene expression after 50nM agonist and antagonist treatment compared to the control in the media-controlled group, no significant differences were observed for CK15 expression in the vehicle controlled group (Figure 6.3 E).

Donor 1 Nestin gene expression was significantly decreased after 50nM agonist treatment compared to the control in the media controlled group, while Nestin gene expression was significantly increased in the vehicle controlled group after 50nM agonist treatment (Figure 6.3 B) compared to the control and 50nM antagonist group. Donor 2 Nestin gene expression was significantly increased after 50nM antagonist treatment compared to 50nM agonist and control treatment in both the media controlled and vehicle controlled groups (Figure 6.3 D). Donor 3 Nestin gene expression was also significantly increased after 50nM antagonist treatment compared control treatment in the media-controlled group (Figure 6.3 F). There were no significant differences observed in Nestin expression in the vehicle controlled groups between treatments in this donor.

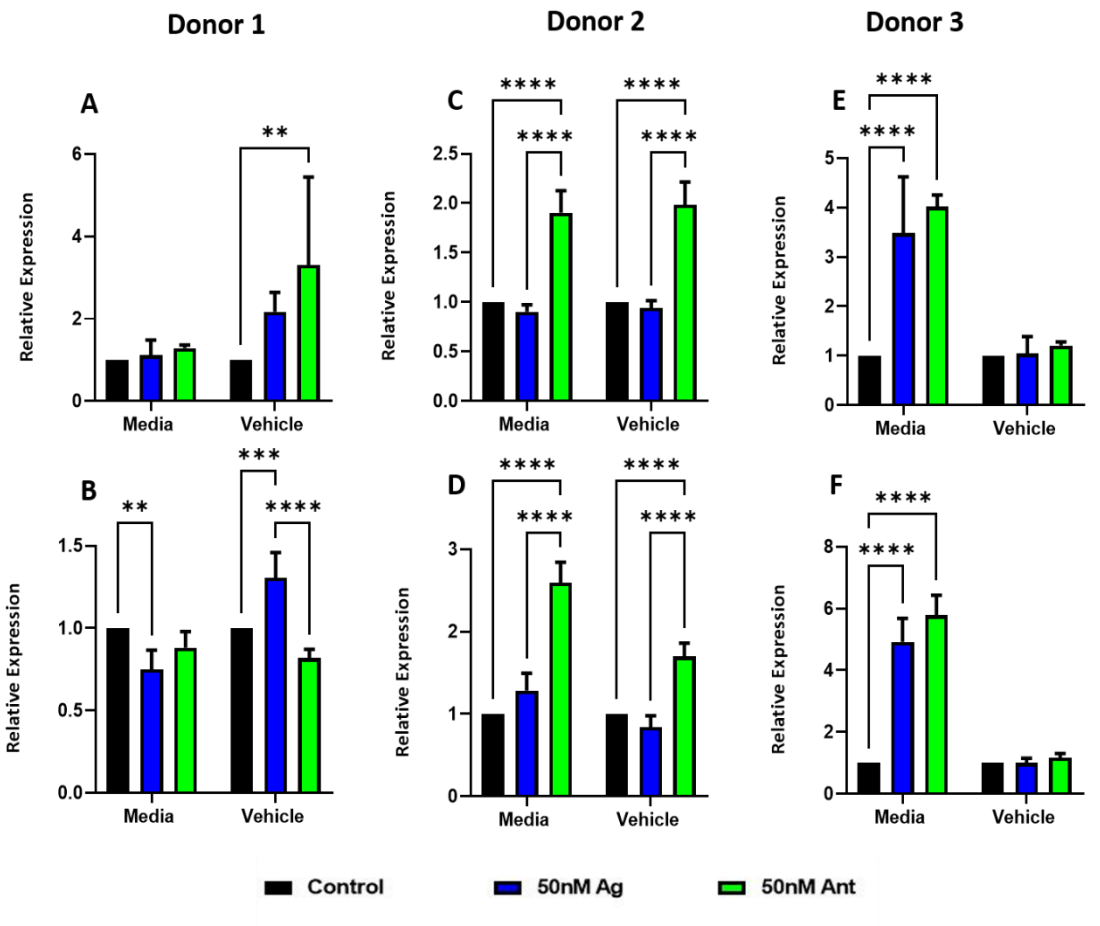

Figure 6.3 Real time PCR of stem cell markers CK15 and Nestin after vehicle, media, 50nM agonist and 50nM antagonist treatment. (A + B) Donor 1, (C + D) Donor 2, (E + F) Donor 3 CK15 and Nestin gene expression. Data are presented as the mean (±SD), normalised to either media or vehicle control significance calculated via two-way ANOVA with a Šídák's multiple comparisons test, N=4, ** = P ≤ 0.01, *** = P ≤ 0.001, **** = P ≤ 0.0001.

6.3.2.2 *Transient amplifying marker expression*

The transient amplifying marker CK14 was also examined as shown in Figure 6.4. There were no significant differences observed in CK14 expression in Donor 1 or 2 (Figure 6.4 A + B). Donor 3 displayed a significant increase in CK14 expression after 50nM antagonist treatment in the media controlled group compared to 50nM agonist and control group (Figure 6.4 C).

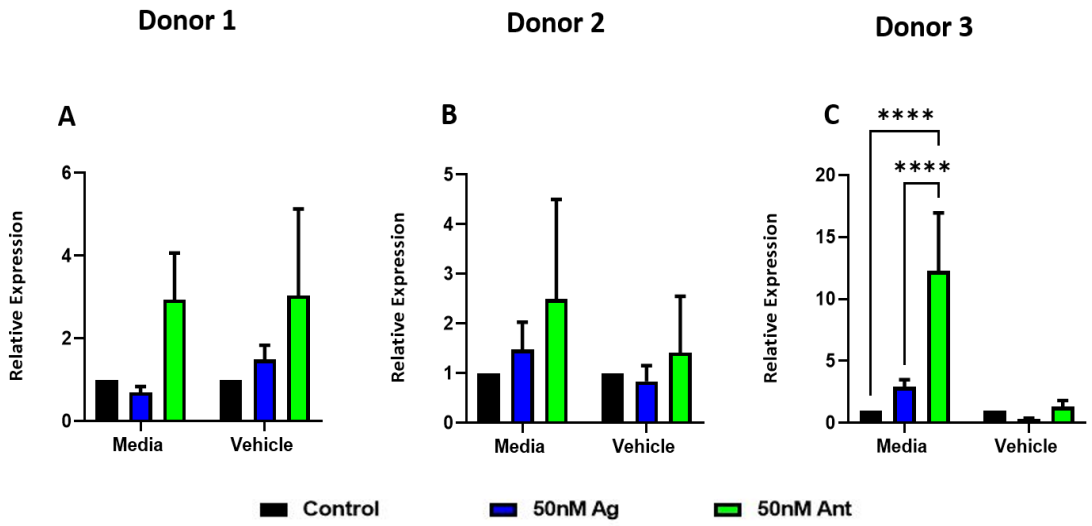

Figure 6.4 Real time PCR of transient amplifying marker CK14 after vehicle, media, 50nM agonist and 50nM antagonist treatment. (A) Donor 1, (B) Donor 2, (C) Donor 3 CK14 gene expression. Data are presented as the mean (±SD), normalised to either media or vehicle control significance calculated via two-way ANOVA with a Šídák's multiple comparisons test, N=4, **** = P ≤ 0.0001.

6.3.2.3 *Mature marker expression*

There were no significant differences in CK3 gene expression in donor 1 and 2 as shown in Figure 6.5 A and C. Donor 1 had increased CK3 expression after 50nM agonist treatment in the media controlled group while CK3 expression was increased after 50nM antagonist treatment in the vehicle controlled group in this donor, albeit not significant (Figure 6.5 A). Donor 2 had increased CK3 expression after 50nM antagonist treatment in both media and vehicle controlled treatment groups (Figure 6.5 C). Donor 3 CK3 expression was significantly increased after 50nM agonist treatment compared to the control in the media controlled treatment group, no significant differences in CK3 expression were observed for the vehicle controlled group in this donor (Figure 6.5 E).

Donor 1 displayed significant differences in CK12 expression (Figure 6.5 B) after 50nM antagonist treatment in the media controlled group compared to 50nM agonist.

While the vehicle-controlled group displayed a significant increase in CK12 expression after 50nM antagonist treatment compared to the 50nM agonist treatment in the media-controlled group. After 50nM agonist treatment in the vehicle-controlled group, CK12 expression was significantly increased compared to the control group and the 50nM agonist and control group in the media-controlled group. Donor 2 (Figure 6.5 D) CK12 expression was significantly increased after 50nM antagonist treatment in the media-controlled group compared to control and 50nM agonist treatment. This was also the case for Donor 3 (Figure 6.5 F).

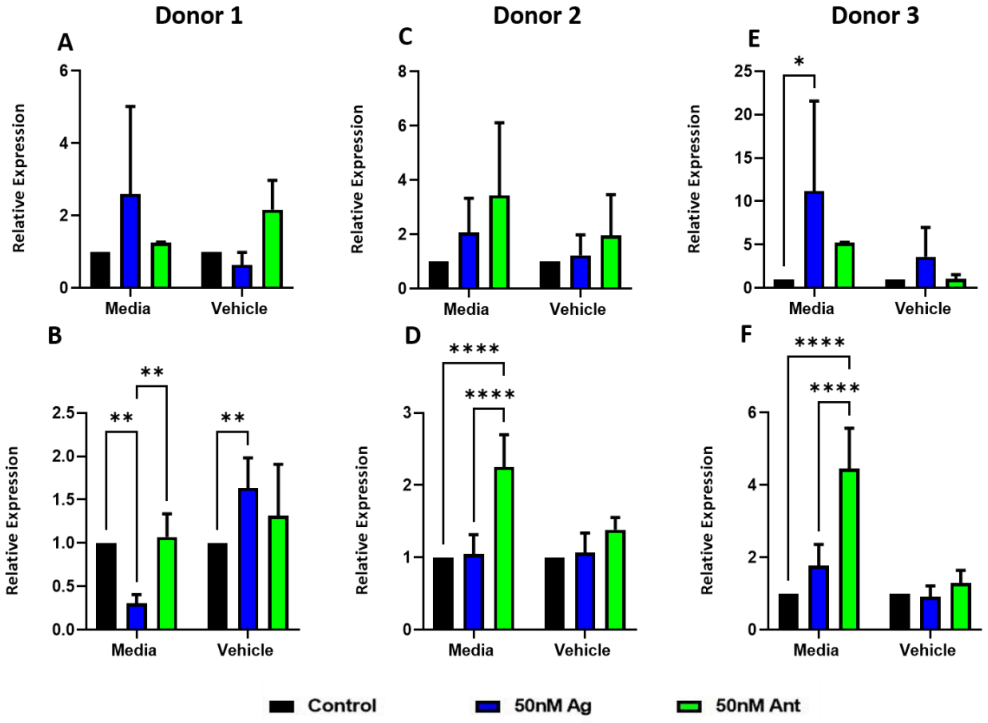

Figure 6.5 Real time PCR of mature markers CK3 and CK12 after vehicle, media, 50nM agonist and 50nM antagonist treatment. (A + B) Donor 1, (C + D) Donor 2, (E + F) Donor 3 CK3 and CK12 gene expression. Data are presented as the mean (±SD), normalised to either media or vehicle control significance calculated via two-way ANOVA with a Šídák's multiple comparisons test, * = P ≤ 0.05, ** = P ≤ 0.01, **** = P ≤ 0.0001.

6.3.2.4 *NP63 and CK3 Expression*

Images of CK3 and NP63 were acquired to look at co-expression of each protein under media treatment alone, vehicle control, 50nM agonist and 50nM antagonist treatment. The middle of each stack is represented in the below images. All donors showed a higher level of NP63 expression, all groups expressed both CK3 and NP63 protein.

NP63 localisation was observed both in the cytoplasm and in the nucleus in the media only group (Figure 6.6 A, E, I); the other groups all had nuclear NP63 expression. Donor 3 had the most visible nuclear NP63 expression compared to the other donors (Figure 6.6 I – L).

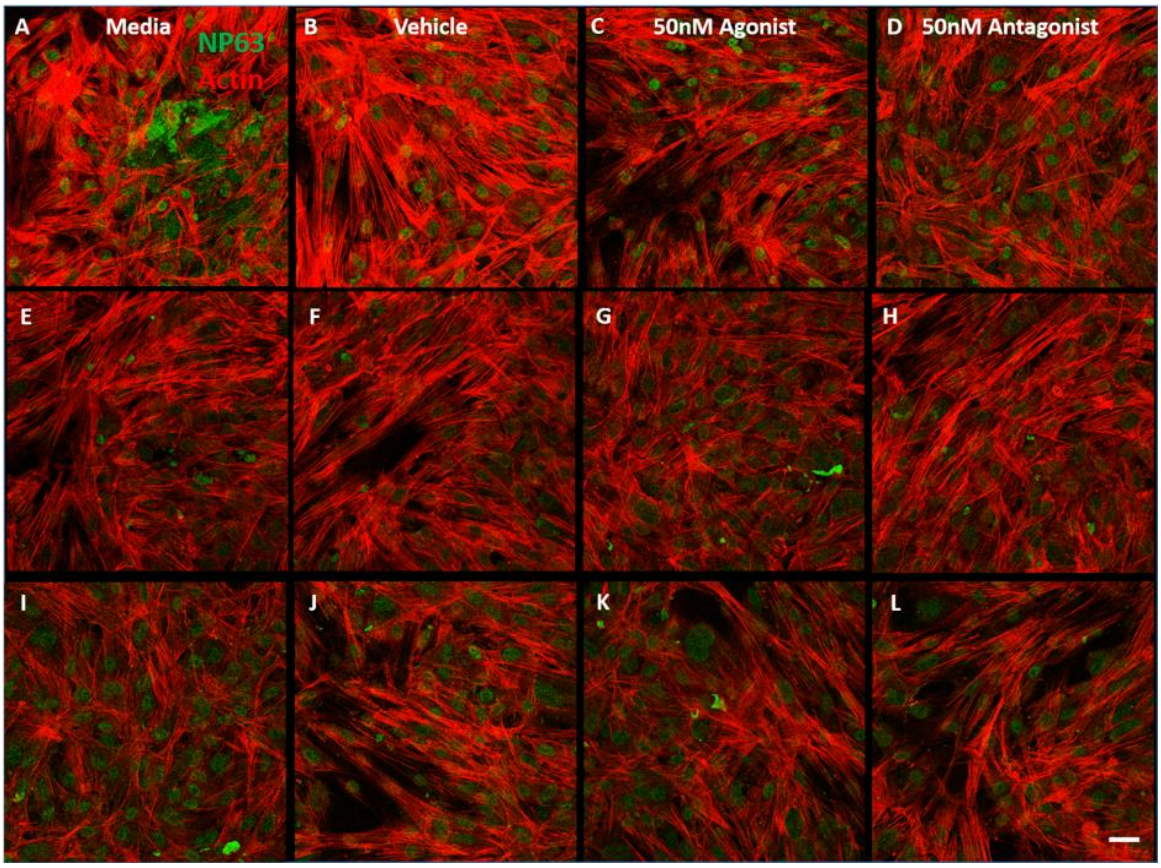

Figure 6.6 All donors Immunocytochemical staining for NP63 expression after media, vehicle, 50nM agonist and 50nM antagonist treatment. (A - D) Donor 1, (E - H) Donor 2, (I - L) Donor 3 NP63 expression. NP63 is stained in green. Cells were counterstained with f-actin (red). Scale bar = 20µm.

CK3 localisation in all groups correlated to actin expression (Figure 6.7), the vehicle control had the highest level of CK3 expression compared to all other groups (Figure 6.7 B). In general, visualisation of CK3 protein under confocal microscopy difficult to image due to the low expression of CK3 protein.

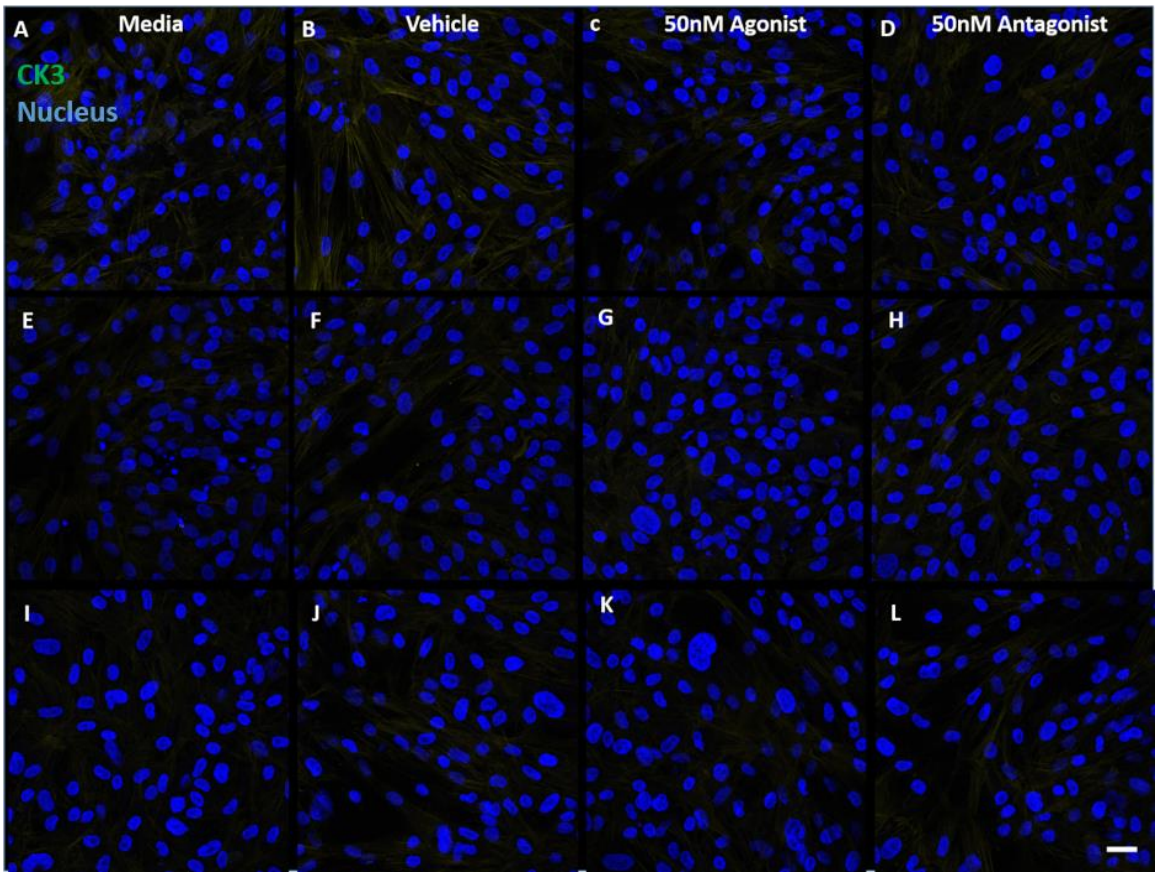

Figure 6.7 All donors Immunocytochemical staining for CK3 expression after media, vehicle, 50nM agonist and 50nM antagonist treatment. (A - D) Donor 1, (E - H) Donor 2, (I - L) Donor 3 CK3 expression. CK3 is stained in green. Cells were counterstained with DAPI (blue). Scale bar = 20µm.

Confocal microscopy was used to quantify protein expression of both NP63 and CK3 expression in the cellular monolayer. Both CK3 (Figure 6.8 A,C,E) and NP63 (Figure 6.8 B,D,F) were expressed under all conditions, with NP63 expressed more so than CK3 (Figure 6.8).

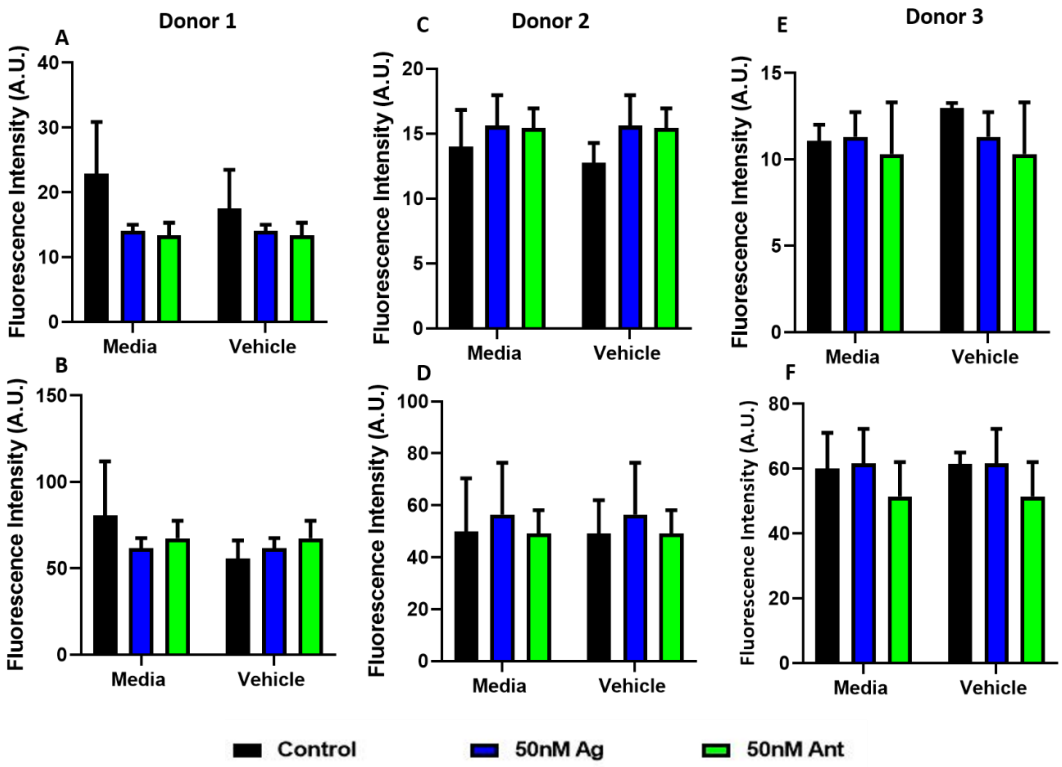

Figure 6.8 Fluorescence intensity of CK3 and NP63 after media, vehicle, 50nM agonist and 50nM antagonist treatment. (A + B) Donor 1, (C + D) Donor 2, (E + F) Donor 3 CK3 and NP63 expression. Data are presented as the mean (±SD), normalised to either media or vehicle control**.**

6.3.3 *Barrier function*

Confocal Microscopy was used to observe ZO-1 protein distribution as a measure of barrier function formation of the cells after treatment with media alone, vehicle control, 50nM agonist or antagonist as shown in Figure 6. 9. Donor 1 showed even distribution of ZO-1 among all groups with no clear tight junctions formed; the protein was distributed inside each cell (Figure 6. 9 A-D). The donor 2 media and vehicle control groups had little ZO-1 protein present in the cells (Figure 6. 9 E-H). The cells treated with 50nM agonist showed concentration of the ZO-1 protein at some cell-to-cell contacts in donor 2 (Figure 6. 9 G). This was also the case for cells treated with 50nM antagonist, with less concentration at cell-to-cell contacts visible (Figure 6. 9 H). Donor 3 showed an even

distribution of ZO-1 production amongst all groups. No tight junction formation was observed in this donor (Figure 6. 9 I – L).

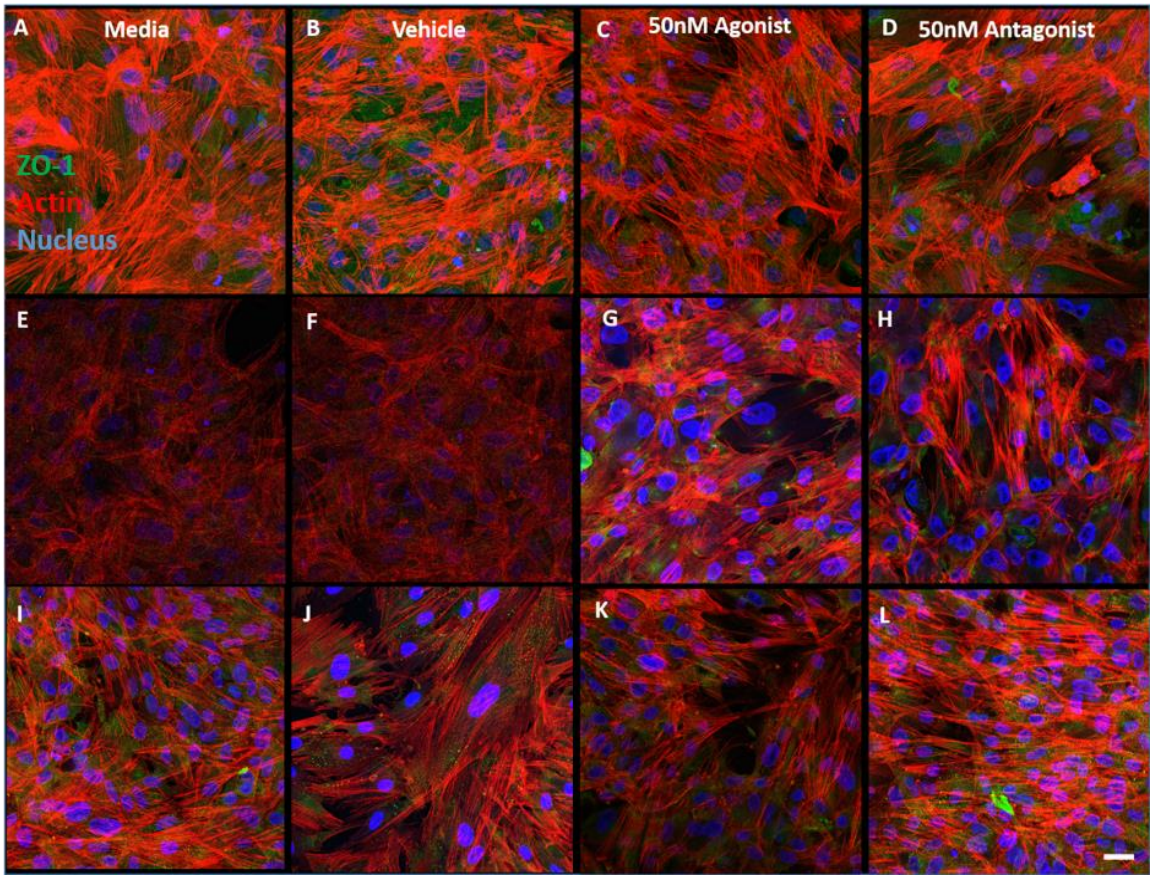

Figure 6. 9 All donors Immunocytochemical staining for ZO-1 expression after media, vehicle, 50nM agonist and 50nM antagonist treatment. (A – D) Donor 1, (E – H) Donor 2, (I – L) Donor 3 ZO-1 expression. ZO-1 is stained in green. Cells were counterstained with f-actin (red) and DAPI (blue). Scale bar = 20µm.

Confocal microscopy was used to quantify protein concentration of the tight junction protein ZO-1 as a measure of barrier function in the LSCs. This was achieved by measuring fluorescence intensity on Image J. All donors were pooled as shown in Figure 6.10 There were no significant differences in ZO-1 expression observed between media and vehicle groups.

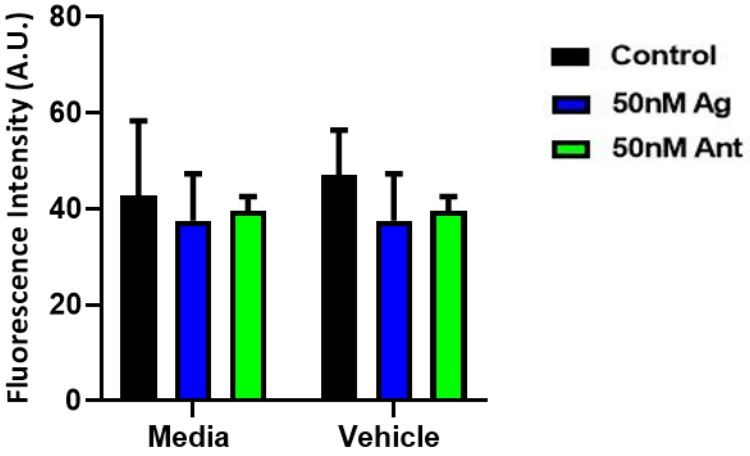

Figure 6.10 All Donors Fluorescence intensity of ZO-1 after vehicle, media, 50nM agonist and 50nM antagonist treatment. Data are presented as the mean (±SD), normalised to either media or vehicle control

6.3.4 *Metabolic Activity*

A presto blue assay was used to determine metabolic activity of cells after treatment with either 50nM agonist, 50nM antagonist, vehicle control or media alone control. Overall, metabolic activity of the cells were similar to the control group.

The donor 1 vehicle control had significantly higher metabolic activity compared to media treatment alone and 50nM agonist treatment (Figure 6.11 A). Donor 2 had a significant upregulation of metabolic activity in the 50nM agonist treatment group compared to all other treatment groups (Figure 6.11 B). Donor 3 showed no significant changes in metabolic activity (Figure 6.11 C).

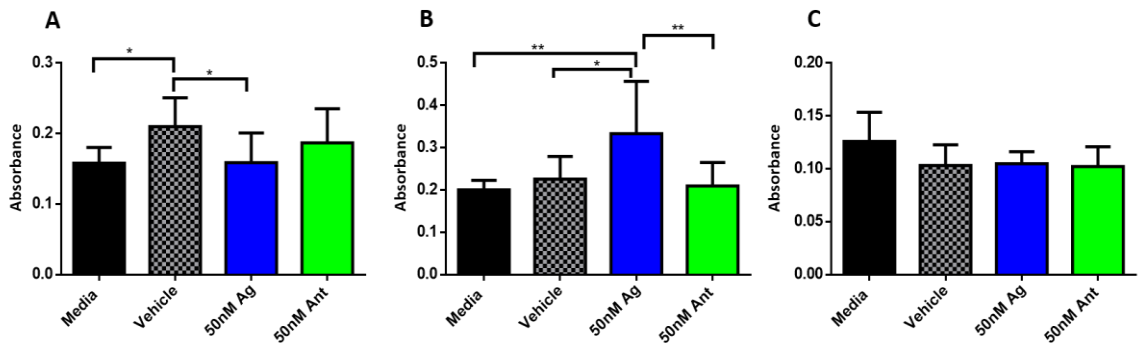

Figure 6.11 Metabolic activity of donor 1,2 and 3 after treatment of media, vehicle, 50nM agonist and 50nM antagonist treatment. (A) Donor 1 metabolic activity, (B) Donor 2 metabolic activity, (C) Donor 3 metabolic activity. Data are presented as the mean (±SD), significance calculated via one-way ANOVA with a Post-Tukey test, N=3, * = $P \leq 0.05$, ** = $P \leq 0.01$.

6.4 Discussion

The mechanosensitive ion channel TRPV4 has been implicated in a number of cell types in response to shear stress but has not been studied in the corneal epithelium previously. In the previous chapter, it was shown that the TRPV4 gene was upregulated under fluidic shear stress. This coupled with its role in TGFβ signalling led to the hypothesis that TRPV4 may be a pathway in which limbal stem cells regulate their shear stress response and could be therapeutically targeted.

Calcium imaging experiments confirmed that TRPV4 agonist treatment successfully opened TRPV4 channels to allow influx of calcium. This allowed for optimisation of the concentrations used for TRPV4 treatment with no cellular toxicity but still evoking a response from calcium signalling experiments to allow for the same agonist and antagonist concentrations. The initial observed response after treatment followed by a decrease in signal was expected due to the nature of calcium signalling in the cell which can act within milliseconds in localized regions (Berridge 2001).

The same panel of markers used to create a phenotypic profile of these limbal stem cells in shear stress experiments were used for this study to assess whether therapeutically targeting TRPV4 would elicit the same responses seen in shear stress experiments. Data was compared between media and vehicle treatment in each donor. A significant increase in stem cell markers was observed after TRPV4 treatment. Specifically, NP63α gene expression was significantly upregulated after 50nM antagonist treatment compared to the control treatment for donor 1, 50nM agonist treatment for donor 2 and the control and 50nM agonist treatment for donor 3 in the media controlled group. However, only donor 2 had a significant increase in NP63α gene expression after 50nM antagonist treatment compared to the 50nM agonist group in the vehicle controlled groups. This suggests that the TRPV4 treatment preparation in DMSO has an effect on NP63α gene expression of these cells. ABCG2, CK15 and Nestin expression showed a similar result among donors with only donor 2 displaying a significant increase in gene expression after 50nM antagonist treatment compared to the control and 50nM agonist group in both the vehicle and media-controlled groups. ABCG2, CK15 and Nestin expression was, however, significantly increased after 50nM antagonist treatment in donor 3 compared to 50nM agonist and control treatment in the media-controlled group.

Based on these results it can be concluded that TRPV4 antagonist treatment has a significant effect on stem cell marker expression. However, further experimentation investigating the effect of DMSO is required to determine how much it effects cellular response to TRPV4 treatment as only one donor (donor 2) displayed significant increases in stem cell expression in vehicle-controlled groups while other donors displayed significant increases in stem cell marker expression compared to the agonist treatment rather than the vehicle control. Chapter 3 of this thesis showed that a low calcium

concentration in the cell media was best at retaining stem cell characteristics with high calcium media concentrations decreasing stem cell marker expression. This coupled with the results of this chapter blocking TRPV4 and thereby reducing calcium in the cells further supports the theory that a TRPV4 inhibitor may be used to promote stem cell marker expression in the corneal epithelium.

The transient amplifying marker CK14 did not show any significant increases in expression among donors of note. Donor 3 did have a significant increase in CK14 gene expression compared to the 50nM agonist treatment in the media-controlled group and no significant differences were observed in the vehicle-controlled group. Again, suggesting that DMSO is having an effect on the expression of CK14.

The mature marker CK3 showed significant increase in gene expression in donor 3 in the 50nM agonist treated media controlled group, which would be expected considering the influx of calcium after TRPV4 treatment. CK12 expression did show significant differences in gene expression among donors. Donor 1 CK12 expression was significantly increased after 50nM antagonist treatment compared to 50nM agonist treatment, which significantly decreased CK12 expression compared to control in the media controlled group. Donor 1 showed a significant increase in CK12 expression after 50nM agonist treatment compared to the vehicle control. Surprisingly, Donor 2 (which did show a significant increase in stem cell expression compared to the vehicle only treatment) and donor 3 showed a significant increase in CK12 expression after 50nM antagonist treatment compared to the 50nM agonist treatment in the media controlled group. No significant differences were observed between groups in the vehicle controlled

groups, for donor 2 and 3 again suggesting that DMSO alone may be causing this effect rather than antagonist treatment alone.

The results from the gene expression analysis shows that DMSO treatment alone plays a role in stem cell marker expression and also suggests that donor variation in the cellular response to these cell treatments occur. Studies in the literature have shown the effects of DMSO on stem cell differentiation as well as survival (Wang, Wang et al. 2017, Fujisawa, Mizuno et al. 2019, Sambo, Li et al. 2019). Therefore, it is probable that in this study TRPV4 treatment is having little effect on the cells and further studies into DMSO treatment alone or increasing TRPV4 concentrations and/or incubation times is required.

Optimisations of the TRPV4 concentrations for cellular treatments were performed which varied from 10nM to 50nM with 50nM agonist displaying positive calcium signalling while also retaining cell viability. Perhaps a higher concentration for future studies may produce a more significant response compared to the vehicle control. Blocking the TRPV4 channel could have further therapeutic effects if optimised correctly; studies have shown in TRPV4 null mice, stromal opacification due to fibrosis in an alkali burn wound healing response was markedly reduced, suggesting that TRPV4 activation contributed to corneal inflammation and fibrosis (Okada, Shirai et al. 2016). For the corneal epithelium specifically, incorporation of a TRPV4 antagonist into an eye drop or therapeutic agent for the eye could possibly restore fibrosis or prevent limbal stem cell deficiency occurring.

Due to the previously observed significant increase in TRPV4 gene expression after shear stress was applied, it was first thought that activating TRPV4 by agonist treatment would induce this increased stem cell expression response. However, as shown in the results the TRPV4 antagonist treatment significantly increased stem cell marker

expression. Shear stress experiments showed that both stem cell and mature marker expression was significantly enhanced. Therefore, the cells exposed to shear stress, which had significant upregulation in stem cell and mature markers, may have caused an upregulation in TRPV4 expression due to increased differentiation of these cells as shown in Figure 6. 12.

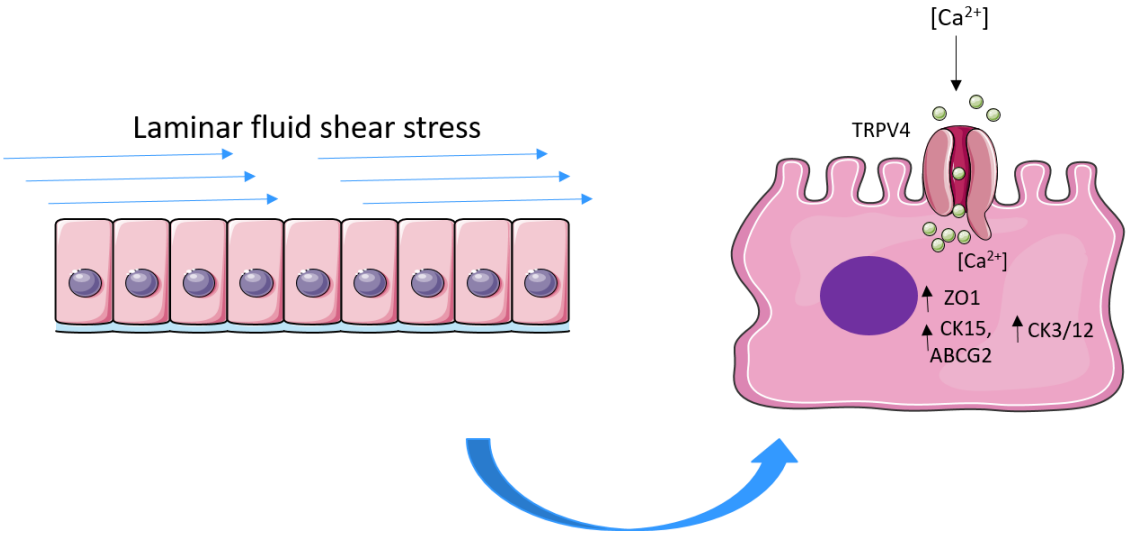

Figure 6. 12 TRPV4 mechanism of action. Under varying laminar shear stress rates and time points, TRPV4 is activated allowing influx of calcium ions resulting in increased stem cell and mature marker expression.

With this in mind, confocal microscopy was performed to determine the protein concentrations of the mature marker CK3 and the stem cell marker NP63 to confirm that these cells had a heterogeneous population of cells expressing both markers. This showed that there was significantly more NP63 protein rather than CK3 protein in all groups compared to vehicle and media controls. This confirmed that the cellular monolayer expressed both mature and stem cell markers on which TRPV4 antagonist or agonist treatment may have an effect.

Barrier function after treatment was examined. There were no significant differences is ZO-1 protein expression among groups. The confocal microscopy images do

not show any clear barrier function formed between cells in any treatments. Previous studies have shown TRPV4 regulates tight junctions and is a late differentiation function in the outermost layer of the stratified corneal epithelia after TRPV4 activation with the same agonist used in this study at a concentration of 100nM (Martínez-Rendón, Sánchez-Guzmán et al. 2017). Further experimentation with longer incubation times with the treatments would be needed to examine this to determine how the cells barrier function is affected when TRPV4 is blocked using antagonist treatment as results from this study were inconclusive.

Finally, metabolic activity was examined under all conditions to ensure that cellular treatment was not harmful to cells. Overall, these experiments showed that metabolic activity was not significantly down regulated after cellular treatment, suggesting that treatment of these cells with either a TRPV4 agonist or antagonist does not induce a reduction in metabolic activity of the cells.

Recent research into the modulation of the TRPV4 channel as a therapeutic target for disease has yielded promising results for the use of TRPV4 antagonism in treating oedema, lung diseases, gastrointestinal disorders and pain. This has lead to human trials for TRPV4 antagonist treatments in healthy participants and stable heart failure patients (Grace, Bonvini et al. 2017). Results from this first in class clinical trial showed that the orally active TRPV4 channel blocker was well tolerated in both patient cohorts with no significant safety issues or serious adverse events, allowing for further evaluation in long-term clinical studies for heart failure and other conditions (Goyal, Skrdla et al. 2019). Therefore, further work into targeting the TRPV4 ion channel for corneal disorders is a promising avenue of research to be explored.

6.5 Conclusion

Overall, this work has provided evidence that the shear stress response observed previously may be mimicked using a TRPV4 antagonist. The results of the gene expression analysis showed a significant upregulation in stem cell markers compared to vehicle treatment alone in some donors (ABCG2, Nestin and CK15 in donor 2 and CK15 in donor 1). Further work looking at observed variations possibly due to DMSO treatment when compared to the vehicle treatment alone is required to understand why these variations are occurring. Longer incubation time with each treatment may be required to allow the cells to adapt to their new cellular medium. The study also shows that no significant harmful metabolic effects were observed after analysis using the presto blue assay, as well as observation of confocal microscopy analysis. No reliable conclusion can be drawn on barrier function capability due to the lack of any obvious barrier function among the cells in the confocal microscopy analysis. Again, longer incubation times may allow tight junction and barrier formation to be observed.

The data shows that supplementation of media with a TRPV4 antagonist may be used as a method to increase stem cell marker expression in LSCs during ex vivo expansion before transplantation. The study has also shown that TRPV4 is implicated in the shear stress response which can be mimicked using this TRPV4 antagonist treatment. This work will aid in future cell culture techniques for limbal epithelial stem cell transplantation while also aiding in the knowledge of corneal epithelial mechanobiology.

Chapter 7

The Combinatorial Effect of Shear Stress and Substrate Stiffness on Culturing Human Corneal Epithelial Cells

7.1 Introduction

As has been previously discussed, the corneal epithelium is subjected to different mechanical cues (Aldrovani, Filezio et al. 2017). This thesis has shown the effect of stiffness (Chapter 4) and shear stress (Chapter 5) on epithelial-limbal derived cells. While there have been studies incorporating different mechanical stimuli to design an in-vitro model of the ocular surface (Seo, Byun et al. 2019), it is unknown if there is a synergistic effect of these two mechanical cues on limbal stem cells.

The ocular surface experiences a number of mechanical stimuli that are difficult to replicate in vitro. Studies in the literature have tried to make in vitro models of the ocular surface for drug toxicity testing as well as for research purposes (Reichl, Kölln et al. 2011, Lu, Yin et al. 2017, Wang, Ghezzi et al. 2017). The corneal epithelium being the outermost layer of the cornea means that it experiences a wide variety of both internal and external stimuli that are difficult to integrate into the in vitro ocular surface models seen in the literature.

This study aimed to combine the two major mechanical stimuli that the corneal epithelium experiences; stiffness and shear stress. Previous work done in the lab showed optimised substrate stiffness and shear stress rates to grow human limbal stem cells to retain stem cell characteristics. This has led to research focused on how the combination of these two stimuli effects the stem cell characteristics of these cells. This may aid in designing future in vitro models of the corneal epithelium while also providing a novel culturing system to allow these cells to be most suited for limbal stem cell transplantation.

7.2 Materials and Methods

7.2.1 *Cell culture*

Cell culture was performed using the same protocol described in Chapter 5. One donor (aged 45 years old) was used for stiffness and flow experiments.

7.2.2 *PDMS fabrication*

PDMS blends of varying stiffnesses were made using a commercially available product of Sylgard 184 and Sylgard 527 (Dow Corning). The softest blend of Sylgard 527 was prepared as per the manufacturer's instructions mixing equal quantities of parts A and B. Sylgard 184, the stiffest substrate, was also prepared as per manufacturer's instructions blending 10 parts base to 1 part curing agent. Sylgard 184 was used for the stiff group in this study, 5 parts of Sylgard 527 to 1 part Sylgard 184 was blended to use for the softer group in this study. All samples were centrifuged at 650 G for 5 minutes to reduce air bubbles before spin coating.

7.2.3 *Mechanical characterisation*

The Young's modulus of PDMS samples were measured using the same procedure described in Chapter 4.

7.2.4 *Spin coating*

Square µ Slide I 0.8 leur ibiTreat polymer coverslips (iBidi) were spin coated at 863 G for 15 seconds using a spin coater (Ossila) with either 184 or 527 PDMS.

7.2.5 *Slide preparation*

After coverslips were spin coated with PDMS, sticky-slide I 0.8 Luer were used to make the slides for the study as shown in Figure 7.1. These slides are bottomless to allow a variety of materials to be mounted to them and used for shear stress experiments. An

ibidi clamp was also used to ensure an even seal of the wet PDMS spin coated coverslip to the sticky slide. Samples were cured at 60 °C overnight followed by ethylene oxide sterilisation to prepare slides for cell culture.

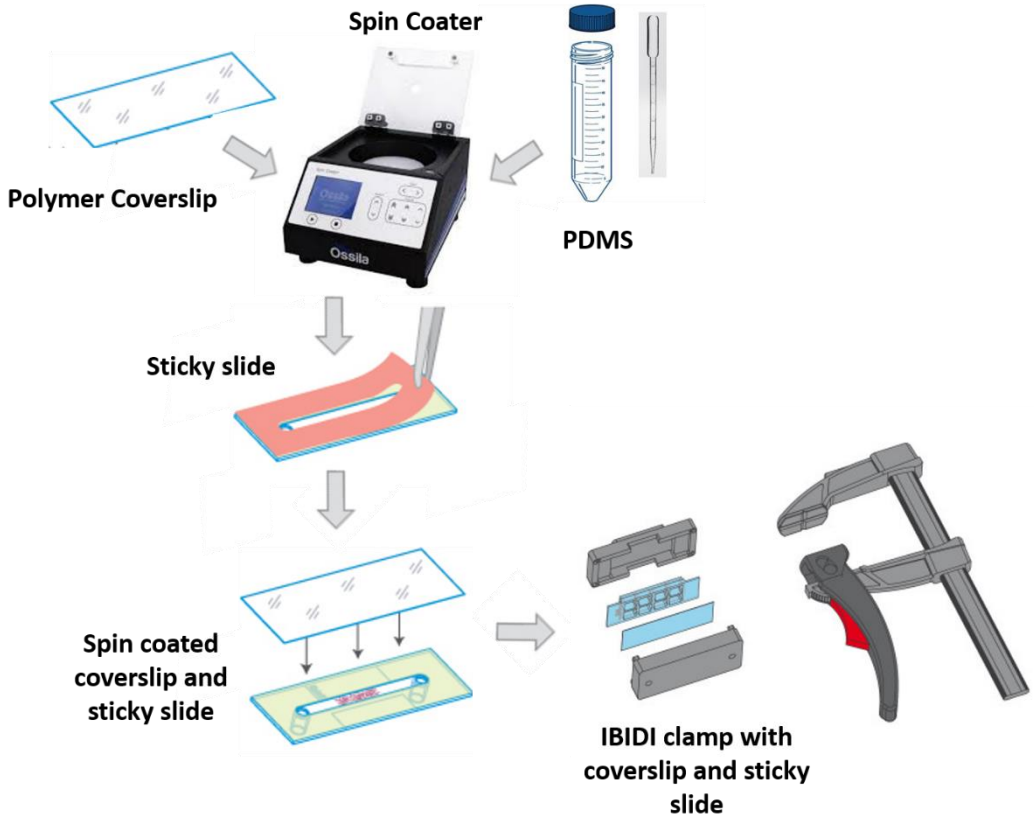

Figure 7.1 Sticky slide preparation. Assembly of the sticky slides uses PDMS to spin coat polymer coverslips, which can be assembled and clamped to create a seal using the IBIDI clamp.

7.2.6 *Fluid flow bioreactor*

Fluid flow was applied to cells using the same protocol described in Chapter 5 with the prepared spin coated slides. The groups used in this study are detailed in Table 5 below. The shear stress used was 1.1 dyn/cm^2 for 1 day or static culture using daily media changes. Previous work done in Chapter 5 showed that this shear stress rate is optimal to grow human limbal stem cells to retain stem cell characteristics.

Table 5 Experimental groups using different substrates and fluid flow conditions.

Group	Elastic Modulus (kPa)	Static culture	Subject to fluid flow
Culture plastic (TCP)	**1 x 10^7**	**TCP static**	**TCP flow**
High stiffness PDMS	**1500**	**Stiff static**	**Stiff flow**
Low stiffness PDMS	**105**	**Soft static**	**Soft flow**

7.2.7 *RT-PCR*

RT-PCR was performed using the same protocol described in Chapter 3. The following primers were used: NP63α (custom made primer sequence adapted from Robertson et al. (Robertson, Ho et al. 2008) ABCG2 (Hs01053790_m1), CK15 (Hs00267035_m1), Nestin (Hs00707120_s1), CK14 (Hs00265033_m1), CK3 (Hs00365080_m1), CK12 (Hs00165015_m1) and GAPDH (Hs02758991_g1).

7.2.8 *Statistical analysis*

All experiments were carried out in triplicate, statistical analysis and outlier calculation was performed using GraphPad Prism software. Data are presented as the mean $\pm$ standard deviation (SD), significance was calculated either via one-way or two-way ANOVA with Post-Tukey test, significance deemed as $p \leq 0.05$ for all data sets.

7.3 Results

7.3.1 *Mechanical characterisation*

Mechanical characterisation of samples were the same as results observed in Chapter 4 for PDMS tensile testing and spin coating thickness.

7.3.2 *Differentiation*

Gene expression analysis was used to determine how stiffness and flow in combination affected differentiation of LSCs. RT-PCR looked at a panel of markers including stem cell markers; NP63α, ABCG2, CK15, Nestin, Transient amplifying marker; CK14 and mature markers; CK3 and CK12. This data was normalised to the stiff static group and all groups were compared. The soft static group was not used as a control group in this data as previous work has shown that a stiffer substrate is more typical of the in vivo stiffness of the cornea as well as representing the stiffness (MPa) of typical biomaterials on which these cells are cultured such as amniotic membrane (Benson-Martin, Zammaretti et al. 2006).

7.3.2.1 *Stem cell marker gene expression*

The stiffer flow group significantly enhanced stem cell marker expression; NP63α, ABCG2, CK15 and Nestin compared to the stiff static group as well as the soft flow group for CK15 gene expression Figure 7.2 A – D. The stiff flow group was the only group to significantly increase NP63α and Nestin expression (Figure 7.2 A + D). The soft flow group did not display any significant changes in gene expression of these markers. The TCP flow group displayed a significant increase in ABCG2 and CK15 expression compared to the stiff static group for ABCG2 and compared to the stiff flow group for CK15 gene expression (Figure 7.2 B + C).

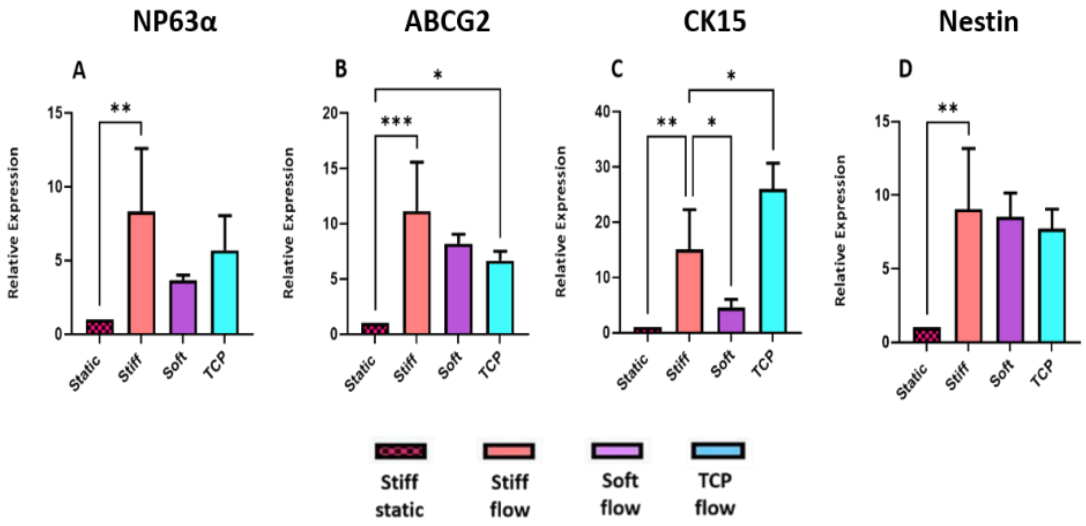

Figure 7.2 Real time PCR of stem cell markers NP63α, ABCG2, CK15 and Nestin after static or flow culture. (A) NP63α, (B) ABCG2, (C) CK15 and (D) Nestin gene expression after static or flow cell culture in combination with the stiff, soft or TCP group. Data are presented as the mean (±SD), significance calculated via one-way ANOVA with a Post-Tukey test, N=4, * = $P \leq 0.05$, ** = $P \leq 0.01$, *** = $P \leq 0.001$.

7.3.2.2 *Transient amplifying gene expression*

The transient amplifying marker CK14 was examined under stiffness and flow conditions. The stiffer flow group significantly enhanced CK14 gene expression compared to the stiff static and soft flow groups as shown in Figure 7.3. The TCP flow group also displayed a significant increase in CK14 gene expression compared to the stiff flow group.

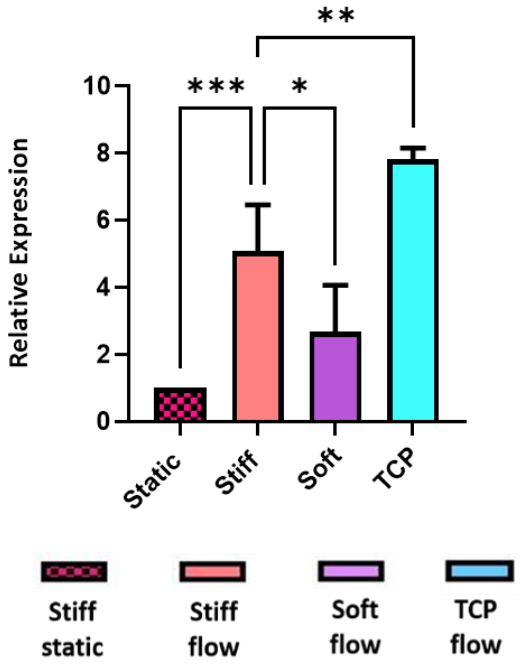

Figure 7.3 Real time PCR of transient amplifying marker CK14 after static or flow culture. CK14 gene expression after static or flow cell culture in combination with the stiff, soft or TCP group. Data are presented as the mean (±SD), significance calculated via one-way ANOVA with a Post-Tukey test, N=4, * = $P \leq 0.05$, ** = $P \leq 0.01$, *** = $P \leq 0.001$.

7.3.2.3 *Mature marker expression*

Gene expression for mature markers CK3 and CK12 under stiffness and flow conditions was examined as shown in Figure 7.4. Both the stiff flow and soft flow groups did not produce any CK3 expression. The TCP flow group did produce CK3 gene expression but this was not significant (Figure 7.4 A). The stiff flow group and TCP flow group expressed CK12 gene expression while the soft flow group did not produce any CK12 expression; no significant differences in CK12 expression were observed (Figure 7.4 B)

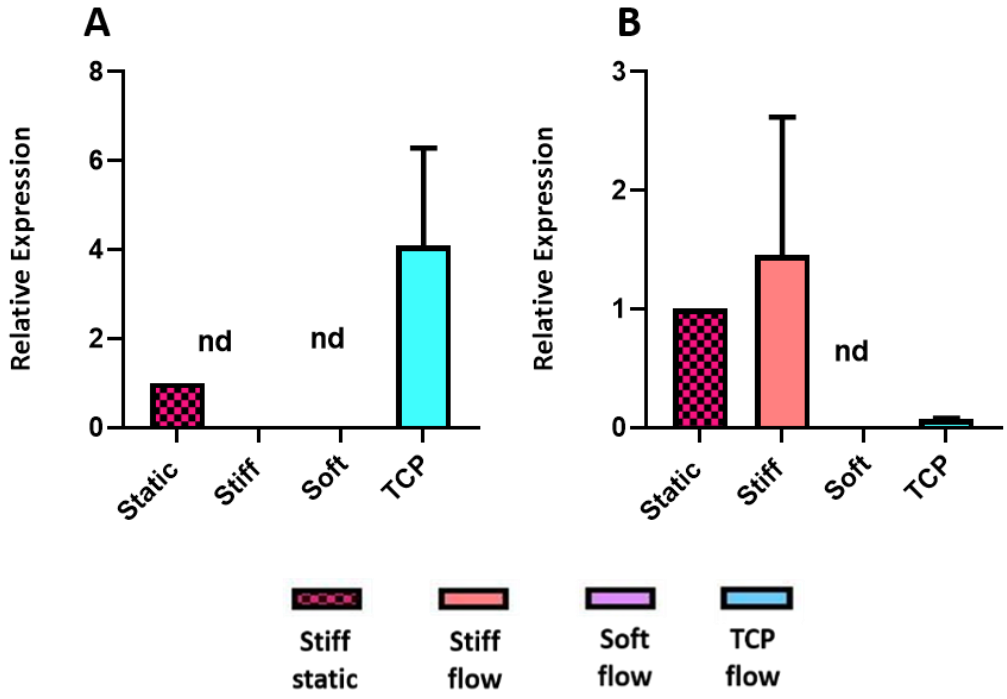

Figure 7.4 Real time PCR of mature markers CK3 and CK12 after static or flow culture. (A) CK3, (B) CK12 gene expression after static or flow cell culture in combination with the stiff, soft or TCP group. Data are presented as the mean (±SD), nd = not detected, N=4.

7.4 Discussion

In Chapter 4, it was shown that culturing corneal epithelial cells on a softer substrates of 105kPa was better at retaining stem cell phenotype compared to a stiffer substrates of 1.5 MPa. However, this study was used a modified cell line rather than primary cells. Chapter 5 showed that culturing human corneal epithelial cells under a low shear stress of 1.22 dyn/cm^2 enhanced stem cell marker expression. This study aimed to combine these two mechanical stimuli to determine whether there is a synergistic effect of these stimuli.

One study has examined shear and tensile behaviour of the stromal lamellae investigating how this affects the cornea's three main layers (epithelium, stroma and endothelium). This study showed that the stromal tissue stress-strain shear behaviour followed an exponential pattern which is an initially low stiffness that increases gradually under higher shear stresses (Elsheikh, Ross et al. 2009). This supports the theory that stiffness and flow together would produce a synergistic effect with softer substrates and low shear stresses working synergistically to increase stem cell expression.

This study showed that the stiffer flow group, which has an elastic modulus of approximately 1.5 MPa, combined with low shear stress for 1 day significantly enhanced both stem cell and transient amplifying expression compared to the stiff static group and soft flow group for ABCG2 expression. This was surprising as the softer group was shown in Chapter 4 to be more suited to culturing corneal epithelial stem cells. However, this study used a cell line as well as a longer culture period. The mature marker CK3 gene expression was not detected in the stiffness and flow groups but the TCP flow group did show expression of CK3 and CK12. The stiff flow group expressed CK12 but this was not

significant. This result shows that combining stiffness and flow cell culture aids in reducing mature marker expression while upregulating stem cell marker gene expression.

The transient amplifying marker CK14 was significantly increased after stiff flow culture compared to the stiff static and soft flow groups. The TCP flow group also significantly enhanced CK14 expression compared to the stiff flow group. While it was increased in the soft flow group, this was not significant. This suggests that cells adopt a phenotype which is stem-like and transient amplifying which may have applications in ex vivo expansion of limbal stem cells before transplantation or for use as an in vitro model for the corneal epithelium.

Research into matrix stiffness and shear stress in 3D organ models have been used to determine how these two mechanical cues regulate cell function by complementing each other's function (Li, Li et al. 2020). While there has been some research in corneal 3D models and optimisation of culturing techniques (Shiju, Carlos de Oliveira et al. 2020), this is mostly focused on full corneal models rather than recapitulating the corneal epithelium specifically. The data presented may aid in optimising future in vitro corneal epithelial models or optimising culture techniques to design better microenvironments and/or biomaterials to culture these cells ex-vivo before transplantation.

Data shows that there is a synergistic effect of the combination of stiffness and shear stress when culturing limbal stem cells. The stiff group combined with shear stress enhanced stem cell marker expression up to 20 fold. Therefore, when culturing limbal stem cells it would be better to combine shear stress with a substrate that has a stiffness of 1-2 MPa.

Further work to examine why stiffer rather than softer substrates in combination with shear stress is required to elucidate this response. Perhaps under shear stress cells require a stiffer underlying substrate similar to the in vivo stiffness of the cornea. This can vary from the basement membrane (modulus ≈ 7.5 kPa) (Last, Liliensiek et al. 2009, Last, Thomasy et al. 2012) to the stiffer corneal stroma (0.17 to 1.5 MPa) (Singh, Han et al. 2018, Xie, Zhang et al. 2018, Zappone, Patil et al. 2018, Karimi, Razaghi et al. 2019). Epithelial cells can become exposed to the stroma following the loss of the bowman's layer after laser photorefractive keratectomy (Lagali, Germundsson et al. 2009). Limbal stem cells have even been cultured on the stiffer amniotic membrane (≈ 2.6 MPa) as a method to generate transplantable sheets for corneal surface repair (Benson-Martin, Zammaretti et al. 2006). Overall, this work aids in the knowledge of the physiological environment experienced by the cornea, combining two major mechanical stimuli experienced by corneal epithelial cells. A stiffer underlying substrate is required when combining with shear stress. This may aid in elucidating the environment that these cells experience in vivo.

7.5 Conclusion

This work shows the combined effect of substrate stiffness and fluid flow can be used to regulate the behaviour of limbal stem cells. This may serve as a novel way to culture these cells to make them more suitable for limbal stem cell transplantation. This work can also help to mimic a more in vivo environment that limbal stem cells experience and may be used as an in vitro model of the corneal epithelium for research or drug toxicity testing purposes.

Chapter 8

Summary, Future Directions, Conclusions

8.1 Summary

The primary objective of this thesis was to use mechanical stimuli to control the cellular phenotype of the corneal epithelium. The two mechanical stimuli investigated were stiffness and shear stress as alternative culturing methods for cultivating corneal epithelial cells.

Initially, a corneal epithelial cell line was used to look at how calcium and glucose concentrations in culture media in combination affect the corneal epithelial cells (Chapter 3). Glucose concentration has been associated with changes in matrix metalloproteinase (MMP) activity (Takahashi, Akiba et al. 2000), immune response (Ni, Yan et al. 2011) and growth factor signalling (Xu, Li et al. 2009) in corneal epithelial cells. Calcium concentration has been shown to affect both the proliferation and differentiation of mice corneal epithelial cells in-vitro (Ma and Liu 2011). While the role of each of these two important reagents has been examined, their reciprocal role on cell behaviour has not previously been explored.

This study showed that the combination of different glucose and calcium concentrations can affect the metabolic activity, proliferative capacity, differentiation and focal adhesion of a corneal epithelial cell line using typical cell culture media used in the literature. The cell line suppliers recommended media appeared to be the best at maintaining stem like characteristics while also promoting proliferation. LG-HC and HG-LC media both had reduced expression of NP63 and enhanced expression of CK3 suggesting that these media formulations may be useful for promoting differentiation towards a mature epithelial phenotype. HG-HC media should be avoided when culturing these cells.

Following these experiments, the supplier's media was used for culturing the cell line and HG-HC media was avoided for any primary cell culture.

The second objective of this thesis was to determine what stiffness was optimal for growing this cell line on (Chapter 4). This study used PDMS and substrates were uncoated unlike most other studies investigating cellular response to stiffness. This study demonstrated that stiffness plays a major role on the differentiation, proliferation and morphology of limbal derived epithelial cells using a corneal epithelial cell line as a model. Culturing cells on a material with a Young's modulus in the range of 10 kPa-105 kPa would appear to be the most suitable for retaining the cells stem like characteristics. Limitations with this study include use of a cell-line rather than primary cells, there was no air-liquid interface when culturing the cells and the topography of the PDMS substrates will differ from the corneas basement membrane. Despite this, these findings could be applied when optimizing the design of biomaterials for limbal epithelial cell culture and transplantation

Chapter 5 explored the effect of shear stress on human primary limbal stem cells. This study showed that culturing corneal epithelial cells under either a low shear stress (1.22 dyn/cm^2) or high shear stress (2.42 dyn/cm^2) significantly affects the corneal epithelial cells stem cell marker expression, wound healing capability and barrier function. This effect is enhanced over time with the cells adopting a more mature phenotype over three days in addition to expressing pro migratory proteins while also expressing stem cell markers, an attractive phenotypic profile for cells to be used in limbal stem cell transplantation. This work has shown that rather than using typical static culture, a new way of culturing these cells under shear stress produces a more conducive cellular

phenotype. This may aid in higher success rates of transplantation while also aiding in our knowledge of the corneal epithelial mechanobiology.

The regulatory mechanism of the shear stress response was investigated in Chapter 6 to determine if this could be therapeutically targeted. TRPV4 was selected as research candidate based off previous work done in the literature which has targeted TRPV4 successfully. Additionally TRPV4 and its role in the corneal epithelium is becoming increasingly important in how it relays mechanical cues and maintains the corneal epithelium. This study concluded that use of 50nM TRPV4 antagonist resulted in a significant increase in stem cell marker expression, successfully mimicking the shear stress response observed in previous studies.

The final study (Chapter 7) combined both stiffness and shear stress to see if these were synergistic or opposing in their expression of stem cell markers. This work showed that a combination of softer substrates compared to the stiff TCP or amniotic membrane used in cell culture of limbal stem cells and shear stress significantly enhances stem cell markers and transient amplifying markers. This may serve as a novel way to culture these cells to make them more suitable for limbal stem cell transplantation. This work can also help to mimic a more in vivo environment that limbal stem cells experience and may be used as an in vitro model of the corneal epithelium for research or drug toxicity testing purposes.

8.2 Limitations and Further Remarks

In earlier Chapters 3 and 4, a human corneal epithelial cell line was used which has been used as a model in previous studies and proven to be a good model of the corneal epithelium (Robertson, Ho et al. 2008). For later chapters primary tissue was sourced and

enabled multiple donors to be used. However, use of primary culture for these earlier studies would have provided more conclusive results but for stiffness experiments this would have been challenging without coating the cells. The results for stiffness experiments using uncoated substrates was not done previously in the literature which provided novel insight into how the corneal epithelial cells relay these mechanical cues.

Primary cell culture used a media that contained xenogeneic components introduced by FBS which is not favourable for applications of these results in an in vivo setting. Applying this work with a media not containing FBS may alter results observed in this thesis and should be considered in future research.

The use of a monolayer culture throughout each study as well as lack of an air liquid interface limits the results of this thesis as the corneal epithelium is a stratified layer which is in an air liquid interface with the external environment. Culturing these cells to produce a stratified layer before applying experimental techniques would provide a more valuable insight into how the cells respond in a more in vivo environment.

While the shear stress results were promising, use of an iBidi pump to perform these experiments in the lab can be cumbersome and for scaling up in a lab to replace traditional culturing methods may not be feasible due to cost and labour. However, elucidating mechanisms of how these cells relayed these shear stress responses allowed for the removal of the shear stress setup which offers alternative cell culture media supplementation rather than using a shear stress bioreactor setup.

The use of a static control group in the shear stress experiments is commonly used throughout the literature. However, a better control may be an extremely low shear stress so that cells are experiencing similar nutritional diffusion and replenished media. Growth

factors and other molecules may also be secreted into circulating media in the cells undergoing shear stress which will affect their response to shear stress. In this study however, the lowest shear stress rate possible was used as an experimental group and the goal was to compare to static cultures. It would however be an important consideration in future experimentation on shear stress and the corneal epithelium.

Using a TRPV4 antagonist as a supplement in cell culture medium to promote expression of stem cell markers may be suitable for culturing these cells to allow for more successful transplantation rates. However, as this study was only 2 days of cell culture, longer cell culture time may be more advantageous and the feasibility of using this long term and how this aids in transplantation success rates needs to be explored with further research.

For stiffness and shear stress in combination, limitations of this study included the use of one donor for proof of concept and the coating of substrates for cellular adhesion. This coating may alter their response to the substrate but it is required for primary cell culture adhesion in limbal stem cells.

8.3 Future Work

To look at how the stiffness ranges in this study affects primary cell culture rather than the use of a cell line would require the ability to use PDMS without a coating similar to the cell line study design. PDMS may be plasma treated to enhance cell adhesion, however this treatment is known to change the mechanical characteristics of the substrate (Bartalena, Loosli et al. 2012). How stiffness affects the migration of corneal epithelial cells would be advantageous to determine for biomaterial or scaffold design. During the course of this PhD, a PDMS gradient was created using a syringe pump to

achieve a PDMS material, which achieved stiffness ranging from 12 kPa to 1.5 MPa. However, due to the thickness of this material it was not possible to observe live cellular migration.

Mechanical memory of the corneal epithelium has not been researched in depth with regards to stiffness or shear stress. There has been work done on this in MSCs and adipose-derived stem cells with implications for biomaterial design and stem cell-based therapies (Dunham, Havlioglu et al. 2020, Wei, Liu et al. 2020). Growing cells on different stiffnesses or under different shear stress rates and determining if these cells remember their past mechanical environments may be of interest to determine how the cells will behave in a new mechanical environment (such as the eye). This work would help to determine whether the corneal epithelial cells may be 'primed' using mechanical stimuli that enhance stem cell marker or migratory expression to aid in repopulating the stem cell niche in the eye.

For TRPV4 experimentation, the early cellular response was determined with promising results showing this channel as a candidate for drug targeting using media supplementation. However, longer incubation times and a lower cell density would be advantageous to determine how the cells adapt to these altered TRPV4 signals as well as how this affects barrier function in the cells.

8.4 Conclusions

This thesis has explored in depth two mechanical stimuli that the corneal epithelium experiences in vivo – stiffness and shear stress. This work has provided several different optimisations of the culturing environments for corneal epithelial cells before transplantation.

The media used for a corneal epithelial cell line was optimised focusing on glucose and calcium combinations. This provided insight into how the use of a typical media used for isolation of primary cells effects these cell lines.

An optimum stiffness range was determined using uncoated substrates. This may aid in biomaterial design and improving culture environments of human corneal epithelial cells.

Culturing human limbal stem cells under defined shear stresses demonstrated a more conducive cellular phenotype. This may facilitate higher success rates of transplantation and aid in our knowledge of the corneal epithelial mechanobiology.

Insight into the regulatory mechanism of the corneal epithelium in its shear stress response was elucidated. This response was successfully mimicked while also presenting a drug target for the corneal epithelium removing the need for the shear stress setup and also improving cell culture techniques for the ex vivo expansion of these cells before transplantation.

The final study was able to combine both of these mechanical stimuli to show a synergistic effect of mechanical stimuli when culturing corneal epithelial cells. This may be used to improve cell culture environments or mimic in vivo environments of the corneal epithelium.

To conclude, the data presented herein provides novel insights into corneal mechanobiology, highlighting the crucial role of the mechanical environment on limbal and corneal epithelial cell behaviour. It is hoped that these insights will actuate

development of improved corneal tissue culturing techniques as a method to address the global shortage of donated corneal tissue.

References

Abdalkader, R. and K. I. Kamei (2020). "Multi-corneal barrier-on-a-chip to recapitulate eye blinking shear stress forces." Lab Chip **20**(8): 1410-1417.

Abou Neel, E. A., U. Cheema, J. C. Knowles, R. A. Brown and S. N. Nazhat (2006). "Use of multiple unconfined compression for control of collagen gel scaffold density and mechanical properties." Soft Matter **2**(11): 986-992.

Abrams, G. A., S. S. Schaus, S. L. Goodman, P. F. Nealey and C. J. Murphy (2000). "Nanoscale Topography of the Corneal Epithelial Basement Membrane and Descemet's Membrane of the Human." Cornea **19**(1): 57-64.

Ahearne, M. (2014). "Introduction to cell-hydrogel mechanosensing." Interface Focus **4**(2): 20130038.

Ahearne, M., K. K. Liu, A. J. El Haj, K. Y. Then, S. Rauz and Y. Yang (2010). "Online monitoring of the mechanical behavior of collagen hydrogels: influence of corneal fibroblasts on elastic modulus." Tissue Eng Part C Methods **16**(2): 319-327.

Ahearne, M., Y. Liu and D. J. Kelly (2014). "Combining freshly isolated chondroprogenitor cells from the infrapatellar fat pad with a growth factor delivery hydrogel as a putative single stage therapy for articular cartilage repair." Tissue Eng Part A **20**(5-6): 930-939.

Ahearne, M. and A. P. Lynch (2015). "Early Observation of Extracellular Matrix-Derived Hydrogels for Corneal Stroma Regeneration." Tissue Eng Part C Methods **21**(10): 1059-1069.

Ahearne, M., Y. Yang, K. Y. Then and K. K. Liu (2007). "An indentation technique to characterize the mechanical and viscoelastic properties of human and porcine corneas." Ann Biomed Eng **35**(9): 1608-1616.

Ahmad, S., C. Osei-Bempong, R. Dana and U. Jurkunas (2010). "The culture and transplantation of human limbal stem cells." Journal of Cellular Physiology **225**(1): 15-19.

Aldrovani, M., M. R. Filezio and J. L. Laus (2017). "A supramolecular look at microenvironmental regulation of limbal epithelial stem cells and the differentiation of their progeny." Arq Bras Oftalmol **80**(4): 268-272.

Alexander, M. R. and P. Williams (2017). "Water contact angle is not a good predictor of biological responses to materials." Biointerphases **12**(2): 02C201.

Atallah, M. R., S. Palioura, V. L. Perez and G. Amescua (2016). "Limbal stem cell transplantation: current perspectives." Clinical Ophthalmology (Auckland, N.Z.) **10**: 593-602.

Aureille, J., N. Belaadi and C. Guilluy (2017). "Mechanotransduction via the nuclear envelope: a distant reflection of the cell surface." Curr Opin Cell Biol **44**: 59-67.

Azkargorta, M., J. Soria, A. Acera, I. Iloro and F. Elortza (2017). "Human tear proteomics and peptidomics in ophthalmology: Toward the translation of proteomic biomarkers into clinical practice." Journal of Proteomics **150**: 359-367.

Azuma, E., M. Hirayama, H. Yamamoto and Y. Komada (2002). "The role of donor age in naive T-cell recovery following allogeneic hematopoietic stem cell transplantation: the younger the better." Leuk Lymphoma **43**(4): 735-739.

Balasubramanian, S. A., D. C. Pye and M. D. P. Willcox (2013). "Effects of eye rubbing on the levels of protease, protease activity and cytokines in tears: relevance in keratoconus." Clinical and Experimental Optometry **96**(2): 214-218.

Bartalena, G., Y. Loosli, T. Zambelli and J. G. Snedeker (2012). "Biomaterial surface modifications can dominate cell–substrate mechanics: the impact of PDMS plasma treatment on a quantitative assay of cell stiffness." Soft Matter **8**(3): 673-681.

Barut Selver, O., A. Yagci, S. Egrilmez, M. Gurdal, M. Palamar, T. Cavusoglu, U. Ates, A. Veral, C. Guven and J. M. Wolosin (2017). "Limbal Stem Cell Deficiency and Treatment with Stem Cell Transplantation." Turk J Ophthalmol **47**(5): 285-291.

Baylis, O., P. Rooney, F. Figueiredo, M. Lako and S. Ahmad (2013). "An investigation of donor and culture parameters which influence epithelial outgrowths from cultured human cadaveric limbal explants." J Cell Physiol **228**(5): 1025-1030.

Benson-Martin, J., P. Zammaretti, G. Bilic, T. Schweizer, B. Portmann-Lanz, T. Burkhardt, R. Zimmermann and N. Ochsenbein-Kolble (2006). "The Young's modulus of fetal preterm and term amniotic membranes." Eur J Obstet Gynecol Reprod Biol **128**(1-2): 103-107.

Benson-Martin, J., P. Zammaretti, G. Bilic, T. Schweizer, B. Portmann-Lanz, T. Burkhardt, R. Zimmermann and N. Ochsenbein-Kölble (2006). "The Young's modulus of fetal preterm and term amniotic membranes." European Journal of Obstetrics & Gynecology and Reproductive Biology **128**(1): 103-107.

Berridge, M. J. (2001). "The versatility and complexity of calcium signalling." Novartis Found Symp **239**: 52-64; discussion 64-57, 150-159.

Boussinesq, M., G. Fobi and A. C. Kuesel (2018). "Alternative treatment strategies to accelerate the elimination of onchocerciasis." International Health **10**(suppl_1): i40-i48.

Braun, R. J., P. E. King-Smith, C. G. Begley, L. Li and N. R. Gewecke (2015). "Dynamics and function of the tear film in relation to the blink cycle." Prog Retin Eye Res **45**: 132-164.

Bray, L. J., K. A. George, S. L. Ainscough, D. W. Hutmacher, T. V. Chirila and D. G. Harkin (2011). "Human corneal epithelial equivalents constructed on Bombyx mori silk fibroin membranes." Biomaterials **32**(22): 5086-5091.

Brocklehurst, P. (2000). "Interventions for treating gonorrhoea in pregnancy." Cochrane Database Syst Rev(2): Cd000098.

Carter, R. T. (2009). "The role of integrins in corneal wound healing." Veterinary Ophthalmology **12**(s1): 2-9.

Castro-Munozledo, F., D. G. Meza-Aguilar, R. Dominguez-Castillo, V. Hernandez-Zequinely and E. Sanchez-Guzman (2017). "Vimentin as a Marker of Early Differentiating, Highly Motile Corneal Epithelial Cells." J Cell Physiol **232**(4): 818-830.

Chakraborty, A., J. Dutta, S. Das and H. Datta (2013). "Comparison of ex vivo cultivated human limbal epithelial stem cell viability and proliferation on different substrates." Int Ophthalmol **33**(6): 665-670.

Cheema, U., C. B. Chuo, P. Sarathchandra, S. N. Nazhat and R. A. Brown (2007). "Engineering functional collagen scaffolds: Cyclical loading increases material strength and fibril aggregation." Advanced Functional Materials **17**(14): 2426-2431.

Chen, B., R. R. Jones, S. Mi, J. Foster, S. G. Alcock, I. W. Hamley and C. J. Connon (2012). "The mechanical properties of amniotic membrane influence its effect as a biomaterial for ocular surface repair." Soft Matter **8**(32): 8379-8387.

Chen, C. S. (2008). "Mechanotransduction – a field pulling together?" Journal of Cell Science **121**(20): 3285-3292.

Chen, F.-M. and X. Liu (2016). "Advancing biomaterials of human origin for tissue engineering." Progress in polymer science **53**: 86-168.

Chen, J., J. Lan, D. Liu, L. J. Backman, W. Zhang, Q. Zhou and P. Danielson (2017). "Ascorbic Acid Promotes the Stemness of Corneal Epithelial Stem/Progenitor Cells and Accelerates Epithelial Wound Healing in the Cornea." Stem Cells Transl Med **6**(5): 1356-1365.

Chen, S.-Y., C. Xie, H. Zhu and Y. Shen (2020). "Effects of epidermal growth factor on transforming growth factor-beta1-induced epithelial-mesenchymal transition and potential mechanism in human corneal epithelial cells." International journal of ophthalmology **13**(1): 11-20.

Chen, Z., C. S. de Paiva, L. Luo, F. L. Kretzer, S. C. Pflugfelder and D.-Q. Li (2004). "Characterization of putative stem cell phenotype in human limbal epithelia." Stem cells (Dayton, Ohio) **22**(3): 355-366.

Chew, H. F. (2011). "Limbal stem cell disease: Treatment and advances in technology." Saudi journal of ophthalmology : official journal of the Saudi Ophthalmological Society **25**(3): 213-218.

Corrigan, M. A., G. P. Johnson, E. Stavenschi, M. Riffault, M.-N. Labour and D. A. Hoey (2018). "TRPV4-mediates oscillatory fluid shear mechanotransduction in mesenchymal stem cells in part via the primary cilium." Scientific Reports **8**(1): 3824.

Dart, J. K., C. F. Radford, D. Minassian, S. Verma and F. Stapleton (2008). "Risk factors for microbial keratitis with contemporary contact lenses: a case-control study." Ophthalmology **115**(10): 1647-1654, 1654 e1641-1643.

Daxer, A., K. Misof, B. Grabner, A. Ettl and P. Fratzl (1998). "Collagen fibrils in the human corneal stroma: structure and aging." Investigative Ophthalmology & Visual Science **39**(3): 644-648.

Dayoub, J. C., F. Cortese, A. Anžič, T. Grum and J. P. de Magalhães (2018). "The effects of donor age on organ transplants: A review and implications for aging research." Exp Gerontol **110**: 230-240.

Di Girolamo, N. (2015). "Moving epithelia: Tracking the fate of mammalian limbal epithelial stem cells." Prog Retin Eye Res **48**: 203-225.

Di Gregorio, J., I. Robuffo, S. Spalletta, G. Giambuzzi, V. De Iuliis, E. Toniato, S. Martinotti, P. Conti and V. Flati (2020). "The Epithelial-to-Mesenchymal Transition as a Possible Therapeutic Target in Fibrotic Disorders." Frontiers in cell and developmental biology **8**: 607483-607483.

Di Iorio, E., V. Barbaro, A. Ruzza, D. Ponzin, G. Pellegrini and M. De Luca (2005). "Isoforms of DeltaNp63 and the migration of ocular limbal cells in human corneal regeneration." Proc Natl Acad Sci U S A **102**(27): 9523-9528.

Discher, D. E., P. Janmey and Y. L. Wang (2005). "Tissue cells feel and respond to the stiffness of their substrate." Science **310**(5751): 1139-1143.

Doñate-Macián, P., J. Enrich-Bengoa, R. I. Dégano, G. D. Quintana and A. Perálvarez-Marín (2019). "Trafficking of Stretch-Regulated TRPV2 and TRPV4 Channels Inferred Through Interactomics." Biomolecules **9**(12).

Dowling, D. P., I. S. Miller, M. Ardhaoui and W. M. Gallagher (2011). "Effect of surface wettability and topography on the adhesion of osteosarcoma cells on plasma-modified polystyrene." J Biomater Appl **26**(3): 327-347.

Dreier, B., V. K. Raghunathan, P. Russell and C. J. Murphy (2012). "Focal adhesion kinase knockdown modulates the response of human corneal epithelial cells to topographic cues." Acta Biomaterialia **8**(12): 4285-4294.

Dunham, C., N. Havlioglu, A. Chamberlain, S. Lake and G. Meyer (2020). "Adipose stem cells exhibit mechanical memory and reduce fibrotic contracture in a rat elbow injury model." Faseb j **34**(9): 12976-12990.

Dunn, S. P., R. L. Gal, C. Kollman, D. Raghinaru, M. Dontchev, C. L. Blanton, E. J. Holland, J. H. Lass, K. R. Kenyon, M. J. Mannis, S. I. Mian, C. J. Rapuano, W. J. Stark and R. W. Beck (2014). "Corneal Graft Rejection Ten Years after Penetrating Keratoplasty in the Cornea Donor Study." Cornea **33**(10): 1003-1009.

Dupont, S., L. Morsut, M. Aragona, E. Enzo, S. Giulitti, M. Cordenonsi, F. Zanconato, J. Le Digabel, M. Forcato, S. Bicciato, N. Elvassore and S. Piccolo (2011). "Role of YAP/TAZ in mechanotransduction." Nature **474**(7350): 179-183.

Eberwein, P. and T. Reinhard (2015). "Concise reviews: the role of biomechanics in the limbal stem cell niche: new insights for our understanding of this structure." Stem Cells **33**(3): 916-924.

Eghrari, A. O., S. A. Riazuddin and J. D. Gottsch (2015). "Overview of the Cornea: Structure, Function, and Development." Prog Mol Biol Transl Sci **134**: 7-23.

Elkins, C. M., Q. M. Qi and G. G. Fuller (2014). "Corneal Cell Adhesion to Contact Lens Hydrogel Materials Enhanced via Tear Film Protein Deposition." PLOS ONE **9**(8): e105512.

Elsheikh, A. and K. Anderson (2005). "Comparative study of corneal strip extensometry and inflation tests." Journal of the Royal Society Interface **2**(3): 177-185.

Elsheikh, A., S. Ross, D. Alhasso and P. Rama (2009). "Numerical study of the effect of corneal layered structure on ocular biomechanics." Curr Eye Res **34**(1): 26-35.

Elsheikh, A., D. Wang and D. Pye (2007). "Determination of the modulus of elasticity of the human cornea." J Refract Surg **23**(8): 808-818.

Engler, A. J., S. Sen, H. L. Sweeney and D. E. Discher (2006). "Matrix Elasticity Directs Stem Cell Lineage Specification." Cell **126**(4): 677-689.

Engler, A. J., S. Sen, H. L. Sweeney and D. E. Discher (2006). "Matrix elasticity directs stem cell lineage specification." Cell **126**(4): 677-689.

Eslani, M., A. Baradaran-Rafii, A. Y. Cheung, K. H. Kurji, H. Hasani, A. R. Djalilian and E. J. Holland (2019). "Amniotic Membrane Transplantation in Acute Severe Ocular Chemical Injury: A Randomized Clinical Trial." Am J Ophthalmol **199**: 209-215.

Fan, T.-J., B. Xu, J. Zhao, H.-S. Yang, R.-X. Wang and X.-Z. Hu (2011). "Establishment of an untransfected human corneal epithelial cell line and its biocompatibility with denuded amniotic membrane." International journal of ophthalmology **4**(3): 228-234.

Fang, Y., L. Liu, S. Liu, L. Hu, W. Cai, X. Wan, D. Liu, Y. He and Z. Zhu (2020). "Calcium-sensing receptor promotes tumor proliferation and migration in human intrahepatic cholangiocarcinoma by targeting ERK signaling pathway." Eur J Pharmacol **872**: 172915.

Findlay, A. S., D. A. Panzica, P. Walczysko, A. B. Holt, D. J. Henderson, J. D. West, A. M. Rajnicek and J. M. Collinson "The core planar cell polarity gene, Vangl2, directs adult corneal epithelial cell alignment and migration." Royal Society Open Science **3**(10): 160658.

Fitt, A. D. and G. Gonzalez (2006). "Fluid mechanics of the human eye: aqueous humour flow in the anterior chamber." Bull Math Biol **68**(1): 53-71.

Foster, J. W., R. R. Jones, C. A. Bippes, R. M. Gouveia and C. J. Connon (2014). "Differential nuclear expression of Yap in basal epithelial cells across the cornea and substrates of differing stiffness." Exp Eye Res **127**: 37-41.

Fournié, P., D. Touboul, J. L. Arné, J. Colin and F. Malecaze (2013). "[Keratoconus]." J Fr Ophtalmol **36**(7): 618-626.

Fujisawa, R., M. Mizuno, H. Katano, K. Otabe, N. Ozeki, K. Tsuji, H. Koga and I. Sekiya (2019). "Cryopreservation in 95% serum with 5% DMSO maintains colony formation and chondrogenic abilities in human synovial mesenchymal stem cells." BMC Musculoskelet Disord **20**(1): 316.

Fujita, M., T. Igarashi, T. Kurai, M. Sakane, S. Yoshino and H. Takahashi (2005). "Correlation between dry eye and rheumatoid arthritis activity." Am J Ophthalmol **140**(5): 808-813.

Garcia-Porta, N., P. Fernandes, A. Queiros, J. Salgado-Borges, M. Parafita-Mato and J. M. González-Méijome (2014). "Corneal biomechanical properties in different ocular conditions and new measurement techniques." ISRN ophthalmology **2014**: 724546-724546.

Geerling, G., C. S. C. Liu, J. R. O. Collin and J. K. G. Dart (2002). "Costs and gains of complex procedures to rehabilitate end stage ocular surface disease." The British journal of ophthalmology **86**(11): 1220-1221.

Glatt, V., C. H. Evans and K. Tetsworth (2016). "A Concert between Biology and Biomechanics: The Influence of the Mechanical Environment on Bone Healing." Front Physiol **7**: 678.

Gouveia, R. M., G. Lepert, S. Gupta, R. R. Mohan, C. Paterson and C. J. Connon (2019). "Assessment of corneal substrate biomechanics and its effect on epithelial stem cell maintenance and differentiation." Nat Commun **10**(1): 1496.

Gouveia, R. M., F. Vajda, J. A. Wibowo, F. Figueiredo and C. J. Connon (2019). "YAP, ΔNp63, and β-Catenin Signaling Pathways Are Involved in the Modulation of Corneal Epithelial Stem Cell Phenotype Induced by Substrate Stiffness." Cells **8**(4): 347.

Goyal, N., P. Skrdla, R. Schroyer, S. Kumar, D. Fernando, A. Oughton, N. Norton, D. L. Sprecher and J. Cheriyan (2019). "Clinical Pharmacokinetics, Safety, and Tolerability of a Novel, First-in-Class TRPV4 Ion Channel Inhibitor, GSK2798745, in Healthy and Heart Failure Subjects." Am J Cardiovasc Drugs **19**(3): 335-342.

Grace, M. S., S. J. Bonvini, M. G. Belvisi and P. McIntyre (2017). "Modulation of the TRPV4 ion channel as a therapeutic target for disease." Pharmacol Ther **177**: 9-22.

Guarino, B. D., S. Paruchuri and C. K. Thodeti (2020). "The role of TRPV4 channels in ocular function and pathologies." Exp Eye Res **201**: 108257.

Guo, Z. H., Y. Y. S. Jia, Y. M. Zeng, Z. F. Li and J. S. Lin (2021). "Transcriptome analysis identifies the differentially expressed genes related to the stemness of limbal stem cells in mice." Gene **775**: 145447.

Guo, Z. H., W. Zhang, Y. Y. S. Jia, Q. X. Liu, Z. F. Li and J. S. Lin (2018). "An Insight into the Difficulties in the Discovery of Specific Biomarkers of Limbal Stem Cells." International journal of molecular sciences **19**(7): 1982.

Haagdorens, M., S. I. Van Acker, V. Van Gerwen, S. Ní Dhubhghaill, C. Koppen, M.-J. Tassignon and N. Zakaria (2016). "Limbal Stem Cell Deficiency: Current Treatment Options and Emerging Therapies." Stem cells international **2016**: 9798374-9798374.

Hamill, O. P. and B. Martinac (2001). "Molecular Basis of Mechanotransduction in Living Cells." Physiological Reviews **81**(2): 685.

Hampel, U., F. Garreis, F. Burgemeister, N. Essel and F. Paulsen (2018). "Effect of intermittent shear stress on corneal epithelial cells using an in vitro flow culture model." Ocul Surf.

Hancox, Z., S. Heidari Keshel, S. Yousaf, M. Saeinasab, M. A. Shahbazi and F. Sefat (2020). "The progress in corneal translational medicine." Biomater Sci.

Harthan, J. S. and E. Shorter (2018). "Therapeutic uses of scleral contact lenses for ocular surface disease: patient selection and special considerations." Clinical optometry **10**: 65-74.

Hatami-Marbini, H. and A. Rahimi (2014). "Effects of bathing solution on tensile properties of the cornea." Exp Eye Res **120**: 103-108.

Hernáez-Moya, R., S. González, A. Urkaregi, J. I. Pijoan, S. X. Deng and N. Andollo (2020). "Expansion of Human Limbal Epithelial Stem/Progenitor Cells Using Different Human Sera: A Multivariate Statistical Analysis." Int J Mol Sci **21**(17).

Heryudono, A., R. J. Braun, T. A. Driscoll, K. L. Maki, L. P. Cook and P. E. King-Smith (2007). "Single-equation models for the tear film in a blink cycle: realistic lid motion." Math Med Biol **24**(4): 347-377.

Hjortdal, J. O. (1994). "Young's modulus of elasticity for the human cornea." J Cataract Refract Surg **20**(6): 672.

Hodson, S. and R. Earlam (1994). "Of an extracellular matrix in human pre-corneal tear film." J Theor Biol **168**(4): 395-398.

Hoffmann, F. and G. Curio (2003). "[REM sleep and recurrent corneal erosion--a hypothesis]." Klin Monbl Augenheilkd **220**(1-2): 51-53.

Hong, W. and K.-L. Guan (2012). "The YAP and TAZ transcription co-activators: Key downstream effectors of the mammalian Hippo pathway." Seminars in Cell & Developmental Biology **23**(7): 785-793.

Hossler, P., C. Racicot, C. Chumsae, S. McDermott and K. Cochran (2017). "Cell culture media supplementation of infrequently used sugars for the targeted shifting of protein glycosylation profiles." Biotechnol Prog **33**(2): 511-522.

Hubbell, J. A. (1995). "Biomaterials in Tissue Engineering." Nat Biotech **13**(6): 565-576.

Iannaccone, S., Y. Zhou, D. Walterhouse, G. Taborn, G. Landini and P. Iannaccone (2012). "Three Dimensional Visualization and Fractal Analysis of Mosaic Patches in Rat Chimeras: Cell Assortment in Liver, Adrenal Cortex and Cornea." PLOS ONE **7**(2): e31609.

IBTS. (2021). "Ocular Tissue." Retrieved Jan 29th 2021, from https://www.giveblood.ie/clinical-services/tissue-bank/ocular_tissue/.

Ingber, D. E. (2006). "Cellular mechanotransduction: putting all the pieces together again." The FASEB Journal **20**(7): 811-827.

Ioannidis, A. S., L. Speedwell and K. K. Nischal (2005). "Unilateral keratoconus in a child with chronic and persistent eye rubbing." Am J Ophthalmol **139**(2): 356-357.

Jackson, C. J., I. T. Myklebust Ernø, H. Ringstad, K. A. Tønseth, D. A. Dartt and T. P. Utheim (2020). "Simple limbal epithelial transplantation: Current status and future perspectives." Stem Cells Transl Med **9**(3): 316-327.

Jafri, B., H. Lichter and R. D. Stulting (2004). "Asymmetric keratoconus attributed to eye rubbing." Cornea **23**(6): 560-564.

Jain, R., N. Sharma, S. Basu, G. Iyer, M. Ueta, C. Sotozono, C. Kannabiran, V. M. Rathi, N. Gupta, S. Kinoshita, J. A. Gomes, J. Chodosh and V. S. Sangwan (2016). "Stevens-Johnson syndrome: The role of an ophthalmologist." Surv Ophthalmol **61**(4): 369-399.

Jannie, K. M., S. M. Ellerbroek, D. W. Zhou, S. Chen, D. J. Crompton, A. J. Garcia and K. A. DeMali (2015). "Vinculin-dependent actin bundling regulates cell migration and traction forces." Biochem J **465**(3): 383-393.

Jia, L., C. E. Ghezzi and D. L. Kaplan (2016). "Optimization of silk films as substrate for functional corneal epithelium growth." J Biomed Mater Res B Appl Biomater **104**(2): 431-441.

Johnson, C. S., S. I. Mian, S. Moroi, D. Epstein, J. Izatt and N. A. Afshari (2007). "Role of Corneal Elasticity in Damping of Intraocular Pressure." Investigative Ophthalmology & Visual Science **48**(6): 2540-2544.

Johnson, D. H., W. M. Bourne and R. Campbell (1982). "The ultrastructure of descemet's membrane: I. changes with age in normal corneas." Archives of Ophthalmology **100**(12): 1942-1947.

Jones, M. B., G. R. Fulford, C. P. Please, D. L. S. McElwain and M. J. Collins (2008). "Elastohydrodynamics of the Eyelid Wiper." Bulletin of Mathematical Biology **70**(2): 323-343.

Jones, R. R., I. W. Hamley and C. J. Connon (2012). "Ex vivo expansion of limbal stem cells is affected by substrate properties." Stem Cell Res **8**(3): 403-409.

Joseph Antony, S. (2015). "Imaging shear stress distribution and evaluating the stress concentration factor of the human eye." Scientific Reports **5**(1): 8899.

Joyce, N. C. (2003). "Proliferative capacity of the corneal endothelium." Prog Retin Eye Res **22**(3): 359-389.

Kang, Y. G., J. W. Shin, S. H. Park, M. J. Oh, H. S. Park, J. W. Shin and S. H. Kim (2014). "Effects of flow-induced shear stress on limbal epithelial stem cell growth and enrichment." PLoS One **9**(3): e93023.

Karimi, A., R. Razaghi, T. Sera and S. Kudo (2019). "A combination of the finite element analysis and experimental indentation via the cornea." Journal of the Mechanical Behavior of Biomedical Materials **90**: 146-154.

Khatry, S. K., K. P. West, Jr., J. Katz, S. C. LeClerq, E. K. Pradhan, L. S. Wu, M. D. Thapa and R. P. Pokhrel (1995). "Epidemiology of xerophthalmia in Nepal. A pattern of household poverty, childhood illness, and mortality. The Sarlahi Study Group." Arch Ophthalmol **113**(4): 425-429.

Kim, I. S., J. C. Shin, C. Y. Im and E. K. Kim (2005). "Three Cases of Descemet's Membrane Detachment after Cataract Surgery." Yonsei Medical Journal **46**(5): 719-723.

Kosaku, K., T. Harada, T. Jike, I. Tsuboi and S. Aizawa (2018). "Long-Term Hypoxic Tolerance in Murine Cornea." High Alt Med Biol **19**(1): 35-41.

Kruse, F. E. and S. C. Tseng (1992). "Proliferative and differentiative response of corneal and limbal epithelium to extracellular calcium in serum-free clonal cultures." J Cell Physiol **151**(2): 347-360.

Ladage, P. M., D. H. Ren, W. M. Petroll, J. V. Jester, J. P. Bergmanson and H. D. Cavanagh (2003). "Effects of eyelid closure and disposable and silicone hydrogel extended contact lens wear on rabbit corneal epithelial proliferation." Invest Ophthalmol Vis Sci **44**(5): 1843-1849.

Lagali, N., J. Germundsson and P. Fagerholm (2009). "The Role of Bowman's Layer in Corneal Regeneration after Phototherapeutic Keratectomy: A Prospective Study Using In Vivo Confocal Microscopy." Investigative Ophthalmology & Visual Science **50**(9): 4192-4198.

Lagali, N., J. Germundsson and P. Fagerholm (2009). "The Role of Bowman’s Layer in Corneal Regeneration after Phototherapeutic Keratectomy: A Prospective Study Using In Vivo Confocal Microscopy." Investigative Ophthalmology & Visual Science **50**(9): 4192-4198.

Lagali, N., U. Stenevi, M. Claesson, P. Fagerholm, C. Hanson and B. Weijdegård (2009). "Survival of donor-derived cells in human corneal transplants." Invest Ophthalmol Vis Sci **50**(6): 2673-2678.

Lapajne, L., M. Lakk, O. Yarishkin, L. Gubeljak, M. Hawlina and D. Križaj (2020). "Polymodal Sensory Transduction in Mouse Corneal Epithelial Cells." Investigative Ophthalmology & Visual Science **61**(4): 2-2.

Last, J. A., S. J. Liliensiek, P. F. Nealey and C. J. Murphy (2009). "Determining the mechanical properties of human corneal basement membranes with atomic force microscopy." Journal of Structural Biology **167**(1): 19-24.

Last, J. A., S. M. Thomasy, C. R. Croasdale, P. Russell and C. J. Murphy (2012). "Compliance profile of the human cornea as measured by atomic force microscopy." Micron **43**(12): 1293-1298.

Le-Bel, G., L. P. Guérin, P. Carrier, F. Mouriaux, L. Germain, S. L. Guérin and R. Bazin (2019). "Grafting of an autologous tissue-engineered human corneal epithelium to a patient with limbal stem cell deficiency (LSCD)." Am J Ophthalmol Case Rep **15**: 100532.

Lee, S. E., S. R. Kim and M. Park (2015). "Oxygen permeability of soft contact lenses in different pH, osmolality and buffering solution." International Journal of Ophthalmology **8**(5): 1037-1042.

Leong, Y. Y. and L. Tong (2015). "Barrier function in the ocular surface: from conventional paradigms to new opportunities." Ocul Surf **13**(2): 103-109.

Leung, B. K., J. A. Bonanno and C. J. Radke (2011). "Oxygen-deficient metabolism and corneal edema." Prog Retin Eye Res **30**(6): 471-492.

Levis, H. J., R. A. Brown and J. T. Daniels (2010). "Plastic compressed collagen as a biomimetic substrate for human limbal epithelial cell culture." Biomaterials **31**(30): 7726-7737.

Li, W., P. Li, N. Li, Y. Du, S. Lü, D. Elad and M. Long (2020). "Matrix stiffness and shear stresses modulate hepatocyte functions in a fibrotic liver sinusoidal model." Am J Physiol Gastrointest Liver Physiol.

Lian, I., J. Kim, H. Okazawa, J. Zhao, B. Zhao, J. Yu, A. Chinnaiyan, M. A. Israel, L. S. Goldstein, R. Abujarour, S. Ding and K. L. Guan (2010). "The role of YAP transcription coactivator in regulating stem cell self-renewal and differentiation." Genes Dev **24**(11): 1106-1118.

Lin, M. C., A. D. Graham, K. A. Polse, R. B. Mandell and N. A. McNamara (1999). "Measurement of post-lens tear thickness." Invest Ophthalmol Vis Sci **40**(12): 2833-2839.

Lin, X. and B. P. Helmke (2009). "Cell Structure Controls Endothelial Cell Migration under Fluid Shear Stress." Cell Mol Bioeng **2**(2): 231-243.

Lindsay, R. G., A. S. Bruce and I. F. Gutteridge (2000). "Keratoconus associated with continual eye rubbing due to punctal agenesis." Cornea **19**(4): 567-569.

Liu, C. Y. and W. W. Kao (2015). "Corneal Epithelial Wound Healing." Prog Mol Biol Transl Sci **134**: 61-71.

Liu, T. and X. G. Dong (2008). "[The progress of epithelial-mesenchymal transition in ophthalmology]." Zhonghua Yan Ke Za Zhi **44**(3): 285-288.

Liu, W.-C., S.-M. Lee, A. D. Graham and M. C. Lin (2011). "Effects of Eye Rubbing and Breath Holding on Corneal Biomechanical Properties and Intraocular Pressure." Cornea **30**(8): 855-860.

Ljubimov, A. V. and M. Saghizadeh (2015). "Progress in corneal wound healing." Progress in retinal and eye research **49**: 17-45.

Lo, C.-M., H.-B. Wang, M. Dembo and Y.-l. Wang (2000). "Cell Movement Is Guided by the Rigidity of the Substrate." Biophysical Journal **79**(1): 144-152.

Long, B., H. Schweizer, H. Bleshoy and F. Zeri (2009). "Expanding your use of silicone hydrogel contact lenses: using lotrafilcon A for daily wear." Eye Contact Lens **35**(2): 59-64.

López-Paniagua, M., T. Nieto-Miguel, A. de la Mata, S. Galindo, J. M. Herreras, R. M. Corrales and M. Calonge (2013). "Consecutive Expansion of Limbal Epithelial Stem Cells from a Single Limbal Biopsy." Current Eye Research **38**(5): 537-549.

Lozano Cerrada, S., S. Y. Altaf and E. Olavarria (2018). "Allogeneic stem cell transplantation from unrelated donors in acute leukaemia." Curr Opin Oncol **30**(6): 418-424.

Lu, L. W., G. Sheyla, D. Wei, D. Sophie and Luo (2016). "Effect of Hypoxia-regulated Plk3 On Human Limbal Stem Cell Differentiation." Journal of Biological Chemistry **291**: 16519-16529.

Lu, Q., H. Yin, M. P. Grant and J. H. Elisseeff (2017). "An In Vitro Model for the Ocular Surface and Tear Film System." Sci Rep **7**(1): 6163.

Lu, Y. W., N. Martino, B. D. Gerlach, J. M. Lamar, P. A. Vincent, A. P. Adam and J. J. Schwarz (2021). "MEF2 (Myocyte Enhancer Factor 2) Is Essential for Endothelial Homeostasis and the Atheroprotective Gene Expression Program." Arterioscler Thromb Vasc Biol: Atvbaha120314978.

Ludwig, P. E., M. J. Lopez and K. E. Sevensma (2020). Anatomy, Head and Neck, Eye Cornea. StatPearls. Treasure Island (FL), StatPearls Publishing

Lynch, A. P. and M. Ahearne (2017). "Retinoic Acid Enhances the Differentiation of Adipose-Derived Stem Cells to Keratocytes In Vitro." Transl Vis Sci Technol **6**(1): 6.

Lynch, A. P., F. O'Sullivan and M. Ahearne (2016). "The effect of growth factor supplementation on corneal stromal cell phenotype in vitro using a serum-free media." Exp Eye Res **151**: 26-37.

Ma, X.-L. and H.-Q. Liu (2011). "Effect of calcium on the proliferation and differentiation of murine corneal epithelial cells in vitro." International Journal of Ophthalmology **4**(3): 247-249.

Ma, X. L. and H. Q. Liu (2011). "Effect of calcium on the proliferation and differentiation of murine corneal epithelial cells in vitro." Int J Ophthalmol **4**(3): 247-249.

Maïssa, C. and M. Guillon (2010). "Tear film dynamics and lipid layer characteristics—Effect of age and gender." Contact Lens and Anterior Eye **33**(4): 176-182.

Malhotra, C. and A. K. Jain (2014). "Human amniotic membrane transplantation: Different modalities of its use in ophthalmology." World Journal of Transplantation **4**(2): 111-121.

Mann, A. and B. Tighe (2013). "Contact lens interactions with the tear film." Exp Eye Res **117**: 88-98.

Marroquin, L. D., J. Hynes, J. A. Dykens, J. D. Jamieson and Y. Will (2007). "Circumventing the Crabtree effect: replacing media glucose with galactose increases susceptibility of HepG2 cells to mitochondrial toxicants." Toxicol Sci **97**(2): 539-547.

Martin, I., D. Wendt and M. Heberer (2004). "The role of bioreactors in tissue engineering." Trends Biotechnol **22**(2): 80-86.

Martínez-Rendón, J., E. Sánchez-Guzmán, A. Rueda, J. González, R. Gulias-Cañizo, G. Aquino-Jarquín, F. Castro-Muñozledo and R. García-Villegas (2017). "TRPV4 Regulates Tight Junctions and Affects Differentiation in a Cell Culture Model of the Corneal Epithelium." J Cell Physiol **232**(7): 1794-1807.

Martinez, J. and J. F. Santibanez (1993). "Extracellular calcium modulates proliferation of factor dependent hemopoietic cells." Cell Biochem Funct **11**(2): 101-105.

Mason, S. L., R. M. K. Stewart, C. M. Sheridan, F. Keshtkar, P. Rooney, E. Austin, U. Schlötzer-Schrehardt, F. E. Kruse and S. B. Kaye (2016). "Yield and Viability of Human Limbal Stem Cells From Fresh and Stored Tissue." Investigative Ophthalmology & Visual Science **57**(8): 3708-3713.

Matthaei, M., A. Hribek, T. Clahsen, B. Bachmann, C. Cursiefen and A. S. Jun (2019). "Fuchs Endothelial Corneal Dystrophy: Clinical, Genetic, Pathophysiologic, and Therapeutic Aspects." Annu Rev Vis Sci **5**: 151-175.

Maurice, D. M. (1957). "The structure and transparency of the cornea." The Journal of Physiology **136**(2): 263-286.

McCarey, B. E. and F. H. Schmidt (1990). "Modeling glucose distribution in the cornea." Curr Eye Res **9**(11): 1025-1039.

McElwain, S., M. B. Jones, G. Fulford, C. P. Please and M. J. Collins (2007). Effect of tear additives on the shear stress and normal stress acting on the ocular surface. 16th Australasian Fluid Mechanics Conference**:** 616-620.

McMahon, F. W., C. Gallagher, N. O'Reilly, M. Clynes, F. O'Sullivan and K. Kavanagh (2014). "Exposure of a Corneal Epithelial Cell Line (hTCEpi) to Demodex-Associated Bacillus Proteins Results in an Inflammatory Response." Investigative Ophthalmology & Visual Science **55**(10).

McMonnies, C. W., A. Alharbi and G. C. Boneham (2010). "Epithelial Responses to Rubbing-Related Mechanical Forces." Cornea **29**(11): 1223-1231.

Mebratu, Y. and Y. Tesfaigzi (2009). "How ERK1/2 Activation Controls Cell Proliferation and Cell Death Is Subcellular Localization the Answer?" Cell cycle (Georgetown, Tex.) **8**(8): 1168-1175.

Meek, K. M. and C. Boote (2004). "The organization of collagen in the corneal stroma." Experimental Eye Research **78**(3): 503-512.

Meek, K. M. and C. Knupp (2015). "Corneal structure and transparency." Progress in Retinal and Eye Research **49**: 1-16.

Mei, H., S. Gonzalez and S. X. Deng (2012). "Extracellular Matrix is an Important Component of Limbal Stem Cell Niche." Journal of Functional Biomaterials **3**(4): 879-894.

Meller, D., M. Pauklin, H. Thomasen, H. Westekemper and K.-P. Steuhl (2011). "Amniotic Membrane Transplantation in the Human Eye." Deutsches Ärzteblatt International **108**(14): 243-248.

Meng, J. X., G. Yang, L. Liu, Y. Y. Song, L. Jiang and S. T. Wang (2017). "Cell adhesive spectra along surface wettability gradient from superhydrophilicity to superhydrophobicity." Science China-Chemistry **60**(5): 614-620.

Merjava, S., A. Neuwirth, M. Tanzerova and K. Jirsova (2011). "The spectrum of cytokeratins expressed in the adult human cornea, limbus and perilimbal conjunctiva." Histol Histopathol **26**(3): 323-331.

Michalaki, E., V. N. Surya, G. G. Fuller and A. R. Dunn (2020). "Perpendicular alignment of lymphatic endothelial cells in response to spatial gradients in wall shear stress." Commun Biol **3**(1): 57.

Miesfeld, J. B. and N. L. Brown (2019). "Eye organogenesis: A hierarchical view of ocular development." Curr Top Dev Biol **132**: 351-393.

Miller, I., M. Min, C. Yang, C. Tian, S. Gookin, D. Carter and S. L. Spencer (2018). "Ki67 is a Graded Rather than a Binary Marker of Proliferation versus Quiescence." Cell reports **24**(5): 1105-1112.e1105.

Mitragotri, S. and J. Lahann (2009). "Physical approaches to biomaterial design." Nature materials **8**(1): 15-23.

Modarreszadeh, S., O. Abouali, A. Ghaffarieh and G. Ahmadi (2014). "Physiology of aqueous humor dynamic in the anterior chamber due to rapid eye movement." Physiol Behav **135**: 112-118.

Molladavoodi, S., H. J. Kwon, J. Medley and M. Gorbet (2015). "Human corneal epithelial cell response to substrate stiffness." Acta Biomater **11**: 324-332.

Molladavoodi, S., M. Robichaud, D. Wulff and M. Gorbet (2017). "Corneal epithelial cells exposed to shear stress show altered cytoskeleton and migratory behaviour." PLoS ONE **12**(6): e0178981.

Montes-Mico, R., J. L. Alio and W. N. Charman (2005). "Dynamic changes in the tear film in dry eyes." Invest Ophthalmol Vis Sci **46**(5): 1615-1619.

Montés-Micó, R., J. L. Alió and W. N. Charman (2005). "Dynamic changes in the tear film in dry eyes." Invest Ophthalmol Vis Sci **46**(5): 1615-1619.

Moon, C. H., J. Y. Kim, M. J. Kim, H. Tchah, B. G. Lim and J. K. Chung (2016). "Effect of Three-Dimensional Printed Personalized Moisture Chamber Spectacles on the Periocular Humidity." Journal of Ophthalmology **2016**: 7.

Mort, R. L., P. Douvaras, S. D. Morley, N. Dorà, R. E. Hill, J. M. Collinson and J. D. West (2012). "Stem cells and corneal epithelial maintenance – insights from the mouse and other animal models." Results and problems in cell differentiation **55**: 357-394.

Mullen, C. A., T. J. Vaughan, K. L. Billiar and L. M. McNamara (2015). "The effect of substrate stiffness, thickness, and cross-linking density on osteogenic cell behavior." Biophysical journal **108**(7): 1604-1612.

Munaron, L., S. Antoniotti and D. Lovisolo (2004). "Intracellular calcium signals and control of cell proliferation: how many mechanisms?" J Cell Mol Med **8**(2): 161-168.

Muntz, A., L. N. Subbaraman, L. Sorbara and L. Jones (2015). "Tear exchange and contact lenses: a review." J Optom **8**(1): 2-11.

Murakami, J., T. Nishida and T. Otori (1992). "Coordinated appearance of beta 1 integrins and fibronectin during corneal wound healing." J Lab Clin Med **120**(1): 86-93.

Nakamura, T., N. Koizumi, M. Tsuzuki, K. Inoki, Y. Sano, C. Sotozono and S. Kinoshita (2003). "Successful regrafting of cultivated corneal epithelium using amniotic membrane as a carrier in severe ocular surface disease." Cornea **22**(1): 70-71.

Nasser, W., A. Amitai-Lange, D. Soteriou, R. Hanna, B. Tiosano, Y. Fuchs and R. Shalom-Feuerstein (2018). "Corneal-Committed Cells Restore the Stem Cell Pool and Tissue Boundary following Injury." Cell Reports **22**(2): 323-331.

Ngan, N. D., H. M. Chau, P. N. Dong, L. X. Cung, N. T. Thuy, P. T. Thang, T. V. Thai, V. T. Nga and N. D. Bac (2019). "Tissue-Cultured Human Cord Lining Epithelial Cells in Treatment of Persistent Corneal Epithelial Defect." Open Access Maced J Med Sci **7**(24): 4266-4271.

Ni, H., X. Yan, Z. Lin and X. Jin (2011). "High glucose may decrease the innate immune through TLRs in cornea epithelium." Mol Vis **17**: 3384-3391.

Nichols, J. J. and P. E. King-Smith (2003). "Thickness of the pre- and post-contact lens tear film measured in vivo by interferometry." Invest Ophthalmol Vis Sci **44**(1): 68-77.

Nowell, C. S., P. D. Odermatt, L. Azzolin, S. Hohnel, E. F. Wagner, G. E. Fantner, M. P. Lutolf, Y. Barrandon, S. Piccolo and F. Radtke (2016). "Chronic inflammation imposes aberrant cell fate in regenerating epithelia through mechanotransduction." Nat Cell Biol **18**(2): 168-180.

Nowell, C. S. and F. Radtke (2017). "Corneal epithelial stem cells and their niche at a glance." Journal of Cell Science **130**(6): 1021.

O'Keefe, E. J., R. A. Briggaman and B. Herman (1987). "Calcium-induced assembly of adherens junctions in keratinocytes." J Cell Biol **105**(2): 807-817.

O'Sullivan, F. and M. Clynes (2007). "Limbal stem cells, a review of their identification and culture for clinical use." Cytotechnology **53**(1-3): 101-106.

Okada, Y., K. Shirai, M. Miyajima, P. S. Reinach, O. Yamanaka, T. Sumioka, M. Kokado, K. Tomoyose and S. Saika (2016). "Loss of TRPV4 Function Suppresses Inflammatory Fibrosis Induced by Alkali-Burning Mouse Corneas." PLoS One **11**(12): e0167200.

Okada, Y., T. Sumioka, K. Ichikawa, H. Sano, A. Nambu, K. Kobayashi, K. Uchida, Y. Suzuki, M. Tominaga, P. S. Reinach, S. I. Hirai, J. V. Jester, M. Miyajima, K. Shirai, H. Iwanishi, W. W. Kao, C. Y. Liu and S. Saika (2019). "Sensory nerve supports epithelial stem cell function in healing of corneal epithelium in mice: the role of trigeminal nerve transient receptor potential vanilloid 4." Lab Invest **99**(2): 210-230.

Oliva, M. S., T. Schottman and M. Gulati (2012). "Turning the tide of corneal blindness." Indian Journal of Ophthalmology **60**(5): 423-427.

Onochie, O. E., A. Zollinger, C. B. Rich, M. Smith and V. Trinkaus-Randall (2019). "Epithelial cells exert differential traction stress in response to substrate stiffness." Exp Eye Res **181**: 25-37.

Orr, A. W., B. P. Helmke, B. R. Blackman and M. A. Schwartz (2006). "Mechanisms of Mechanotransduction." Developmental Cell **10**(1): 11-20.

Ortiz-Melo, M. T., M. J. Garcia-Murillo, V. M. Salazar-Rojas, J. E. Campos and F. Castro-Muñozledo (2021). "Transcriptional profiles along cell programming into corneal epithelial differentiation." Experimental Eye Research **202**: 108302.

Ostrin, L. A. (2019). "Ocular and systemic melatonin and the influence of light exposure." Clin Exp Optom **102**(2): 99-108.

Palchesko, R. N., K. L. Lathrop, J. L. Funderburgh and A. W. Feinberg (2015). "In vitro expansion of corneal endothelial cells on biomimetic substrates." Sci Rep **5**: 7955.

Palchesko, R. N., L. Zhang, Y. Sun and A. W. Feinberg (2012). "Development of polydimethylsiloxane substrates with tunable elastic modulus to study cell mechanobiology in muscle and nerve." PLoS One **7**(12): e51499.

Parini, R., F. Deodato, M. Di Rocco, E. Lanino, F. Locatelli, C. Messina, A. Rovelli and M. Scarpa (2017). "Open issues in Mucopolysaccharidosis type I-Hurler." Orphanet J Rare Dis **12**(1): 112.

Park, M., A. Richardson, E. Pandzic, E. P. Lobo, R. Whan, S. L. Watson, J. G. Lyons, D. Wakefield and N. Di Girolamo (2019). "Visualizing the Contribution of Keratin-14+ Limbal Epithelial Precursors in Corneal Wound Healing." Stem Cell Reports **12**(1): 14-28.

Paugh, J. R., J. Tse, T. Nguyen, A. Sasai, E. Chen, M. T. De Jesus, J. Kwan, A. L. Nguyen, M. Farid, S. Garg and J. V. Jester (2020). "Efficacy of the Fluorescein Tear Breakup Time Test in Dry Eye." Cornea **39**(1): 92-98.

Pauklin, M., K. P. Steuhl and D. Meller (2009). "Characterization of the corneal surface in limbal stem cell deficiency and after transplantation of cultivated limbal epithelium." Ophthalmology **116**(6): 1048-1056.

Pellegrini, G., C. E. Traverso, A. T. Franzi, M. Zingirian, R. Cancedda and M. De Luca (1997). "Long-term restoration of damaged corneal surfaces with autologous cultivated corneal epithelium." Lancet **349**(9057): 990-993.

Pellegrini, G., C. E. Traverso, A. T. Franzi, M. Zingirian, R. Cancedda and M. DeLuca (1997). "Long-term restoration of damaged corneal surfaces with autologous cultivated corneal epithelium." Lancet **349**(9057): 990-993.

Pellegrini, M., C. Senni, F. Bernabei, A. F. G. Cicero, A. Vagge, A. Maestri, V. Scorcia and G. Giannaccare (2020). "The Role of Nutrition and Nutritional Supplements in Ocular Surface Diseases." Nutrients **12**(4).

Peng, H., J. Katsnelson, W. Yang, M. A. Brown and R. M. Lavker (2013). "FIH-1/c-Kit Signaling: A Novel Contributor to Corneal Epithelial Glycogen Metabolism." Investigative Ophthalmology & Visual Science **54**(4): 2781-2786.

Pierscionek, B. K., M. Asejczyk-Widlicka and R. A. Schachar (2007). "The effect of changing intraocular pressure on the corneal and scleral curvatures in the fresh porcine eye." The British Journal of Ophthalmology **91**(6): 801-803.

Pinto, M. C., A. H. Kihara, V. A. Goulart, F. M. Tonelli, K. N. Gomes, H. Ulrich and R. R. Resende (2015). "Calcium signaling and cell proliferation." Cell Signal **27**(11): 2139-2149.

Prakasam, R. K., M. Schwiede, W. W. Hutz, R. F. Guthoff and O. Stachs (2012). "Corneal responses to eye rubbing with spectral domain optical coherence tomography." Curr Eye Res **37**(1): 25-32.

Püspöki, Z., M. Storath, D. Sage and M. Unser (2016). "Transforms and Operators for Directional Bioimage Analysis: A Survey." Adv Anat Embryol Cell Biol **219**: 69-93.

Qi, X., L. Xie, J. Cheng, H. Zhai and Q. Zhou (2013). "Characteristics of immune rejection after allogeneic cultivated limbal epithelial transplantation." Ophthalmology **120**(5): 931-936.

Quent, V. M., D. Loessner, T. Friis, J. C. Reichert and D. W. Hutmacher (2010). "Discrepancies between metabolic activity and DNA content as tool to assess cell proliferation in cancer research." J Cell Mol Med **14**(4): 1003-1013.

Raghunathan, V. K., B. Dreier, J. T. Morgan, B. C. Tuyen, B. W. Rose, C. M. Reilly, P. Russell and C. J. Murphy (2014). "Involvement of YAP, TAZ and HSP90 in contact guidance and intercellular junction formation in corneal epithelial cells." PLoS One **9**(10): e109811.

Rahman, I., D. G. Said, V. S. Maharajan and H. S. Dua (2009). "Amniotic membrane in ophthalmology: indications and limitations." Eye **23**(10): 1954-1961.

Rama, P., S. Bonini, A. Lambiase, O. Golisano, P. Paterna, M. De Luca and G. Pellegrini (2001). "Autologous fibrin-cultured limbal stem cells permanently restore the corneal surface of patients with total limbal stem cell deficiency." Transplantation **72**(9): 1478-1485.

Ramachandran, C., S. Basu, V. S. Sangwan and D. Balasubramanian (2014). "Concise Review: The Coming of Age of Stem Cell Treatment for Corneal Surface Damage." STEM CELLS Translational Medicine **3**(10): 1160-1168.

Reichl, S., C. Kölln, M. Hahne and J. Verstraelen (2011). "In vitro cell culture models to study the corneal drug absorption." Expert Opin Drug Metab Toxicol **7**(5): 559-578.

Ren, H. and G. Wilson (1996). "Apoptosis in the corneal epithelium." Invest Ophthalmol Vis Sci **37**(6): 1017-1025.

Ren, H. and G. Wilson (1997). "The effect of a shear force on the cell shedding rate of the corneal epithelium." Acta Ophthalmologica Scandinavica **75**(4): 383-387.

Resan, M., M. Vukosavljevic and M. Millvojevic (2012). Wavefront Abberations Advances in Ophthalmology. S. Rumelt, InTech.

Resnick, N., H. Yahav, A. Shay-Salit, M. Shushy, S. Schubert, L. C. Zilberman and E. Wofovitz (2003). "Fluid shear stress and the vascular endothelium: for better and for worse." Prog Biophys Mol Biol **81**(3): 177-199.

Robertson, D. M. (2013). "The Effects of Silicone Hydrogel Lens Wear on the Corneal Epithelium and Risk for Microbial Keratitis." Eye & contact lens **39**(1): 67-72.

Robertson, D. M., S. I. Ho and H. D. Cavanagh (2008). "Characterization of DeltaNp63 isoforms in normal cornea and telomerase-immortalized human corneal epithelial cells." Exp Eye Res **86**(4): 576-585.

Robertson, D. M., L. Li, S. Fisher, V. P. Pearce, J. W. Shay, W. E. Wright, H. D. Cavanagh and J. V. Jester (2005). "Characterization of growth and differentiation in a telomerase-immortalized human corneal epithelial cell line." Investigative Ophthalmology & Visual Science **46**(2): 470-478.

Ruberti, J. W., A. S. Roy and C. J. Roberts (2011). "Corneal Biomechanics and Biomaterials." Annual Review of Biomedical Engineering **13**(1): 269-295.

Sabater, A. L. and V. L. Perez (2017). "Amniotic membrane use for management of corneal limbal stem cell deficiency." Curr Opin Ophthalmol **28**(4): 363-369.

Sacchetti, M., P. Rama, A. Bruscolini and A. Lambiase (2018). "Limbal Stem Cell Transplantation: Clinical Results, Limits, and Perspectives." Stem cells international **2018**: 8086269-8086269.

Safvati, A., N. Cole, E. Hume and M. Willcox (2009). "Mediators of neovascularization and the hypoxic cornea." Curr Eye Res **34**(6): 501-514.

Sambo, D., J. Li, T. Brickler and S. Chetty (2019). "Transient Treatment of Human Pluripotent Stem Cells with DMSO to Promote Differentiation." J Vis Exp(149).

Sartaj, R., C. Zhang, P. Wan, Z. Pasha, V. Guaiquil, A. Liu, J. Liu, Y. Luo, E. Fuchs and M. I. Rosenblatt (2017). "Characterization of slow cycling corneal limbal epithelial cells identifies putative stem cell markers." Scientific reports **7**(1): 3793-3793.

Schrader, J., T. T. Gordon-Walker, R. L. Aucott, M. van Deemter, A. Quaas, S. Walsh, D. Benten, S. J. Forbes, R. G. Wells and J. P. Iredale (2011). "Matrix stiffness modulates proliferation, chemotherapeutic response, and dormancy in hepatocellular carcinoma cells." Hepatology (Baltimore, Md.) **53**(4): 1192-1205.

Seo, J., W. Y. Byun, F. Alisafaei, A. Georgescu, Y.-S. Yi, M. Massaro-Giordano, V. B. Shenoy, V. Lee, V. Y. Bunya and D. Huh (2019). "Multiscale reverse engineering of the human ocular surface." Nature Medicine **25**(8): 1310-1318.

Seyed-Safi, A. G. and J. T. Daniels (2020). "The limbus: Structure and function." Experimental Eye Research **197**: 108074.

Shanbhag, S. S., C. N. Patel, R. Goyal, P. R. Donthineni, V. Singh and S. Basu (2019). "Simple limbal epithelial transplantation (SLET): Review of indications, surgical technique, mechanism, outcomes, limitations, and impact." Indian J Ophthalmol **67**(8): 1265-1277.

Sharma, S., R. Goswami, D. X. Zhang and S. O. Rahaman (2019). "TRPV4 regulates matrix stiffness and TGFβ1-induced epithelial-mesenchymal transition." J Cell Mol Med **23**(2): 761-774.

Shiju, T. M., R. Carlos de Oliveira and S. E. Wilson (2020). "3D in vitro corneal models: A review of current technologies." Exp Eye Res **200**: 108213.

Singh, M., Z. Han, J. Li, S. Vantipalli, S. R. Aglyamov, M. D. Twa and K. V. Larin (2018). "Quantifying the effects of hydration on corneal stiffness with noncontact optical coherence elastography." J Cataract Refract Surg **44**(8): 1023-1031.

Sonnaert, M., I. Papantoniou, F. P. Luyten and J. I. Schrooten (2015). "Quantitative Validation of the Presto Blue Metabolic Assay for Online Monitoring of Cell Proliferation in a 3D Perfusion Bioreactor System." Tissue engineering. Part C, Methods **21**(6): 519-529.

Sonnaert, M., I. Papantoniou, F. P. Luyten and J. I. Schrooten (2015). "Quantitative Validation of the Presto Blue Metabolic Assay for Online Monitoring of Cell Proliferation in a 3D Perfusion Bioreactor System." Tissue Eng Part C Methods **21**(6): 519-529.

Soong, H. K. (1987). "Vinculin in focal cell-to-substrate attachments of spreading corneal epithelial cells." Arch Ophthalmol **105**(8): 1129-1132.

Sridhar, M. S. (2018). "Anatomy of cornea and ocular surface." Indian journal of ophthalmology **66**(2): 190-194.

Sridharan, R., B. Cavanagh, A. R. Cameron, D. J. Kelly and F. J. O'Brien (2019). "Material stiffness influences the polarization state, function and migration mode of macrophages." Acta Biomater.

Stahl, U., M. Willcox and F. Stapleton (2012). "Osmolality and tear film dynamics." Clinical and Experimental Optometry **95**(1): 3-11.

Stamer, W. D., A. M. Williams, S. Pflugfelder and S. E. Coupland (2018). "Accessibility to and Quality of Human Eye Tissue for Research: A Cross-Sectional Survey of ARVO Members." Invest Ophthalmol Vis Sci **59**(12): 4783-4792.

Stepp, M. A., S. Spurr-Michaud and I. K. Gipson (1993). "Integrins in the wounded and unwounded stratified squamous epithelium of the cornea." Invest Ophthalmol Vis Sci **34**(5): 1829-1844.

Sugrue, S. P. and J. D. Zieske (1997). "ZO1 in corneal epithelium: association to the zonula occludens and adherens junctions." Exp Eye Res **64**(1): 11-20.

SundarRaj, N., J. D. Rizzo, S. C. Anderson and J. P. Gesiotto (1992). "Expression of vimentin by rabbit corneal epithelial cells during wound repair." Cell Tissue Res **267**(2): 347-356.

Svitova, T. F. and M. C. Lin (2016). "Dynamic interfacial properties of human tear-lipid films and their interactions with model-tear proteins in vitro." Adv Colloid Interface Sci **233**: 4-24.

Swat, A., I. Dolado, J. M. Rojas and A. R. Nebreda (2009). "Cell density-dependent inhibition of epidermal growth factor receptor signaling by p38alpha mitogen-activated protein kinase via Sprouty2 downregulation." Molecular and cellular biology **29**(12): 3332-3343.

Takahashi, H., K. Akiba, T. Noguchi, T. Ohmura, R. Takahashi, Y. Ezure, K. Ohara and J. D. Zieske (2000). "Matrix metalloproteinase activity is enhanced during corneal wound repair in high glucose condition." Curr Eye Res **21**(2): 608-615.

Takahashi, H., K. Akiba, T. Noguchi, T. Ohmura, R. Takahashi, Y. Ezure, K. Ohara and J. D. Zieske (2000). "Matrix metalloproteinase activity is enhanced during corneal wound repair in high glucose condition." Current Eye Research **21**(2): 608-615.

Takatori, S. C., P. Lazon de la Jara, B. Holden, K. Ehrmann, A. Ho and C. J. Radke (2013). "In vivo corneal oxygen uptake during soft-contact-lens wear." Invest Ophthalmol Vis Sci **54**(5): 3472-3479.

Tamura, M., A. Osajima, S. Nakayamada, H. Anai, N. Kabashima, K. Kanegae, T. Ota, Y. Tanaka and Y. Nakashima (2003). "High glucose levels inhibit focal adhesion kinase-mediated wound healing of rat peritoneal mesothelial cells." Kidney Int **63**(2): 722-731.

Tang, Z. L., Y. Akiyama and T. Okano (2012). "Temperature-Responsive Polymer Modified Surface for Cell Sheet Engineering." Polymers **4**(3): 1478-1498.

Taylor, H. R., M. J. Burton, D. Haddad, S. West and H. Wright (2014). "Trachoma." Lancet **384**(9960): 2142-2152.

Thoft, R. A. (1984). "Keratoepithelioplasty." American Journal of Ophthalmology **97**(1): 1-6.

Tiffany, J. M. (2008). "The normal tear film." Dev Ophthalmol **41**: 1-20.

Tilghman, R. W., C. R. Cowan, J. D. Mih, Y. Koryakina, D. Gioeli, J. K. Slack-Davis, B. R. Blackman, D. J. Tschumperlin and J. T. Parsons (2010). "Matrix rigidity regulates cancer cell growth and cellular phenotype." PLoS One **5**(9): e12905.

Tong, C. M., K. van Dijk and G. R. J. Melles (2019). "Update on Bowman layer transplantation." Curr Opin Ophthalmol **30**(4): 249-255.

Trappmann, B., J. E. Gautrot, J. T. Connelly, D. G. T. Strange, Y. Li, M. L. Oyen, M. A. C. Stuart, H. Boehm, B. J. Li, V. Vogel, J. P. Spatz, F. M. Watt and W. T. S. Huck (2012). "Extracellular-matrix tethering regulates stem-cell fate." Nature Materials **11**(7): 642-649.

Tseng, S. C. G., S. Y. Chen, O. G. Mead and S. Tighe (2020). "Niche regulation of limbal epithelial stem cells: HC-HA/PTX3 as surrogate matrix niche." Exp Eye Res **199**: 108181.

Tusan, C. G., Y. H. Man, H. Zarkoob, D. A. Johnston, O. G. Andriotis, P. J. Thurner, S. F. Yang, E. A. Sander, E. Gentleman, B. G. Sengers and N. D. Evans (2018). "Collective Cell Behavior in Mechanosensing of Substrate Thickness." Biophysical Journal **114**(11): 2743-2755.

Utheim, T. P., Ø. Aass Utheim, P. Salvanos, C. J. Jackson, S. Schrader, G. Geerling and A. Sehic (2018). "Concise Review: Altered Versus Unaltered Amniotic Membrane as a Substrate for Limbal Epithelial Cells." Stem cells translational medicine **7**(5): 415-427.

Utsunomiya, T., A. Ishibazawa, T. Nagaoka, K. Hanada, H. Yokota, N. Ishii and A. Yoshida (2016). "Transforming Growth Factor-beta Signaling Cascade Induced by Mechanical Stimulation of Fluid Shear Stress in Cultured Corneal Epithelial Cells." Invest Ophthalmol Vis Sci **57**(14): 6382-6388.

Van Buskirk, E. M. (1989). "The anatomy of the limbus." Eye (Lond) **3 (Pt 2)**: 101-108.

Van Meter, W. S., D. G. Katz, H. White and R. Gayheart (2005). "Effect of death-to-preservation time on donor corneal epithelium." Trans Am Ophthalmol Soc **103**: 209-222; discussion 222-204.

Walker, J. L., B. M. Bleaken, A. R. Romisher, A. A. Alnwibit and A. S. Menko (2018). "In wound repair vimentin mediates the transition of mesenchymal leader cells to a myofibroblast phenotype." Mol Biol Cell **29**(13): 1555-1570.

Wang, H. T., M. G. Wang, X. Liu, P. Su, L. S. Zhang, C. C. Liu, Y. Wang, D. Wu, Q. Tu and J. X. Zhou (2017). "[DMSO Promotes Hematopoietic Differentiation of Human Embryonic Stem Cells in vitro]." Zhongguo Shi Yan Xue Ye Xue Za Zhi **25**(3): 644-649.

Wang, J., D. Fonn, T. L. Simpson and L. Jones (2003). "Precorneal and pre- and postlens tear film thickness measured indirectly with optical coherence tomography." Invest Ophthalmol Vis Sci **44**(6): 2524-2528.

Wang, S., C. E. Ghezzi, R. Gomes, R. E. Pollard, J. L. Funderburgh and D. L. Kaplan (2017). "In vitro 3D corneal tissue model with epithelium, stroma, and innervation." Biomaterials **112**: 1-9.

Wang, Y., J. Xu, X. Sun, R. Chu, H. Zhuang and J. C. He (2009). "Dynamic wavefront aberrations and visual acuity in normal and dry eyes." Clinical and Experimental Optometry **92**(3): 267-273.

Wei, D., A. Liu, J. Sun, S. Chen, C. Wu, H. Zhu, Y. Chen, H. Luo and H. Fan (2020). "Mechanics-Controlled Dynamic Cell Niches Guided Osteogenic Differentiation of Stem Cells via Preserved Cellular Mechanical Memory." ACS Appl Mater Interfaces **12**(1): 260-274.

Wei, J., M. Yoshinari, S. Takemoto, M. Hattori, E. Kawada, B. Liu and Y. Oda (2007). "Adhesion of mouse fibroblasts on hexamethyldisiloxane surfaces with wide range of wettability." J Biomed Mater Res B Appl Biomater **81**(1): 66-75.

Wei, M. L., P. Duan, Z. M. Wang, M. Ding and P. Tu (2017). "High glucose and high insulin conditions promote MCF-7 cell proliferation and invasion by upregulating IRS1 and activating the Ras/Raf/ERK pathway." Mol Med Rep **16**(5): 6690-6696.

Wen, J. H., L. G. Vincent, A. Fuhrmann, Y. S. Choi, K. C. Hribar, H. Taylor-Weiner, S. Chen and A. J. Engler (2014). "Interplay of matrix stiffness and protein tethering in stem cell differentiation." Nat Mater **13**(10): 979-987.

West-Mays, J. A. and D. J. Dwivedi (2006). "The keratocyte: Corneal stromal cell with variable repair phenotypes." The international journal of biochemistry & cell biology **38**(10): 1625-1631.

West, J. D., N. J. Dorà and J. M. Collinson (2015). "Evaluating alternative stem cell hypotheses for adult corneal epithelial maintenance." World journal of stem cells **7**(2): 281-299.

Weyand, B., M. Israelowitz, H. P. von Schroeder and P. M. Vogt (2009). "Fluid dynamics in bioreactor design: considerations for the theoretical and practical approach." Adv Biochem Eng Biotechnol **112**: 251-268.

WHO. (2016). "Priority eye diseases ", from http://www.who.int/blindness/causes/priority/en/index8.html.

Wilson, S. E. and J.-W. Hong (2000). "Bowman's Layer Structure and Function: Critical or Dispensable to Corneal Function? A Hypothesis." Cornea **19**(4): 417-420.

Winter, K. N., D. M. Anderson and R. J. Braun (2010). "A model for wetting and evaporation of a post-blink precorneal tear film." Math Med Biol **27**(3): 211-225.

Wizert, A., D. R. Iskander and L. Cwiklik (2014). "Organization of lipids in the tear film: a molecular-level view." PLoS One **9**(3): e92461.

Xie, J., D. Zhang, C. Zhou, Q. Yuan, L. Ye and X. Zhou (2018). "Substrate elasticity regulates adipose-derived stromal cell differentiation towards osteogenesis and adipogenesis through beta-catenin transduction." Acta Biomater **79**: 83-95.

Xu, K.-P., Y. Li, A. V. Ljubimov and F.-S. X. Yu (2009). "High Glucose Suppresses Epidermal Growth Factor Receptor/Phosphatidylinositol 3-Kinase/Akt Signaling Pathway and Attenuates Corneal Epithelial Wound Healing." Diabetes **58**(5): 1077-1085.

Xu, K. P., Y. Li, A. V. Ljubimov and F. S. Yu (2009). "High glucose suppresses epidermal growth factor receptor/phosphatidylinositol 3-kinase/Akt signaling pathway and attenuates corneal epithelial wound healing." Diabetes **58**(5): 1077-1085.

Xu, M., D. J. McCanna and J. G. Sivak (2015). "Use of the viability reagent PrestoBlue in comparison with alamarBlue and MTT to assess the viability of human corneal epithelial cells." Journal of Pharmacological and Toxicological Methods **71**: 1-7.

Yamaguchi, S., N. Horie, K. Satoh, T. Ishikawa, T. Mori, H. Maeda, Y. Fukuda, S. Ishizaka, T. Hiu, Y. Morofuji, T. Izumo, N. Nishida and T. Matsuo (2018). "Age of donor of human

mesenchymal stem cells affects structural and functional recovery after cell therapy following ischaemic stroke." J Cereb Blood Flow Metab **38**(7): 1199-1212.

Yang, H. (1991). "[Selection of culture media for human and rabbit corneal epithelia]." Zhonghua Yan Ke Za Zhi **27**(6): 351-353.

Yang, H. J., K. J. Kim, M. K. Kim, S. J. Lee, Y. H. Ryu, B. F. Seo, D. Y. Oh, S. T. Ahn, H. Y. Lee and J. W. Rhie (2014). "The stem cell potential and multipotency of human adipose tissue-derived stem cells vary by cell donor and are different from those of other types of stem cells." Cells Tissues Organs **199**(5-6): 373-383.

Yazdanpanah, G., Z. Haq, K. Kang, S. Jabbehdari, M. L. Rosenblatt and A. R. Djalilian (2019). "Strategies for reconstructing the limbal stem cell niche." Ocul Surf **17**(2): 230-240.

Ye, J., W. Ai, F. Zhang, X. Zhu, G. Shu, L. Wang, P. Gao, Q. Xi, Y. Zhang, Q. Jiang and S. Wang (2016). "Enhanced Proliferation of Porcine Bone Marrow Mesenchymal Stem Cells Induced by Extracellular Calcium is Associated with the Activation of the Calcium-Sensing Receptor and ERK Signaling Pathway." Stem Cells Int **2016**: 6570671.

Yeh, S. I., T. W. Chu, H. C. Cheng, C. H. Wu and Y. P. Tsao (2020). "The Use of Autologous Serum to Reverse Severe Contact Lens-induced Limbal Stem Cell Deficiency." Cornea **39**(6): 736-741.

Yin, J. and U. Jurkunas (2018). "Limbal Stem Cell Transplantation and Complications." Semin Ophthalmol **33**(1): 134-141.

Yokoi, N., A. J. Bron and G. A. Georgiev (2014). "The precorneal tear film as a fluid shell: the effect of blinking and saccades on tear film distribution and dynamics." Ocul Surf **12**(4): 252-266.

Yoon, J. J., S. Ismail and T. Sherwin (2014). "Limbal stem cells: Central concepts of corneal epithelial homeostasis." World J Stem Cells **6**(4): 391-403.

Ytteborg, J. and C. H. Dohlman (1965). "Corneal edema and intraocular pressure: Ii. clinical results." Archives of Ophthalmology **74**(4): 477-484.

Zappone, B., N. J. Patil, M. Lombardo and G. Lombardo (2018). "Transient viscous response of the human cornea probed with the Surface Force Apparatus." PLoS One **13**(5): e0197779.

Zeng, B., P. Wang, L. J. Xu, X. Y. Li, H. Zhang and G. G. Li (2014). "Amniotic membrane covering promotes healing of cornea epithelium and improves visual acuity after debridement for fungal keratitis." Int J Ophthalmol **7**(5): 785-789.

Zhang, J., C. W. Zhang, L. Q. Du and X. Y. Wu (2016). "Acellular porcine corneal matrix as a carrier scaffold for cultivating human corneal epithelial cells and fibroblasts in vitro." Int J Ophthalmol **9**(1): 1-8.

Zhang, L., D. Zou, S. Li, J. Wang, Y. Qu, S. Ou, C. Jia, J. Li, H. He, T. Liu, J. Yang, Y. Chen, Z. Liu and W. Li (2016). "An Ultra-thin Amniotic Membrane as Carrier in Corneal Epithelium Tissue-Engineering." **6**: 21021.

Zhang, X., H. Sun, X. Tang, J. Ji, X. Li, J. Sun, Z. Ma, J. Yuan and Z. C. Han (2005). "Comparison of cell-suspension and explant culture of rabbit limbal epithelial cells." Exp Eye Res **80**(2): 227-233.

Zhao, Y., Y. Shen, Z. Yan, M. Tian, J. Zhao and X. Zhou (2019). "Relationship Among Corneal Stiffness, Thickness, and Biomechanical Parameters Measured by Corvis ST, Pentacam and ORA in Keratoconus." Frontiers in physiology **10**: 740-740.

Zhu, C., L. Li and B. Zhao (2015). "The regulation and function of YAP transcription co-activator." Acta Biochim Biophys Sin (Shanghai) **47**(1): 16-28.

Zieske, J. D., G. Bukusoglu and I. K. Gipson (1989). "Enhancement of Vinculin Synthesis by Migrating Stratified Squamous Epithelium." Journal of Cell Biology **109**(2): 571-576.